MAKERERE UNIVERSITY

ENCAPSULATED AND NANO-ORGANIC FERTILIZERS FOR WATER RETENTION AND CONTROLLED NUTRIENT RELEASE

13/02/2026

Hadijah R. Nantambi
MSc. Technology Innovation and Industrial Development, (Mak),
BSc. Industrial Chemistry (Mak)

13/02/2026

Dr. Julia Kigozi, Ph.D
Dean, Department of Agricultural and Biosystems Engineering,
College of Agricultural and Environmental Sciences
Makerere University, Kampala – UGANDA

13/2/2026

Assoc. Prof. Michael, Lubwama, Ph.D
Associate Professor, Department of Mechanical Engineering,
School of Engineering,
College of Engineering, Design, Art and Technology
Makerere University, Kampala – UGANDA

A THESIS SUBMITTED IN PARTIAL FULFILLMENT OF THE REQUIREMENTS FOR THE AWARD OF THE DEGREE OF DOCTOR OF PHILOSOPHY OF MAKERERE UNIVERSITY, KAMPALA UGANDA

February 13th, 2026

DECLARATION

I hereby declare that this thesis, titled "Encapsulated and Nano-Organic Fertilizers for Water Retention and Controlled Nutrient Release," is my original work and has not been submitted, in whole or in part, to any other institution of higher learning for the award of a degree or any other academic qualification. Where the work of others has been used, it has been duly acknowledged and referenced in accordance with academic standards.

13|02|2026

…… ……

Hadijah R. Nantambi **Date**
2018/HD08/19391U
1800743718

DEDICATION

This thesis is dedicated to my virtuous husband, Michael Ssekyondwa, and our children, Morris, Philip, Keren, and Efraim, who have sustained me throughout this journey with their unwavering love, encouragement, and sacrifices. Their patience and constant support have inspired me to persevere through every challenge.

Above all, I dedicate this work to the Ecolife farmers and partners, whose real-world challenges have given my research purpose and strengthened my commitment to impactful, human-centered innovations.

TABLE OF CONTENTS

LIST OF TABLES

LIST OF FIGURES

ACKNOWLEDGEMENT

I express my deepest gratitude to my supervisors, Assoc. Prof. Michael Lubwama, Dr. Julia Kigozi, Dr. Herbert Kalibala, and examiners for their exceptional guidance, constructive feedback, and unwavering support throughout this research. Their expertise in composting, thin-film coatings, materials science, and environmental technology profoundly shaped the direction and quality of this work from inception to completion.

I am sincerely grateful to the Department of Food and Drug, Government Analytical Laboratory, for providing the research facilities and technical assistance essential to this study. My appreciation also goes to the National Agricultural Research Organization (NARO) for supporting composting trials, physicochemical analyses, and semi-field experiments. I extend special thanks to Mr. Andrew Wabwire, Mr. Thomas Mwanawakunno, and Mr. Ronald Tumwesigye for their contribution to the XRD, SEM, and FT-IR characterizations, and to Mr. Stephen Ssebulime for his support with nutrient analyses and ICP-MS data processing. I gratefully acknowledge MAPRONANO, MakRIF, and Ecolife for their financial commitment, without which this work would not have been possible.

I further appreciate the academic, social, psychological, and spiritual support provided by my peers and colleagues, including Ms. Sylvia Namazzi, Dr. Ronald Kayiwa, Dr. Vianney A. Yiga, Mr. and Mrs. Nyanzi, Dr. Derrick Kajjoba, Dr. Stephen Ndawula, Dr. Robinah Kulabako, Dr. Harriet Muyinza Kayongo, Ms. Joyce Ateesa, Mr. Eria Maseruka, Mr. Stephen Ogaba, Mr. Fredrick Semalago, Mr. Emmanuel Nsubuga, the Reawakened Revival community, and the Makerere University CEDAT School of Engineering PhD fraternity. Their encouragement enriched both my academic and personal journey.

I express my sincere gratitude to my husband, Michael Ssekyondwa, for his unwavering encouragement, patience, and financial support throughout this challenging journey. I also extend my heartfelt appreciation to my mother-in-law and dear parents, Mr. and Mrs. Ssekandi, as well as my siblings, Rashidah, Haawa, and Isma, for their continuous support and cheer. Above all, I am grateful to God for awakening my life in 2005 and for sustaining me with joy, strength, and purpose ever since.

LIST OF ACRONYMS AND ABBREVIATIONS

AAS	Atomic Absorption Spectrometry
ANOVA	Analysis of Variance
BBC	Biochar Blended Compost
C/N	Carbon to Nitrogen Ratio
CAADP	Comprehensive Africa Agriculture Development Programme
CCD	Central Composite Design
CEC	Cation Exchange Capacity
CRF	Controlled-Release Fertilizer
DLS	Dynamic Light Scattering
EBBC	Encapsulated Biochar-Blended Compost
EC	Electrical Conductivity
EDX	Energy Dispersive X-ray Spectroscopy
FT-IR	Fourier Transform Infrared Spectroscopy
ICP-MS	Inductively Coupled Plasma Mass Spectrometry
NARO	National Agricultural Research Organization
NDP	National Development Plan
Nano-BBC	Nano-Biochar-Blended Compost
PTE	Potentially Toxic Elements
PVC	Polyvinyl Chloride
RSM	Response Surface Methodology
SBT	Soil Burial Test
SEM	Scanning Electron Microscopy
SR	Swelling Ratio
SSA	Sub-Saharan Africa
TDS	Total Dissolved Solids
WHC	Water Holding Capacity
XRD	X-ray Diffraction

LIST OF PUBLICATIONS

i. Nantambi, H. R., Lubwama, M., & Kigozi, J. (2025). Preparation and characterization of encapsulated biochar-blended compost pellets with biopolymer coating for controlled nutrient release and water retention. *Journal of Material Cycles and Waste Management 2025 27:5*, *27*(5), 3762–3778. https://doi.org/10.1007/S10163-025-02338-W

ii. Nantambi, H. R., Lubwama, M., & Kigozi, J. (2026). Optimised co-composting of chicken manure with biochar and Tithonia diversifolia for enhanced nutrient recovery and reduced phytotoxicity. *Environmental Technology, 1–14.* https://doi.org/10.1080/09593330.2026.2629044

iii. Nantambi, H. R., Lubwama, M., & Kigozi, J. Synthesis and optimization of biochar-compost nanocomposites developed from *Tithonia diversifolia*, chicken manure and rice husk biochar for enhanced seed germination. Discover materials (*Under review)*

ABSTRACT

Declining soil fertility, low nutrient-use efficiency, and heavy dependence on imported synthetic fertilizers remain critical constraints to agricultural productivity in Uganda. This research developed and evaluated advanced organic fertilizers derived from biochar-blended compost (BBC), specifically focusing on two engineered derivatives: Encapsulated Biochar-Blended Compost (EBBC) and Nano-Biochar-Blended Compost (Nano-BBC). An optimized co-composting matrix (60% *Tithonia diversifolia* and 5.7% rice husk biochar) was established using Response Surface Methodology and Central Composite Design. The quadratic models developed for nitrogen, phosphorus, and potassium were highly significant (*F*-values of 33.70, 50.64, and 86.60, respectively) and exhibited a non-significant lack of fit ($p < 0.05$). Model robustness was confirmed by high coefficients of determination ($R^2 \geq 0.97$) and adjusted $R^2 \geq 0.94$, and low coefficients of variation (3.24%–6.24%), indicating high reproducibility. *Tithonia diversifolia* most influenced N and K enrichment, while P availability depended on quadratic effects of both substrates. The enriched mature compost served as the base for enhancements. Nano-BBC synthesis was optimized via high-energy ball milling, and a reduced quadratic model identified the milling solvent mass and ball-to-powder ratio as key factors for particle size reduction. Chitosan–starch biopolymer encapsulation further enhanced performance. Under simulated 20-mm rainfall, EBBC reduced leachate volume to 6.5 mL (65% less than conventional BBC and mineral fertilizers) while eliminating nitrate-N leaching. Nitrogen-release assays showed controlled release: EBBC pellets released 56.9–70% of total N over 30 days via Fickian diffusion, unlike uncoated BBC, which exceeded 100% by day 25 via non-Fickian kinetics. EBBC also improved soil moisture retention in sandy loam to 4.4% at 30 days via hydrogel effects. In semi-field *Zea mays* L. (Maize) trials under drought, EBBC produced the highest plant height and shoot biomass, outperforming BBC, Nano-BBC, and synthetics. All formulations met FAO/EU heavy-metal thresholds. This scalable, climate-smart framework transforms organic waste into high-performance fertilizers, synchronizing nutrient delivery with drought resilience in Uganda.

Keywords: Biochar-blended compost, Encapsulation, Controlled-release fertilizer, Organic fertilizer, Germination Index, Drought, Maize, Uganda, Climate-smart agriculture

CHAPTER 1: INTRODUCTION

1.1 Background

Global agriculture faces the urgent challenge of feeding a rapidly growing population while boosting productivity and safeguarding the environment (Islam, 2025; Shrestha & Mahat, 2022). Despite this, conventional farming practices continue to degrade soils, deplete nutrients, and intensify water scarcity and greenhouse gas emissions, all of which threaten long-term food security (Islam, 2025; Shrestha & Mahat, 2022). As a result, sustainable agriculture, particularly practices that restore soil health, has become central to mitigating these interconnected crises (Sharma et al., 2024). In Uganda, as in many Sub-Saharan African (SSA) economies, these challenges are intensified by critically low soil fertility and limited fertilizer use, despite heavy reliance on imported inputs (Njoroge et al., 2023). Uganda imports over 95% of its fertilizers, spending an estimated USD 60–70 million annually, a cost burden that is projected to rise with increasing global prices and transport constraints (Veljanoska, 2016). Nonetheless, national fertilizer use remains extremely low: only 20% of households apply any fertilizer, and a mere 4% use inorganic types (Veljanoska, 2016). Adoption rates vary by region, for example, only 32% of maize farmers in Western Uganda use inorganic fertilizers (Midamba et al., 2025). Without fertilizer inputs, crop productivity remains severely constrained; soils across Uganda have experienced persistent nutrient mining, resulting in 1.2% annual topsoil nutrient depletion (Nkonya et al., 2008), and yield gains among fertilizer adopters remain modest, around 55.38 kg/acre (Midamba et al., 2025). These conditions reinforce persistent cycles of low productivity, poverty, and food insecurity (Minai et al., 2023), while knowledge on how cropping systems affect soil fertility dynamics in Uganda remains limited (Nataliya & Andrew, 2018).

A particularly urgent concern is the inefficiency of nitrogen (N) fertilizers. It is typically estimated that only 30–50% of applied N is utilized by crops (Halbert-Howard et al., 2021), with the remainder lost through processes such as volatilization, leaching, and denitrification (Ali et al., 2025; Govindasamy et al., 2023). Nitrate leaching is especially problematic in tropical agroecosystems, where high rainfall and irrigation can accelerate nutrient movement into groundwater (Jankowski et al., 2018). For example, prolonged excessive N application has resulted in the buildup of large quantities of nitrate-N in agricultural soils within temperate regions, making them susceptible to occasional leaching and subsequent groundwater nitrate

contamination (Bijay-Singh & Craswell, 2021a). Similar inefficiencies are observed with phosphorus. Phosphorus availability in soil is often limited by high adsorption and a tendency to precipitate with ions such as calcium, iron, and aluminum, leading to sequestration and reduced plant availability (Fan et al., 2025; Fathy et al., 2025). Excess phosphorus can be readily transported in surface runoff, leading to eutrophication and the deterioration of aquatic ecosystems (Akinnawo, 2023; Altamira-Algarra et al., 2022; A. Rahman et al., 2024). These patterns collectively show a fundamental limitation of conventional synthetic fertilizers. While they boost productivity, they are poorly aligned with ecological sustainability, creating a trade-off between short-term yields and long-term environmental health (Dobermann et al., 2021; Peñuelas et al., 2023).

In response, there has been increasing interest in organic fertilizers, such as composts and animal manures, as more sustainable nutrient sources. Organic amendments are recognized for their ability to improve soil structure, increase organic carbon storage, and restore microbial diversity, thereby contributing to long-term soil fertility and agroecosystem resilience (Mishra et al., 2025; Urra et al., 2019). By providing a broad spectrum of nutrients in organic forms, they also support circular nutrient cycling and reduce dependence on synthetic inputs (Badagliacca et al., 2024). Nevertheless, organic fertilizers are not without challenges. Their nutrient density is often low, their mineralization can be slow and inconsistent, and their quality highly variable depending on feedstock composition and processing (Panday et al., 2024). Moreover, they can contribute to gas emissions during composting and after application, particularly when poorly managed (Badagliacca et al., 2024). Long-term experiments, such as those at the Rothamsted Experimental Station, have shown that farmyard manure plots can have estimated nitrate-N leaching losses of 124 kg N ha^{-1} $year^{-1}$, compared to only 25 kg N ha^{-1} $year^{-1}$ from mineral fertilizer-treated plots (Bijay-Singh & Craswell, 2021a). These findings illustrate the dual nature of organic fertilizers: while they offer ecological benefits, they can also pose environmental risks if not carefully engineered and managed.

To overcome these limitations, recent advances have explored technological innovations in fertilizer design. Biochar, a carbon-rich product of biomass pyrolysis, has emerged as a promising compost amendment due to its high porosity, sorptive capacity, and ability to improve water-holding capacity (Anyebe et al., 2025). When co-composted with organic

matter, biochar enhances nutrient retention, stabilizes labile compounds, and supports beneficial microbial activity (Hagemann et al., 2017; Mikajlo et al., 2024; Sanchez-Monedero et al., 2018). Biochar can also influence soil P availability by inhibiting P-complexation with metal ions and facilitating its retention in exchangeable forms through adsorption or complexation with mineral-biochar complexes. Parallel advances in nanotechnology have led to the development of nanofertilizers, which exploit their high surface area and reactivity to improve nutrient uptake efficiency, reduce nutrient fixation, and allow lower application rate (Madzokere et al., 2021; Nongbet et al., 2022). Similarly, encapsulation technologies using biodegradable polymers have demonstrated the ability to regulate nutrient release, synchronize nutrient supply with plant demand, and reduce losses through leaching and volatilization (Fincheira et al., 2023; Khaliq et al., 2023). Biochar-blended compost occupies a strategic middle ground, shown to enhance nutrient retention, soil structure, and microbial activity more effectively than compost alone (Agegnehu et al., 2015; D'Hose et al., 2020; Vandecasteele et al., 2016). Nano-structuring and encapsulation can enhance biochar-blended compost, creating next-generation fertilizers for controlled nutrient delivery and restoration.

Despite this promise, critical knowledge gaps remain. Many studies on advanced fertilizers, including nanotechnology-based solutions, often lack real-field trials and are limited to laboratory or controlled greenhouse conditions, making it difficult to validate their effectiveness under realistic agricultural settings (Gigli et al., 2022; Maaz et al., 2025; Miguel-Rojas & Pérez-de-Luque, 2023). There has been little comprehensive work on the impact of organic amendments in combination with biochar on maize growth and yield (Agegnehu et al., 2016). Consequently, there is a distinct scarcity of systematic evaluations of biochar-blended compost, polymer-coated composites, and nanostructured amendments in drought-prone maize systems in tropical regions, where leaching and water stress severely compromise fertilizer efficiency. This study addresses these deficiencies by developing and evaluating biopolymer-encapsulated biochar-blended compost (EBBC) and nanocomposites (Nano-BBC), benchmarking them against conventional biochar-blended compost (BBC) and mineral fertilizers. The novelty of this study resides in the establishment of a precision feedstock formulation for encapsulated and nano-structured biochar-blended compost.

1.2 Problem statement

Soil fertility decline remains a major constraint to agricultural productivity in Uganda, where highly weathered soils severely limit crop yields. Although organic fertilizers are widely promoted as sustainable alternatives to synthetic inputs, their effectiveness in tropical agroecosystems is often compromised by uncontrolled mineralization, low nutrient concentration, weak nutrient-binding capacity, and high susceptibility to leaching losses. These limitations result in poor nutrient-use efficiency and inconsistent crop response, undermining the potential of organic amendments to support climate-resilient agriculture. Biochar-blended compost has emerged as a promising organic fertilizer due to its ability to enhance nutrient retention, improve soil structure, and stimulate microbial activity. However, the performance of such composites is strongly influenced by feedstock composition and composting conditions, which remain insufficiently optimized for maximizing nutrient enrichment and stabilization. Furthermore, conventional biochar-blended composts still suffer from uncontrolled nutrient release under fluctuating soil moisture and temperature regimes. Recent advances in fertilizer engineering, including biodegradable polymer encapsulation and nanoscale modification, offer new opportunities to overcome these constraints by regulating nutrient release, enhancing water retention, and improving soil–plant nutrient interactions. However, empirical evidence on the comparative performance of encapsulated and nanosized biochar-blended compost fertilizers relative to unmodified formulations remains limited under semi-field soil–water–plant conditions. Specifically, the effects of encapsulation and nanoscale refinement on nutrient-release kinetics, leaching behaviour, water-retention dynamics, and crop nutrient uptake are poorly quantified in tropical soil systems.

1.3 Objectives

1.3.1 Main Objective

The main objective of the study was to develop and evaluate encapsulated and nanosized biochar-blended organic fertilizers to improve water retention and nutrient release.

1.3.2 Specific Objective

i. To optimize a nutrient-rich biochar-blended compost from biochar, chicken manure, and *Tithonia diversifolia* with quantified nutrient enrichment and agronomic performance.

ii. To develop fertilizer formulations by creating EBBC with biodegradable polymer coatings and nano-BBC through high-energy ball milling.
iii. To determine the nutrient release kinetics, leaching behavior, and water-retention capacity of the developed EBBC and Nano-BBC in comparison with conventional biochar composites.
iv. To assess the agronomic performance of EBBC and Nano-BBC under laboratory and field conditions.

1.4 Research Questions

The questions that guided the study were:

i. How do varying proportions of biochar and *Tithonia diversifolia* influence nutrient retention and compost maturity in chicken-manure thermophilic composting systems?
ii. To what extent do encapsulation and nanoscale refinement enhance the controlled-release behaviour of biochar-blended compost relative to unmodified formulation?
iii. How do the nutrient-release dynamics and water-retention properties of encapsulated and nanosized amendments compare with those of the conventional biochar-blended compost?
iv. How do biopolymer-coated biochar composites and nanostructured amendments affect crop nutrient uptake and physiological performance when benchmarked against synthetic fertilizers and conversional formulation?

1.5 Scope

This research focuses on the engineering, characterization, and performance assessment of advanced biochar-blended compost fertilizers. The technical scope encompasses the optimization of co-composting protocols using chicken manure, *Tithonia diversifolia*, and rice husk biochar, alongside the synthesis of EBBC via chitosan–starch encapsulation and Nano-BBC through high-energy mechanochemical milling. Analytical evaluations examine nutrient enrichment, release kinetics, and hydrogel-mediated water-retention properties. Agronomic assessment is limited to laboratory and controlled-pot experiments using white radish (*Raphanus sativus* L.) and maize (*Zea mays L.*) as model crops to quantify nutrient-use efficiency under simulated drought. Consequently, the study is constrained to lab-scale

synthesis and semi-field trials; broad field-level validation and longitudinal environmental impact assessments remain outside the current scope of investigation.

1.6 Significance of Study

This study is significant in light of the persistent decline in soil fertility, low fertilizer-use efficiency, and increasing climate stresses that continue to limit agricultural productivity in Uganda and across Sub-Saharan Africa. As highlighted in the background, Uganda faces severe nutrient depletion, a heavy reliance on imported fertilizers, and limited access to affordable, sustainable soil amendments. Addressing these constraints directly aligns national, regional, and global development priorities. Scientifically, the research advances understanding engineered organic fertilizers by integrating composting and biochar technology with nanoscale modification and biodegradable polymer encapsulation. This combined approach offers crucial insights into nutrient-release kinetics, water-retention behaviour, mineral stabilization, and structural performance of next-generation BBC formulations. These areas remain insufficiently explored under tropical soil conditions. Agronomically, the study introduces practical innovations with demonstrated potential to improve nutrient-use efficiency, early crop establishment, drought resilience, and biomass accumulation.

The EBBC and Nano-BBC formulations provide controlled nutrient delivery, overcoming key limitations of conventional organic and synthetic fertilizers, whose nutrient release often poorly aligns with crop demand. These features make the technologies highly suitable for Uganda's predominantly rain-fed, smallholder farming systems. Sustainably, the work supports SDG 2 by improving soil fertility and productivity, SDG 12 through efficient nutrient recycling and biomass valorization, and SDG 13 by reducing environmental losses associated with fertilizer inefficiency. Nationally, it aligns with Uganda's NDP IV priorities on climate-smart agriculture and soil fertility restoration. Regionally, it contributes to CAADP goals and Agenda 2063 aspirations for environmentally responsible agro-industrial development. Overall, the study provides robust, policy-relevant evidence for scalable, climate-resilient organic fertilizer innovations.

1.7 Justification

The justification for this study arises from the pressing need to combat declining soil fertility and the prohibitive costs of synthetic fertilizers, which threaten food security in Uganda's smallholder farming systems. Tropical soils are highly susceptible to rapid nutrient mineralization and leaching; for example, nitrogen leaching in sub-Saharan soils frequently exceeds 30%, while Nitrogen utilization efficiency remains limited to 30–50% (Bijay-Singh & Craswell, 2021). To address these challenges, this research valorizes local biomass, chicken manure, rice husks, and *Tithonia diversifolia*, into nutrient-stabilized organic amendments (Agbede & Oyewumi, 2022; Ravindran et al., 2017). The study transitions composting from trial-and-error to a model-driven approach, employing Response Surface Methodology alongside struvite-mediated stabilization, which recovers over 80–90% phosphorus from waste streams, to identify optimal blending ratios for maximum nutrient retention (Qian et al., 2023). This overcomes inconsistencies in raw organic matter, yielding reproducible high-quality biochar-blended compost. Technologically, it develops engineered fertilizers via biopolymer encapsulation and nano-processing to boost nutrient use efficiency, which currently stands at 30–50% globally for conventional nitrogenous fertilizers by synchronizing release with plant demand and enhancing reactivity in rain-fed, high-leaching systems (Naghdi et al., 2017).

1.8 Conceptual Framework

The framework (**Figure 1.1**) centers on transitioning raw tropical feedstocks into precision-engineered fertilizers through three integrated pillars: structural functionalization, regulatory mechanisms, and agronomic stabilization. Structural functionalization utilizes biopolymer encapsulation and high-energy ball milling to modify the physical architecture of Biochar-Blended Compost (BBC), creating a robust matrix, characterized by optimized swelling ratios, particle sizes, and specific gravity, that resists rapid hydraulic leaching. This is reinforced by regulatory mechanisms, where encapsulation enables diffusion-limited release to prevent the nutrient losses typical of conventional fertilizers, while nanosizing increases functional-group density for enhanced ion adsorption and improved bioavailability. Finally, agronomic stabilization ensures rhizosphere resilience through increased water-holding capacity, using nutrient recovery efficiency as the critical metric for bridging laboratory-scale validation to performance in tropical semi-field conditions.

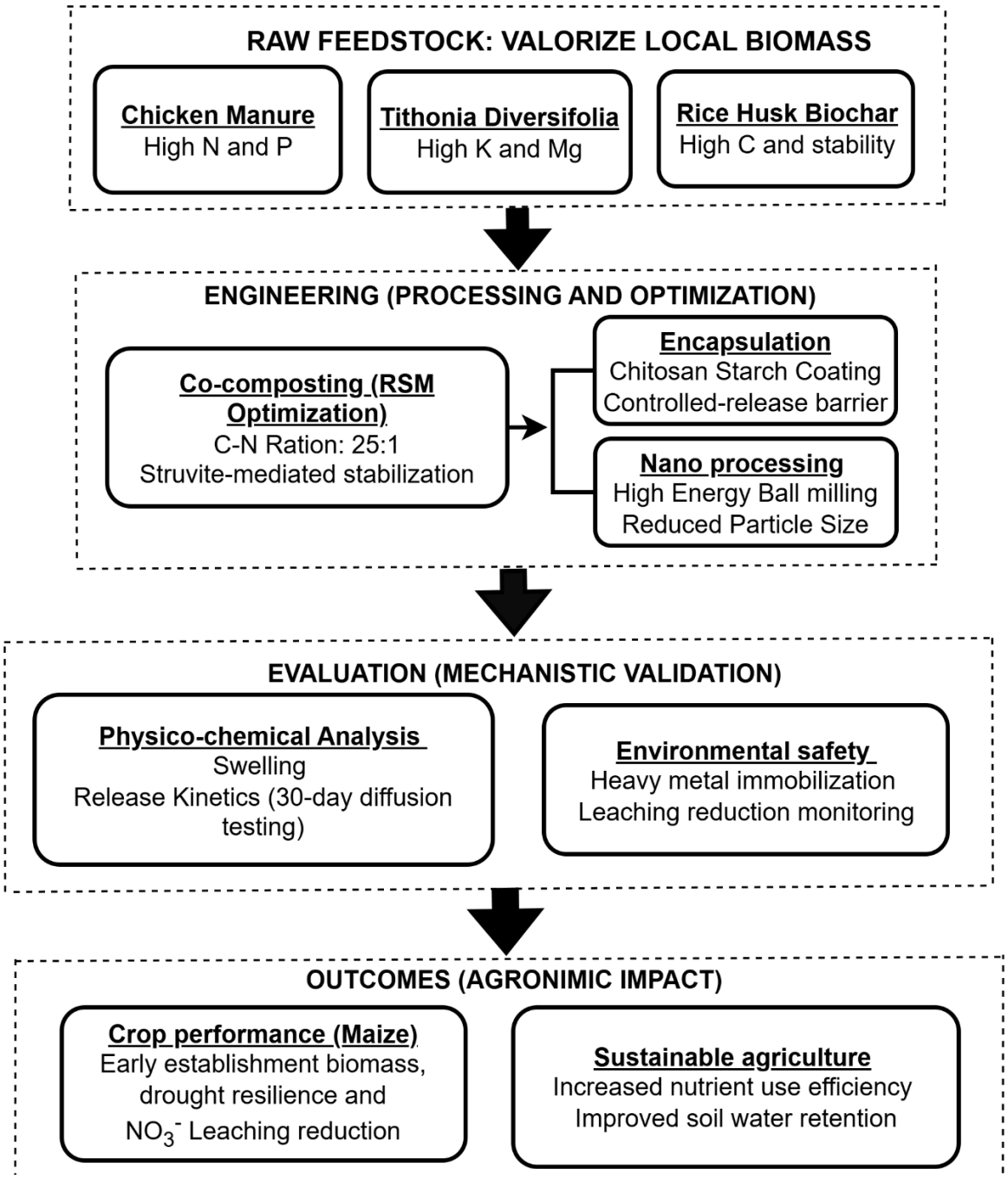

Figure 1.1: Conceptual framework of advanced fertilizer development integrating biochar-blended compost (BBC), nanosizing, and encapsulation technologies

CHAPTER 2: LITERATURE REVIEW

2.1 Overview

This chapter critically examines emerging fertilizer technologies aimed at improving nutrient-use efficiency and reducing environmental impacts. Emphasis is placed on biochar-blended composts, encapsulated and nanosized fertilizers, and strategies that optimize nutrient composition, release dynamics, and water retention. Key advancements reviewed include struvite crystallization for nutrient stabilization, polymer-encapsulated biochar composites and ball-milling-based amendments, and the use of germination assays and pot experiments to evaluate agronomic performance. Together, these approaches provide a framework for designing fertilizers that are both effective and sustainable under diverse soil and climatic conditions.

2.2 Biochar-Blended Compost (BBC) for Nutrient Enrichment.

Developing a nutrient-rich compost begins with understanding how biochar fundamentally transforms the composting process. When biochar is composted with chicken manure and *Tithonia diversifolia*, it creates a powerful nutrient enrichment platform that outperforms either material used alone (Antonangelo et al., 2021a; Casini et al., 2021). Chicken manure provides readily mineralizable nitrogen and phosphorus, while *Tithonia diversifolia* contributes potassium-rich, labile organic biomass that promotes microbial activity and balanced decomposition. The incorporation of biochar, characterized by a porous carbon matrix and highly reactive surfaces, enhances the retention of ammonium, phosphate, and potassium, thereby minimizing nutrient losses commonly associated with conventional composting processes (Khan et al., 2023). The co-composting process facilitates dynamic interactions between multiple feedstock materials, leading to improved nutrient mineralization, decreased gaseous emissions, and modifications to biochar's inherent physicochemical properties (Melo & Sánchez-Monedero, 2024). Within the compost pile, biochar improves cation exchange capacity, buffers pH, and enhances aeration conditions that accelerate mineralization and stabilize nutrients (Antonangelo et al., 2021). This synergistic effect has proven highly effective in improving soil degradation and reducing abiotic stresses, including drought, salinity, and heavy metal contamination (Hassan et al., 2023; Tran et al., 2023). These interactions promote the formation of organo-mineral complexes that lock nutrients onto biochar surfaces, increasing their long-term availability to crops. Co-composting also reduces

emissions of ammonia and nitrous oxide, further preserving nitrogen that would otherwise be lost to the atmosphere (Gao et al., 2023; Jia et al., 2016; hang et al., 2025),. The combined effect is a nutrient-dense, environmentally stable amendment with superior retention of N, P, and K and improved resistance to leaching (Godlewska et al., 2017; Joseph et al., 2018; Ramos et al., 2021).

2.2.1 Feedstock Ratios for High-Nutrient Biochar-Blended Compost

The production of a nutrient-rich biochar-blended compost is strongly dependent on the optimization of feedstock proportions, particularly rice husk biochar, chicken manure, and *Tithonia diversifolia*. While the theoretical role of these components in governing nutrient retention (N, P, and K), microbial activity, and compost stability is well recognized, optimal blending ratios remain highly context-specific and insufficiently resolved for tropical systems (Nepal et al., 2023). Appropriate feedstock combinations are expected to improve porosity, moisture balance, and aeration, thereby accelerating organic matter decomposition and enhancing nutrient sequestration. Moreover, specific ratios may facilitate the formation of organo-mineral complexes on biochar surfaces, improving hydrophilicity, water retention, and long-term nutrient adsorption, which collectively enhance nutrient-use efficiency following soil application (Agegnehu et al., 2016; Rani et al., 2026).

Previous studies indicate that moderate biochar additions, generally ranging from 10% to 30%, can enhance compost maturity and improve nutrient retention across diverse organic substrates. Biochar-to-compost ratios of approximately 30:70 have been shown to significantly increase plant nutrient uptake, while additions of 10–15% biochar to manure-based composts increase the availability of P, K, Ca, and Mg (Lebrun et al., 2023; Melo & Sánchez-Monedero, 2024). Even lower biochar proportions, around 4%, have been reported to stimulate nitrogen cycling in lignocellulosic composts (López-Cano et al., 2016). As shown in **Table 2.1**, across a wide range of feedstocks and applications, these composite blends consistently outperform individual components (Casini et al., 2021) showing the importance of precise feedstock ratio optimization for maximizing nutrient retention, compost quality, and agronomic effectiveness.

Despite these general findings, a significant knowledge gap remains in identifying optimal blending ratios for locally available tropical feedstocks, particularly rice husk biochar, chicken manure, and *Tithonia diversifolia*. Existing literature rarely provides systematic, comparative

evaluations of how varying proportions of these specific materials influence composting dynamics, nutrient enrichment, and agronomic performance in smallholder farming systems (Kavitha et al., 2018). This study addresses this gap by systematically optimizing and quantifying nutrient enrichment in biochar-blended compost derived from these locally available feedstocks, providing evidence-based guidance for the development of efficient, high-performance organic fertilizers for tropical agriculture.

Table 2.1: Comparative data summarizing typical NPK compositions for various optimized formulations

Material Type	N (%)	P (%)	K (%)	Key Findings	Reference
COMBI-mix (Biochar + Compost)	1.15	0.20	0.66	Nutrient content comparable to compost alone, with synergistic benefits to soil organic matter and water holding capacity.	(Bass et al., 2016)
Compost	1.19	0.22	0.63	Baseline for compost, showing slightly higher N than some COMBI-mixes but generally lower P and K.	
Biochar	0.24	0.03	0.38	Biochar alone consistently demonstrates the lowest NPK content.	
Sheep manure compost with biochar	2.43	0.38	3.28	Biochar addition improved N cycling, doubled mineral N content, and minimized N losses in mature composts, resulting in high NPK.	(López-Cano et al., 2016)
Biochar	0.84	0.19	0.72	Baseline for biochar, demonstrating lower NPK compared to the blended product.	
Pig Manure Compost	2.91	0.17	1.45	Accumulated amounts of NH_4-N, PO_4-P, and K were highest in pig manure compost, indicating effective nutrient retention.	(Shin & Park, 2018)
Biochar	0.20	0.01	2.02	Baseline for biochar, showing lower N and P, but potentially higher K.	

2.2.2 Using Response Surface Methodology to Optimize Biochar–Chicken Manure–Tithonia diversifolia Compost Formulations

Developing nutrient-rich compost from biochar, chicken manure, and *Tithonia diversifolia* requires more than simply mixing feedstock materials. It demands a systematic approach that identifies the precise blend that maximizes nutrient enrichment and compost stability. Response Surface Methodology (RSM) provides this level of precision, making it an indispensable tool. RSM enables researchers to move beyond trial-and-error by quantitatively modeling how key composting variables, biochar proportion, moisture content, C/N ratio, aeration, and temperature, interact to influence compost maturity and nutrient concentration (Khuri, 2017; País-Chanfrau et al., 2021). By mapping these interactions, RSM reveals the most efficient pathways to enhance nitrogen retention, phosphorus stabilization, and potassium availability, all of which are critical for producing an agronomically superior compost. Across diverse organic waste systems, RSM has proven highly effective for optimizing biofertilizer formulations (Asadu et al., 2019; Iqbal et al., 2014; Nurin et al., 2024). It enables the identification of optimal biochar-to-waste ratios to maximize NPK retention (Asadu et al., 2019) and the adjustment of composting parameters to enhance microbial activity and nutrient mineralization (Iqbal et al., 2014). Furthermore, it helps evaluate the influence of biochar pyrolysis conditions and feedstock characteristics on nutrient dynamics (Qian et al., 2023; Saeed et al., 2021; Zhou et al., 2019). Beyond improving nutrient profiles, RSM reduces experimental time and cost by minimizing the number of required trials while maximizing information gained (Ferrazza et al., 2018). Its ability to capture complex non-linear behaviour makes it invaluable for designing high-quality, nutrient-stable composts tailored for smallholder farming systems (Arefizadeh et al., 2024; Roy et al., 2024). By integrating RSM, the development of a nutrient-rich biochar–chicken manure–*Tithonia diversifolia* compost becomes not only more efficient but also more scientifically grounded, ensuring the final formulation is optimized for maximum agronomic performance and minimal environmental loss.

2.2.3 Struvite Nutrient Recovery and Stabilization during Co-Composting of Biochar, Chicken Manure, and Tithonia diversifolia

Developing a nutrient-rich compost requires not only optimizing feedstock ratios but also ensuring that valuable nutrients are stabilized rather than lost during decomposition. One of the

most promising mechanisms for achieving this is struvite formation, a natural mineralization process that converts soluble nitrogen and phosphorus into a slow-release crystalline fertilizer. Struvite (magnesium ammonium phosphate hexahydrate, $MgNH_4PO_4 \cdot 6H_2O$) precipitates under alkaline conditions when magnesium, ammonium, and phosphate ions interact, a reaction known to capture nutrients that would otherwise volatilize or leach (Liang et al., 2018; Su et al., 2022). In optimized systems, struvite can recover over 85–90% of phosphorus and up to 52% of nitrogen from waste streams, dramatically reducing nutrient losses while improving fertilizer value (Aguilar-Pozo et al., 2023; Corona et al., 2022).

The co-composting mixture employed in this study, comprising biochar, chicken manure, and *Tithonia diversifolia*, creates an ideal environment for struvite formation. Chicken manure supplies abundant ammonium and phosphate but typically suffers major ammonia volatilization. Biochar helps counter this by providing nucleation surfaces, buffering pH, and adsorbing ammonium, thereby stabilizing precursors needed for struvite crystallization (Pantoja et al., 2023; Wang et al., 2022; Yu, 2022). *Tithonia diversifolia* augments this process through its elevated magnesium content and alkaline ash, which raise local pH and ionic activity, thereby engendering microenvironments conducive to mineral precipitation (Omolola, 2019). Studies have shown that supplementation with magnesium salts, such as $MgSO_4$, further augments precipitation efficacy (Rabinovich et al., 2021). By intentionally fostering struvite formation within the composting system, this approach transforms nutrient-rich but unstable feedstocks into a high-value, slow-release fertilizer. The resulting compost is more nutrient-dense, environmentally stable, and better aligned with the needs of smallholder farming systems in tropical regions.

2.3 Developing Advanced Organic Fertilizer Formulations:

Building on the successful development of nutrient-rich biochar-blended compost in section 2.2, the next critical step is to transform this enriched material into advanced fertilizer formulations that deliver nutrients more efficiently and reliably under tropical soil conditions. While optimized biochar-blended compost provides a stable, nutrient-dense foundation, its agronomic effectiveness is still limited by the natural variability of organic mineralization and the risk of nutrient losses through leaching and volatilization challenges that are especially pronounced in the highly weathered, drought-prone soils typical of Uganda's smallholder

systems. Therefore, this section examines two complementary formulation strategies, biopolymer encapsulation and nanosizing, that transform biochar-blended compost into high-performance fertilizers capable of delivering nutrients more efficiently, reducing losses, and improving plant resilience.

2.3.1 Biopolymer Encapsulation

Biopolymer encapsulation has emerged as a promising strategy for transforming biochar-blended compost fertilizers into controlled-release systems capable of synchronizing nutrient supply with plant demand. These systems typically employ biodegradable polymers, such as chitosan, starch, alginate, or cellulose derivatives, to form semi-permeable coatings around fertilizer granules or pellets. By regulating nutrient diffusion, encapsulation aims to reduce nutrient losses through leaching, volatilization, and denitrification, which are major constraints to fertilizer efficiency in tropical agroecosystems (Benlamlih et al., 2021; Demirci et al., 2024; Govil et al., 2024; Negi et al., 2022; Qiao et al., 2025).

For organic fertilizers such as biochar-blended compost, encapsulation is particularly attractive because it offers a potential solution to inconsistent and moisture-dependent mineralization. Polymer coatings are expected to moderate nutrient release, enhance moisture retention in the root zone, and stabilize rhizosphere conditions, thereby supporting improved plant growth and stress tolerance. Empirical studies report enhanced root development, sustained microbial activity, and improved crop resilience to drought and nutrient stress in encapsulated fertilizer systems (Gong et al., 2023). However, these benefits are not universal. Their effectiveness depends strongly on polymer properties such as permeability, swelling behavior, and degradation rate, as well as on soil moisture regimes and temperature dynamics. In many cases, variable polymer degradation leads to unpredictable nutrient-release kinetics, complicating synchronization with crop uptake. Moreover, not all controlled-release fertilizers significantly improve soil water retention, limiting their utility in water-scarce environments (Kottegoda et al., 2023).

The integration of biochar into encapsulated systems is hypothesized to amplify fertilizer performance. Biochar's porous structure and surface functionality promote nutrient adsorption, enhance moisture retention, and improve soil physicochemical conditions that favor beneficial microbial activity (Chi et al., 2024; Schofield et al., 2019). When biochar-blended compost is

enclosed within a biopolymer shell, a composite slow-release matrix is formed, potentially extending nutrient availability and substantially reducing nitrate leaching (Rafique et al., 2024). Recent advances in semi-interpenetrating polymer networks further suggest opportunities to improve coating biodegradability, water-holding capacity, and release control. Nevertheless, the complexity of encapsulating heterogeneous organic matrices; including biochar, composted biomass, and microbial residues, means that the influence of processing parameters on nutrient dynamics and microbial functioning remains insufficiently explored (Rubel et al., 2024).

Despite strong conceptual foundations, critical knowledge gaps persist regarding the application of biopolymer encapsulation to biochar-blended composts under tropical conditions. Comparative data on the medium-term performance, stability, and biodegradation behaviour of specific biopolymer coatings under high temperatures, intense rainfall, and frequent wet–dry cycles are limited. Optimal biopolymer formulations, coating thicknesses, and biochar loadings for locally available tropical feedstocks, such as rice husk biochar, chicken manure, and *Tithonia diversifolia*, are not well established, constraining precise nutrient delivery. Furthermore, nutrient-release kinetics of encapsulated biochar-blended composts derived from local materials remain poorly quantified, and the lack of standardized assessment protocols limits cross-study comparison (Negi et al., 2022). Collectively, these gaps hinder the rational design and field-level optimization of encapsulated biochar-blended compost fertilizers for tropical smallholder farming systems. Addressing these limitations is essential to developing robust, water-retentive, and nutrient-efficient organic fertilizers capable of enhancing crop productivity and resilience in nutrient-depleted and climate-stressed tropical soils.

2.3.2 Nanosizing

High-energy ball milling has emerged as an innovative and complementary strategy for transforming biochar-blended compost into a nanosized fertilizer, offering capabilities that far exceed conventional organic amendments. At the core of this approach is intense mechanical fracturing, which reduces bulk biochar and compost–mineral aggregates to submicron dimensions (<1000 nm). This nanoscale transformation dramatically increases surface area, porosity, oxygenated functional groups, and negative zeta potential, properties that collectively enhance nutrient retention and soil conditioning (Kumar et al., 2024; Verma et al., 2023). As a result, nanosized composites exhibit improved cation-exchange capacity and stronger

adsorption affinities for NH_4^+, PO_4^{3-}, and K^+, while also improving water-holding ability (Dong et al., 2025; Liu et al., 2022). These enhanced physicochemical traits support more efficient nutrient delivery and significantly reduce leaching losses, a significant limitation of conventional fertilizers and composts (Shafiq et al., 2023). Beyond its technical advantages, ball milling is increasingly viewed as a practical and scalable solution. The method's low operational cost and environmentally responsible design make it suitable for fertilizer innovation in resource-limited agricultural systems (Awasthi et al., 2020; Dubadi et al., 2023; Peterson et al., 2012; Yu et al., 2025). Operating at the nanoscale further strengthens the agronomic value of Nano-BBC, enabling nutrient carriers to overcome diffusion barriers, interact more closely with root surfaces, and sustain nutrient uptake even under challenging environmental conditions (Madzokere et al., 2021; Mim et al., 2025; Nongbet et al., 2022). Moreover, the mechanochemical forces produced during milling not only reduce particle size but also expose new reactive surfaces and promote the formation of biochar–iron oxide composites. These composites enhance nutrient immobilization, contaminant sorption, and catalytic activity, broadening the functional scope of Nano-BBC (Dong et al., 2025; Liu et al., 2022). When applied within biochar-blended compost systems, nanosizing amplifies beneficial interactions between biochar particles, decomposing organic matter, and compost minerals. This combination improves organo-mineral complex formation and sustains microbial activity both during composting and in the soil after application. Consistently, nanosized formulations outperform their bulk counterparts by improving soil structure, stimulating microbial colonization, and boosting nutrient use efficiency under both optimal and stress-prone conditions (Shafiq et al., 2023). Collectively, these advances position Nano-BBC developed through high-energy ball milling as a next-generation fertilizer innovation, one capable of delivering highly reactive, nutrient-stabilizing, and water-retentive organic inputs that align with the goals of sustainable intensification in tropical agriculture.

2.4 Nutrient Release Kinetics, Water Retention, and Leaching Behaviour in EBBC and Nano-BBC

Having established the engineering principles behind Encapsulated Biochar-Blended Compost and Nano-Biochar-Blended Compost, the subsequent critical step involves a comprehensive evaluation of their performance within water-soil systems. This assessment focuses on their nutrient-release dynamics, water-retention capacity, and leaching patterns. These parameters

are crucial for determining whether the engineered properties translate into tangible agronomic and environmental benefits, especially when validated against conventional Biochar-Blended Compost. Such an evaluation is essential for demonstrating their suitability as climate-smart agricultural inputs in tropical, water-limited smallholder farming systems.

2.4.1 Approaches for Characterizing Nutrient Release Kinetics

Investigating nutrient-release kinetics provides crucial insight into how fertilizers deliver nutrients over time, differentiating between rapid-release amendments and controlled-release formulations. A variety of laboratory and field methods are employed, each with distinct advantages and limitations for understanding complex soil-fertilizer interactions. Laboratory methods often aim to replicate soil moisture, temperature, and microbial conditions. Batch equilibrium experiments are useful for measuring initial burst release and equilibrium concentrations, while column-leaching assays simulate rainfall-driven percolation and quantify nutrient losses (Ransom et al., 2020). Dissolution tests specifically assess the solubilization rate of coated granules in aqueous environments. In contrast, soil incubation studies are vital for capturing long-term nutrient transformations within the complex biological and mineral soil environment (Piash et al., 2021). For instance, one study determined nitrogen release in tropical conditions by analysing fertilizer nitrogen content at various intervals over 220 days using dry combustion (Borges et al., 2020). Another approach involves placing fertilizer in nylon bags buried in paddy soil or in bottles with water for laboratory analysis (Nayak et al., 2024). While these methods generate comprehensive release profiles, a significant knowledge gap lies in standardizing these approaches, particularly for heterogeneous organic formulations like EBBC and Nano-BBC and ensuring their direct relevance to the dynamic conditions of diverse tropical soils. Traditional laboratory methods often simplify complex field interactions, potentially overestimating or underestimating actual release rates (Ransom et al., 2020).

2.4.2 Determinants of Nutrient Release Behaviour

Nutrient-release kinetics are a dynamic interplay between fertilizer properties and environmental conditions. For encapsulated EBBC, coating characteristics are paramount: porosity, thickness, and polymer composition directly regulate the diffusion of water and solutes into and out of the fertilizer. Thicker or more hydrophobic films generally slow nutrient release, influencing the nutrient use efficiency (Khuntia et al., 2022). However, the choice of

polymer coating has shifted significantly towards biodegradable options to prevent environmental accumulation associated with non-degradable thermoplastics (Fertahi et al., 2020; Negi et al., 2022). The challenge lies in optimizing these biodegradable polymers, as their degradation rates and long-term stability vary considerably, impacting release predictability (Kalita & Vaid, 2025). For Nano-BBC, particle size plays a key role. Nanoscale particles exhibit a significantly greater surface area and higher reactivity compared to their bulk counterparts. This can accelerate early nutrient desorption and potentially improve plant uptake efficiency over time (Chaubey et al., 2024; Sheokand et al., 2023). However, this rapid initial release can sometimes be a double-edged sword, as a sudden influx of nutrients might still lead to some initial losses if not properly managed (Chaubey et al., 2024). Environmental conditions further complicate these dynamics. Soil temperature, pH, and microbial activity directly influence coating degradation, nutrient solubility, and overall mineralization rates, creating highly dynamic release environments that vary across seasons and soil types. Therefore, understanding these complex interactions is crucial, but detailed comparative studies across different tropical soil types are still needed to predict performance accurately.

In encapsulated fertilizers, nutrient movement is commonly described by Fickian diffusion, where concentration gradients across the polymer barrier govern the flux. Fick's laws have been widely applied to model nutrient transport, incorporating parameters such as granule radius, coating thickness, diffusion coefficients, and soil water content. These models are instrumental for predicting release kinetics and designing coatings that match nutrient supply with plant uptake demands. However, a critical analysis reveals that while Fickian diffusion often provides a foundational understanding, it may not fully capture the complexities of nutrient release from organic, biochar-containing encapsulated systems. The heterogeneous nature of biochar-blended compost, the potential for physiochemical interactions between biochar, organic matter, and nutrients, and the variable degradation of biodegradable polymer coatings introduce additional complexities. For instance, some studies indicate that potassium release from certain biochar-based fertilizers might follow a non-Fickian diffusional module (Hamed et al., 2024). Furthermore, the presence of biochar can alter the rate of nutrient release without necessarily changing the fundamental release mechanism (Sim et al., 2021). This suggests that more models, potentially incorporating relaxation-controlled mechanisms or a combination of diffusion and degradation, might be necessary for accurate prediction,

especially in diverse tropical soil environments where biological activity and moisture fluctuations are pronounced. A significant knowledge gap exists in developing and validating such advanced models specifically for EBBC and Nano-BBC in tropical contexts.

2.4.3 Water-Retention Capacity

Water retention is a crucial indicator of fertilizer performance, especially in drought-prone agricultural systems characteristic of many tropical regions. Water retention curves, quantify how soil–fertilizer mixtures store water across varying suction pressures. Water-holding capacity (WHC) measurements further illustrate the maximum amount of water retained. Biochar consistently improves both water retention and WHC, with some soils experiencing a doubling of WHC following biochar addition (Endriani & Listyarini, 2023) . This enhancement stems from biochar's porous architecture, which provides substantial micropore and mesopore storage for water (El-Moaty et al., 2024; Guarnieri et al., 2021). The impact is often more pronounced in coarse-textured soils, where biochar can fill large pore spaces, thereby increasing moisture retention and decreasing water flow rate (El-Moaty et al., 2024). Biochar has been shown to have a greater effect on increasing water storage capacity than compost (Duarte et al., 2022). The combination of biochar and compost further enhances available water in sandy clay loam soils (Endriani & Listyarini, 2023). Nano-BBC is expected to exhibit the highest water-retention capacity due to its significantly increased surface area and enhanced porosity (El-Moaty et al., 2024). Small biochar particle sizes (e.g., 21.86 nm) can fit easily into large pores of sandy soils, greatly increasing mesoporosity and water retention even at lower application rates (El-Moaty et al., 2024). This intensified effect arises from increased capillary action and accessible surface area, thereby enhancing water retention even in coarse-textured soils. Encapsulated EBBC may also improve soil moisture by moderating nutrient dissolution and influencing soil–polymer interactions. A significant knowledge gap lies in precisely quantifying the *plant-available* water supplied by each formulation in tropical soils, as some water retained in micropores might not be accessible to plants (Duarte et al., 2022). Comparative studies are needed to determine which formulation offers the most significant advantage in specific water-limited environments, considering both total water retention and WHC.

2.5 Bridging Laboratory Findings with Field Performance

Translating promising laboratory findings into reliable real-world agricultural outcomes remains a critical challenge, particularly for innovative soil amendments like Encapsulated Biochar-Blended Compost and Nano-Biochar-Blended Compost. This section critically analyses the methodologies employed to bridge this gap, highlighting inherent limitations, justifying the selection of specific experimental approaches, and emphasizing implications for smallholder farmers in tropical systems. The successful deployment of biochar-blended compost amendments in agricultural systems mandates rigorous verification of their maturity and the absence of phytotoxic compounds. Phytotoxicity testing serves as an essential safety check, ensuring that the amendments promote, rather than inhibit, plant growth

2.5.1 Germination bioassay

The white radish germination bioassay is widely recognized as a rapid and reliable tool for detecting toxic residues in organic materials, including biochar-enriched composts (Milon et al., 2021). The Germination Index, which integrates relative seed germination and root elongation, provides a robust indicator of compost phytotoxicity and stabilization (Milon et al., 2021). Values above 80% indicate mature compost, while values below 50% suggest high phytotoxicity (Kong et al., 2023; Yuan, et al., 2022; Yang et al., 2021). GI values exceeding 100% often reflect phyto-stimulatory effects (Thu & Loan, 2024) . This initial screening is non-negotiable; amendments failing this test risk detrimental effects on crop establishment. While the GI provides a critical initial screen, a knowledge gap persists in establishing comprehensive GI benchmarks for the diverse, often recalcitrant, feedstocks used in tropical biochar-blended composts under varying processing conditions (Kong et al., 2023). Applying bioassay to EBBC and Nano-BBC formulations derived from local tropical feedstocks is necessary to determine ecological safety and maturity before field application

2.5.2 Pot Experiments Under Field Conditions: A Semi-Field Approach

After excluding phytotoxicity, crop-based evaluations become essential for assessing nutrient release, uptake, and overall growth performance. Controlled pot experiments conducted under field conditions serve as a crucial intermediate step, effectively bridging the gap between laboratory validation and the inherent variability of full-scale agricultural trials (Ransom et al., 2020; Verburg et al., 2022). These "semi-field" setups simulate natural environmental

conditions, including ambient temperature, rainfall, and solar radiation, while retaining critical experimental control through defined soil volumes and precise treatment applications. This approach allows for a more accurate assessment of plant response, soil health, and the ecological safety of advanced fertilizer formulations under real-world climatic factors, a key advantage over constant laboratory conditions where temperature fluctuations significantly impact nutrient release and overall efficacy (Kottegoda et al., 2023; Ransom et al., 2020). The advisability of a specific product depends on soil properties and climatic zones, necessitating local investigations (Wesołowska et al., 2021). Maize is frequently employed in nutrient management research due to its high nutrient demand, rapid biomass accumulation, and sensitivity to changes in soil fertility (Kakar et al., 2021; Mahmoud et al., 2023). These traits make maize an ideal model for evaluating nutrient-use efficiency, water dynamics, and yield response to controlled-release and nanosized formulations (Sary & Abd El-Aziz, 2025). Such pot experiments are particularly informative when conducted using nutrient-depleted or chemically constrained soils, common in tropical regions. For instance, Ferrosols, widespread in Sub-Saharan Africa, are characterized by extremely low native chemical fertility, resulting from very low nutrient reserves, low pH (usually < 5), high phosphorus retention by oxide minerals (iron and aluminium oxides), and low cation exchange capacity (Bruand et al., 2023). These conditions amplify the effects of nutrient-release dynamics, providing an ideal testbed for evaluating whether EBBC and Nano-BBC can enhance nutrient availability, overcome fixation, and improve plant growth. Given the prevalence of drought in tropical agriculture, integrating controlled water-stress treatments into these pot experiments is essential. This allows for rigorous assessment of water-use efficiency, root development, and physiological resilience under sub-optimal moisture conditions. Combining field-simulated pot conditions with water-deficit regimes provides a robust framework for evaluating advanced fertilizer formulations under both optimal and stress-prone environments, directly addressing their potential for improving nutrient retention and soil water availability. This study uses real tropical soils and climate, coupled with a highly responsive crop like maize, will strengthen the predictive power of the findings, bridging the gap more effectively than purely laboratory-based studies.

2.5.3 Experimental Treatments

Comparative studies of advanced fertilizers typically employ multiple treatment levels, including conventional biochar-blended compost, encapsulated composites, and nanosized formulations. Essential controls such as unamended soil, synthetic fertilizers, and compost-only treatments are crucial for benchmarking performance against current practices and for isolating the specific benefits of the innovative formulations (Piash et al., 2024). For instance, nano-biochar has been investigated as a coating material for smart di-ammonium phosphate fertilizer, with different concentrations (2.5%, 5%, and 10% w/w) to control P and N release and enhance maize productivity (Shah et al., 2024). Application techniques, such as broadcasting and localized banding, are adapted for pot conditions to optimize nutrient availability and minimize leaching. Experimental designs often follow randomized complete block, enabling statistical rigor and the detection of interactions among fertilizer type, dosage, and water regime. This robust design is critical given that the benefits of enhanced-efficiency fertilizers are often inconsistent in the field due to complex interactions between crop, management, and seasonal climate (Verburg et al., 2022). A key knowledge gap relates to the optimization of application methods and doses for EBBC and Nano-BBC within smallholder farming contexts, where resources and precise application tools may be limited. There is a need to comparatively evaluate practical application techniques adaptable to smallholder systems, providing data on optimal dosages that maximize nutrient efficiency and minimize costs, directly informing farmer adoption.

2.5.4 Assessing and Evaluating Agronomic Performance

The assessment of fertilizer efficiency under pot-based semi-field conditions is inherently multidimensional, integrating indicators of plant performance, nutrient dynamics, Crop growth metrics, including germination rate, plant height, leaf development, biomass accumulation, and root architecture, which provide early and sensitive signals of fertilizer response (Raza et al., 2023). Yield-related parameters and nutrient use efficiency, assessed through tissue nutrient concentrations and apparent nutrient recovery, quantify the effectiveness of nutrient delivery and plant (Novak et al., 2023; Rosa et al., 2024). Collectively, these evaluations offer a holistic understanding of the agronomic and ecological performance of EBBC and Nano-BBC under semi-field-simulated conditions, highlighting their capacity to enhance nutrient retention,

improve water availability, and support climate-resilient resource-efficient agricultural systems through stabilized nutrient matrices, including struvite crystallization.

2.6 Summary of literature review

This research addresses the challenges of developing advanced biochar-based fertilizers for smallholder farmers in tropical systems. While biochar-blended compost, encapsulated biochar-blended compost, and Nano-biochar-blended compost show potential to enhance nutrient use efficiency, a disconnect persists between laboratory findings and real-world tropical applications. This study aims to bridge this gap by optimizing feedstock combinations, developing innovative formulations, and characterizing their agronomic efficacy. Maximizing nutrient retention requires optimizing feedstock ratios to enhance porosity and water-holding capacity. Despite the known benefits of biochar-compost mixtures, precise ratios for local tropical feedstocks, such as rice husk biochar, chicken manure, and *Tithonia diversifolia*, remain undefined. This study systematically optimizes these mixing ratios to produce nutrient-rich BBC and evaluates its performance under laboratory and semi-field conditions.

The study introduces two innovative formulations: EBBC and Nano-BBC. Using biopolymers like chitosan and starch, EBBC encapsulation regulates nutrient diffusion and stabilizes mineralization. Integrating biochar further reduces nutrient loss while improving microbial viability. Concurrently, Nano-BBC is produced via high-energy ball milling, transforming the materials into submicron particles (<1000 nm) to significantly increase surface area, cation-exchange capacity, and water retention. Key research gaps addressed include the long-term stability of biopolymer coatings, optimization of milling parameters for heterogeneous feedstocks, and the ecological impact of nanoscale materials on the tropical soil microbiome.
Engineered fertilizers are designed to synchronize nutrient release with plant demand. However, standardized methods to characterize these kinetics under variable tropical moisture and temperature are lacking. This study develops tailored methodologies to quantify plant-available water and nitrogen leaching, compared with conventional composite methods. Finally, agronomic evaluation begins with the white radish bioassay to ensure ecological safety. Following safety confirmation, controlled pot experiments using *Zea mays* L. in nutrient-depleted Ferrosols bridge the gap between laboratory and field trials, establishing evidence-based application guidelines for tropical smallholder agriculture.

CHAPTER 3: METHODOLOGY

3.1 Introduction

This methodological framework provides a clear, reproducible pathway for producing nutrient-rich biochar-blended compost, enabling the enhancement of nutrient use efficiency through local resources. The co-composting process is designed to foster nutrient enrichment, microbial activity, and structural stability, creating a foundational matrix for advanced formulations. To maintain scientific rigor, the methodology is structured into interconnected stages that directly address each specific objective. Including feedstock characterization and co-composting optimization, encapsulation of the compost matrix, nano-processing for particle size reduction, evaluation of nutrient release kinetics, and validation of agronomic performance. This integrated design supports both fundamental understanding and application in small-holder farming systems.

3.2 Develop and optimize a nutrient-rich biochar-blended compost

The synthesis of the nutrient-rich biochar-blended compost (BBC) was predicated on the strategic selection and preparation of organic feedstocks with complementary physicochemical profiles. To ensure scalability and practical relevance for smallholder systems, the study prioritized locally sourced, low-cost, and sustainable materials. Comprehensive feedstock analysis was conducted to determine optimal blending ratios, precise moisture balancing, and carbon-to-nitrogen (C/N) adjustments, thereby establishing the necessary conditions for efficient thermophilic decomposition and maximum nutrient retention. Furthermore, the study integrated rigorous biosafety and environmental safeguards. Thermophilic composting temperatures (55–65 °C) were maintained to effectively sanitize chicken manure against pathogens, while biochar inclusion sequestered and immobilized heavy metals. These combined measures ensured that the final organic fertilizer posed no risk of pathogen transmission or soil contamination and aligned with international standards for sustainable soil management.

3.2.1 Feedstock Preparation

Fresh, bedding-free chicken manure (**Figure 3.1**) was sourced from the poultry facility at Makerere University Agricultural Research Institute, approximately 19 km north of Kampala. Before transportation for immediate use, on-site manual sorting removed feathers and ensured

feedstock uniformity. Chicken manure was used within 24 hours. Fresh *Tithonia diversifolia* biomass, represented in **Figure 3.1c**, was carefully harvested from the National Agricultural Research Organization in Kawanda, Uganda. To ensure optimal freshness and prevent degradation, the biomass was immediately transported to the designated composting site on the very day of its collection. Upon arrival, the large plant material was prepared for composting by manual chopping. A linear knife was used to cut the biomass into smaller fragments, each approximately 3–5 cm long. This precise size reduction was crucial for two primary reasons: to promote uniform decomposition throughout the compost pile, ensuring all material breaks down at a similar rate, and to facilitate better aeration within the pile, which is vital for aerobic composting processes. Following this preparation, the chopped *Tithonia diversifolia* biomass was then stored under control conditions at 15 °C for 24 hours. This interim storage period was implemented before the biomass was transferred to the composting reactor to standardize initial feedstock conditions.

The biochar used in this investigation was produced from Kaiso (K85) rice husks (**Figure 3.1**b) obtained from a commercial mill and subsequently sun-dried to a moisture content of 15%. A portion of the rice husks was milled using a hammer mill, while the remainder was reserved for thermochemical conversion. Carbonization was conducted in a modified 200-liter steel drum kiln (**Figure 3.1e**), measuring 1.0 m in height and 0.5 m in diameter. The kiln featured 70 evenly distributed perforations (2 cm in diameter) designed to regulate airflow. To establish and maintain the oxygen-limited conditions necessary for high-quality biochar production, these perforations were sealed using a specialized soil-cement lute. This mixture was prepared using a 3:1 ratio of Ferralsol soil to Portland Cement, with water added incrementally until a stiff, dough-like consistency was achieved. The cement provided the structural integrity needed to prevent the plugs from crumbling under thermal expansion. Each batch consisted of 700 g of rice husk feedstock, a proportion optimized based on prior studies to minimize ash content. The process was initiated by igniting a fire beneath the kiln for 25–30 minutes. Once ignition was stabilized, the soil-cement mixture was applied to the perforations to restrict oxygen intake. A chimney was utilized to facilitate smoke venting during the active phase. Following carbonization, the resulting biochar (**Figure 3.1d**) was cooled for 1 hour to prevent post-process oxidation. The air-dried biochar was then transferred to and stored in air-tight containers to preserve its functional properties.

3.2.2 Determination of Initial Feedstock C/N Ratio

The initial carbon-to-nitrogen (C/N) ratio was optimized by blending fresh chicken manure with milled rice husks before incorporating *Tithonia diversifolia* and rice husk biochar. After laboratory determination of baseline carbon, nitrogen, and moisture contents, an experimental design was established using substrate mass. This configuration enabled a theoretical C/N range of 7.5:1 to 38:1 and a moisture content of 13.2% to 55.2%. To achieve a target ratio of 25:1, Minitab Statistical Software was used for predictive modeling using a regression equation, which identified an optimal mixture of 334 kg of manure and 166 kg of rice husks. Laboratory validation confirmed an actual C/N ratio of 25.7:1, verifying the model's accuracy. This optimized manure-husk pre-mix provided a stable foundation for the treatment piles and served as the control experiment, with quantities determined via mass balance. While biochar and *Tithonia diversifolia* dosages were varied independently according to the Response Surface Methodology design to evaluate interactive effects, the pre-mix was dynamically adjusted to maintain a constant total mass in each reactor. This approach ensured that variations in nutrient stabilization were attributable to feedstock ratios rather than to differences in total pile volume.

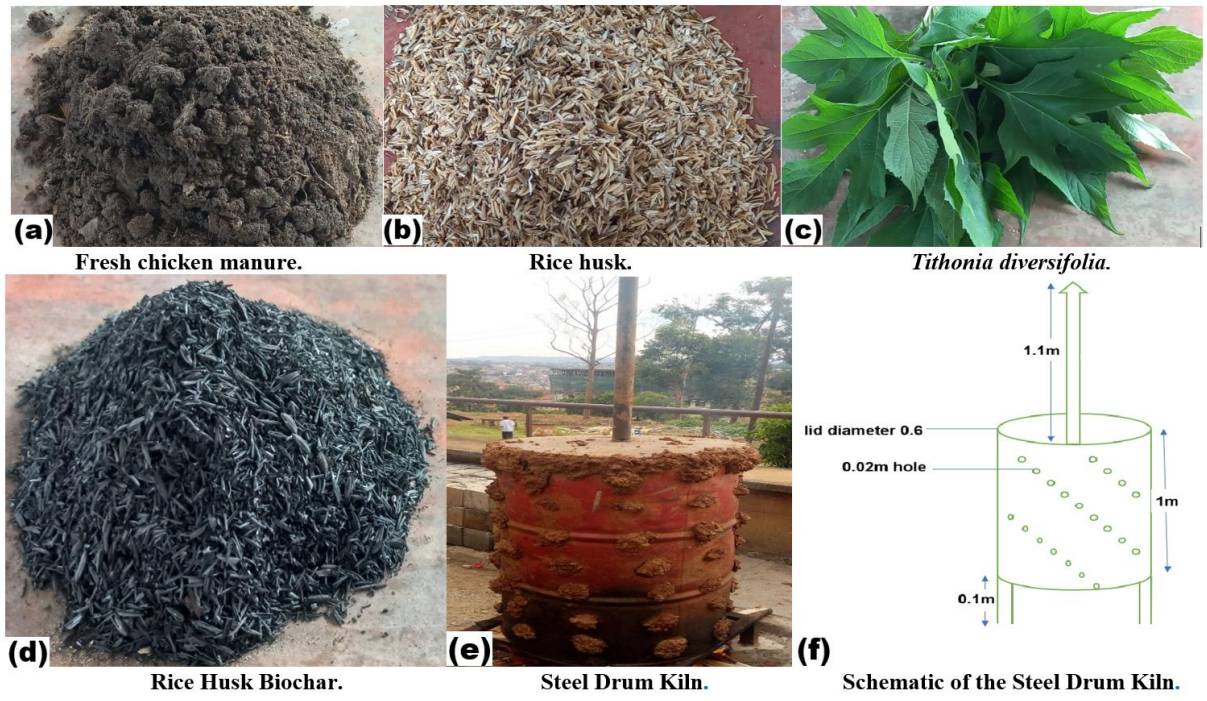

Figure 3.1: Feedstock materials

3.2.3 Feedstock Characterization

Proximate analysis was employed to partition the feedstocks into their fundamental constituents: moisture, volatile matter, fixed carbon, and ash. Moisture content was determined by drying samples at 105 °C for 24 hours, while the organic matter fraction, representing gases released during thermal decomposition, was quantified via loss on ignition at 440 ± 1 °C (Chaher et al., 2020). For air-dried biochar, ash content was determined by heating samples to 800 ± 1 °C. The Fixed Carbon (FC) content was subsequently derived by subtracting the organic matter from the initial sample weight as described by Yang et al. (2021). The specific gravimetric calculations for Moisture Content (MC) and Ash Content were performed using Equation 1 and Equation 2, respectively:

$$\%\ Moisture\ content = \frac{M_x - M_y}{M_x} \times 100 \qquad \text{Equation 1}$$

$$\%\ Ash\ content = \frac{M_{ash}}{M_x} \times 100 \qquad \text{Equation 2}$$

where M_x is the initial sample mass in grams, M_y is the mass in grams of the sample after oven drying at 105 °C, and M_{ash} is the sample mass in grams after combustion at 730 °C for 8 hours. The percentage volatile matter (% VM) was determined using Equation (3).

$$\%\ Volatile\ Matter\ (VM) = \frac{M_x - M_{FC}}{M_x} \qquad \text{Equation 3}$$

Where M_{FC} is the mass in grams of fixed carbon and ash in the sample at 730 °C. Total organic carbon was calculated as VM/1.8. To measure compost pH, EC, and TDS, fresh samples were mixed with deionized water (1:10, w/v) and shaken at 300 rpm for 1 h. The pH, EC and TDS values were determined using a multiparameter pH-meter (In-lab®731-15M/1-xpert pro-ISM, Metter Toledo, Precision/sensitivity 0.001/USA).

For sample mineralization, 200 mg of each material underwent acid digestion using a mixture of 7 mL nitric acid (HNO_3) and 2 mL hydrogen peroxide (H_2O_2). Following digestion, the solutions were filtered and diluted to a final volume of 100 Ml. The concentrations of trace and heavy metals, including aluminum, iron, zinc, lead, cadmium, chromium, magnesium, copper, and calcium, were determined via Atomic Absorption Spectroscopy (Ravindran et al., 2017).

Total phosphorus levels were quantified using Inductively Coupled Plasma Mass Spectrometry. For alkali metals such as sodium and potassium, flame photometry was employed (Gondek et al., 2020).

Surface functional groups were characterized using a Jasco FT/IR-6600 Fourier Transform Infrared spectrometer (Lin et al., 2022). Spectra were acquired across the 400–4000 range at a resolution of 4, with 30 scans per sample. The Cation Exchange Capacity was determined by the summation of exchangeable cations quantified via AAS, following the standardized approach for nano-biochar and compost materials described in earlier green synthesis methodologies (Naghdi et al., 2017). This parameter serves as a critical indicator of the nanocomposite's potential for nutrient retention and long-term exchange in agricultural applications. Certified reference materials from the Directorate of Government Analytical Laboratory in Kampala, Uganda, were utilized as benchmarks. The surface morphology and elemental distribution of the vacuum-dried, gold-sputtered samples were examined using Scanning Electron Microscopy (SEM) coupled with Energy-Dispersive X-ray Spectroscopy at an accelerating voltage of 10 kV (Mujtaba et al., 2021). This approach facilitates visualization of the internal pore architecture and quantitative confirmation of surface-level elemental composition.

3.2.4 Ancillary Materials

Materials such as planting seeds, corn starch, and chitosan were carefully selected to ensure accurate evaluation of compost functionality, environmental safety, and agronomic relevance across subsequent experimental phases. These materials enabled controlled testing of nutrient stabilization, biological compatibility, and soil–plant interactions arising from the optimized compost formulations. A sandy loam soil was selected for field and pot trials due to its inherently low organic matter content, limited water-holding capacity, and high susceptibility to nutrient leaching (Libutti et al., 2021). These characteristics provided a stringent test environment for assessing the capacity of the biochar-enriched compost to improve nutrient retention and water-use efficiency, thereby directly reflecting the performance of the co-composted material. The same soil was homogenized and used as a burial medium in biodegradation assays to evaluate the environmental compatibility of encapsulating materials under realistic soil conditions. Biological test systems were incorporated to assess compost

maturity, safety, and agronomic performance. White radish seeds were used for germination and phytotoxicity assays owing to their sensitivity to residual toxicity and rapid response to compost quality (Gezahegn et al., 2020; Parra-Orobio et al., 2021). These assays provided an early biological validation of the co-composting process and confirmed that nutrient enrichment did not compromise plant safety.

For agronomic evaluation, a widely cultivated hybrid maize (H520) was selected to assess nutrient availability, biomass accumulation, and growth response under conditions representative of smallholder tropical agriculture. Together, these plant systems enabled a comprehensive evaluation of the functional outcomes of the nutrient-rich compost. Biodegradable polymers were also selected to facilitate subsequent modification of the optimized compost through encapsulation, building directly on the stabilized nutrient matrix developed during co-composting. Corn starch, composed of 70% amylose and 30% amylopectin, was selected for its low cost, food-grade safety, and hydrogel-forming ability. At the same time, chitosan contributed antimicrobial properties and enhanced mechanical strength to the composite coating (Hu et al., 2024; Mendes et al., 2016). Their combined use was guided by demonstrated biodegradability, low toxicity, and capacity to regulate nutrient-release kinetics in sustainable fertilizer formulations (Eddarai et al., 2024; Kusumastuti et al., 2019; Sofyane et al., 2024). All additional chemicals and solvents, including analytical-grade ethanol, hexane, methanol, hydrogen peroxide, hydrochloric acid, and distilled water, were procured at high purity and used without further purification. These reagents supported feedstock preparation, nutrient analysis, and physicochemical characterization, ensuring methodological precision and adherence to international laboratory standards throughout the study.

3.2.5 Thermophilic Composting

Biochar-blended compost was prepared in self-constructed aerated static polyethylene bins, each measuring 1.0 × 0.8 × 1.0 m. To systematically assess strategies for nutrient stabilization and compost quality improvement, varying ratios of fresh *Tithonia diversifolia* biomass and rice husk biochar were incorporated into different treatment groups. A control treatment, devoid of both *Tithonia diversifolia* and biochar, served as a baseline for comparison. Moisture content was maintained at 60–65% to optimize microbial metabolism and activity in the composting matrix (Melo et al., 2020; Pezzolla et al., 2021). Thin layers of chopped *Tithonia*

diversifolia stems were added to enhance structural porosity. Compost piles were manually turned every 10 days to promote uniform decomposition and adequate oxygen distribution (Bryndum et al., 2017; Ma et al., 2024). Internal temperatures were monitored daily using long-rod thermometers and digital probes to evaluate microbial activity and composting progress. Concurrently, oxygen and carbon dioxide concentrations were measured daily with a portable biogas analyzer (BSK-602). Representative samples were collected on days 0, 15, 30, 45, and 60 and subdivided. Following the composting period, samples were subdivided for comprehensive physicochemical, biological, and maturity analyses. into physicochemical, biological, and maturity analyses. All measurements were conducted in triplicate, with final samples analyzed immediately or stored at −20 °C prior to testing

3.2.6 Process Optimization using Response Surface Methodology

To quantitatively optimize the co-composting process, response surface methodology was applied to assess the interactive influences of feedstock composition on nutrient enrichment and compost maturity (Asadu et al., 2019; Nurin et al., 2024). RSM, integrated with Central Composite Design, represents a robust statistical approach for devising, refining, and optimizing processes influenced by several variables (Md Saleh et al., 2020). A Central Composite Design (CCD) was utilized to formulate a predictive quadratic model that characterizes the system's response within the experimental space. CCD was selected for its ability to examine the interactive effects of feedstock composition on nutrient enrichment and compost maturity, enabling the evaluation of linear, quadratic, and interaction effects among independent variables with fewer experimental runs (Md Saleh et al., 2020). The independent variables, biochar proportion and *Tithonia diversifolia* proportion, were selected based on prior research on co-composting (Matheri et al., 2025). The lower and upper limits for these variables were determined from existing literature and preliminary experiments to ensure practicality and relevance for process optimization. These variables were tested at five coded levels to fully capture linear, quadratic, and interaction effects, as detailed in the treatment combinations of **Table 3.1.** The runs consisted of four factorial points, four axial points, and five replicates at the center points as determined from Equation 4. The center points were employed to determine the experimental error and repeatability

$$N = 2^k + 2k + n_c = 2^2 + 2(2) + 5 = 13 \qquad \text{Equation 4}$$

where N is the total number of experiments required, k is the number of process variables, and n_c is the number of replicates for 2-factor.

The optimized response variables included the nitrogen, phosphorus, and potassium contents in the final compost (Asadu et al., 2019). To model the relationships between independent variables and these responses, second-order polynomial equations were employed, following the approach of Menya et al. (2020). The experimental design, model development, and optimization were conducted using Stat-Ease Design-Expert® 360 software. Experimental data were fitted to second-order polynomial models, and term significance was evaluated using analysis of variance at the 95% confidence level. Model adequacy was confirmed through values, lack-of-fit tests, and residual analysis (Nurin et al., 2024). Three-dimensional response surface and contour plots were generated to visualize the effects of biochar, chicken manure, and *Tithonia diversifolia* proportions on nutrient retention and compost maturity. Optimization was achieved using a desirability function, with values approaching 1 indicating optimal N, P, and K retention (El-Damarawy et al., 2025).

Table 3.1: The coded and actual values of the two independent variables

Factor	-∂	Low (-1)	Average (0)	High (+1)	+∂
A: Biochar (%)	-2.07	0.0	5.0	10.0	12.07
B: *Tithonia diversifolia* (%)	-0.35	10.0	35.0	60.0	70.35

3.2.7 Characterization of Biochar-Blended Compost

The final compost was comprehensively characterized to confirm its maturity, stability, and agricultural suitability. Weekly analyses followed standardized protocols for organic fertilizers to monitor organic matter transformation and microbial activity. Temperatures were tracked daily with a Reotemp compost thermometer until ambient stabilization, as temperature indicates decomposition rates and process progression. For chemical analysis, fresh samples were processed for pH, electrical conductivity, and total dissolved solids using a Metter Toledo multiparameter meter after preparing a 1:10 (w/v) water extract. Moisture content was determined via oven-drying at 105 °C to a constant weight. Subsequently, loss-on-ignition at 550 °C was performed to quantify total organic matter, a widely accepted method for estimating organic matter content in compost and soil. Total Nitrogen was determined through Kjeldahl

digestion and analyzed using a VELP Scientifica UDK-159 automated analyzer. Total organic carbon and humification indices were assessed to calculate the C/N ratio, a primary indicator of compost stability and maturity. For nutrient and elemental profiling, dried and ground samples underwent microwave-assisted acid digestion; heavy metals were quantified by atomic absorption spectroscopy, and phosphorus by inductively coupled plasma mass spectrometry. Fourier transform infrared spectroscopy identified crystalline phases such as struvite—potentially promoted by high Mg and N in *Tithonia diversifolia*, to evaluate nutrient immobilization.

To achieve the second specific objective, two complementary modification pathways were adopted: encapsulation for external diffusion control of nutrient release and water interaction, and nano-sizing for internal enhancement of surface reactivity, nutrient accessibility, and soil–material interactions. Although each technique targets different regulatory mechanisms, both were designed to improve nutrient-use efficiency and functional stability in the BBC.

3.3 Develop fertilizer formulations by creating EBBC with biodegradable polymer coatings and Nano-BBC through high-energy ball milling

Post-processing strategies were used to enhance the functional performance of optimized biochar-blended compost (BBC). The BBC was milled using a Mixer Mill MM 500 Nano to achieve a mean particle size of approximately 2000 µm, ensuring material homogeneity and enhanced pellet cohesion. The milled compost was then pelletized using a laboratory-scale twin-screw extruder to produce uniform cylindrical pellets. Standardizing pellet dimensions minimized variability in coating thickness and ensured consistent encapsulation performance and reproducible nutrient-release behavior during subsequent evaluations.

3.3.1 Formulation of Biodegradable Chitosan–Starch Coating Films

A biodegradable chitosan–starch matrix was developed as the encapsulating medium due to its renewability, biodegradability, and proven suitability for controlled-release fertilizer systems functionality (Fertahi et al., 2020). A 2% (w/v) chitosan solution was prepared by dissolving 10 g of chitosan in 500 mL of 1% acetic acid under continuous stirring until complete solubilization (Kusumastuti et al., 2019; Wang, Lou, et al., 2016). In parallel, 8 g of food-grade corn starch was gelatinized in distilled water at 70 °C to form a homogeneous viscous paste

functionality (Fertahi et al., 2020). After cooling, the gelatinized starch was incorporated into the chitosan solution at controlled volumetric ratios to generate four coating formulations (**Table 3.2**). The mixture was heated in a water bath at 60–70 °C to promote hydrogen bonding and polyelectrolyte complexation between the protonated amine groups of chitosan and the hydroxyl groups of starch, thereby enhancing film cohesion and permeability control (Wan Yusof et al., 2024). The synergistic blending of chitosan and starch produced semi-permeable films with barrier properties suitable for regulating nutrient diffusion (Chiaregato & Faez, 2021; Magaletti et al., 2023).

Table 3.2: Formulation of Film-Forming Biopolymer Solutions for Coating Biochar-blended Compost Pellets

EBBC pellet	Corn starch (ml)*	Chitosan solution (ml)*	Coating film composite
B	0	100	CH
D	50	50	CH/S-50
E	67	33	CH/S-33
F	33	67	CH/S-67

*Refers to the respective amounts of prepared film-forming solutions used in the coating process.

3.3.2 Formulation of Encapsulated biochar-blended compost

Encapsulation of biochar-blended compost into controlled-release fertilizer pellets was achieved by immersing individual BBC pellets in a preheated chitosan–starch biopolymer solution at 70 °C for 2 minutes, forming a uniform coating. Upon withdrawal, the pellets were placed on a mesh screen for 60 seconds to drain excess solution under gravity, thereby removing surplus biopolymer and developing a consistent, homogeneous film around each pellet, resulting in encapsulated BBC pellets. The EBBC pellets were then oven-dried at 30 °C for 12 hours to solidify the biopolymer coating, a crucial step for maintaining their mechanical and chemical properties during handling and storage (Sarlaki et al., 2021). Following drying, the pellets were conditioned in a desiccator at 25 °C and 50% relative humidity for 72 hours to achieve uniform moisture content. Finally, to ensure batch uniformity and the integrity of the controlled-release mechanism, all pellets were inspected under ultraviolet light; those exhibiting discontinuous, fractured, or brittle coatings were systematically discarded.

3.3.3 Characterization of Encapsulated biochar-blended compost.

Characterization focused on the microstructural integrity, chemical functionality, and biodegradability of the EBBC coating films, as these properties directly govern nutrient-release kinetics, moisture interactions, and long-term stability. Surface morphology and porosity were assessed via SEM. Samples were mounted on aluminum stubs using conductive carbon tape and sputter-coated with a 5 nm chromium layer for 90 seconds in a Quorum 150T ES sputter coater. Images were acquired using a Sigma 300 VP SEM operated at 10–15 kV (Gao et al., 2021; Krystyjan et al., 2021)., revealing pore distribution, coating continuity, surface roughness, and EBBC bead microstructure. These factors influence nutrient diffusion, water ingress, and retention. Supplementary image analysis and sieving ensured a uniform bead-size distribution, resulting in consistent nutrient release and field application. Chemical interactions between the BBC core and the chitosan–starch coating were evaluated using FT-IR spectroscopy (Jasco FT/IR-6600) over the range 4000–500 cm^{-1}, with 200 scans and a spectral resolution of 2 cm^{-1}. The spectra were analyzed to identify functional groups and intermolecular interactions associated with coating formation. Characterization focused on understanding the microstructure, chemical functionality, and biodegradability of the biopolymer films, since these properties directly influence nutrient-release dynamics, moisture interactions, and coating stability.

Lastly, the biodegradation potential of the developed films was assessed using a modified Soil Burial Test (SBT) adapted from the protocol outlined by Othman et al. (2023). Circular film samples with a uniform diameter of 20 mm were prepared and weighed to an accuracy of 0.01 g before burial to determine the initial dry weight, which ranged from 1.00 to 1.06 g. The burial medium consisted of loam soil, homogenized and placed in plastic containers to ensure consistent conditions across replicates. Each film was buried at a depth of 4.5 cm within the soil matrix. The containers were maintained under controlled laboratory conditions, with soil moisture regulated at approximately 60% of field capacity throughout the test duration (Seligra et al., 2016; Zain et al., 2017). Film samples were exhumed and analyzed at 5, 10, 15, and 20 days to evaluate the extent of degradation over time. Post-excavation samples were gently washed, dried to constant weight, and reweighed to determine the residual mass, facilitating quantification of weight loss and visual analysis as a function of exposure time.

3.3.4 Nanosizing

The development of Nano-BBC represents an advanced approach to enhancing the reactivity and nutrient availability of biochar-blended compost. Nano-BBC synthesis was achieved via high-energy mechanochemical processing using a Nano planetary ball mill operated at a speed of 575 RPM (Mixer Mill MM 500 Nano, Retsch GmbH, Germany). Zirconia grinding bowls (80 mL) and 5 mm ZrO_2 balls were selected to ensure optimal impact force while preserving surface functional groups (Dudnik et al., 2025; Kucio et al., 2020; Lopez-Tenllado et al., 2021). Each milling batch consisted of 1.6 g of pre-ground biochar-blended compost to maintain uniform energy input. Wet milling was adopted to suppress agglomeration, reduce temperature rise, and prevent the loss of oxygen-containing functional groups (Peterson et al., 2012; Yan et al., 2019; ang et al., 2021). Solvents with differing polarities, like, hexane, ethanol, and deionized water were employed to modulate particle dispersion and energy dissipation during milling (Xu et al., 2021). After milling, the resulting Nano-BBC slurry was air-dried and preserved in airtight containers inside a vacuum desiccator to maintain structural and chemical stability.

3.3.5 Optimization of Milling Parameters using Response Surface methodology

To optimize particle size reduction of biochar-blended compost while maintaining its structural integrity and functional properties, Response Surface Methodology based on a Central Composite Design was employed following the approach of Naghdi et al. (2017). Three independent variables were systematically evaluated: milling time, solvent volume, and ball-to-powder ratio. Other parameters, such as rotational speed, milling jar material, and grinding ball diameter, were held constant. These operational conditions were selected based on prior studies demonstrating that controlled rotational speed and optimized ball dimensions effectively minimize excessive surface energy accumulation, thereby preventing cold welding, particle agglomeration, and adhesion within the milling chamber (Kumar et al., 2020).

For solvent-free milling, a pulsed-milling strategy was adopted to control temperature rise and mitigate thermal degradation. Milling was conducted in 1-hour active cycles followed by 15-minute cooling intervals, as described by Lopez-Tenllado et al. (2021). The reported milling times represent net processing durations, excluding rest intervals, to enable accurate comparisons across treatments. The central composite design included 17 experimental runs,

with three replicated center points to estimate experimental error and enhance model reliability. The coded and actual levels for the three independent variables (milling time, solvent volume, and ball-to-powder ratio) are summarized in **Table 3.3**.

RSM was used to develop empirical regression models relating these independent factors to the response variable, volume mean particle size. This design enabled a systematic evaluation of how process parameters influence nanoscale structural refinement, including particle morphology, pore development, and surface functional group density, key factors for adsorption efficiency, nutrient retention, and overall agronomic performance. ANOVA was performed using Design-Expert® V13.0 to assess parameter significance and identify (Kumar et al., 2020b; Pohshna et al., 2023).

Table 3.3. The Coded and Actual Levels For the Three Independent Variables

Factor	Name (Units)	-$\dot{\alpha}$	Low (-1)	Average (0)	High (+1)	+$\dot{\alpha}$
A	Milling Time (h)	0.64	2.0	4.0	6.0	7.36
B	Solvent Volume (mL)	0	0.8	5.2	9.6	12.60
C	Ball-to-powder ratio	7.95	25	50	75	92.05

3.3.6 Characterization of Nano biochar-blended compost

A thorough characterization was conducted to investigate the effects of nanoscale refinement on the structural and chemical properties of nano-biochar-blended compost. Sample preparation entailed dispersing 1 mg of Nano-BBC in 200 mL of distilled water supplemented with 1% ethanol to improve wettability and prevent aggregation. Dispersion was performed using a sequential two-stage protocol: initial magnetic stirring for 60 min, followed by ultrasonication in an ice bath for a further 60 min to prevent heat-mediated structural modifications (Naghdi et al., 2017). Water-holding capacity was determined gravimetrically: oven-dried samples were saturated with deionized water in Büchner funnels, and excess water was allowed to drain under gravity. Retained water was quantified per gram of dry Nano-BBC, excluding contributions from filter paper. This metric indicates moisture retention capacity of Nano-BBC, a critical attribute for use as a soil amendment.

Morphological and surface features were characterized using scanning electron microscopy coupled with energy-dispersive X-ray spectroscopy. For SEM analysis, an oven-dried 1 mg

aliquot of Nano-BBC was dispersed in 200 ml of 1% ethanol and applied to clean aluminium foil stubs suitable for SEM vacuum. The samples were then oven-dried at 40 ± 1 °C to prevent imaging artifacts from residual moisture while protecting the organic matrix from thermal damage. A 15 nm gold coating was sputtered onto the samples to mitigate charging effects typical of insulating organics, with thickness optimized for conductivity and morphological fidelity. Imaging was performed using a Zeiss Sigma SEM equipped with a Bruker EDS detector at a working distance of 8–10 mm and an accelerating voltage of 5–10 kV, adjusted for sample topography and resolution. X-ray diffraction revealed alterations in crystalline architecture, including partial breakdown of crystalline regions and increased amorphous content, indicating elevated surface energy and improved nutrient solubility. Fourier Transform Infrared spectroscopy identified key surface functional groups (e.g., hydroxyl, carboxyl, and amine) on the Nano-BBC matrix. These groups enable cation exchange, robust nutrient binding, and gradual nutrient release. Specific gravity was determined per ASTM D854 using a pycnometer, with density calculated from mass differences before and after filling with distilled water. Potassium, phosphorus, and heavy metal analyses were conducted per the method described in Section 3.2.3.

3.4 Determine the nutrient release kinetics, leaching behaviour, and water-retention capacity of the developed EBBC and Nano-BBC

A combination of batch dissolution and column leaching experiments was conducted under controlled laboratory conditions to quantify the nutrient release kinetics, leaching behaviour, and water-retention performance of conventional biochar-blended compost, EBBC, and Nano-BBC.

3.4.1 Nutrient release kinetic

Batch dissolution tests were first employed to determine cumulative nitrogen release over 28 days in both deionized water and soil slurry systems, enabling direct comparison of release behavior among formulations. Controlled nitrogen release was evaluated by immersing EBBC pellets in distilled water at room temperature and sampling at intervals up to 30 days. Samples were wrapped in filter paper and placed in sealed beakers. At specific intervals (1, 5, 10, 15, 20, and 30 days), aliquots were taken for nitrogen analysis using the Kjeldahl method, which involved digestion at 370 °C for 2 hours, followed by titration and distillation with a Vapodest

500 distillation unit (VELP Scientifica UDK-159, Italy). All experiments were conducted in triplicate. The cumulative release percentage was calculated using the equation (5).

$$\text{Nutrient release (\%)} = \left(\frac{\text{MV}}{\text{MC}}\right) * 100 \qquad \text{Equation 5}$$

where MV (mg/l) is the released amount and MC (mg/l) is the total nutrient concentration of EBBC. The release data were analyzed using established kinetic models, such as the Korsmeyer–Peppas and Fickian diffusion models. These models effectively describe and predict the complex nutrient-release behaviour of each formulation (Ganetri et al., 2020; Hamed et al., 2024; Lee et al., 2022; Vadhel et al., 2023; Wang et al., 2021). Grounded in Fick's laws of diffusion, dominant release mechanisms, quantified key parameters, including diffusion coefficients, release rate constants, and release exponents, were determined and provided quantitative insights into product sustained-release capabilities. Moreover, the models provided a mechanistic framework that incorporated factors such as coating thickness, polymer composition, biodegradability, hydrophobicity, and nanoscale size reduction. The framework evaluates impact on nutrient transport dynamics in fertilizers, enabling the development of release profiles tailored to crop nutrient demands that maximize nutrient use efficiency while minimizing environmental losses (Lawrencia et al., 2021; Rubel et al., 2024; Sim et al., 2021).

3.4.2 Column Leaching Test

To complement batch tests and assess nitrogen mobility under simulated field conditions, column leaching experiments were performed using a Ferralsol soil collected from the National Agricultural Research Organization (NARO). This soil was selected for its acidity, strong phosphorus fixation, and low organic matter content, typical of highly weathered tropical soils (Hamed et al., 2024; Vadhel et al., 2023). Air-dried soil (<2 mm) was packed into PVC columns (15 cm height, 3 cm internal diameter) at a bulk density of approximately 1.5 g cm^{-3} and a gravimetric moisture content of 0.43 g g^{-1}, with each column containing 0.159 kg of soil. After pre-saturation and equilibration to remove residual mineral nitrogen, fertilizer treatments (BBC, EBBC, and Nano-BBC) were incorporated into the upper 1–2 cm of soil to simulate field banding practices (Rychel et al., 2023). At the same time, unamended columns served as controls. Nitrogen was applied at a rate of 76.5 mg N per column, and simulated rainfall events

(20 mm per event) were delivered using filtered water (pH 5.55) at a controlled rate of 0.17 ml min^{-1} to ensure uniform infiltration. Columns were subjected to alternating wet–dry cycles at 27–30 °C, repeated twice to generate a cumulative rainfall depth of approximately 40 mm, corresponding to 29% of the mean dry season rainfall in Uganda. Leachates were collected after each drainage event and analyzed for pH, electrical conductivity, total dissolved solids, salinity, and nitrate nitrogen (NO_3^--N) using a HACH-DR6000 UV–Vis spectrophotometer following benzene-sulfonic acid derivatization, with nitrogen losses expressed as mg/L (Rychel et al., 2023). Together, the combined batch and column approaches enabled robust comparison of nutrient release kinetics, leaching resistance, and water-mediated nutrient transport across BBC, EBBC, and Nano-BBC formulations under conditions representative of tropical agroecosystems.

3.4.3 Water retention

Water absorbency was measured by placing 1 g of dried EBBC in distilled water. Samples were taken every 30 minutes. Excess water was removed using Whatman No.1 filter paper, followed by weighing the samples (Rashidzadeh et al., 2015). The swelling ratio (%SR) of the EBBC was calculated according to the equation below:

$$\%SR = \frac{W - W_O}{W_O} X\ 100 \qquad \text{Equation 6}$$

Where, W and Wo denote the weight of the swollen EBBC and the weight of the dry EBBC, respectively, and SR is the water absorbency per gram of dried EBBC. To evaluate EBBC's capacity to improve soil moisture retention, 1 g of encapsulated pellets was mixed with 200 g of dry sandy soil and placed in a 100 mL conical flask. The sandy soil used in this study was representative of the Kampala metropolitan area, located in the central region of Uganda and characterized by a tropical rainforest climate. The bottom of the flask was sealed with nylon fabric to prevent soil loss during the experiment. The soil mixture was then slowly drenched with distilled water from the top of the flask until water seeped out from the bottom. The flask's weight was recorded (W1) before the addition of water. The flask was weighed again after ensuring no more water seeped from the bottom (W3). The flask weight during the soaking process was recorded as W2. A control experiment was conducted without EBBC addition for

comparison. The soil's water retention capacity (WR%) was calculated using the following equation.

$$\%WR = \frac{W3-W2}{W1} \quad \text{Equation 7}$$

3.5 Agronomic Validation

Agronomic performance of the developed EBBC and Nano-BBC was first evaluated under controlled laboratory conditions using a standardized seed germination bioassay, followed by pot-based trials designed to simulate field conditions.

3.5.1 Germination index

Compost phytotoxicity was evaluated through white radish germination bioassay. White radish was selected due to its rapid germination, high sensitivity to phytotoxic compounds, and established use as a bioindicator in compost maturity studies. Sampling followed representative procedures: 500 g of compost was collected from three depths in each treatment pile, homogenized, and subsampled. Extracts were prepared by suspending 10 g of fresh compost in 100 mL of distilled water, shaking at 180 rpm for 3 h, and centrifuging at 4,000 rpm for 20 min. The supernatant served as the test solution. Sterile Petri dishes lined with filter paper (Whatman No. 1) were moistened with 10 mL of extract, and ten white radish seeds were placed in each dish (distilled water as a control). Treatments were conducted in triplicate and incubated in darkness at 25 ± 1 °C for 72 h. Relative seed germination, root elongation, and germination Index were calculated in equation (10) by multiplying the relative seed germination (RSG) (equation 8) and relative radicle length (RRL) (equation 2) and expressed as a percentage (Siles-Castellano et al., 2020). Statistical differences among treatments were evaluated using one-way ANOVA, and only formulations demonstrating biological safety were advanced to pot-based agronomic trials, with phytotoxicity classified as strong (GI ≤ 50%), moderate (50–70%), or absent (GI > 80%) (Kong et al., 2022; Wang et al., 2022).

$$RSG = \frac{number\ of\ germinated\ seeds\ in\ compost}{number\ of\ germinated\ seeds\ in\ control} \quad \text{Equation 8}$$

$$RRL = \frac{Total\ radicle\ length\ of\ germinated\ seeds\ in\ sample}{Total\ radicle\ legth\ of\ germinated\ seeds\ in\ control} \quad \text{Equation 9}$$

$$GI = \frac{RSG\ x\ RRL}{100} \quad \text{Equation 10}$$

3.5.2 Semi-field experiments

Following laboratory validation, pot experiments were conducted in triplicate using a completely randomized design to assess crop growth response and nutrient use efficiency under semi-field conditions. The trials used ferrosol soil with low organic matter content and moderate nutrient deficiency, representative of smallholder farming systems in tropical regions (Bruun et al., 2023; Huang et al., 2021; Novak et al., 2023). Treatments included unamended control, standard biochar-blended compost, encapsulated BBC, Nano-BBC, and synthetic NPK (18-18-18) fertilizer reference. Each serially numbered pot, placed on a brickwork top, received compost-based treatments at nitrogen-equivalent rates of 0.00006 kg N per kg soil. Five maize seeds were sown at a uniform depth of 2 cm and irrigated to maintain ~70% field capacity when rainfall was inadequate, while exposed to ambient climatic conditions. Seedlings were thinned to two plants per pot seven days after emergence. Agronomic parameters were monitored throughout growth, including seed emergence and germination (3–7 days after sowing) and weekly plant height. At harvest, above- and below-ground biomass and root morphological traits (length and mass) were measured. Soil and plant nutrient analysis, including heavy metal uptake, were conducted before planting and after harvest; plant tissues were oven-dried, ground, digested and analysed using methods described in section 3.2.3.

3.6 Data Analysis

One-way analysis of variance was conducted on the experimental data using Minitab and Design-Expert software to identify significant differences among treatments, with subsequent mean separation tests. Fertilizer effectiveness was assessed via nutrient recovery efficiency, calculated using the difference method that compares nutrient uptake in amended treatments relative to the unamended control and the total nutrient applied.

CHAPTER 4: RESULTS AND DISCUSSION

4.1 Overview

This chapter presents the results from feedstock selection, characterization, and co-composting processes used to develop biochar-blended composts, including their encapsulated and nanosized formulations. It emphasizes how the physicochemical, structural, and chemical properties of *Tithonia diversifolia*, chicken manure, and rice husk biochar influenced composting dynamics, nutrient stabilization, and material maturation. The results first demonstrate the suitability and functional complementarity of the feedstocks, followed by an evaluation of composting process indicators that collectively define the compost's quality and stability. This is then followed by encapsulation and ball milling to enhance controlled release and bioavailability. Finally, the results demonstrate the agronomic functionality of the developed BBC formulations.

4.2 Feedstock Characterization

The physicochemical composition of the selected feedstocks strongly influenced their functional roles during co-composting (**Table 4.1**). *Tithonia diversifolia* exhibited elevated total organic carbon (41.16%), nitrogen (5.46%), and potassium (5.32%), alongside a low C/N ratio (7.54). These results confirm its status as a high-quality biomass capable of accelerating compost stabilization (Matheri et al., 2025). Consistent with its reputation as a concentrated nutrient reservoir, the chicken manure had high phosphorus (5.86%) and ash (59.49%) content. This phosphorus level was significantly high, potentially reflecting the use of high-mineral feed additives in local poultry systems. The moderate C/N ratio (13.30) and alkaline pH (7.79) are well within the ranges documented by Malomo et al. (2018). Heavy metal concentrations (Zn: 186 mg/kg; Cu: 24.88 mg/kg) were elevated but remained below safety thresholds established for organic amendments. Raw rice husks had high lignocellulosic content and a wide C/N ratio, reflecting low biodegradability. Carbonization markedly altered these properties, producing rice husk biochar with increased aromatic carbon, reduced salinity, total dissolved solids, and enhanced magnesium content. These changes improved its suitability as a structural and chemical stabilizer within the composting matrix, consistent with earlier findings (Cecire et al., 2024 and Siles-Castellano et al., 2020).

Table 4.1. Comparative Analysis of the Physicochemical Composition of feedstocks (mean values, n = 3).

Parameter	*Tithonia Diversifolia*	Chicken manure	Rice Husk	Rice Husk Biochar
Ash (%)	29.04[a]	59.49[a]	44.87[a]	33.38[a]
TDS (mg/L)	3015.81	1297.51	648.10	204.6
Salinity (ppt)	4.13	1.66	0.77	0.18
pH	7.28	7.79	7.13	7.06
EC (µS/cm)	7.67	4.26	0.92	0.98
C/N ratio	7.54	13.30	38.52	38.86
TOC (%)	41.16	23.50	33.07	38.64
N (%)	5.46	1.77	0.86	0.99
K (%)	5.32	1.12	0.68	0.79
P (%)	0.97	5.86	2.29	0.83
Lignin (%)	N/A	N/A	16.29[a]	10.87[a]
Cellulose (%)	N/A	N/A	41.38[a]	17.04[a]
Hemicellulose (%)	N/A	N/A	16.30[a]	7.81[a]
Cr (mg/kg)	45.50[a]	37.065[a]	101.23[b]	42.25[b]
Cu (mg/kg)	10.25[a]	24.88[b]	5.17[a]	3.96[a]
Pb (mg/kg)	9.95[b]	24.51[b]	12.50[b]	9.95[b]
Ni (mg/kg)	4.93[b]	4.93[b]	4.93[b]	5.00[b]
Zn (mg/kg)	74.58[b]	186.01[b]	152.64[b]	59.38[b]
Fe (mg/kg)	814.78[b]	4,645.31[b]	9,046.80[b]	5,347.51[b]
Mg (mg/kg)	2,789.80[a]	2,246.40[a]	446.85[b]	3,012.51[b]
Na (mg/kg)	891.16b	4,738.79[b]	3,097.04[b]	1,816.55[b]

*TDS - Total Dissolved Solids; TOC - Total Organic Carbon; TKN - Total Kjeldahl Nitrogen; EC - Electrical Conductivity; N/A - Not Analysed. [a] Value Based on Dry Matter, [b] Value Based on Wet Matter.

4.2.1 Feedstock microstructural and elemental features

SEM analysis revealed distinct morphological features that influenced aeration, microbial colonization, and nutrient stabilization during composting (**Figure 4.1**). Chicken manure exhibited a porous and loosely aggregated structure, facilitating oxygen diffusion and microbial access, which is critical for rapid mineralization (Jindo et al., 2025). *Tithonia diversifolia* displayed compact, fibrous aggregates rich in labile organic matter, explaining its strong thermophilic response and rapid C/N reduction during composting (Matheri et al., 2025; Mlangeni, 2013). Rice husk biochar maintained a rigid, microporous framework with heterogeneous surface features. This structure prevented pile compaction, enhanced airflow, and created microhabitats favorable for microbial proliferation (Godlewska et al., 2017; Sánchez-Monedero et al., 2019; Stacey et al., 2024). EDX spectra confirmed the presence of key macro- and secondary elements (C, N, P, K, Mg, Ca, Si), supporting complementary

nutrient contributions across feedstocks. Elemental mapping further demonstrated spatial heterogeneity, reinforcing the synergistic interaction between nutrient-rich biomass and biochar as a stabilizing matrix.

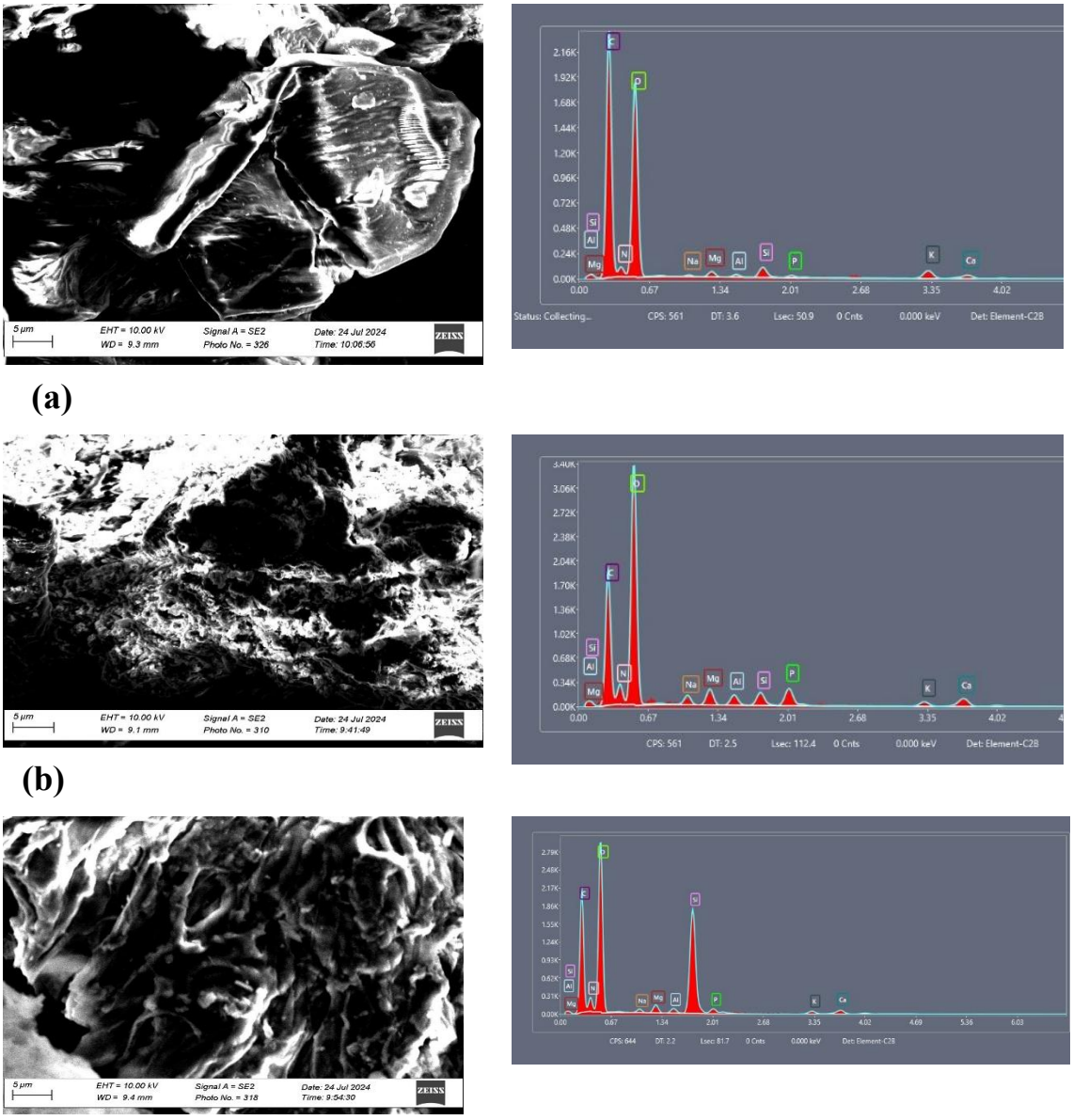

Figure 4.1. Surface Morphology and Elemental Composition (SEM–EDX) of Composting Feedstocks. (a) *Tithonia Diversifolia*, (b) Chicken Manure, and (c) Rice Husk Biochar.

4.2.2 Surface Functional Groups and Nutrient Retention Potential

The FT-IR spectrum of rice husk biochar (**Figure 4.2**) reveals a transition from raw biomass to a stable, carbonized matrix, marked by an intense Si-O-Si asymmetric stretching band at

1060–1080 cm^{-1}. This confirms the concentration of inherent silica after thermal degradation of organics. Supporting peaks at 793 cm^{-1} and 465 cm^{-1} indicate silicate structures that enhance mechanical strength and heavy metal adsorption. Aromatic C=C stretching near 1600 cm^{-1} signals stable benzenoid rings promoting recalcitrance and carbon sequestration. Unlike raw husks, broad O-H and aliphatic C-H bands are attenuated by dehydration and dealkylation during pyrolysis, while persistent carbonyls near 1700 cm^{-1} maintain cation exchange capacity. Overall, these features define a porous, silica-rich, aromatically stable framework ideal for struvite nucleation in compost. In comparison, the FT-IR spectrum of *Tithonia diversifolia* (**Figure 4.3**) shows a profile typical of nutrient-dense biomass, characterized by a broad O-H stretching band at approximately 3300–3400 cm^{-1} from alcohols and phenols, alongside aliphatic C-H stretching peaks near 2920–2850 cm^{-1} derived from leaf lipids. The presence of nitrogenous compounds is confirmed by the Amide I (1650 cm^{-1}) and Amide II (1540 cm^{-1}) bands, which correspond to C=O stretching and N-H bending in proteins, supporting the high nitrogen and amino acid content essential for green manure. A prominent peak near 1076 cm^{-1} (within the 1156–1060 cm^{-1} range) reflects C-O and C-N stretching vibrations associated with carbohydrates and lignocellulosic cell walls. These diverse O- and N-containing functional groups promote nutrient mineralization and microbial colonization.

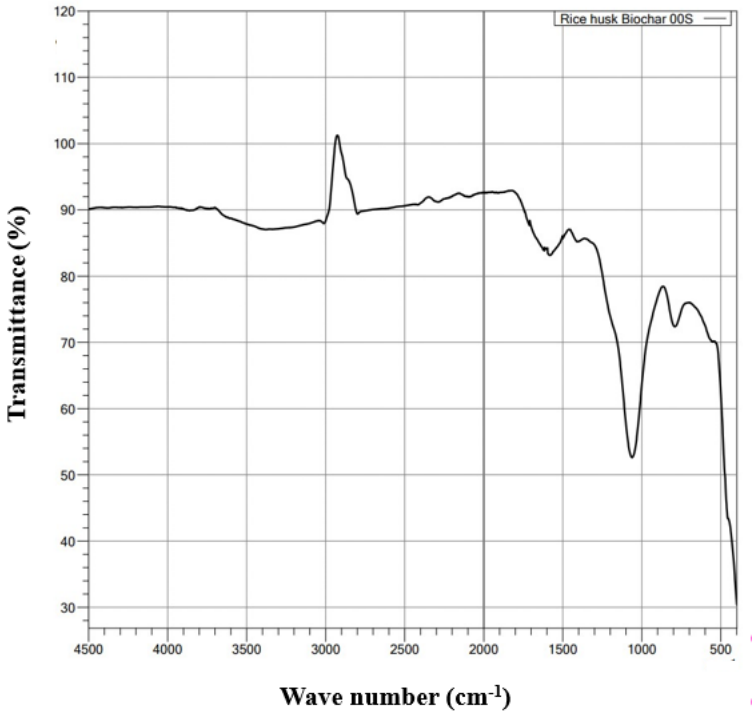

Figure 4.2: FT-IR Spectra of Rice Husk Biochar

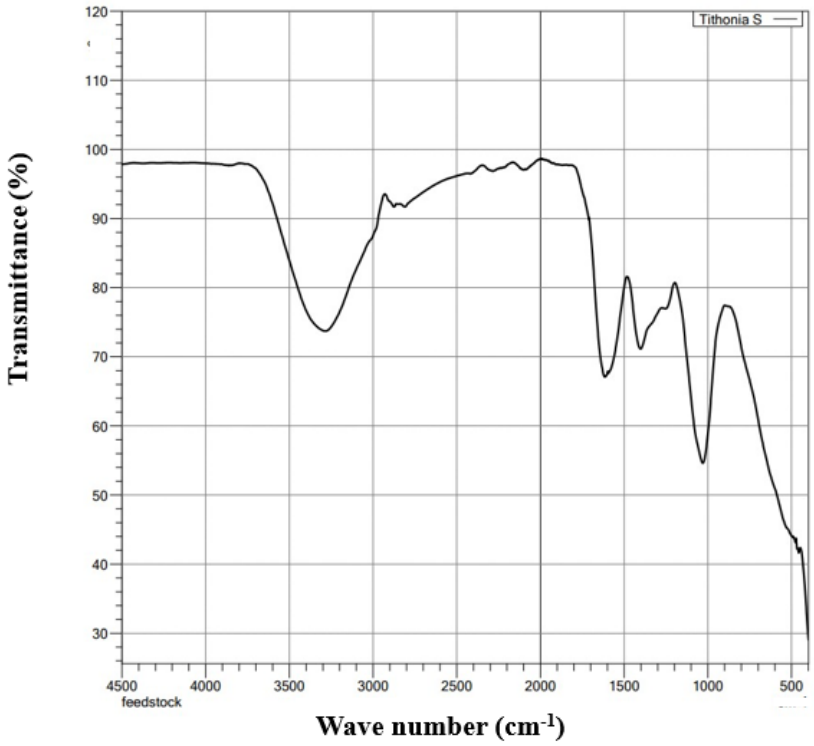

Figure 4.3: FT-IR spectra of *Tithonia diversifolia*

4.3 Composting Dynamics and Nutrient Stabilization

This section examines the temporal evolution of composting parameters that reflect microbial activity, organic matter transformation, and system stabilization. Temperature, pH, electrical conductivity, salinity, and gaseous indicators were used to evaluate composting efficiency and maturity development under different feedstock combinations.

4.3.1 Temperature evolution

All composting treatments exhibited the classical mesophilic–thermophilic–maturation sequence, indicating effective microbial decomposition and process stability (Mlangeni, 2013). As illustrated in **Figure 4.4**, temperatures increased rapidly during the first five days, reaching maximum values of 60.1 °C in the *Tithonia diversifolia*–manure treatment and 56.3 °C in the *Tithonia diversifolia*–biochar–manure mixture. These elevated temperatures reflect intense microbial oxidation of readily degradable substrates and confirm the strong stimulatory role of *Tithonia diversifolia* as a nitrogen-rich biomass input. Notably, thermophilic conditions were maintained above 50 °C for 3–5 days across most treatments, meeting sanitation thresholds required for pathogen and weed seed inactivation (Miguel et al., 2025). The biochar-free

treatment (M7) exhibited the highest temperature peak, suggesting that the abundance of labile organic matter in *Tithonia diversifolia* strongly stimulated microbial metabolism (Mlangeni et al., 2013). In contrast, biochar-amended treatments displayed more regulated thermal profiles, achieving thermophilic temperatures rapidly and sustaining them for longer. This moderating effect is attributed to biochar's porous structure and high surface area, which improve aeration, moisture retention, and microbial habitat formation (Jindo et al., 2012; Melo et al., 2020). For example, the *Tithonia diversifolia*–biochar mixture (M2) reached 56.3 °C, reflecting synergistic interactions between labile organic inputs and biochar's structural stability. Similar temperature regulation effects of biochar during composting have been widely reported and linked to improved heat distribution and microbial efficiency (Alarefee et al., 2023; Stacey et al., 2024). Overall, the thermal profiles confirm that *Tithonia diversifolia* accelerates composting through nutrient supply, while biochar moderates process intensity, creating a balanced system conducive to efficient decomposition.

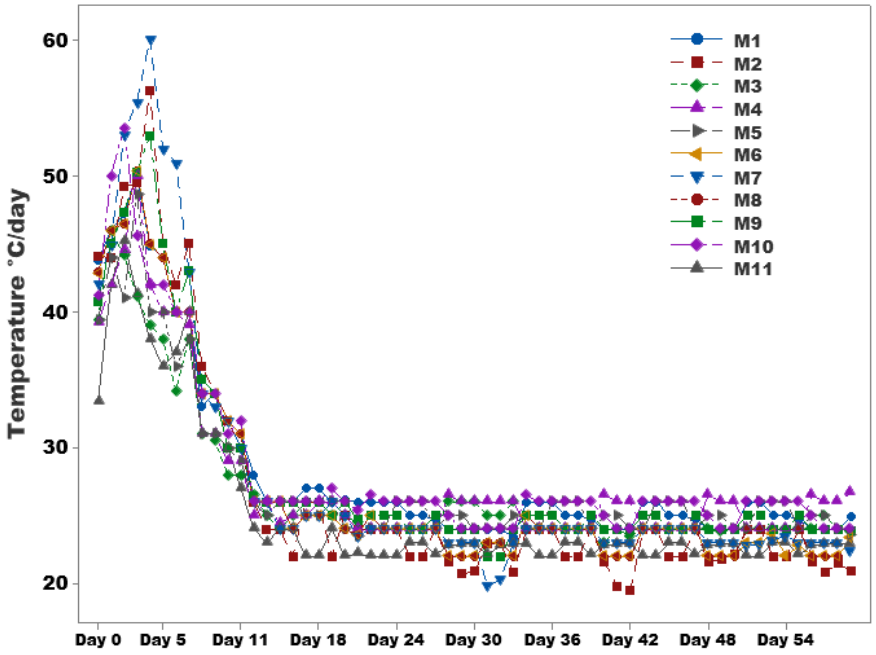

Figure 4.4: Variation of Temperature in all 11 Composting Treatments

4.3.2 pH evolution and Chemical Stabilization

The evolution of pH during the 60-day composting period reflects key biochemical transformations typical of manure- and biochar-based systems (**Figure 4.5**). All treatments initially displayed alkaline pH levels (8.3–8.8), which further rose during the thermophilic

phase due to ammonification and protein mineralization. Peak pH values (8.9–9.2) were recorded around Day 30, signaling active microbial turnover and the degradation of organic nitrogen. Treatments containing higher proportions of *Tithonia diversifolia* and biochar exhibited more stable pH trajectories than control or low-biochar mixtures. This buffering behaviour is attributed to biochar's alkaline ash content and acid-neutralizing capacity, which dampens fluctuations arising from microbial metabolism (Wang et al., 2016a). Alkaline conditions during the thermophilic stage are particularly significant because they favour the crystallization of struvite ($MgNH_4PO_4 \cdot 6H_2O$), a key mechanism for stabilizing ammonium and phosphate (Krishnamoorthy et al., 2021; Talboys et al., 2015). After Day 30, pH values gradually declined across all treatments, reaching 8.0–8.6 by Day 60. This decline reflects compost maturation processes, including ammonia volatilization, nitrification, and humic substance formation. The sharper pH decline in treatments with lower biochar content indicates reduced buffering capacity and more rapid humification. Overall, the pH trajectory confirms effective compost stabilization and the production of mature compost suitable for acidic tropical soils.

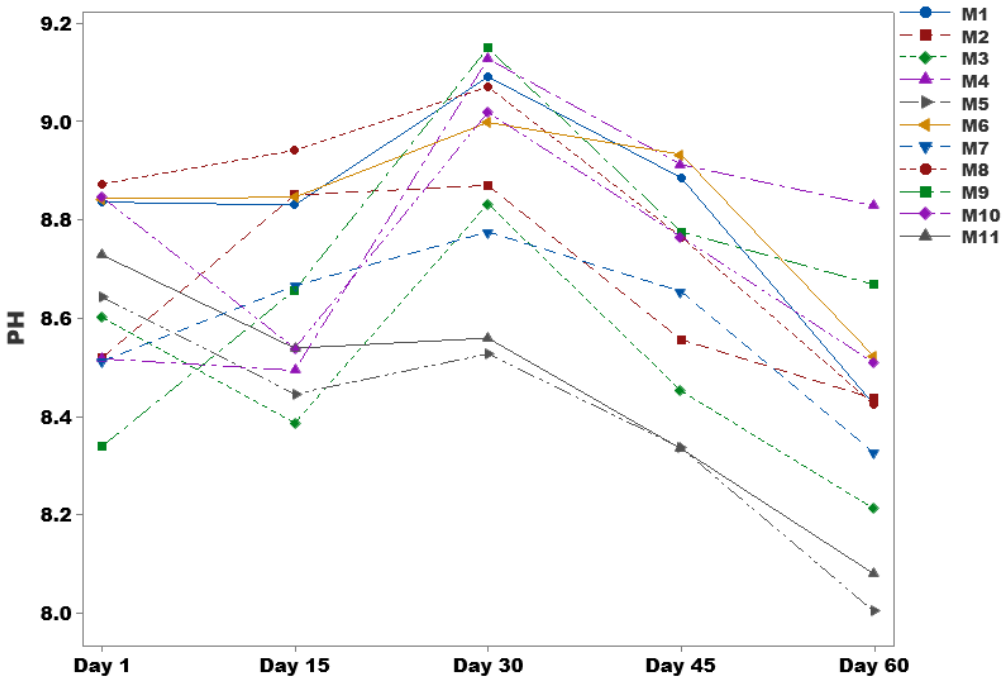

Figure 4.5: Changes in Compost pH Over a 60-Day Co-Composting Period for Different Feedstock Ratios

4.3.3 Electrical Conductivity and Salinity Dynamics

Electrical conductivity (EC) trends (**Figure 4.6**) provide insight into soluble salt release and stabilization during composting. Across all treatments, EC increased during the first 30 days, corresponding to the thermophilic phase and accelerated organic matter mineralization. The highest EC values were observed in treatments M2, M7, and M8, reflecting higher inputs of chicken manure and/or biochar and the associated release of soluble ions such as $NH4^{+}$, K^{+}, and Mg^{2+}. Following the thermophilic peak, EC declined steadily across all formulations, reaching acceptable levels by Day 60. This reduction reflects nutrient stabilization processes, including microbial uptake, nitrification, humification, and the formation of less soluble organomineral complexes. Treatments with higher *Tithonia diversifolia* content and moderate biochar levels (e.g., M3, M9, M10) exhibited faster EC decline, indicating efficient salt stabilization and advanced compost maturity. These findings align with previous reports that biochar addition reduces salinity by immobilizing ions and enhancing microbial efficiency (Wang et al., 2016b).

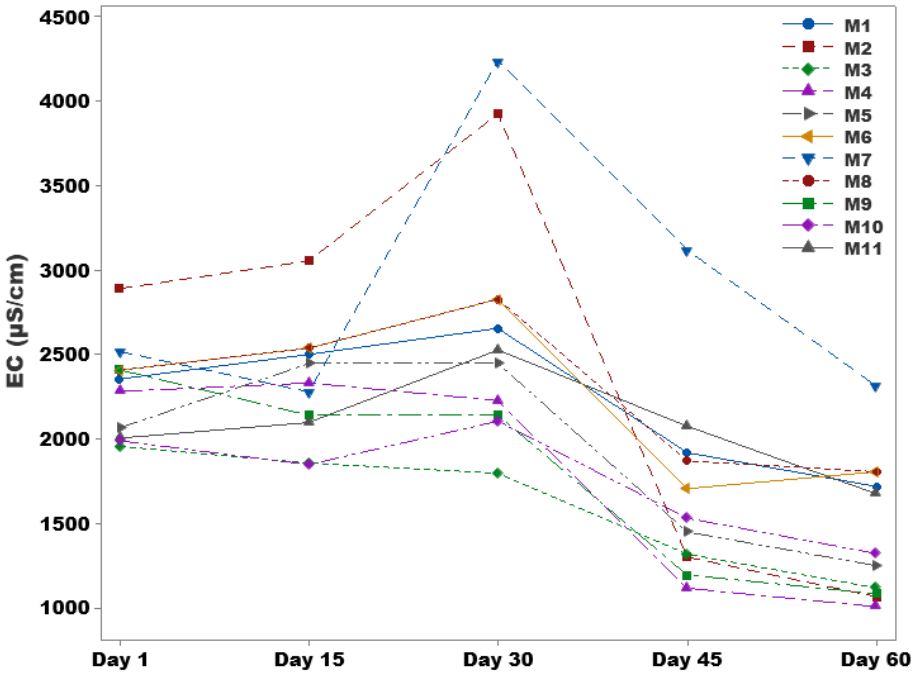

Figure 4.6. Variation in Electrical Conductivity (EC, µS/cm) of Biochar-Enhanced Compost Mixtures Over a 60-Day Composting Cycle

4.3.4 Total Dissolved Solids and Nutrient Retention

Total dissolved solids trends further corroborated the stabilizing role of biochar during composting (**Figure 4.7**). The Tithonia–biochar blend (M2) consistently exhibited lower TDS while maintaining higher nutrient concentrations, indicating effective adsorption of ammonium and nitrate ions (Ksheem et al., 2015; Purakayastha et al., 2019). In contrast, treatments with high *Tithonia diversifolia* inputs but limited biochar buffering showed elevated TDS, highlighting the risk of salinity buildup when labile biomass is applied without adequate stabilization (Opala, 2020). Excessive biochar, however, may immobilize nutrients to the point of reducing short-term availability (Joseph et al., 2021; Sanchez-Monedero et al., 2018), showing the need for balanced feedstock ratios.

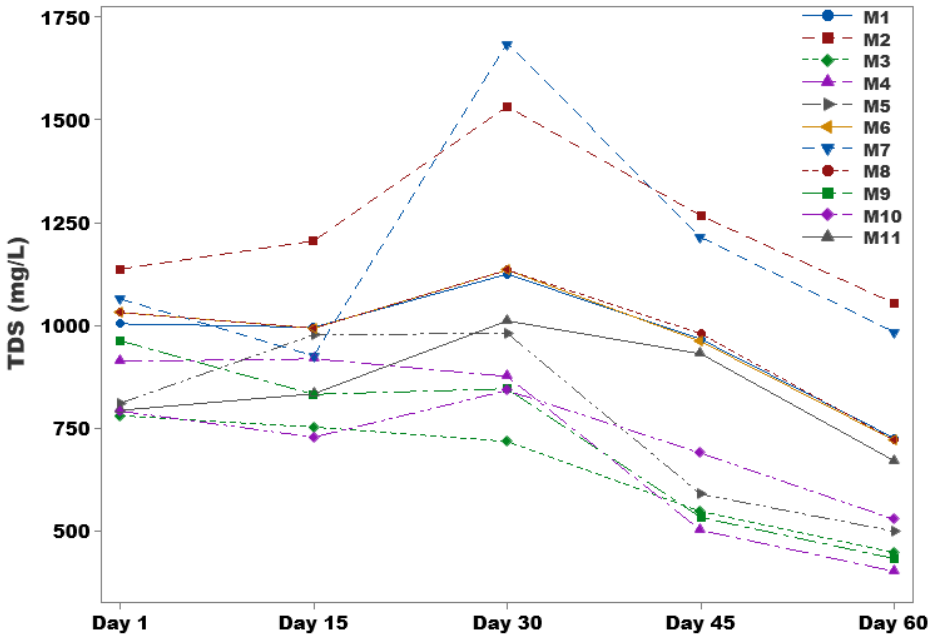

Figure 4.7: Variation in Total Dissolved Solids (TDS, mg/L) of Biochar-Enhanced Compost Mixtures Over a 60-Day Composting Cycle

4.3.5 Gaseous Exchange and Compost Stabilization

Gas composition monitoring provided direct evidence of microbial respiration dynamics (**Figure 4.8**). During the first week, carbon dioxide levels increased, reflecting intense microbial oxidation during the thermophilic phase. By approximately Day 10, CO_2 declined to 1–6%, indicating reduced metabolic intensity and transition toward maturation. Biochar-amended treatments showed more moderate CO_2 fluctuations, consistent with improved

aeration and reduced anaerobic microsites. This behaviour is attributed to biochar's porous architecture, which enhances oxygen diffusion and microbial efficiency (Agyarko-Mintah et al., 2017; Sayara et al., 2020). The gas exchange patterns confirm that *Tithonia diversifolia*–biochar co-composting accelerates stabilization while improving nitrogen conservation through adsorption and mineral precipitation mechanisms.

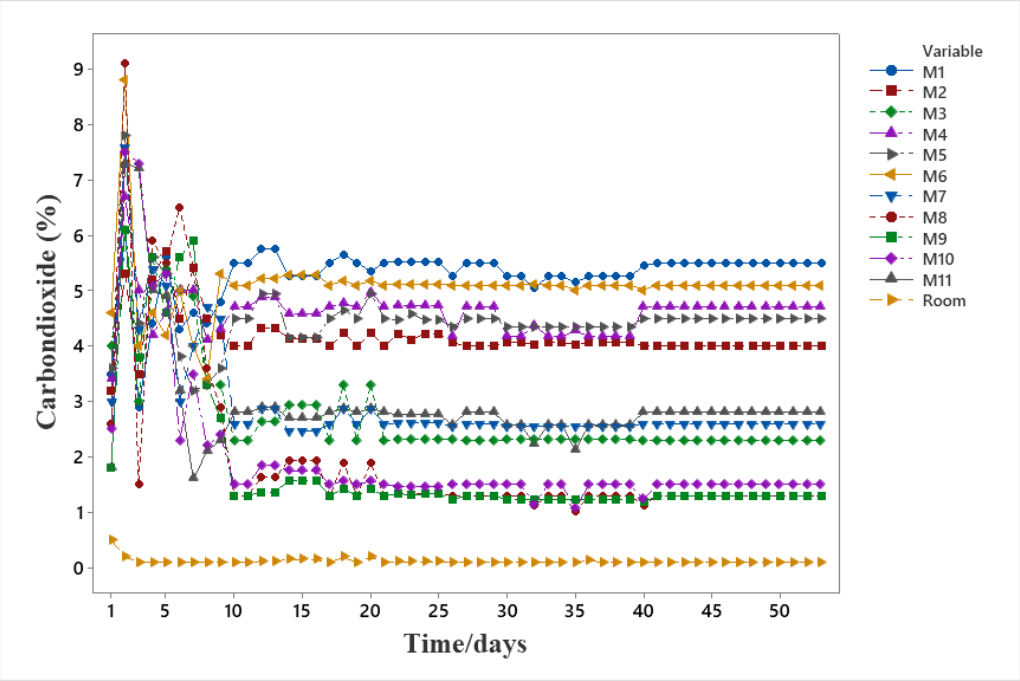

Figure 4.8: Variations in Carbon Dioxide (CO_2) Evolution During Co-composting of Different Feedstock Ratios

4.3.6 Spectroscopic Characterization and Functional Group Transformation of Optimized BBC Formulations

The FT-IR spectra of formulations M1–M11 exhibit high structural similarity, confirming that the optimized composting process yields a chemically consistent, mature product. Analysis across 4000–400 cm^{-1} reveals transformations in functional groups, including a broad, intense band at 3330–3400 cm^{-1} that corresponds to O-H and N-H stretching vibrations from alcohols, phenols, and protein-derived compounds in chicken manure and *Tithonia diversifolia*. This persistent O-H stretch reflects origins in lignocellulosic materials and their stabilized decomposition products. Indicators of stable organic matter include sharp peaks at 2920 cm^{-1} and a prominent peak at 1630 cm^{-1}, which reflect benzenoid rings from biochar alongside nitrogen stabilization. All formulations show a sharp nitrate band at 1384 cm^{-1}, confirming

mineralization of polypeptides and polysaccharides, its intensity was highest in M7, lower in high-biochar reactors, and lowest in M10 (low biochar and *Tithonia diversifolia* content), thus highlighting biochar's influence on nitrogen mineralization and retention. Previous studies have similarly demonstrated that biochar incorporation can enhance nitrogen retention during composting, primarily through its porous structure and surface chemistry (Joseph et al., 2018). The structural framework features an intense band at 1030 cm^{-1}, providing nucleation sites for struvite-mediated stabilization. Similar peaks are also evident in the biochar-amended composts (Hagemann, et al., 2017). Lower-frequency peaks at 470 cm^{-1} and 560 cm^{-1} represent Si–O bending and mineral vibrations, collectively verifying a robust silicate matrix that transforms unstable feedstocks into a stable, nutrient-dense organic fertilizer.

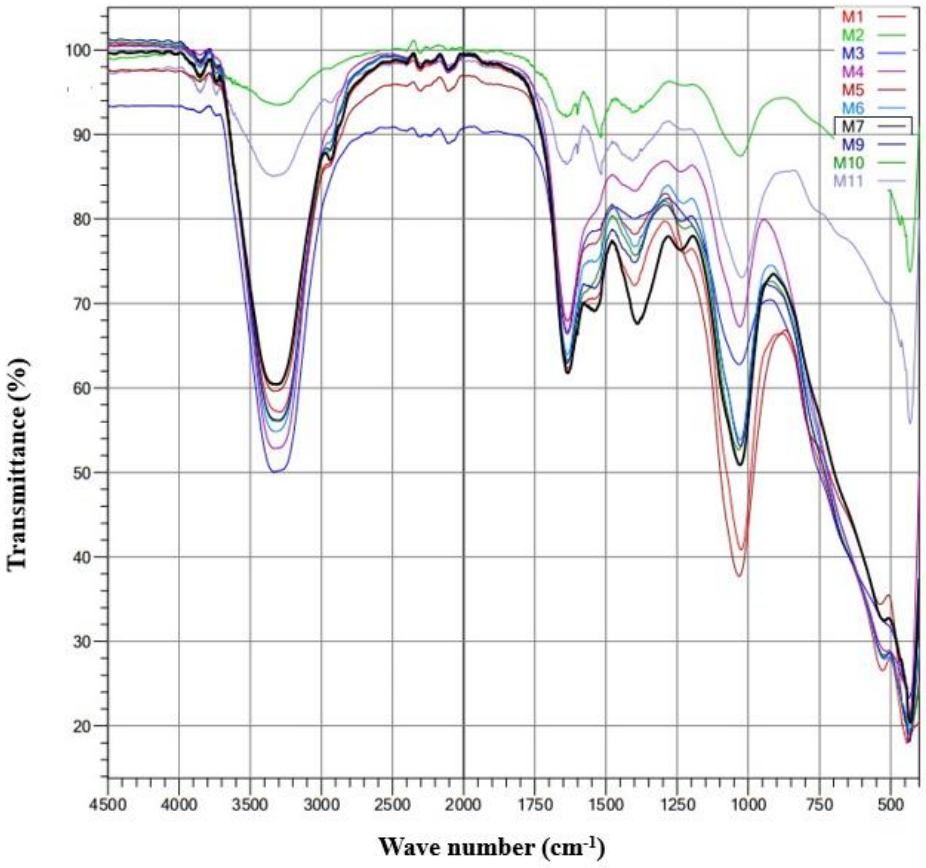

Figure 4.9: Comparative FT-IR spectra of biochar-blended compost (BBC) formulations (M1–M11) optimized via Response Surface Methodology

4.4 Development of regression model equations

CCD was employed to develop correlations between the proportions of composting feedstocks (*Tithonia diversifolia* and biochar) and the responses (nitrogen, phosphorus, and potassium contents) as shown in Equations 11-13. The experimental design and corresponding experimental values for each response are shown in **Table 4.2**. Runs M1, M6, and M8 at the center point were employed out of five points to determine the experimental error and the reproducibility of the data. As shown in **Table 4.2**, nitrogen, phosphorus, and potassium contents ranged from 1.32–2.68 g/kg, 1.10–2.05 g/kg, and 1.20–2.91 g/kg, respectively. These relatively wide ranges are attributed to the varying extents to which the synergistic effects of labile organic nitrogen from *Tithonia diversifolia* and the adsorption mechanisms of biochar influenced nutrient stabilization across different mixing ratios.

To find the best fit for each response, the respective sequential model's sum of squares was used. From each of these, the highest-order polynomial for which the additional terms are significant, and the model is not aliased, was chosen. In this study, the quadratic model best fit the responses, as indicated by high coefficients of determination ($R^2 > 0.97$). These values indicate that more than 97% of the observed variability in macronutrient concentrations was explained by the model terms, confirming the robustness of the RSM framework (Asadu et al. 2019; Vandecasteele et al., 2016). For the coded factors, the reduced quadratic response surface models for nitrogen, phosphorus, and potassium, without excluding insignificant terms, are given in Equations 11-13, respectively. The fitted regression equations revealed both linear and quadratic effects of *Tithonia diversifolia* and biochar, confirming that nutrient responses were governed by nonlinear interactions rather than simple additive effects.

$$\mathrm{N} = 1.66 + 0.5205A + 0.1387B + 0.0032AB + 0.4330A^2 - 0.1005B^2 \quad \text{Equation 11}$$

$$\mathrm{P} = 1.59 - 0.0283A + 0.1350B - 0.07AB + 0.4834A^2 - 0.3266B^2 \quad \text{Equation 12}$$

$$K = 2.32 + 0.6875A + 0.1917B - 0.2575AB - 0.0849A^2 - 0.1374B^2 \quad \text{Equation 13}$$

Where A is the *tithonia diversifolia* (kg), B rice husk biochar (kg)

Table 4.2: CCD and Experimental Results

Run	Composting Feedstock			Responses		
	A (*Tithonia Diversifolia*, kg)	B (Biochar, kg)	Chicken manure mixture	N (Nitrogen, g/kg)	P (Phosphorus g/kg)	K (Potassium g/kg)
M1	35	5	60	1.70	1.53	2.34
M2	60	10	30	2.68	1.79	2.75
M3	10	10	80	1.67	1.78	1.87
M4	35	0	35	1.32	1.10	1.89
M5	10	5	85	1.44	2.05	1.50
M6	35	5	60	1.67	1.64	2.22
M7	60	0	40	2.40	1.66	2.91
M8	35	5	60	1.79	1.64	2.36
M9	60	5	35	2.55	2.04	2.83
M10	35	10	40	1.60	1.37	2.33
M11	10	0	90	1.40	1.60	1.20

4.5 Diagnostics and adequacy checking

The adequacy of the fitted models was verified using normal probability plots of the externally studentized residuals **(Figure 4.10**) and predicted versus actual values **(Figure 4.11**). Plots of nitrogen, phosphorus, and potassium showed points that fit a straight line closely, confirming a normal distribution and the absence of significant outliers. Thus, the response surface models effectively describe the functional relationship between the experimental factors and responses. The plots of externally studentized residuals versus predicted values for nitrogen **(Figure 4.11j**), phosphorus (**Figure 4.12h**), and Potassium (**Figure 4.12i)** do not show any particular pattern. The lack of any particular nonlinear patterns in these plots suggests random distribution of the residues, fulfilling the requirements of a statistically robust and reliable model (Kumar et al., 2023).

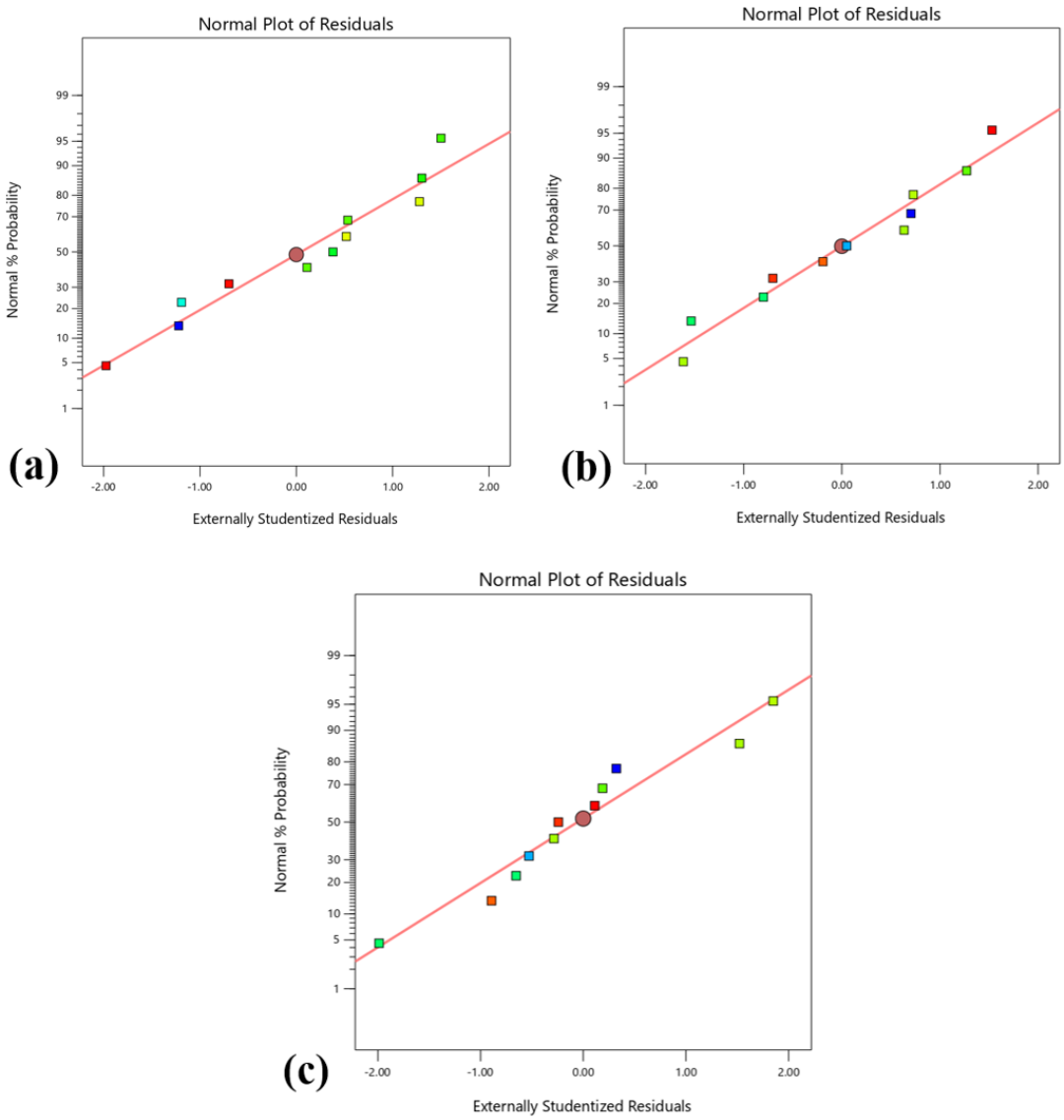

Figure 4.10: Normal probability plot of residues for: (a) Nitrogen, (b) phosphorus, and (c) Potassium

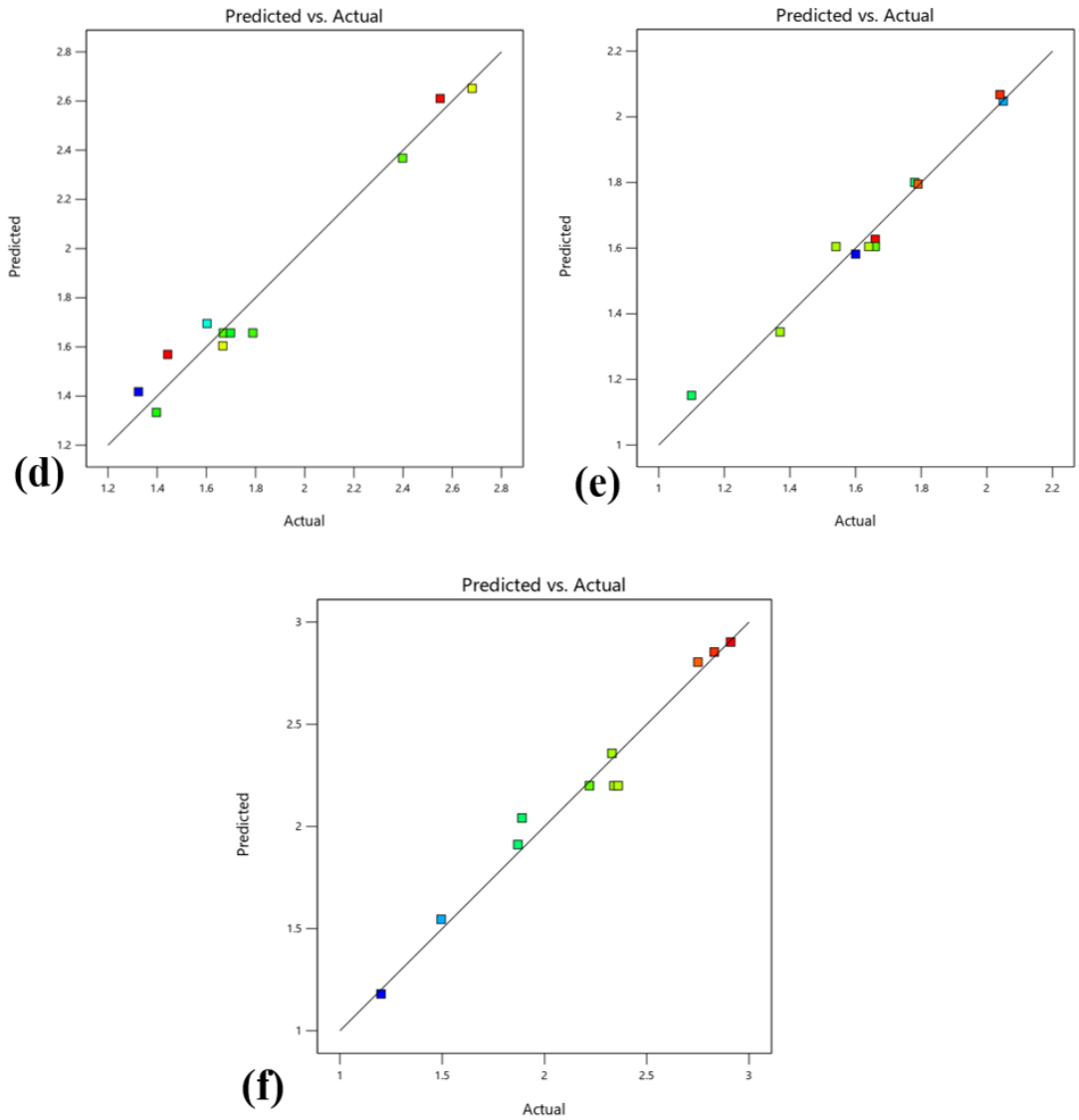

Figure 4.11: Predicted versus experimental values for: (d) Nitrogen, (e) phosphorus, and (f) Potassium

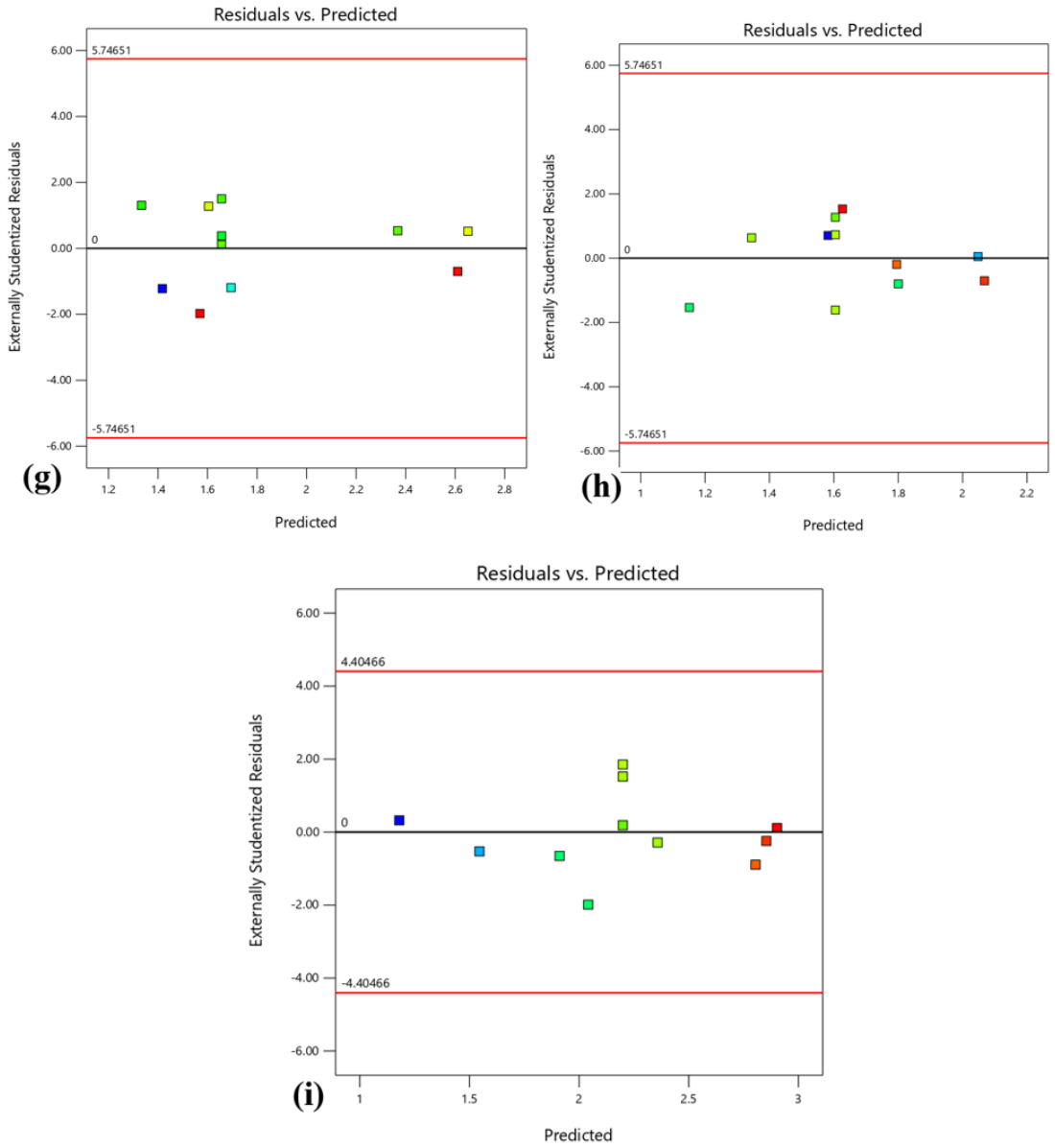

Figure 4.12: Residues versus predicted for (g) Nitrogen, (h) Phosphorus, and (i) Potassium

4.6 Analysis of Variance

ANOVA was used to evaluate the statistical significance of the quadratic models, their lack-of-fit, and the significance of their respective model coefficients. As shown in **Table 4.3**, the model F-values of 33.70, 50.64, and 86.60 for the quadratic models of Nitrogen, Phosphorus, and Potassium, respectively, indicate that the developed models are significant (p-values < 0.05). Besides, the lack of fits for the developed models are not significant (p-values > 0.05), further suggesting that the quadratic models adequately describe the functional relationship between the experimental factors (*Tithonia diversifolia* and Biochar) and the response variables.

Because model terms are significant at $p < 0.05$, A, B, and A^2 are significant terms in the response surface model for Nitrogen. Out of these, *Tithonia diversifolia* (F-value 123.58) was found to be the most significant factor influencing nitrogen content, followed by the quadratic effect of *Tithonia diversifolia* (F-value 36.11), and lastly the main effect of Biochar (F-value 8.77) (**Table 4.3**). The interactive effect (AB) and the quadratic effect of Biochar (B2) were not significant for Nitrogen, as their p-values were greater than 0.05.

Table 4.3: ANOVA for response surface reduced quadratic models for N(a), P(b), and K(c)

Source	Sum of Squares	df	Mean Square	F-value	p-value	Comment
Response 1: Nitrogen						
Model	2.22	5	0.4433	33.70	0.0007	significant
A-Tithonia	1.63	1	1.63	123.58	0.0001	significant
B-Rice husk Biochar	0.1154	1	0.1154	8.77	0.0315	significant
AB	0.0000	1	0.0000	0.0032	0.9570	Not significant
A^2	0.4750	1	0.4750	36.11	0.0018	significant
B^2	0.0256	1	0.0256	1.94	0.2220	Not significant
Residual	0.0658	5	0.0132			
Lack of Fit	0.0579	3	0.0193	4.93	0.1734	not significant
Pure Error	0.0078	2	0.0039			
Cor Total	2.28	10				
Response 2: Phosphorus						
Model	0.7294	5	0.1459	50.64	0.0003	significant
A-Tithonia	0.0006	1	0.0006	0.2083	0.6673	Not significant
B-Rice husk Biochar	0.0561	1	0.0561	19.46	0.0069	significant
AB	0.0006	1	0.0006	0.2170	0.6609	Not significant
A^2	0.5202	1	0.5202	180.60	< 0.0001	significant
B^2	0.3226	1	0.3226	111.98	0.0001	significant
Residual	0.0144	5	0.0029			
Lack of Fit	0.0061	3	0.0020	0.4949	0.7219	not significant
Pure Error	0.0083	2	0.0041			
Cor Total	0.7438	10				
Response 2: Potassium						
Model	2.89	3	0.9627	86.60	< 0.0001	significant
A-Tithonia	2.57	1	2.57	230.85	< 0.0001	significant
B-Rice husk Biochar	0.1501	1	0.1501	13.50	0.0079	significant
AB	0.1718	1	0.1718	15.45	0.0057	significant
Residual	0.0778	7	0.0111			
Lack of Fit	0.0664	5	0.0133	2.31	0.3287	not significant
Pure Error	0.0115	2	0.0057			
Cor Total	2.97	10				

The significant terms for the model corresponding to Phosphorus content include B, A^2, and B^2. Out of these, the quadratic effect of *Tithonia diversifolia* (F-value 180.60) was found to

have the most significant influence, followed by the quadratic effect of Biochar (F-value 111.98), and the main effect of Biochar (F-value 19.46). Similar to Nitrogen, the interactive term (AB) was not significant for phosphorus. Similar findings were reported by Asadu et al., (2019). The findings in this study also agree with previous studies, which revealed that when organic amendments are co-composted with biochar, phosphorus availability is primarily governed by adsorption-desorption equilibria rather than simple additive effects (Antonange lo et al., 2021; Joseph et al., 2018). Moreover, the quadratic effect of high-nutrient biomass, such as *Tithonia diversifolia*, reaches a critical threshold beyond which further increases do not significantly enhance phosphorus mineralization.

For Potassium content, the significant terms include A, B, and the interaction AB. *Tithonia diversifolia* (F-value 230.85) was the most significant factor, followed by the interactive effect between *Tithonia diversifolia* and Biochar (F-value 15.45), and the main effect of Biochar (F-value 13.50). These findings agree with previous studies (Asadu et al., 2019), which highlighted that nutrient responses in compost optimization are often governed by nonlinear interactions rather than simple additive effects. The goodness-of-fit of the model to the experimental data was evaluated using standard deviation, coefficient of variation, adjusted R-squared, predicted R^2, and adequate precision (**Table 4.4**). Low standard deviations for each response indicate robust models (Md Saleh et al., 2020). Coefficient of variation values below 10% for the responses suggest high reproducibility (Kumar et al., 2023). Elevated R2 values confirm satisfactory alignment of the data with the models.

Table 4.4: Model summary statistics indicating goodness of fit of the

Statistical parameter	**Nitrogen**	**Phosphorous**	**Potassium**
Standard deviation	0.1147	0.0537	0.1054
Mean	1.84	1.66	2.20
Coefficient of variation (%)	6.24	3.24	4.79
R^2	0.9712	0.9806	0.9780
Adjusted R^2	0.9424	0.9613	0.9625
Predicted R^2	0.8174	0.8975	0.9485
Adequate Precision	15.5639	23.1254	27.0916

Specifically, the models explain 97.12%, 98.06%, and 97.80% of the variability in Nitrogen, phosphorus, and potassium content, respectively, as shown in Equations 11-13. Moreover, the adjusted and predicted values for each response were in reasonable agreement (difference < 0.2), supporting the model's suitability. The adequate precision values exceeding 4 indicate that the models can effectively navigate the design space (Md Saleh et al., 2020).

4.7 Response surfaces

4.7.1 Nitrogen Retention

Nitrogen was the most responsive macronutrient across the experimental domain, as indicated by the strong positive linear and quadratic coefficients associated with *Tithonia diversifolia*. Increasing *Tithonia diversifolia* input consistently enhanced total nitrogen concentration, with a pronounced nonlinear increase at higher biomass levels (**Figure 4.13**). This response reflects the high labile organic nitrogen content in *Tithonia diversifolia*, which stimulates microbial proliferation and accelerates organic matter mineralization. Similar nitrogen enrichment patterns have been widely reported for *Tithonia*-based composts and green manures (Mlangeni, 2013; Matheri et al., 2025). Biochar exerted a dual, dose-dependent influence on nitrogen dynamics. Moderate additions improved nitrogen retention through ammonium (NH_4^+) adsorption and reduced volatilization losses (Abban-Baidoo et al., 2024). However, excessive biochar loading resulted in a slight decline in total nitrogen, likely due to physical immobilization of ammonium within biochar pore networks and reduced microbial accessibility. High biochar doses may also alter aeration and moisture regimes but can also suppress microbial activity and slow decomposition (Chen et al., 2020; Sanchez-Monedero et al., 2018). The curvature of the nitrogen response surface, therefore, identifies a clear threshold beyond which biochar shifts from a retention enhancer to a limiting factor (Pokharel & Chang, 2023; Tsai & Chang, 2020).

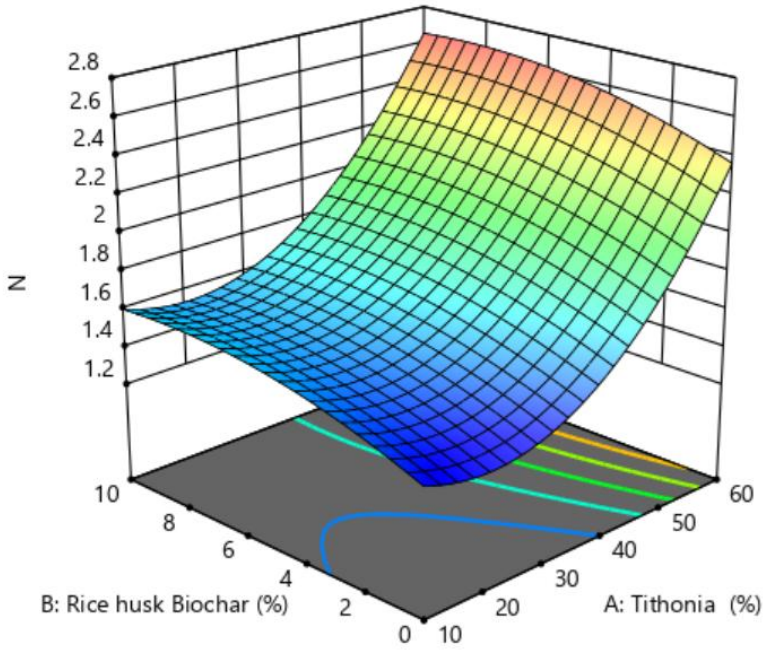

Figure 4.13: Three-Dimensional Response Surface Plots of Nutrient Dynamics Nitrogen with Varying Proportions of *Tithonia diversifolia* and Biochar

4.7.2 Phosphorus

Phosphorus exhibited a distinct nonlinear response, with biochar exerting a stronger influence than *Tithonia diversifolia* (**Figure 4.14**). Biochar enhanced phosphorus retention primarily through surface adsorption, ion exchange, and complexation mediated by oxygen-containing functional groups (Li et al., 2022; Luo et al., 2022). These mechanisms effectively reduced phosphate mobility and leaching losses during composting. In contrast, increasing *Tithonia diversifolia* input showed a weakly negative association with measured phosphorus concentration. This effect likely reflects nutrient dilution and competitive sorption processes, as rapid *decomposition of Tithonia diversifolia* releases large quantities of soluble nitrogen and potassium, which compete with phosphate ions for sorption sites (Rashidzadeh et al., 2015). Additionally, intense microbial activity stimulated by *Tithonia diversifolia* may temporarily immobilize phosphorus within microbial biomass, reducing extractable concentrations during active composting phases (Talboys et al., 2015). The response surface patterns indicate that phosphorus stabilization is maximized within an optimal biochar range. This finding reconciles contrasting reports in the literature, where biochar has been shown to either enhance phosphorus availability (Wei et al., 2021) or reduce it through over-adsorption (Iqbal et al., 2015), depending on application rate and system chemistry.

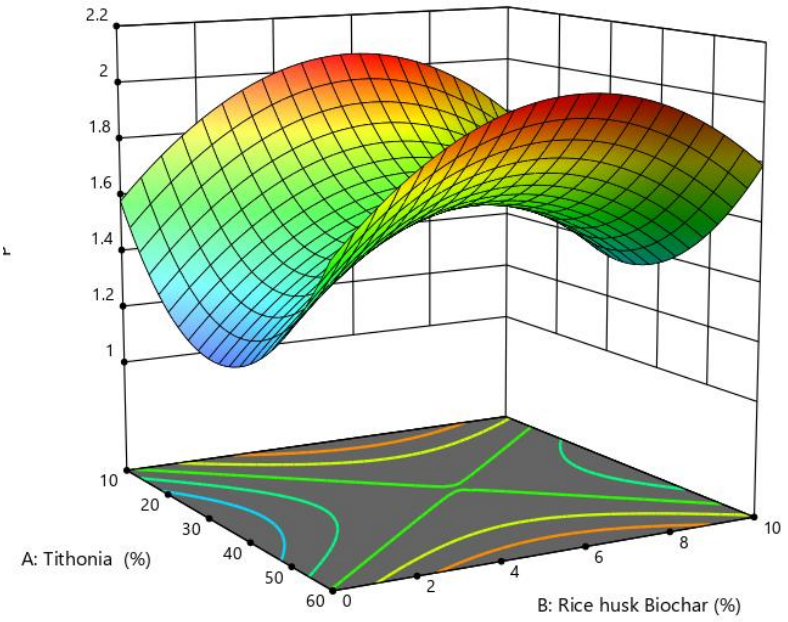

Figure 4.14: Three-Dimensional Response Surface Plots of Nutrient Dynamics Showing Phosphorus in Compost Formulations (M1–M11) with Varying Proportions of Tithonia diversifolia and Biochar

4.7.3 ***Potassium***

Potassium dynamics showed significant variability due to its high solubility and mobility during composting. Integrating *Tithonia diversifolia* and rice husk biochar markedly enriched potassium, as shown by the upward-sloping response surface in Figure 4.15. *Tithonia diversifolia* served as the primary biogenic K source, rapidly releasing bioavailable K during enzymatic decomposition of its biomass. Biochar stabilized this mobile fraction through its high cation exchange capacity and oxygen-containing functional groups (e.g., carboxyl and hydroxyl groups, discussed Section 4.4.2), retaining exchangeable potassium via electrostatic surface adsorption and mitigating leaching during composting. The combined application of these materials proved essential: whereas excessive *Tithonia diversifolia* posed a leaching risk due to rapid mineralization, the biochar buffered K solubility. Ultimately, this interplay enhances the compost's agronomic efficacy by extending K availability to support osmotic regulation, enzyme activation, and drought resilience.

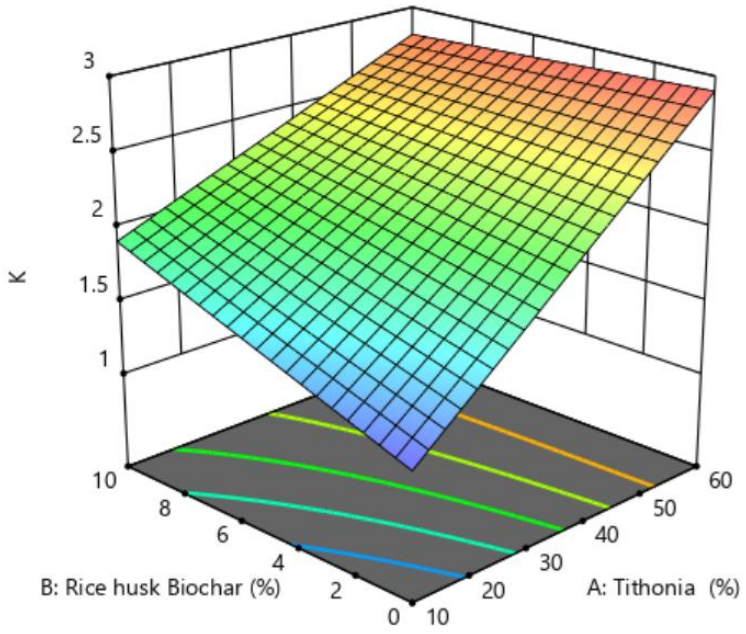

Figure 4.15: 3D Response Surface Depicting Potassium Variation as a Function of *Tithonia diversifolia* and Biochar Proportions

4.8 Optimization Outcomes and Model Validation

After model simulation using Design-Expert software and numerical optimization, the optimal composting formulation was determined as *Tithonia diversifolia* (60.0%) and biochar (5.7%). If the feedstocks are blended with 34.3 chicken manure pre-mix, the N, P, and K contents, as predicted by the respective models, would be 2.648, 2.050, and 2.873%, respectively. To verify the predictive capability of the developed models, compost was produced using the suggested substrate quantities. The mean experimental values were 2.648, 2.306, and 2.793% for N, P, and K, respectively. These values fell within both the low and high bounds of the 95% prediction interval, indicating model validity and good predictive capability (Iqbal et al., 2014; Md Saleh et al., 2020). The mean experimental values for each response were within the 95% PI, suggesting that the developed models are valid. The deviations between the actual and the predicted values were considerably small, further confirming the good agreement between the experimental and predicted values. This high level of precision indicates that the RSM models effectively captured the complex interactions within the matrix.

4.9 Struvite Formation and Spectroscopic Evidence of Mineralization

The FT-IR spectra (**Figure 4.16**) provide definitive evidence of structural and compositional shifts between the control compost (MC) and the biochar–*Tithonia diversifolia* –amended treatments (M2, M3, M7, M11). The control compost (MC) exhibited relatively flat spectral profiles with weak O–H stretching (3200 – 3600 cm^{-1}) and faint NH_4^+ bending vibrations (1400 – 1450 cm^{-1}). These features reflect a system dominated by conventional organic decomposition with minimal mineral stabilization, often resulting in significant nitrogen loss through volatilization (Jiang et al., 2016). In contrast, the amended samples (particularly M2, M3, and M7) showed a marked intensification of key diagnostic bands. The pronounced peaks at 1430–1470 cm^{-1} (NH_4^+ bending) and 1600 – 1700 cm^{-1} (H–O–H bending), coupled with the broad, deep absorption band in the 2650 – 3650 cm^{-1} region (O–H stretching), signify a transition toward a more structured mineral phase. These spectral are diagnostic of hydrated magnesium ammonium phosphate (struvite) crystallization (Sidorczuk et al., 2020).

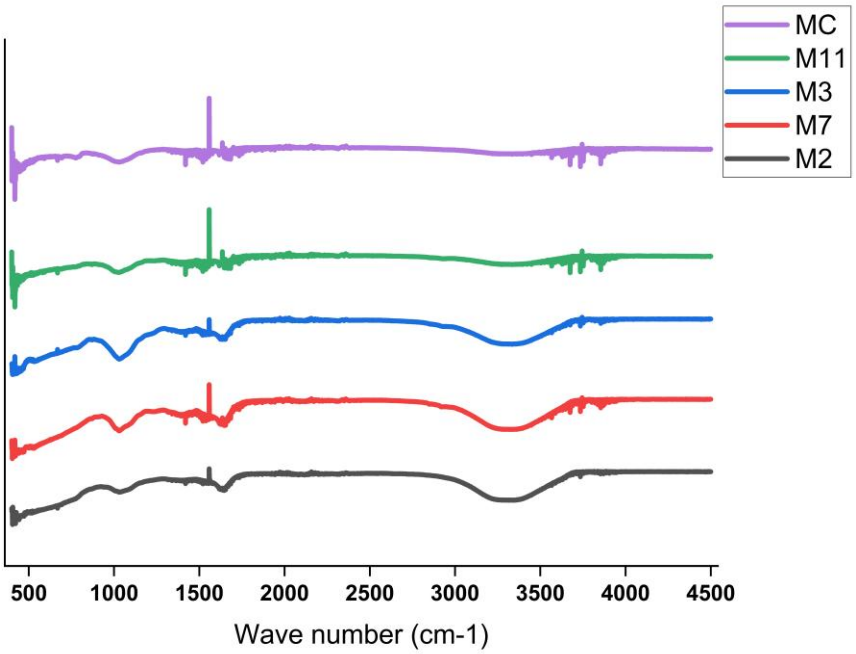

Figure 4.16. Stacked FT-IR spectra showing the functional group profiles of MC, M11, M3, M7, and M2 samples.

These results indicate that nitrogen stabilization in the amended compost was driven by mineral precipitation rather than simple organic complexation. The biochar functioned as a critical nucleation and sorption matrix, while the mineral phases (struvite) effectively locked ammonium and phosphate ions into semi-crystalline forms. The results are consistent with the

those of Kékedy-Nagy et al. (2020), who demonstrated that agricultural waste can fundamentally alter nutrient retention pathways, transforming volatile components into stable, slow-release fertilizers.

4.9.1 Magnesium and Sodium Dynamics and Implications for Compost Quality

Magnesium concentrations increased consistently with increasing proportions of *Tithonia diversifolia* and biochar (**Figure 4.17**), reflecting progressive microbial solubilization of organically bound Mg^{2+} and its subsequent participation in nutrient-stabilization processes. Notably, the study demonstrated that *Tithonia diversifolia* alone supplied sufficient bioavailable Mg^{2+} to support struvite formation, eliminating the need for external magnesium additives commonly required in conventional composting systems. The highest magnesium accumulation, observed in treatment M2 at day 60, coincided with peak struvite formation, confirming the intrinsic mineralization capacity of *Tithonia diversifolia*. Biochar played a complementary role by enhancing compost cation exchange capacity and providing reactive sorption sites for Mg^{2+}, NH_4^+, and PO_4^{3-} ions, thereby facilitating ion retention and crystal nucleation (Wang et al., 2016a). This synergistic interaction, nutrient supply from *Tithonia diversifolia* and ionic stabilization by biochar, created favorable conditions for sustained struvite precipitation. Statistical analysis confirmed a strong linear relationship between feedstock proportions and magnesium concentration, with a high coefficient of determination validating the robustness of the predictive model. Beyond enrichment, magnesium dynamics provided insights into compost maturation and nutrient stabilization. Magnesium concentrations increased from approximately 3,985.5 mg kg^{-1} at compost initiation to 6,665.7 mg kg^{-1} by day 28, consistent with reports by Omolola (2019). This trend indicates continued mineralization during maturation and enhanced nutrient availability. The concurrent stabilization of ammonium and phosphate occurred through struvite precipitation ($MgNH_4PO_4 \cdot 6H_2O$), a process that effectively reduces nitrogen volatilization and phosphorus leaching (Mancho et al., 2023). Biochar further reinforced this mechanism by retaining Mg^{2+} through cation exchange and surface sorption, minimizing ionic losses and improving nutrient recovery efficiency (Abban-Baidoo et al., 2024; Tran et al., 2023). The reaction below describes the simultaneous stabilization of ammonium and phosphate through struvite precipitation:

$$Mg^{2+} + NH_4^+ + PO_4^{3-} + 6H_2O \rightarrow MgNH_4PO_4 \cdot 6H_2O$$

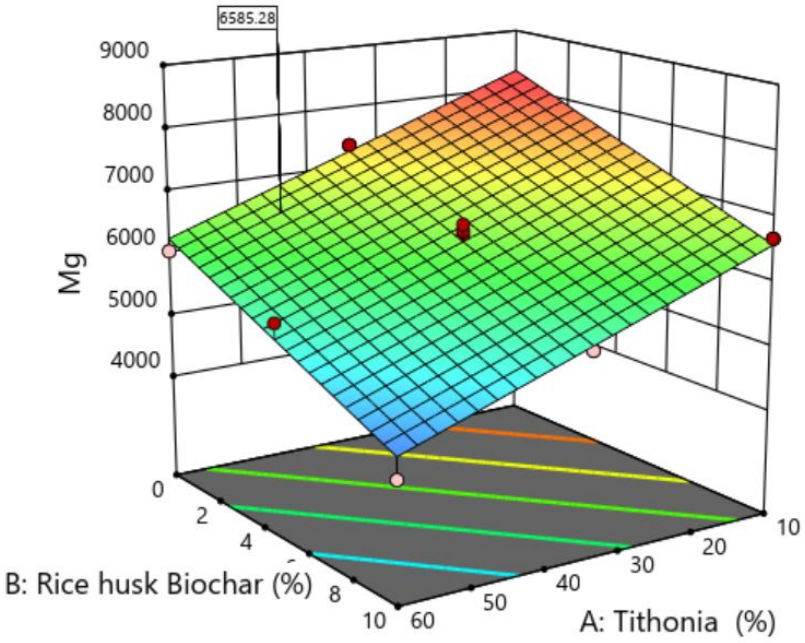

Figure 4.17. Three-Dimensional Response Surface Plots of Magnesium Concentrations Showing Enrichment Trends with Increasing *Tithonia Diversifolia* and Biochar Inputs.

Collectively, the results presented in Sections 4.2 through 4.9.1 demonstrate that the optimized co-composting of *Tithonia diversifolia* and biochar significantly enhances macronutrient retention, promotes mineral stabilization via struvite formation, and improves both compost maturity and agronomic safety. The validated Response Surface Methodology models provide a reliable decision-support framework for designing nutrient-efficient, biochar-blended composts tailored to sustainable soil fertility management. To achieve Objective 2, the results below detail the development of advanced formulations:

4.10 Effects of Encapsulation on the Functional Performance of Biochar-Blended Compost

Encapsulation represents a critical step toward achieving controlled nutrient release. The results demonstrate that coating biochar-blended compost with biodegradable polymers fundamentally altered pellet structure and transport properties, thereby regulating nutrient mobility and reducing loss pathways such as leaching and volatilization. The formation of a semi-permeable polymer barrier around the mature BBC matrix enabled diffusion-controlled nutrient release governed by moisture ingress and microbial activity. These findings are

consistent with reports that biodegradable polymers enhance nutrient-use efficiency by prolonging nutrient residence time in soil and limiting off-site nutrient transfer (Azeem, 2025; Singh et al., 2025). Collectively, the results show that encapsulation transforms BBC from a conventional organic amendment into a functionally engineered, controlled-release fertilizer system.

4.10.1 Influence of Biodegradable Coating Films on Pellet Structure and Release Potential

The performance of the encapsulated BBC was strongly governed by the composition of the chitosan–starch coating films. Dip-coating produced pellets with uniform geometry across formulations (**Table 4.5**; **Figure 4.18**), confirming consistent film formation. However, systematic differences in pellet mass and compactness revealed that polymer ratios directly influenced coating density and permeability. As shown in **Table 4.5**, chitosan-rich formulations produced denser, more compact coatings, indicative of tighter polymer packing and reduced diffusivity, whereas starch-dominant coatings, particularly CH/S-33, generated heavier pellets due to starch swelling and increased water affinity. In contrast, the CH/S-50 formulation yielded lighter yet structurally cohesive coatings, reflecting improved polymer compatibility and balanced film integrity. These trends indicate that adjusting the chitosan-to-starch ratio provides a robust strategy for tailoring moisture responsiveness, mechanical stability, and nutrient diffusion, core requirements for controlled-release performance under soil conditions. Comparable relationships between polymer composition and release behaviour have been reported in blended biopolymer systems used for fertilizer and agro-delivery applications (Jiménez-Rosado et al., 2021; Lewicka et al., 2024; Tomadoni et al., 2019), supporting the broader applicability of the encapsulation approach demonstrated in this study.

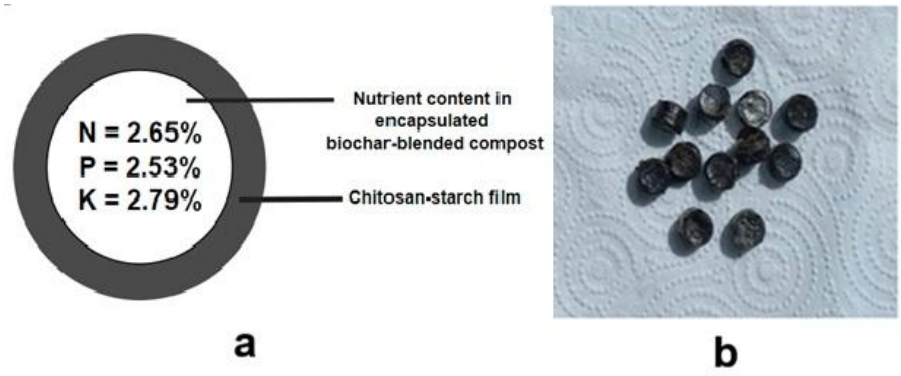

Figure 4.18. Schematic Representation and Visual Illustration of Encapsulated Biochar-Blended Compost Fertilizer (EBBC). **a** Cross-Sectional Diagram Showing the Internal Structure of the Encapsulated Pellet; **b** Photograph of the Fabricated EBBC Pellets

Table 4.5: Formulation and Characterization of Encapsulated Biochar-Blended Compost Pellet

EBBC pellet	Corn starch (ml)*	Chitosan solution (ml)*	Diameter of coated pellet (mm)	Weight of coated pellet (g)	Coating film composite
B	0	100	12.1867	1.0450	CH
D	50	50	12.1633	0.9796	CH/S-50
E	67	33	12.2727	1.0716	CH/S-33
F	33	67	12.1225	1.0460	CH/S-67

*Refers to the respective amounts of prepared film-forming solutions used in the coating process

4.10.2 Biodegradation Behaviour of Biopolymer Films and Implications for Nutrient Release

The environmental responsiveness of the chitosan–starch coatings was evaluated through soil burial tests, where gravimetric mass loss served as a proxy for biodegradation and release potential (**Figure 4.19**). All formulations exhibited measurable degradation, confirming their suitability as biodegradable diffusion barriers in soil. However, degradation rates varied markedly with polymer composition. The CH/S-33 formulation degraded most rapidly, losing more than 80% of its mass within five days, whereas pure chitosan films required approximately 15 days for complete breakdown. Blended films displayed intermediate behaviour, with full degradation occurring between 15 and 20 days. This gradual mass loss suggests that starch incorporation promotes the formation of denser, semi-crystalline polymer

networks that moderate water ingress and microbial penetration, thereby extending functional lifetime in soil (Gao et al., 2021; Wan Yusof et al., 2024; Zhang et al., 2017).

Visual observations during burial (**Figure 4.20**) reinforced these trends. Pure chitosan films showed rapid and extensive disintegration, accompanied by discoloration and shrinkage, indicating limited resistance to microbial attack. In contrast, chitosan–starch composites degraded more progressively, characterized by surface cracking and localized fragmentation rather than complete structural collapse. These patterns reflect selective enzymatic hydrolysis, with starch-rich domains acting as preferential sites for microbial colonization. The loamy soil used in the assay (**Table 4.6**), characterized by higher organic matter (7.40 ± 0.02%) and water-holding capacity (8.60 ± 0.01%) compared to the sandy loam, likely accelerated these processes due to a more robust microbial environment. Furthermore, the loam's superior electrical conductivity (208.58 ± 0.75 mS/l) and higher clay content (1.29 ± 0.24 g/kg) suggest an enhanced nutrient exchange capacity and moisture retention, providing an ideal matrix for rapid microbial degradation.

Table 4.6: Physicochemical Properties of Different Soil Types

Parameter	**Sand-loam**	**Loam**
Organic matter (%)	4.23 ± 0.10	7.40 ± 0.02
Conductivity (mS/l)	125.92 ± 0.56	208.58 ± 0.75
pH	8.13 ± 0.01	5.57 ± 0.7
Water holding capacity (%) *	7.94 ± 0.02	8.60 ± 0.01
Sand (g/kg)	97.98 ± 0.12	95.15 ± 0.36
Silt (g/kg)	1.63 ± 0.01	-
Clay (g/kg)	0.31 ± 0.09	1.29 ± 0.24

*After three hours

Overall degradation followed the sequence CH > CH/S-50 > CH/S-33 > CH/S-67, closely matching gravimetric weight-loss data and confirming the regulatory role of polymer ratio. Initial opacity measurements (**Figure 4.20**, day 0) further revealed increasing turbidity with higher starch content, attributable to dispersed starch granules within the polymer matrix ((De Paola et al., 2021). This microstructural heterogeneity appears to influence both degradation

pathways and film permeability. Collectively, these results demonstrate that chitosan–starch ratios provide an effective lever for tailoring biodegradation kinetics, enabling coatings that persist long enough to regulate nutrient diffusion yet degrade predictably to ensure timely nutrient availability. This balance is critical for transforming encapsulated biochar-blended compost into a responsive, soil-adaptive fertilizer system (Babaee et al., 2022; Gumelar et al., 2020; Zain et al., 2017).

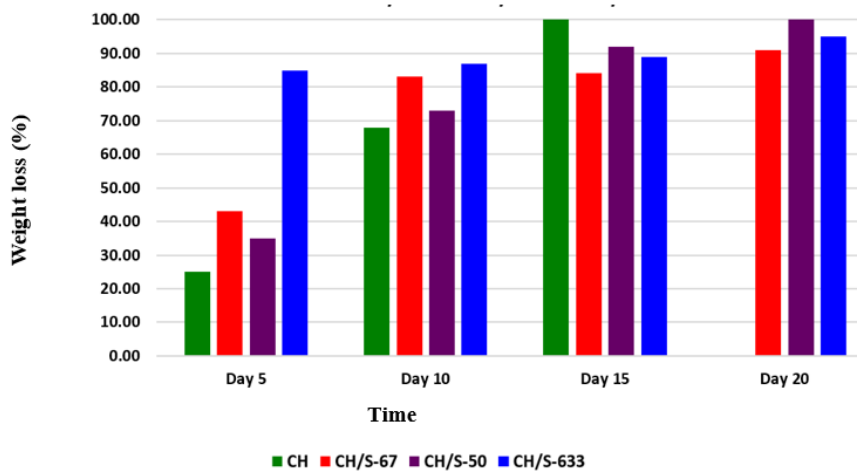

Figure 4.19. Weight Loss and Degradation Profile of Chitosan and Chitosan–Starch Composite Films Over Time.

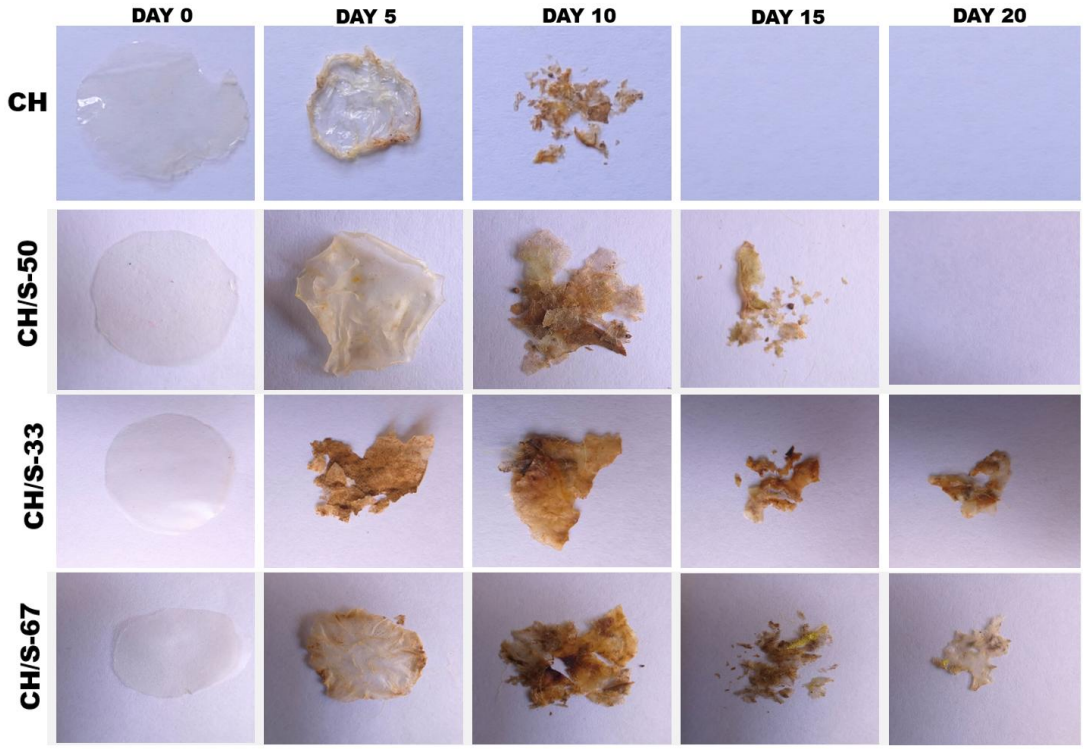

Figure 4.20: The Visual Observation of Film Composites Before and After Burial in Planting Soil

4.10.3 FT-IR Evidence of Coating Structure and Degradation Relevant to Controlled Release

FT-IR spectroscopy provided molecular-level confirmation that the chitosan–starch coatings developed formed stable, interactive polymer networks capable of regulating nutrient release. The spectra of freshly prepared films (**Figure 4.21**) showed broad O–H stretching bands (3200–3500 cm^{-1}), characteristic C–H stretching near 2900 cm^{-1}, and well-defined amide I and II bands (1550–1640 cm^{-1}), indicating successful integration of chitosan and starch through extensive hydrogen bonding (Atakan et al., 2023; Hamdi et al., 2020; Tagliaro et al., 2022; Yusof et al., 2019). The pronounced polysaccharide backbone signal around 1026 cm^{-1} further confirmed effective film formation and structural continuity within the encapsulating matrix (Herniou--Julien et al., 2018; Tagliaro et al., 2022; Zhang et al., 2017). Following soil burial, the coatings exhibited systematic spectral changes consistent with controlled biodegradation. These included a narrowing of the O–H region (Goiana et al., 2021), attenuation of C–H stretching peaks, indicative of the shortening of alkyl chains (dos Santos Cotta et al., 2023), and a reduction in the intensity of amide bands, suggesting structural changes in chitosan components (Rouzi et al., 2017). Shifts and weakening in the C–O and glycosidic linkage regions (notably from 1026 to 1016 cm^{-1}) indicated progressive hydrolysis of polysaccharide bonds, confirming microbial-mediated degradation of the films. Importantly, degradation intensity varied with polymer composition: starch-rich coatings (CH/S-67) showed more rapid structural weakening, while chitosan-rich formulations retained greater integrity, consistent with chitosan's known contribution to mechanical strength and moisture resistance (Jiménez-Regalado et al., 2021; Tan et al., 2022).

Collectively, the FT-IR results demonstrate that the encapsulating films are both structurally robust and biodegradable, with degradation kinetics that can be modulated through the chitosan–starch ratio. This breakdown of behaviour shows the controlled nutrient release mechanism targeted in this study. It ensures gradual nutrient diffusion during early soil exposure while allowing progressive film disintegration to support sustained nutrient release

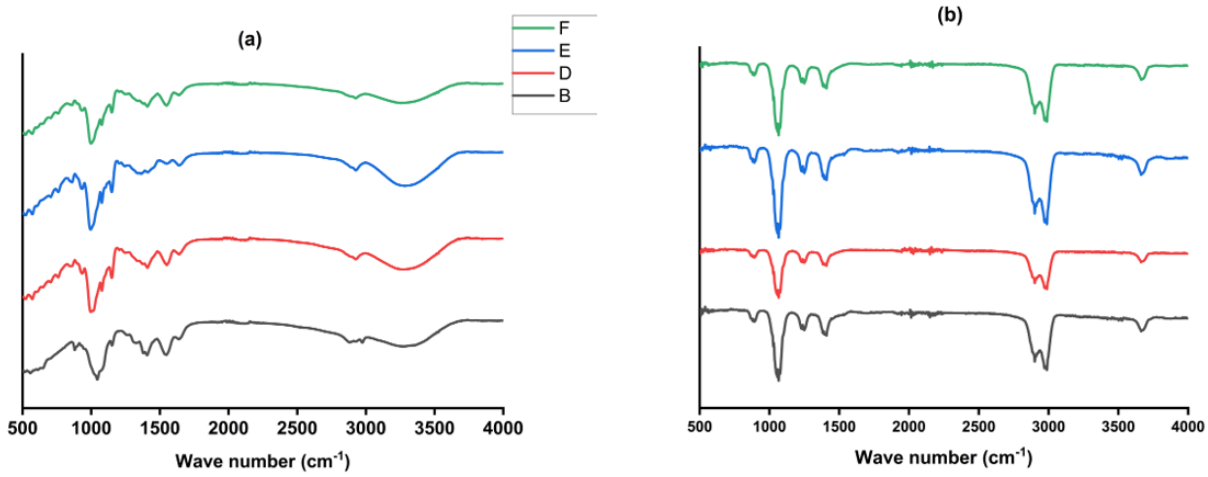

Figure 4.21: FT-IR Spectra Comparison of the Film Samples on Different Days: (**a)** at Day 0, and (**b)** at Day 10 After Burial in Loam Soil

4.10.4 SEM Surface Degradation Features

SEM provided complementary evidence of surface transformation before and after soil burial (**Figure 4.22**). Initially, pure chitosan films exhibited uneven topography with shallow pores caused by trapped air during film formation (Khuntia et al., 2022). Blended films, however, displayed smoother and more homogeneous surfaces, suggesting improved polymer compatibility. The CH/S-67 formulation achieved the most uniform morphology, reflecting strong intermolecular hydrogen bonding. After 10 days of soil exposure, all films showed erosion and crack formation consistent with microbial and enzymatic attack. Starch-rich films degraded faster, while chitosan-dominant blends retained partial structural integrity. These observations corroborate earlier reports highlighting starch's susceptibility to microbial hydrolysis and chitosan's role in enhancing water resistance (Mendes et al., 2016; Othman et al., 2023). Thus, intermediate chitosan–starch ratios achieved a balanced trade-off between durability and biodegradability, rendering them optimal for encapsulation purposes (Firmanda et al., 2022).

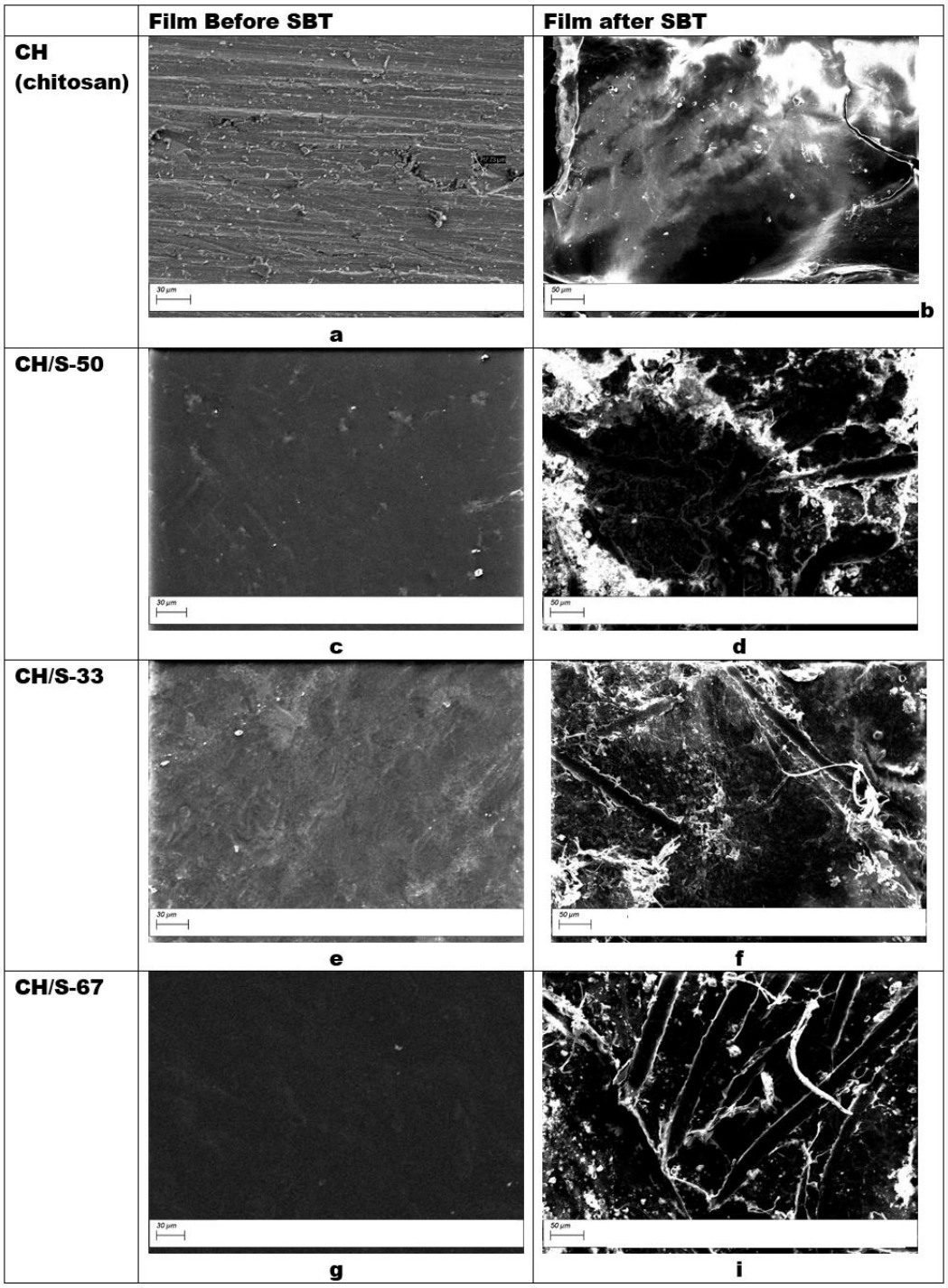

Figure 4.22: SEM micrographs illustrate the surface morphology of unburied chitosan (CH) and chitosan–starch blend films and their corresponding changes after 10 days of soil burial

4.10.5 Hydration Properties

Figure 4.23 illustrates the swelling kinetics of pellets coated with four distinct biopolymer films (B, E, F, and D) over an 82-minute duration. The data reveals that Film B exhibits the most rapid and consistent water absorption, maintaining a dominant swelling ratio that

increases from approximately 146% to nearly 188%. This indicates a highly hydrophilic and porous matrix capable of significant expansion without immediate structural failure. In contrast, Film E demonstrates a steadier, linear progression; although it begins with the lowest absorption capacity, its gradual rise to 148% suggests a more controlled and stable hydration process. The behavior of Films F and D indicates a critical structural threshold around 50 minutes. Both films reach their maximum hydration peaks at this point (158% and 153%, respectively) before experiencing a notable decline in their swelling ratios. This post-peak reduction is characteristic of structural degradation or partial dissolution of the biopolymer chains into the medium. Notably, Film D shows a more precipitous drop to 135% in the final stage, suggesting that while it can achieve high initial hydration, it possesses lower long-term structural resilience compared to the more stable linear growth seen in Films B and E.

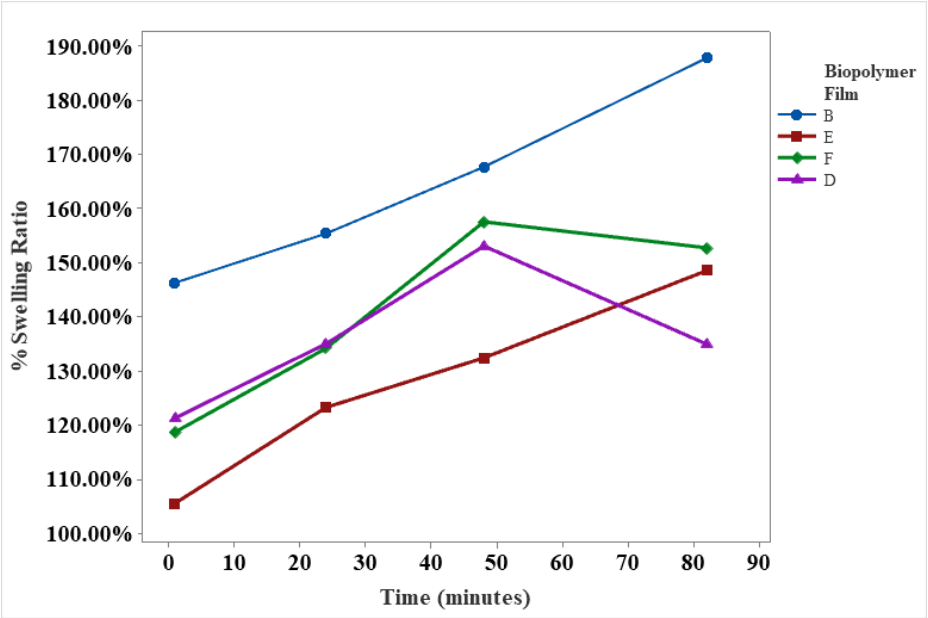

Figure 4.23: Time-Dependent Swelling Behaviour of EBBC Pellets Over a Period of 82 Hours

Furthermore **Figure 4.24** shows the swelling behavior across a temperature range from 25 ºC to 50 ºC. The data reveals a clear thermal threshold at 40 ºC, where nearly all films reach their maximum swelling capacity. Film F exhibits the most dramatic response, surging from 118 ºC to a dominant peak of at 172 ºC at 40 ºC, suggesting a highly temperature-sensitive matrix. Film B follows a similar trajectory, peaking at 164% before declining. These peaks represent the point of maximum hydration, facilitated by the thermal expansion of the amorphous polymer chains. In contrast, pellets coated with Film E maintain the lowest swelling profile,

peaking at 126, which likely indicates a more densely cross-linked or hydrophobic structure. A critical divergence occurs between 40 ºC and 50 ºC; while Films B, E, and F exhibit a sharp decline due to thermal degradation, Film D is the only variant to achieve a stable plateau (155%). This stabilization demonstrates superior thermal resilience, confirming that the Film D matrix maintains its mechanical integrity at elevated temperatures.

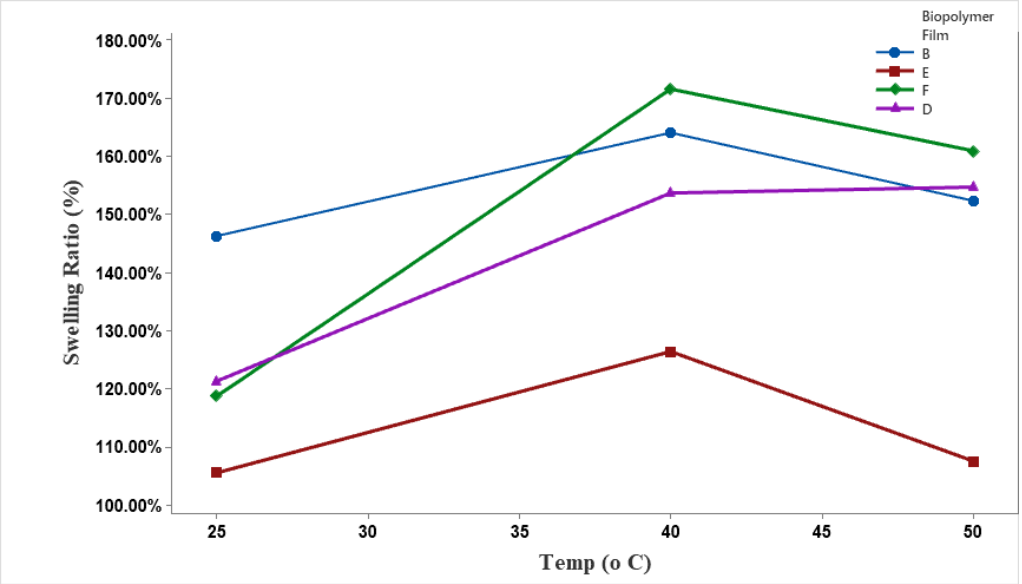

Figure 4.24: Temperature-Dependent Swelling Behaviour of EBBC Pellets

Likewise, **Figure 4.25** illustrates the swelling kinetics of the four biopolymer films as a function of increasing water volume, revealing distinct hydration and structural response phases. Initially, all films exhibited a sharp swelling trend; Film B attained the highest preliminary ratio (149%), while Film E demonstrated the lowest (110%), suggesting that the latter possesses a more hydrophobic or densely cross-linked matrix. However, a "structural disturbance" at the 5 mL threshold triggered a simultaneous decline across all variants, likely due to the disruption of intermolecular hydrogen bonding, which may lead to matrix contraction or the leaching of soluble fractions. Following this, the films reached a saturation peak at 6 mL, with Films F and D reaching maximum expansion at 161% and 155%, respectively. Beyond saturation, a sharp decline was observed, indicating structural failure or partial dissolution. Notably, at the 9 mL mark, Films B and E exhibited a secondary recovery trend. In contrast, Film F continued to decline, highlighting significant differences in the long-term mechanical integrity and stability of the engineered formulations.

Therefore, the plots show that true stabilization, defined by a non-significant change in % SR, was achieved only by Film F at 40 °C and 6 mL hydration peak. While this peak marks the point of maximum matrix expansion, the subsequent declines indicate a transition from hydration to diffusion-controlled release. This suggests that for the engineered formulation, the hydration phase is stable, establishing a reliable semi-permeable barrier that regulates nutrient mobility before the onset of matrix contraction or dissolution.

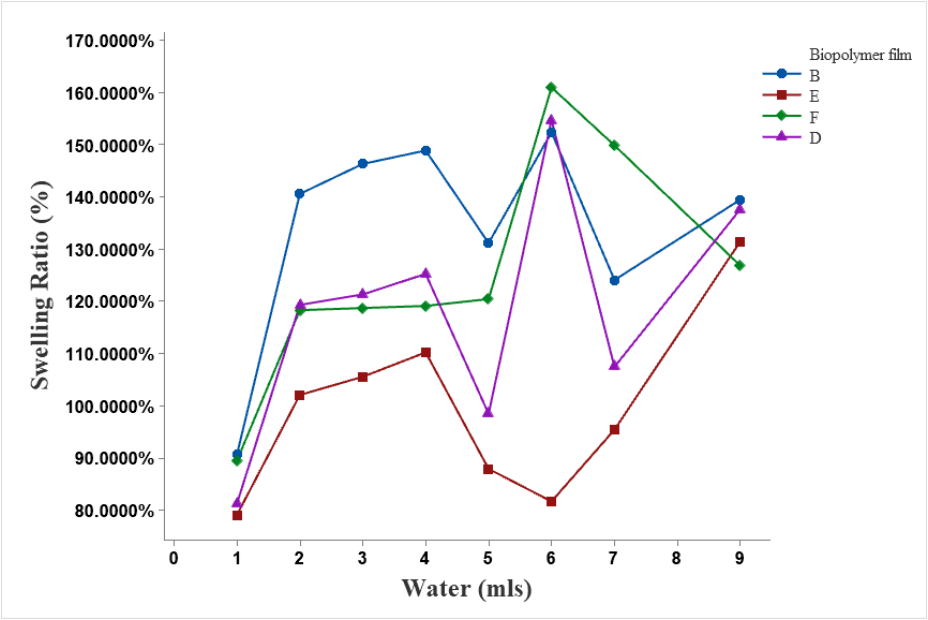

Figure 4.25: Swelling Behaviour of EBBC Pellets as A Function of Increasing Water Volume

4.10.6 Soil moisture retention

Soil moisture retention closely mirrored swelling trends, with water-holding capacity following the order F > E > D > B (**Figure 4.26**). Formulation F (2:1 chitosan–starch ratio) demonstrated superior retention, confirming its hydrogel-like behaviour and resistance to rapid degradation. This combination of moderate swelling and sustained moisture retention makes the formulation particularly effective in moisture-limited conditions (Kabir et al., 2023), functioning simultaneously as a nutrient regulator and a soil water micro-reservoir (Gumelar et al., 2020; Kusumastuti et al., 2019). These hydration dynamics directly govern nutrient release by controlling water penetration, dissolution, and ion diffusion (Jiang et al., 2024). Consequently, formulations like Sample F deliver nutrients more gradually and predictably than highly swellable but structurally unstable alternatives. This balance between water uptake and sustained availability aligns with established controlled-release systems (Jiang et al., 2024),

demonstrating that fine-tuning chitosan–starch ratios is a robust strategy for optimizing encapsulated biochar–blended compost.

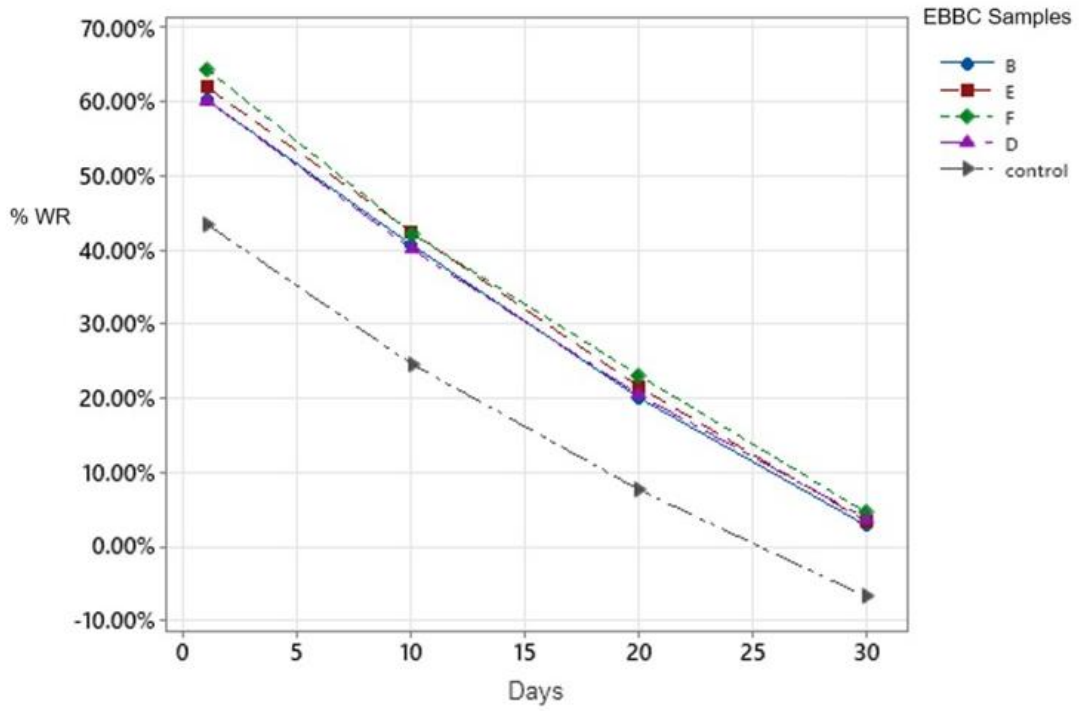

Figure 4.26: Water Retention (WR) of Soil with EBBC Pellet

4.10.7 Surface Morphology of EBBC Fertilizer Pellets

Scanning electron microscopy provided direct evidence of how encapsulation alters pellet surface structure and, by extension, nutrient release behaviour (**Figure 4.27**). Uncoated biochar–blended compost pellets (**Figure 4.27**a) exhibited a highly porous, sponge-like morphology with loosely aggregated particles. This structure is characteristic of co-composted biochar systems and reflects their high surface area and cation-exchange capacity, which favor the adsorption of ammonium, humic substances, and other nutrient species Khan et al., 2016; Prost et al., 2013). While advantageous for nutrient retention, such open porosity also facilitates rapid water penetration and uncontrolled nutrient loss under wet conditions. In contrast, encapsulated pellets showed a markedly different morphology. Fracture-surface micrographs (**Figure 4.27**b, c) revealed a continuous, well-adhered polymer coating tightly integrated with the biochar–compost matrix, with no visible interfacial gaps or delamination. This strong interfacial compatibility confirms effective film adhesion, a prerequisite for mechanical stability and regulated nutrient diffusion (Chen et al., 2018; Lawrencia et al., 2021). The

coating effectively transformed the pellet surface from an open, highly permeable matrix into a semi-permeable barrier capable of modulating water ingress and nutrient release. Clear differences were observed among coating formulations. Pellets coated with pure chitosan (**Figure 4.27**f) exhibited surface fissures and irregular film coverage, with cracks reaching up to 50 μm. These defects are attributed to drying-induced shrinkage and the inherent brittleness of chitosan in the absence of flexible co-polymers or plasticizers (Abraham et al., 2016; Fonseca-García et al., 2021; Gumelar et al., 2020).

In contrast, chitosan–starch composite coatings (**Figure 4.27**e) produced smoother, more uniform, and defect-free surfaces. This improved morphology reflects stronger intermolecular interactions and chain entanglement between chitosan and starch, resulting in cohesive films with enhanced mechanical integrity (Mendes et al., 2016; Ren et al., 2017; Zhang et al., 2020). Notably, the compact and continuous nature of the chitosan–starch coatings effectively limit rapid water infiltration and restricts nutrient diffusion pathways, reinforcing their role as sustained-release barriers. These microstructural observations are consistent with previous studies reporting superior performance of blended biopolymer coatings in controlled-release fertilizer systems (Ren et al., 2017; Wan Yusof et al., 2024). Collectively, the SEM evidence demonstrates that polymer blending not only improves coating integrity but also provides a structural basis for the observed improvements in nutrient retention and release control in encapsulated biochar–blended compost.

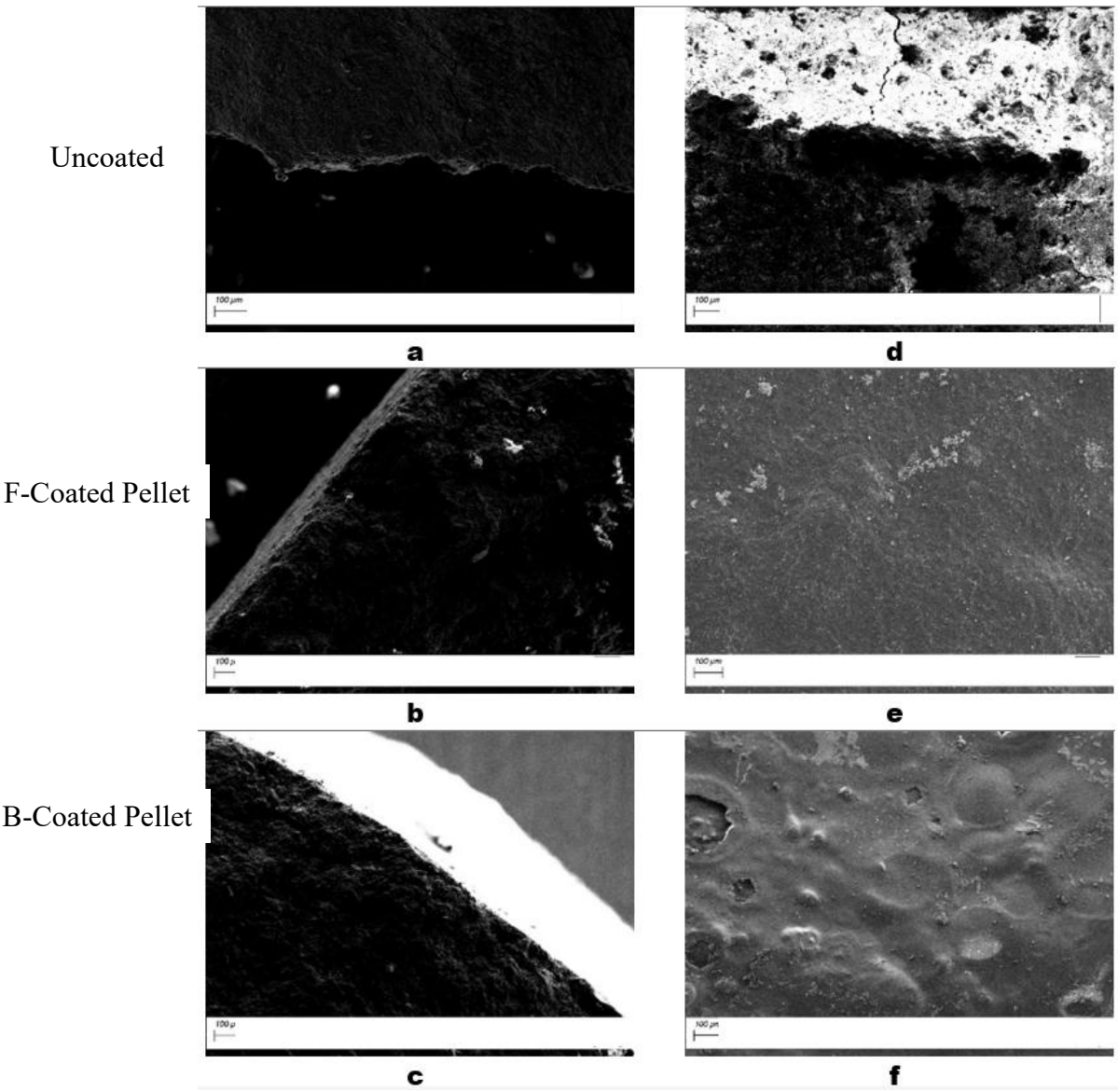

Figure 4.27: Surface and Fracture Morphology of Uncoated and Encapsulated Biochar–Blended Compost with Different Coating Materials

4.11 Effects of Mechanochemical Processing on Biochar–Blended Compost

Mechanochemical processing markedly transformed the structure and functional behaviour of biochar–blended compost, establishing a distinct performance pathway compared with encapsulated formulations. Rather than regulating nutrient release through an external diffusion barrier, mechanochemical activation reconfigured the composite matrix itself, producing nanoscale particles with enhanced surface reactivity and internal accessibility. This structural refinement fundamentally shifted the way nutrients are retained and exchanged within the material. The resulting Nano-BBC exhibited substantial particle size reduction and

a pronounced increase in reactive surface area. These changes are consistent with mechanochemical effects that promote bond rupture, lattice distortion, and the formation of oxygen-containing functional groups, collectively increasing surface charge density and nutrient-binding capacity (Yu et al., 2025). As a result, Nano-BBC functions as an intrinsically active nutrient carrier, capable of interacting dynamically with soil solutions, microbial metabolites, and plant roots at micro- and nanoscale, rather than relying solely on surface-controlled release mechanisms (Shafiq et al., 2023; Shahzadi et al., 2025). Milling conditions strongly influenced the extent of nanoscale refinement. Comparative analysis (**Table 4.7**) showed that ethanol-assisted mechanochemical processing produced the most uniform particle size distribution and the highest degree of dispersion.

Table 4.7: Experimental Matrix and Particle Size (nm) Under Different Milling Conditions

Run	Ball-to-powder ratio	Milling Time (h)	Solvent Volume (ml)	Ethanol (nm)	Water (nm)	Hexane (nm)	Solvent-less (nm)
1	50	4	5.2	465.20	2324.52	1006.83	1017.67
2	75	2	9.6	728.00	1025.01	828.477	1257.17
3	75	2	0.8	691.50	1240.00	1554.8	1149.97
4	75	6	9.6	933.79	1150.79	1543.18	1074.27
5	25	4	5.2	248.00	2415.00	1106.25	1557.13
6	50	4	5.2	466.10	2680.00	1359.00	1017.67
7	25	6	9.6	712.63	1378.61	2583.00	1164.03
8	25	2	0.8	629.00	1230.95	1445.00	2352.73
9	75	4	5.2	315.00	2044.58	667.051	999.00
10	50	6	5.2	573.60	2819.38	2522.25	954.13
11	75	6	0.8	310.00	1361.31	1827.00	1226.73
12	50	2	5.2	570.90	2596.30	2057.05	1483.87
13	50	4	9.6	817.90	1027.98	703.00	1031.27
14	50	4	0.8	540.00	1221.70	248.1.00	1134.73
15	50	4	5.2	465.02	2341.52	662.1.00	1017.67
16	25	2	9.6	300.00	1054.03	1792.68	2298.27
17	25	6	0.8	392.00	1551.33	1887.00	1478.16

Ethanol likely facilitated energy transfer during milling, limited particle agglomeration, and promoted surface functionalization, thereby enhancing the stability and reactivity of the nanosized composite. Together, these results demonstrate that mechanochemical processing enables precise control over particle size and surface chemistry, positioning Nano-BBC as a

highly responsive and efficient platform for nutrient delivery and soil interaction. This supports earlier evidence that solvent-assisted milling improves energy transfer efficiency and stabilizes newly formed reactive surfaces, yielding more homogeneous product dispersions (Kumar et al., 2020). The enhanced dispersion and increased reactivity observed in ethanol-milled Nano-BBC suggest improved nutrient exchange potential and stronger soil interaction during application.

4.11.1 Optimization of Biochar-Blended Compost Particle Size

The mechanochemical treatment of biochar-blended compost (BBC) resulted in substantial nanoscale refinement, with particle sizes ranging from approximately 230 to 2800 nm (Kumar et al., 2020). As shown in **Figure 4.28**, ethanol-based milling consistently produced the smallest and most uniformly dispersed nanoparticles, whereas water-based milling yielded the largest aggregates. Ethanol's performance aligns with its physicochemical properties: its moderate polarity and low surface tension enhanced wetting, reduced interparticle adhesion, and minimized cold welding, all mechanisms known to suppress re-agglomeration during intensive collisions (Naghdi et al., 2017). This stabilizing effect explains why ethanol-milled BBC maintained submicron particle distributions with high suspension stability. In contrast, aqueous milling produced particles as large as 2819.4 nm (Experiment 12), a result attributed to water-induced capillary bridging and stronger surface adhesion forces. This behaviour is well documented in wet-milled biochar and zeolitic systems, where water promotes agglomeration despite high impact energies (Pohshna & Mailapalli, 2023). These relationships are quantified by the regression model for volume mean particle size

$$\text{Volume mean} = 467 + 71\text{A} + 93\text{C} - 44\text{AB} + 84\text{AC} + 155\text{BC} - 195\text{A}^2 + 105\text{B}^2 + 211\text{C}^2$$

Equation 14

Where A is the ball-to-powder ratio, B is the milling time (h) and C is the mass of milling solvent. The negative AB coefficient ($p = 0.0076$) in the optimized regression model indicates that increased ball mass compensates for shorter milling times by intensifying impact energy. However, the negative A^2 term reveals a critical threshold beyond which excessive impact forces trigger agglomeration rather than refinement, an effect also noted in other studies (Pohshna & Mailapalli, 2023).

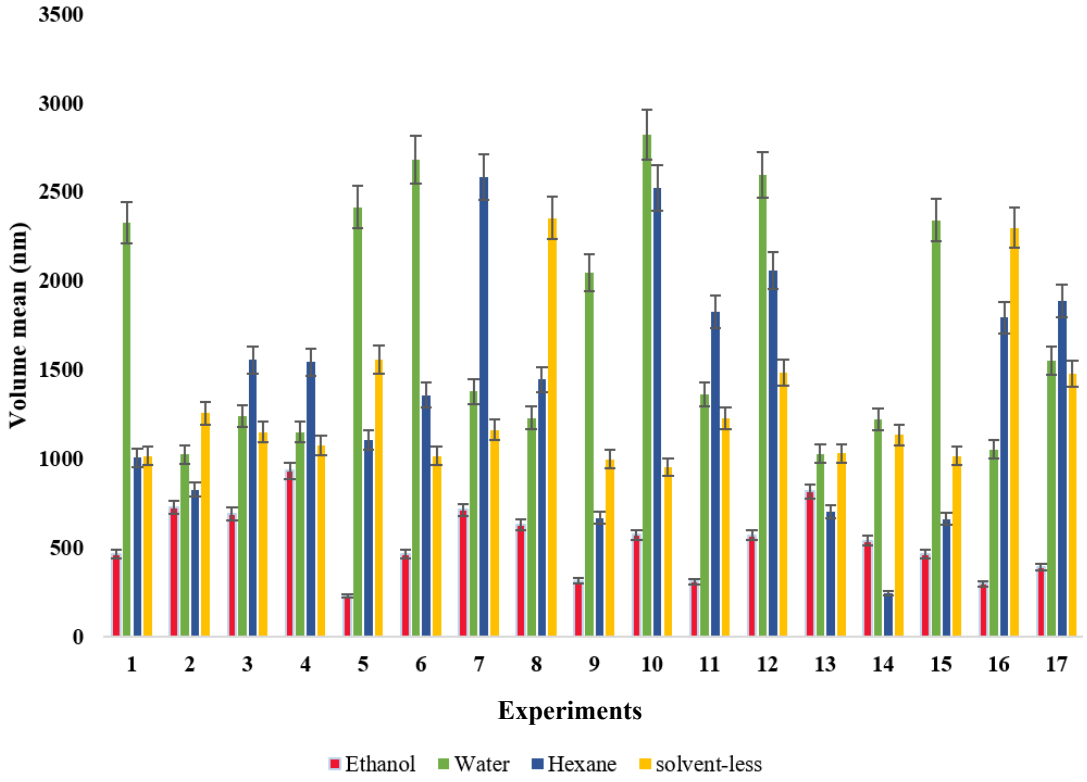

Figure 4.28: Comparison of Volume Mean Particle Size Across 17 Experimental Using Different Milling Solvents.

4.11.2 Analysis of variance

ANOVA was employed to evaluate the statistical significance of the quadratic model for particle size reduction, its lack of fit, and the significance of the individual model coefficients. As shown in **Table 4.8**, the model F-value of 42.91 corresponds to a reduced quadratic model that is highly significant ($p < 0.0001$). There is less than a 0.01% chance that an F-value this large could occur due to noise, confirming the model's reliability in describing the particle size reduction process. Based on the significance threshold ($p < 0.05$), the significant model terms include A, B, C, AB, BC, A^2, B^2, and C^2. Among the primary factors, the mass of milling solvent (C) was found to be the most significant factor influencing particle size reduction (F-value 92.49), closely followed by the ball-to-powder ratio (A) (F-value 87.72). While milling time (B) had a lower F-value (5.07) and a p-value of 0.0591, it remains a critical component of the reduced model structure.

The interaction effects were also prominent, specifically the interaction between milling time and solvent mass (BC) (F-value 61.51) and the interaction between BPR and time (AB) (F-

value 19.57). These results indicate that particle size reduction is not merely a function of individual parameters but depends heavily on the combined effects of the milling environment. Additionally, the significant quadratic terms (A^2, B^2, and C^2) confirm the non-linear nature of the milling process. Although the Lack of Fit was significant ($p < 0.0001$), the high F-value for the overall model and the relatively low residual sum of squares (12796.69) compared to the model sum of squares suggest that the quadratic model still captures the primary trends of the experimental data effectively. Similar observations regarding the dominance of solvent dynamics and ball-to-powder ratio in producing nanoparticles have been noted in related milling optimization studies (Pohshna et al., 2020, 2023).

Table 4.8: ANOVA for response surface reduced model for particle size reduction

Source	Sum of Squares	df	Mean Square	F-value	p-value	comment
Model	7.060E+05	9	78448.64	42.91	< 0.0001	significant
A-Ball-to-powder ratio	1.604E+05	1	1.604E+05	87.72	< 0.0001	significant
B-Milling Time	9261.07	1	9261.07	5.07	0.0591	significant
C-Mass of milling solvent	1.691E+05	1	1.691E+05	92.49	< 0.0001	significant
AB	35783.48	1	35783.48	19.57	0.0031	significant
AC	4057.20	1	4057.20	2.22	0.1799	Not significant
BC	1.124E+05	1	1.124E+05	61.51	0.0001	significant
A^2	1.408E+05	1	1.408E+05	77.02	< 0.0001	significant
B^2	24437.69	1	24437.69	13.37	0.0081	significant
C^2	1.095E+05	1	1.095E+05	59.92	0.0001	significant
Residual	12796.69	7	1828.10			
Lack of Fit	12796.02	5	2559.20	7643.98	0.0001	significant
Pure Error	0.6696	2	0.3348			
Cor Total	7.188E+05	16				
R^2	0.9822					
Adjusted R^2	0.9593					
Predicted R^2	0.8248					
Adeq. Precision	42.76					
Standard Deviation	8.35					
Coefficient of Variation	0.9822					

Furthermore, the model demonstrates a high degree of explanatory power, with an R^2 value of 98.22% (**Table 4.8**), indicating that the selected factors, specifically the ball-to-powder ratio, milling time, and the mass of milling solvent, account for a substantial proportion of the variability observed in particle size reduction. The Adjusted of 95.93% remains robust, even after accounting for the number of predictors. The close alignment between the adjusted values

suggests that the model is well-specified and avoids the inclusion of extraneous variables that might artificially enhance its apparent predictive capability (Bhattacharya, 2021; Md Saleh et al., 2020). A coefficient variation below 10% is considered very good, indicating high reproducibility and that the experimental error is low relative to the mean of the data (Menya et al., 2020).

4.11.3 Response surface

The provided response surface plots (**Figure 4.29**) illustrate the interactive effects of the independent variables, ball-to-powder ratio (A), milling time (B), and mass of wet milling Solvent (C), on particle size reduction (Zeta size). The three-dimensional surface and contour plots visualize how these factors influence the final particle size. In plot (a), increasing the ball-to-powder ratio (A) leads to a significant decrease in Zeta size, with the steepness of the curve indicating that the media ratio has a more pronounced initial effect than milling time (B). Plot (b) highlights the critical interaction between the media ratio and solvent mass (C); the distinct bowl-shaped curvature suggests a nonlinear relationship, where a specific balance is required to achieve the minimum particle size. Plot (c) demonstrates a strong interaction between milling time and solvent mass (BC), which aligns with your significant ANOVA F-value of 61.51. The convergence of the surface toward lower values shows that extended milling times, when paired with optimal solvent levels, effectively

The visual data in these plots further validates the statistical robustness of your model. The clear curvatures and gradients represent the significant linear and quadratic terms (A, C, A^2, B^2, and C^2) identified during analysis. With a high R^2 of 0.9822 and an Adjusted R^2 of 0.9593, the model explains over 98% of the variability in the milling process. Because these values significantly exceed the standard 0.75 threshold for agricultural and engineering models (Pohshna et al., 2023), the response surfaces can be considered highly reliable for predicting and optimizing the production of nanoparticle amendments.

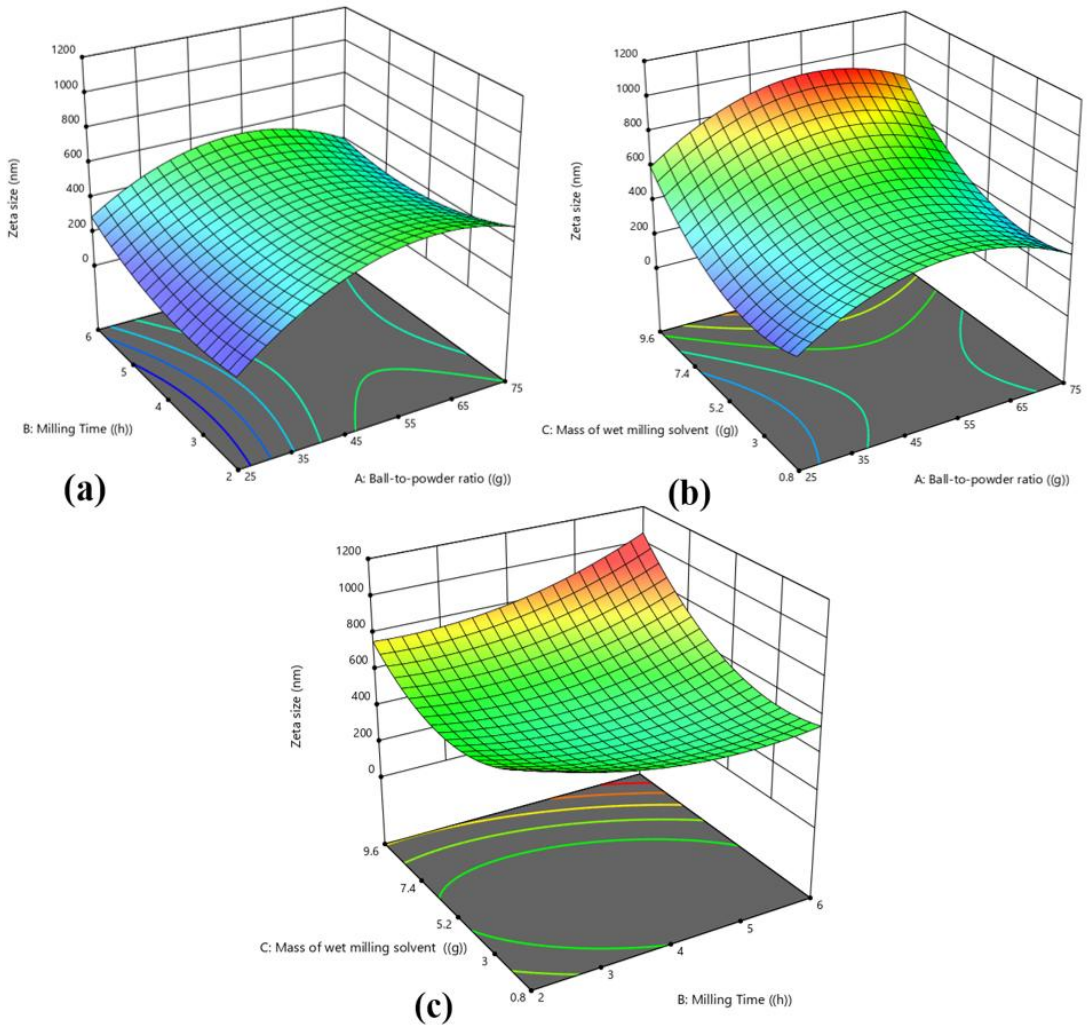

Figure 4.29: Response surface plots showing the interaction effects of ball milling parameters on Zeta size

The diagnostic plots (**Figure 4.30**) affirm the quadratic model's suitability and robustness in predicting particle size reduction. The predicted vs. actual plot shows data points tightly aligned along the diagonal, substantiating the model's strong predictive performance and aligning with its elevated value. The Residuals vs. Predicted plot shows random scatter within control limits, with no systematic patterns such as curvature or funnel shapes, indicating homoscedasticity. The normal plot of externally studentized residuals displays a linear alignment, verifying the normality of errors and upholding a fundamental ANOVA assumption for tests of coefficient significance.

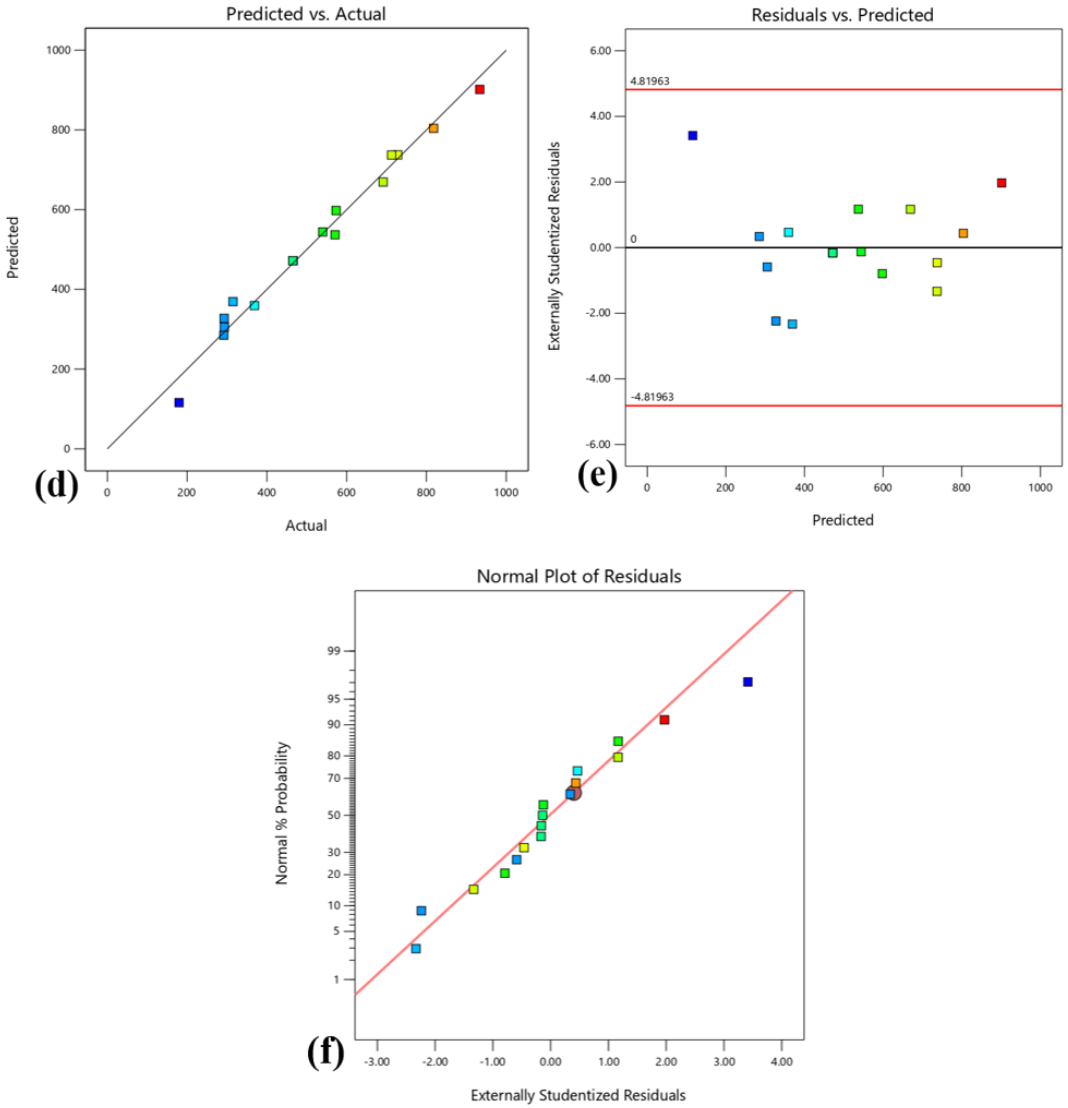

Figure 4.30: Diagnostic Plots for Regression Model Evaluating Adequacy of the Response Surface Methodology

4.11.4 FT-IR Analysis: Functional Group Evolution

The FT-IR spectra (**Figure 4.31**) provided for the BBC samples reveal that the choice of solvent during wet ball milling significantly influences the surface chemistry and functional groups of the resulting material. Across all samples, including the dry-milled No solvent control, characteristic peaks are consistently observed at approximately 1000 cm^{-1}, 1600 cm^{-1}, and 2900-3400 cm^{-1}. The intense peak near 1000 cm^{-1} is typically associated with C-O or Si-O stretching vibrations, while the peak around 1600 cm^{-1} corresponds to aromatic C=C or C=O stretching, both of which are common in carbonaceous materials like biochar. Notably, the sample processed with Water (Blue) exhibits a markedly broader and

more intense band in the 3200-3500 cm^{-1} region, indicating a higher concentration of hydroxyl (O-H) groups likely due to surface hydration or the introduction of oxygen-containing functional groups during the high-energy milling process. Further differences are evident in the C-H stretching region near 2900 cm^{-1}, where the Hexane (Green) and Ethanol (Red) samples show varying peak intensities. These shifts and intensity changes suggest that wet milling is more effective than dry milling at altering the surface functionalization, potentially by exposing internal pore networks or creating new reactive sites through mechanochemical activation. While the fundamental graphitic-like structure of the BBC remains intact across all solvents, the increased presence of oxygenated groups (carboxyl, phenolic, and hydroxyl) in the wet-milled samples, particularly with polar solvents such as water and ethanol, generally leads to improved dispersion and enhanced adsorption performance for environmental applications. Ethanol's polarity enhances hydrogen bond disruption and promotes mechanochemical cleavage, thereby increasing accessible reactive groups (Zouari et al., 2023). These FT-IR trends closely align with SEM morphological patterns. The enhanced exposure of functional groups in milled composite translates into higher cation exchange capacity, stronger nutrient-binding affinity, and improved potential for controlled nutrient release (Hagemann et al., 2017a; Hossain et al., 2020; Liu et al., 2019).

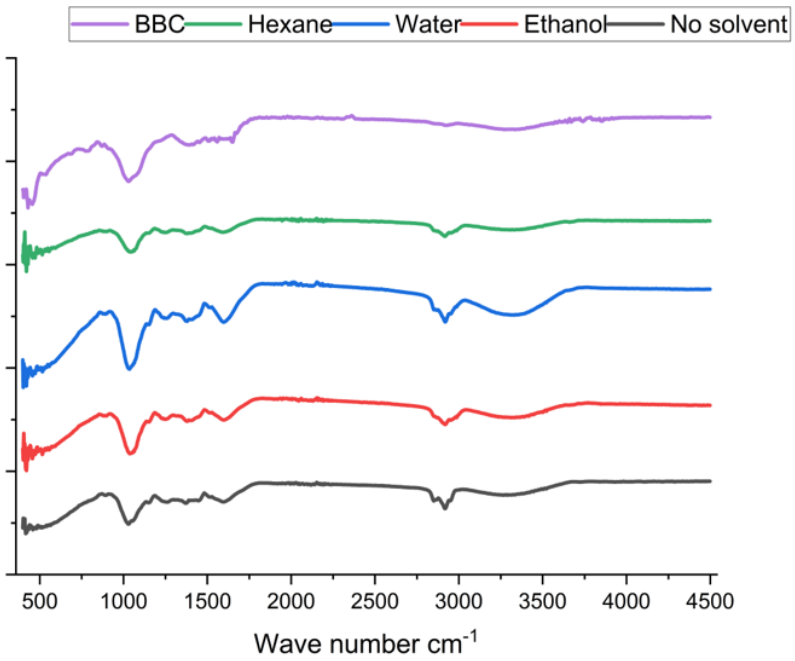

Figure 4.31. FI-TR Spectra of BBC Samples Prepared Using Different Wet Milling Solvents Compared to A Dry Milling (No Solvent) Control.

4.11.5 X-Ray Diffraction

XRD patterns (**Figure 4.32**) exhibited attenuation and broadening of the peak near 2θ ≈ 26°**,** indicative of graphitic disorder and amorphization**.** The X-ray diffraction patterns showed broad, low-intensity features across all samples, confirming the predominantly amorphous nature of the biochar–compost matrix. The unmilled Biochar-Blended Compost exhibited the highest overall intensity, reflecting a more ordered structure with residual mineral phases. A consistent peak near 26° (2θ) indicates the presence of quartz or related silicates, common in compost–biochar mixtures and biomass ash (Radziemska et al., 2022). Ethanol-assisted milling produced the most pronounced amorphous hump (20 – 24°), indicating extensive structural disordering and breakdown of weakly crystalline regions. This enhanced amorphization aligns with FT-IR observations and reflects ethanol's effectiveness in softening the organic matrix, promoting lattice disruption during mechanochemical processing (Kumar et al., 2020; Lyu et al., 2017). The weakening or loss of characteristic carbon diffraction peaks further demonstrates the destruction of ordered carbon domains and the transition toward a more amorphous carbon structure (Radziemska et al., 2022; Wenger & Hanusa, 2023). Such transformations are expected under high-energy milling, which reduces crystallinity and increases structural disorder (Cao et al., 2022; Lyu et al., 2017).

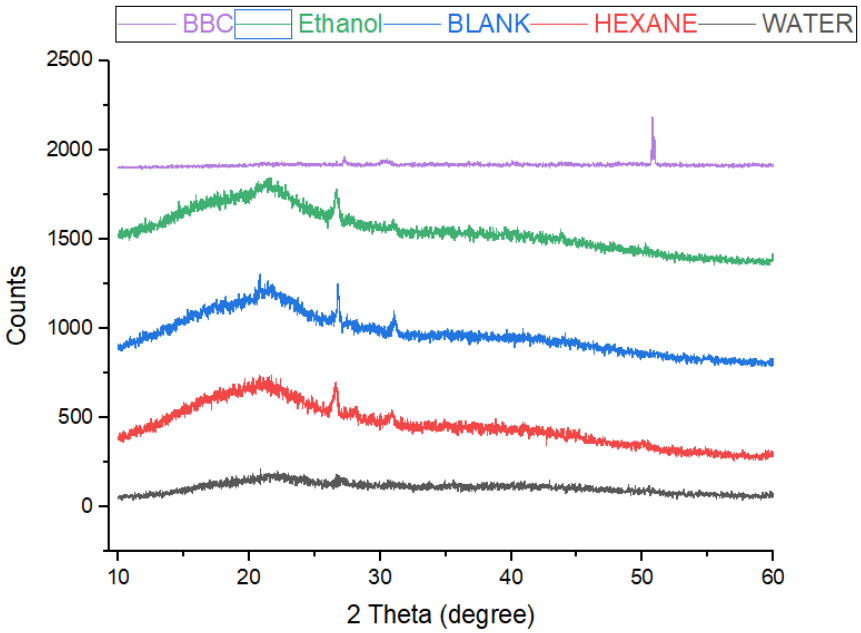

Figure 4.32: XRD Patterns of Biochar–Compost Composites Processed Under Different Mechanochemical Conditions

Water-milled and solvent-less samples showed partial disordering and limited modification. Water-induced swelling and dry-milling inefficiency hindered full amorphization compared to ethanol-milling, reflecting reduced energy transfer and re-agglomeration tendencies. (Kumar et al., 2020; Naghdi et al., 2017). Hexane-milled composites exhibited the weakest amorphous signatures and the lowest intensities, confirming minimal structural alteration. Hexane's nonpolar nature offers little capacity for matrix swelling or bond weakening, which explains the limited mechanochemical activation and is consistent with the subdued morphological and chemical changes observed in FT-IR analyses (Amusat et al., 2023). Overall, the XRD results strongly corroborate the FT-IR findings: ethanol-assisted milling induces the greatest structural reorganization, producing a highly disordered, reactive composite. This reduction in crystallinity and increase in amorphous content enhances cation exchange capacity, nutrient binding affinity, and overall fertilizer reactivity key advantages of mechanochemically modified biochar (Kumar et al., 2020; Wenger & Hanusa, 2023). In contrast, hexane and dry milling yield only minor structural changes, resulting in much lower enhancement potential.

4.11.6 Morphological and surface characteristics

SEM micrographs revealed pronounced structural differences among biochar–compost composites produced by ethanol, hexane, water, and solventless milling, demonstrating that solvent polarity and milling medium strongly dictate particle fragmentation, surface morphology, and micro-aggregate formation. These structural attributes are critical determinants of composite reactivity, nutrient retention, and performance in soil systems. Ethanol-assisted milling produced highly disrupted, fissured, and porous microstructures at both 10 μm and 2 μm scales. (**Figure 4.33**). Extensive microcracking and particle detachment indicate efficient breakdown of organic–biochar associations, consistent with ethanol's intermediate polarity and its capacity to weaken hydrogen bonding and capillary forces within heterogeneous matrices (Ng et al., 2022; Raczkiewicz et al., 2024; Zouari et al., 2023). This enhanced mechanochemical activation aligns with evidence that ball milling can dramatically reduce particle size and increase specific surface area, exposing reactive edge sites and improving adsorption potential (Cao et al., 2022; Kumar et al., 2020; Lyu et al., 2017). The resulting porosity and surface complexity support greater nutrient loading, cation exchange, and microbial colonization, key attributes for improved soil fertility and nutrient-use efficiency (Hao et al., 2024; Hossain et al., 2020; Liu et al., 2019).

Hexane-assisted milling yielded smoother, more compact surfaces with minimal pore development structures indicative of limited particle disruption. The low polarity of hexane likely limited softening of organic domains, resulting in retained plate-like structures and broader lamellar features. These characteristics suggest lower reactive surface area and reduced capacity for nutrient exchange, highlighting the inefficiency of nonpolar milling solvent for composite refinement. Water-assisted milling produced heterogeneous textures with irregular fissures, partially swollen regions, and mixed microporous–dense domains. Water's high polarity facilitated partial softening of lignocellulosic components but simultaneously promoted re-agglomeration through capillary condensation, a known mechanism that drives particle clumping during wet milling (Ng et al., 2022). The outcome reflects moderate but inconsistent particle refinement and reduced uniformity relative to ethanol-assisted milling.

Solvent-less milling produced the least-refined structures, characterized by dense aggregates, broad flakes, and minimal micro-fracturing. Without a liquid medium to dissipate heat or modulate interparticle forces, mechanical impacts alone were insufficient to overcome the cohesive strength of the biochar-blended compost matrix. Such dry milling conditions often promote particle agglomeration due to increased surface energy and cold welding (Naghdi et al., 2017; Rajaonarivony et al., 2022), unless milling parameters are carefully optimized (Kumar et al., 2020; Yameen et al., 2024). Although solvent-free mechanochemical activation can enhance porosity under some conditions (Amusat et al., 2023; Kiani et al., 2023), its effectiveness is limited here by strong biochar–organic cohesion. These morphological trends translate directly into differences in functional agronomic performance. Composites produced with ethanol exhibit the most advantageous architecture, finely textured, highly porous, and rich in reactive sites, properties associated with improved nutrient sorption, controlled release, and stronger soil–microbe interactions (Hossain et al., 2020; Liu et al., 2019). In contrast, the minimally fractured composites from hexane and solvent-less treatments are likely to exhibit slower nutrient exchange and reduced reactivity. Overall, ethanol-assisted milling emerges as the most efficient method for producing structurally optimized biochar–compost composites, offering a superior platform for precision nutrient delivery and long-term soil fertility enhancement.

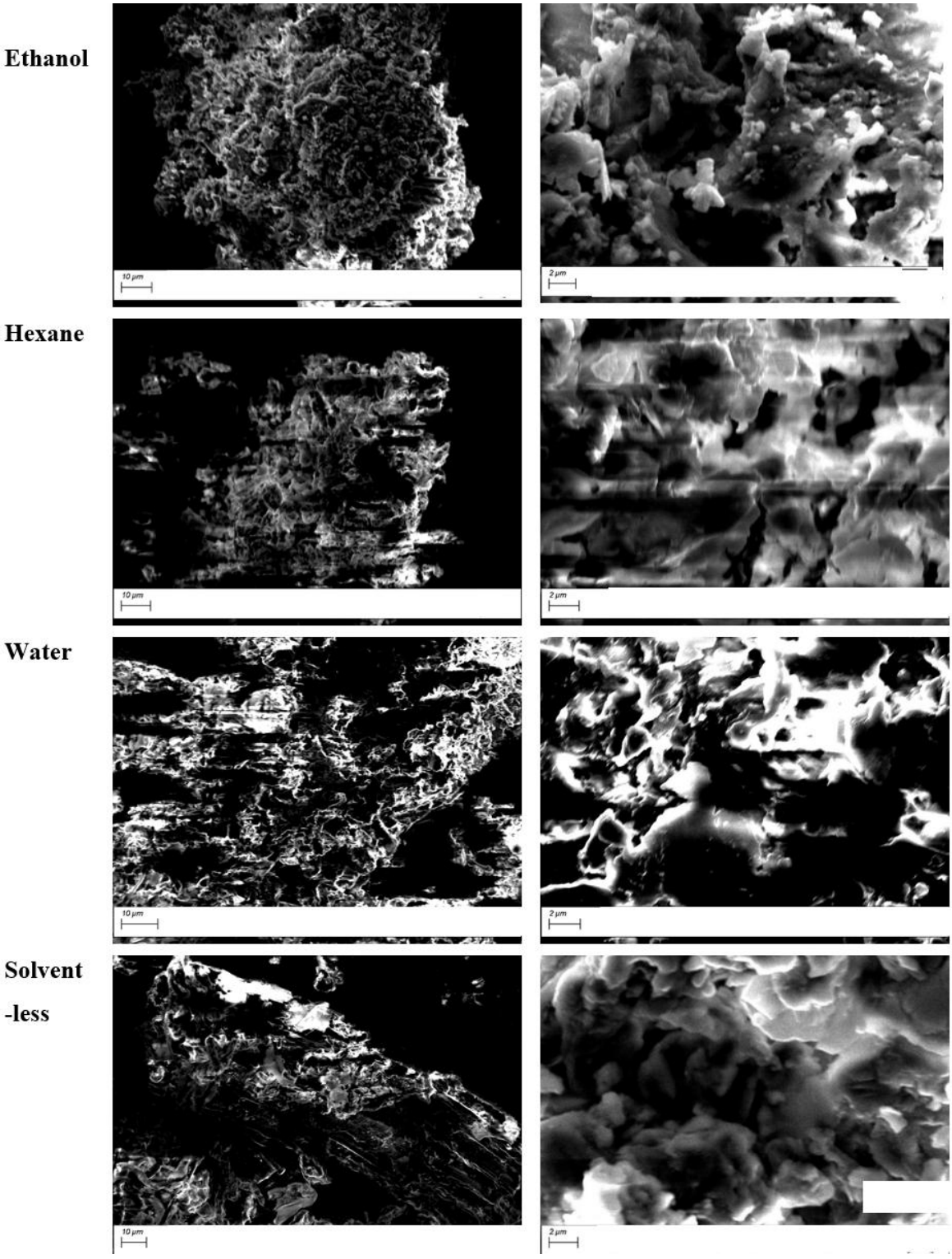

Figure 4.33: Scanning Electron Micrographs of Nano-Biochar-Blended Compost Synthesized Using Different Milling Solvents

4.11.7 EDX Elemental Composition: Surface Oxygen Incorporation

Elemental analysis using Energy-dispersive X-ray spectroscopy (EDX) confirmed that solvent-assisted milling significantly enhances oxygen incorporation into the biochar-blended compost (BBC) matrix. As detailed in **Table 4.9**

Table *4.9*, treatments utilizing ethanol (38.4%) and water (38.0%) achieved the highest oxygen (O) concentrations, representing a substantial increase over the unmilled BBC control (29.97%).

Table 4.9*:* Elemental Composition of Nano-BBC After Milling in Different Solvents

Milling solvent	**Carbon (C) %**	**Oxygen (O) %**
Hexane	53.76	33.13
Solvent-less	67.21	26.2
Ethanol	57.99	38.44
water	58.27	38.02
BBC	64.00	29.97

This enrichment elevates the O/C atomic ratio, a key indicator of surface oxidation and the formation of oxygen-containing functional groups (e.g., carboxyl and hydroxyl groups). These modifications are essential for increasing the material's hydrophilicity and chemical reactivity, thereby improving soil water retention and nutrient-holding capacity. In contrast, the solvent-less (26.2%) and hexane-milled (33.13%) samples showed lower oxygen levels, likely due to restricted oxidative activation in the absence of polar liquid media. This trend aligns with recent findings by Zouari et al. (2023), suggesting that wet milling effectively creates new reactive sites through mechanochemical surface oxygenation

4.11.8 Macronutrient and Metal Content of Nano-BBC

The mechanochemically synthesized Nano-BBC exhibited substantial improvements in the availability and distribution of essential macronutrients. As shown in **Figure 4.34**, ethanol-assisted Nano-BBC contained elevated concentrations of Ca, K, Mg, and Na nutrients vital for plant metabolic and structural processes. The enrichment of these cations can be attributed to the high density of negatively charged functional sites introduced during ethanol-assisted milling, which promotes electrostatic adsorption and ion exchange (Antonangelo et al., 2021;

Kumar et al., 2020). Among these, Ca and Mg play particularly crucial roles in improving soil structure and fertility. Their divalent nature enhances the cation CEC and neutralizes acidic soil conditions, thereby creating a favorable environment for nutrient uptake. These findings are consistent with those of Jindo et al. (2012), who reported enhanced macronutrient availability in biochar–compost systems derived from manure-based feedstocks. The Fe concentration in ethanol-assisted Nano-BBC was also noteworthy. Iron not only functions as an essential micronutrient for chlorophyll synthesis but also acts as a redox buffer in soil systems, aiding in pH regulation and the immobilization of toxic metals (Liang et al., 2024). The elevated Fe levels, therefore, reinforce the capacity of Nano-BBC to support soil remediation and enhance nutrient cycling. Equally important, the concentrations of potentially toxic elements, notably Cd, Pb, and Zn; were either negligible or below detection limits. The recorded negative Pb and Zn values **(Figure 4.34)** suggest concentrations lower than the analytical quantification threshold, a phenomenon commonly observed in bio-based nanoparticles produced via solvent-assisted mechanochemical treatment (Peterson et al., 2012; Zhang et al., 2022). This reduction is likely due to the metal-binding capacity of oxygen-rich functional groups, which stabilize and immobilize trace contaminants, thereby minimizing ecotoxicological risks. These findings bear significant agronomic implications. Heavy metals are known to impair seed germination and early seedling growth even at trace levels (Joseph et al., 2021; Zhang et al., 2022). The observed combination of high nutrient enrichment and low PTE contamination indicates that ethanol-assisted Nano-BBC can serve as a safe, high-performance organic nano-fertilizer. As previously discussed, this unique compositional balance enhances nutrient bioavailability while ensuring environmental protection, thereby advancing sustainable soil fertility management.

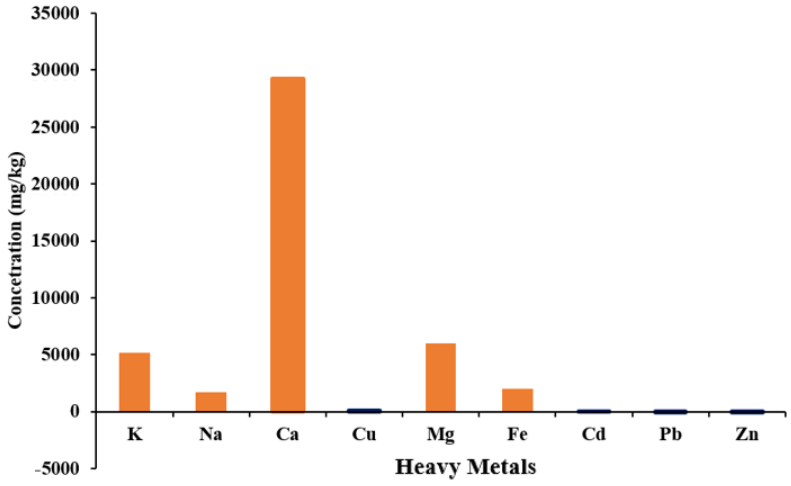

Figure 4.34: Toxic (Black Bars) and Non-Toxic (Orange Bars) Metal Concentration of Nano-Biochar-Blended Compost in mg kg^{-1}

4.11.9 Physicochemical Properties of Nano-BBC

The physicochemical characterization of ethanol-assisted Nano-BBC (**Table 4.10**) revealed distinct modifications that collectively enhance its functional potential as a soil amendment. The material displayed a slightly acidic pH (5.56), which falls within the optimal range for nutrient solubility and micronutrient availability in most agricultural soils. This pH range also complements the alkaline buffering capacity of many tropical soils, facilitating balanced nutrient exchange processes (Tsai & Chang, 2020). The EC of 1328.33 µS/cm indicates a moderate ionic strength conducive to nutrient mobility without causing salinity stress. The organic matter (91.00%) and volatile matter (93.28%) contents were exceptionally high, reflecting the preservation of biologically active organic fractions during mechanochemical processing. These properties suggest a strong potential for improving soil organic carbon pools and stimulating microbial activity, both of which are essential for sustained soil fertility and structure formation (Joseph et al., 2021; Zhang et al., 2022). The ash content (7.42%) and fixed carbon fraction (0.44%) were relatively low compared with conventional BBC formulations, implying that mechanochemical activation increased the proportion of labile, reactive carbon species. This compositional shift promotes rapid nutrient mineralization and bioavailability, an attribute desirable for short-term crop response (Tsai & Chang, 2020).

Elemental analysis revealed macronutrient concentrations of N (2.8%), P (3.0%), and K (5.38%), exceeding those typically reported in standard biochar–compost formulations (Jindo et al., 2012; Vandecasteele et al., 2016). The relatively narrow C:N ratio (9.8) reflects a highly decomposed organic matrix favorable for microbial nitrogen immobilization and steady nutrient release. Furthermore, the CEC (50.64 cmol/kg) was notably high, showing the strong ion-exchange capacity imparted by oxygenated functional groups formed during ethanol-assisted milling (Tsai & Chang, 2020; Yan et al., 2019). Collectively, these physicochemical parameters signify a functionally enhanced material that combines high reactivity, strong nutrient retention, and balanced chemical properties suited for both short-term nutrient delivery and long-term soil conditioning. The combination of moderate acidity, high organic content, and strong cation exchange characteristics positions Nano-BBC as a superior biofertilizer and soil amendment compared to unmodified biochar blended compost.

Table 4.10: Physicochemical properties of nano-biochar-blended compost compared with conventional biochar-blended composts

Parameter	Nano-biochar-blended compost (Nano-BBC) (this study)	Biochar-blended compost (previous studies) (D'Hose, Debode, De Tender, Ruysschaert, & Vandecasteele, 2020; Jindo et al., 2012; Tazebew et al., 2024; Vandecasteele et al., 2016)
Specific gravity	0.81 ± 0.074	0.59 - 1.65
Moisture content (%)	12.44 ± 0.176	1.98 - 66.2
LOI[a] organic matter (%)	91.00 ± 0.048	10.9 - 63.2
Volatile matter (%)	93.28 ± 0.005	69.8 - 96.9
Ash content (%)	7.42 ± 0.005	1.5 - 65.7
Fixed C content (%)	0.44 ± 0.001	1.06 - 40.3
pH	5.56 ± 0.091	6.73 – 10.87
EC[b] (μS/cm)	1328.33 ± 8.733	7 - 4150
TDS (mg/l)	536.23 ± 0.925	-
N (%)	2.85 ± 0.006	1.23 - 2.6
P (%)	3.00 ± 0.090	0.05 - 0.59
K (%)	5.38 ± 0.056	1.35 –
C:N[c]	9.8	8.61 – 11.55
CEC[d]	50.64	49.70 – 58.02
WHC[d] (gH_2O/gBBC)		

[a] Loss on ignition
[b] Electrical Conductivity
[c] Carbon to nitrogen ratio
[d] Cation Exchange Capacity (meq/100)
[d] Water holding capacity

4.11.10 Particle Size Distribution of Nano-BBC

Particle size analysis revealed clear differences between solvent-free and ethanol-assisted milling processes. Dry milling produced a dominant particle-size peak at 2298 nm, yielding submicron fractions consistent with prior mechanochemical studies (Amusat et al., 2021). In contrast, ethanol-assisted milling significantly reduced particle size, yielding a narrow, uniform nanoscale at 230 nm (**Figure 4.35**). This refinement increases surface area and reactive site density, improving nutrient adsorption, retention, and bioavailability in soil systems. Compared to mean particle sizes (296 nm) reported for nano-fertilizers, ethanol-assisted Nano-BBC

showed uniformly dispersed nanoparticles at a polydispersity index of 0.3797. The consistent morphology in **Figure 4.35**, depicting smooth, well-dispersed nanoscale aggregates, demonstrates precise control through solvent-mediated ball milling. Collectively, these results confirm that ethanol-assisted mechanochemical processing achieves a better particle size reduction, colloidal stability, and uniformity. The resulting Nano-BBC, with optimized particle size, enhanced surface chemistry, and nutrient-enriched composition, represents a next-generation biofertilizer with potential for scalable, sustainable agricultural applications.

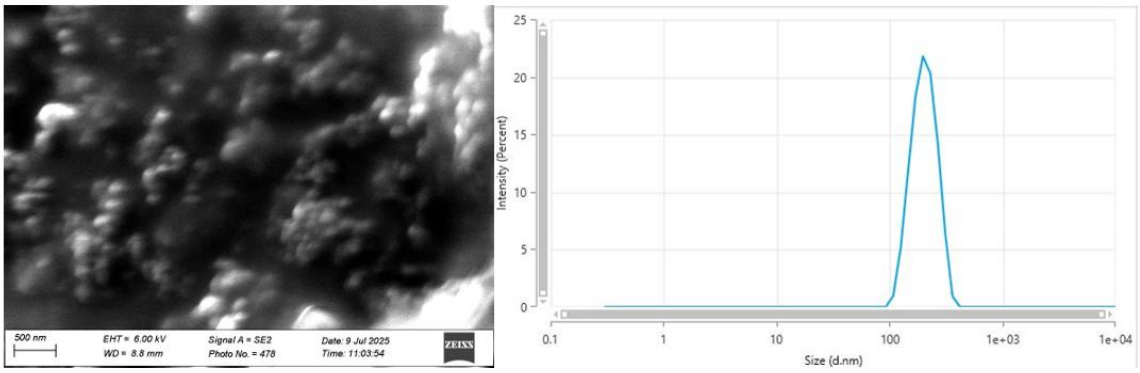

Figure 4.35: Morphological and size characterization of ethanol-assisted Nano-BBC

4.12 Nutrient Release Kinetics of EBBC Pellets and Nano-BBC

Nitrogen release profiles (**Figure 4.36**) demonstrate how encapsulation and nano-sizing distinctly regulate nutrient release behaviour. Encapsulated biochar-blended compost pellets exhibited strong early-stage control over nitrogen diffusion. By day 5, coated formulations (B, D, E, and F) released only 8–12% of total nitrogen, compared with nearly 20% from uncoated BBC. This early retention confirms that intact chitosan–starch films effectively restrict water ingress and delay nitrogen dissolution, consistent with reported behaviour of biopolymer-coated controlled-release fertilizers (Ren et al., 2017; Rubel et al., 2024; Wan Yusof et al., 2024; Yusof et al., 2019; Zhang et al., 2020). As hydration progressed, EBBC pellets maintained a gradual and sustained release pattern, reaching 35–45% nitrogen release by day 20 and 40–48% by day 30. These values satisfy established controlled-release benchmarks (Lawrencia et al., 2021), confirming coating integrity over the test period. Among the formulations, the chitosan-rich CH/S-67 coating (Formulation F) exhibited the slowest release, reflecting enhanced film cohesion driven by strong hydrogen bonding between chitosan amino groups and starch hydroxyl groups (Ren et al., 2017; Wan Yusof et al., 2024). The release

pathway followed a multistage process involving initial film hydration, internal nutrient solubilization, and diffusion-controlled transport through the polymer matrix.

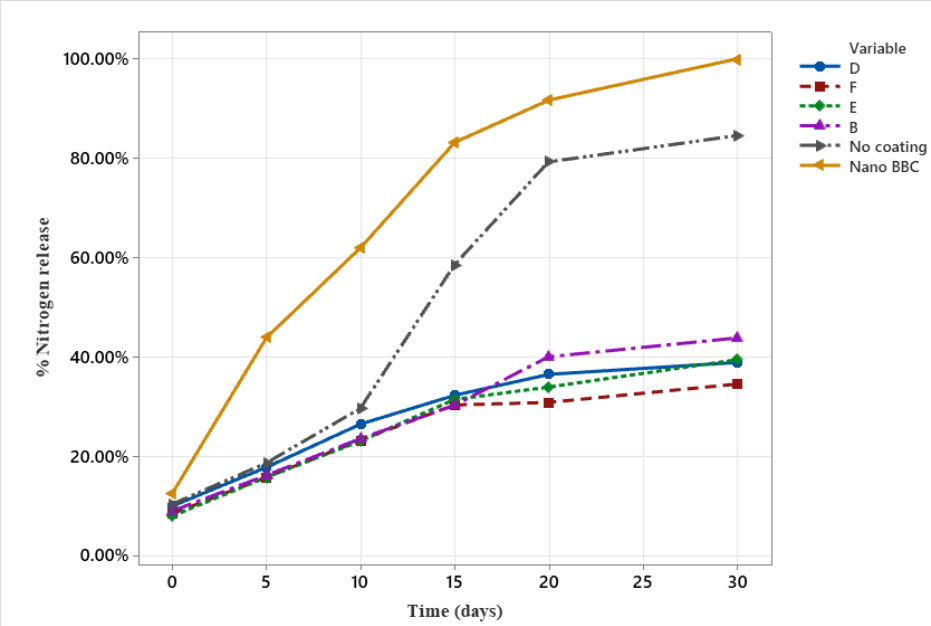

Figure 4.36: Nitrogen release dynamic profiles of encapsulated biochar-blended compost (D, F, E, B), Nano-BBC and uncoated fertilizer pellets over a 30 days in soil-simulated conditions.

In contrast, uncoated compost showed rapid nitrogen mobilization, releasing nearly 60% by day 15 and approximately 85% by day 30. This accelerated release reflects unrestricted water penetration and rapid dissolution of nitrogenous compounds, highlighting the susceptibility of conventional BBC to nutrient loss under aqueous conditions. Nano-BBC displayed a markedly different release regime. More than 40% of nitrogen was released within the first 5 days, exceeding 80% by day 15, with complete release occurring before day 30. This rapid mobilization is attributed to nanoscale particle size, which dramatically increases surface area and exposure of reactive sites, enhancing nutrient exchange with the surrounding solution (Ávila-Quezada et al., 2022; Dhiman et al., 2025; Mim et al., 2025). Unlike EBBC, nutrient regulation in Nano-BBC arises from internal surface reactivity rather than diffusion barriers, favouring fast nutrient availability rather than prolonged release. Release mechanism analysis using the Ritger–Peppas model (**Figure 4.37**) further clarified transport dynamics. The uncoated BBC pellet exhibited an n value of 0.622, indicating anomalous (non-Fickian) transport governed by both diffusion and matrix relaxation or disintegration. In contrast, EBBC formulations showed n values between 0.4162 and 0.4582, confirming Fickian diffusion as the

dominant mechanism, where nitrogen movement is controlled by concentration gradients across structurally stable coatings (Palansooriya et al., 2025; Wang et al., 2021). All experiments were conducted under controlled aqueous conditions, minimizing microbial activity and ionic interactions. While this preserved coating stability, previous studies indicate that enzymatic degradation and multivalent ion interactions in soil can increase coating permeability and alter release kinetics (Mendes et al., 2021; Yan et al., 2023; Song et al., 2024). These findings therefore establish a mechanistic baseline for interpreting EBBC and Nano-BBC behaviour under field-relevant conditions assessed in subsequent sections.

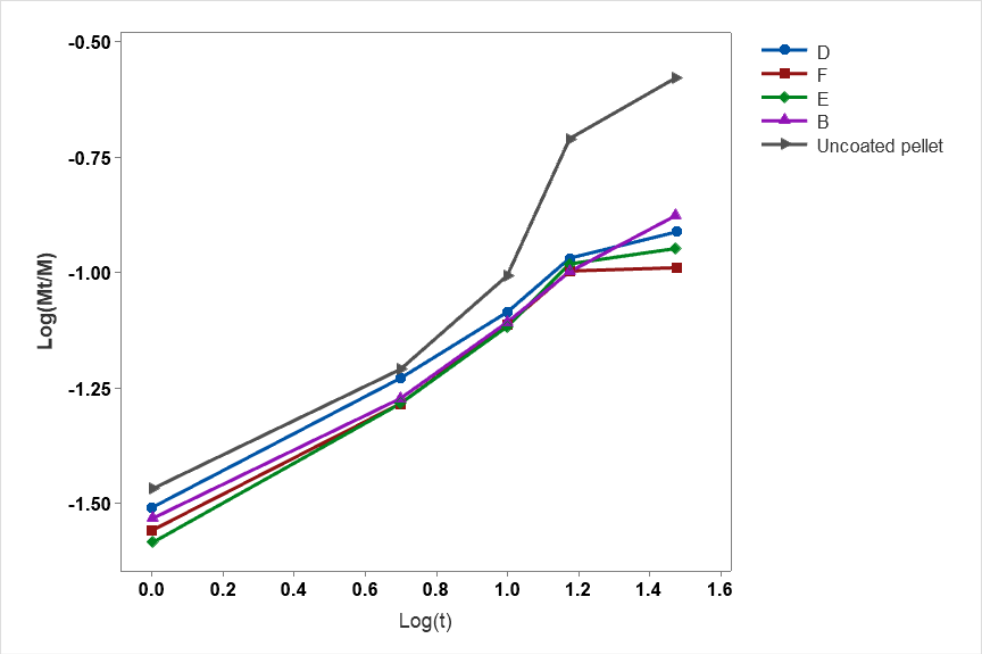

Figure 4.37: Log–Log Plot of Nitrogen Release Profiles of encapsulated biochar-blended compost (D, F, E, B) and uncoated fertilizer pellets

Table 4.11: Kinetic Parameters for Nitrogen Release from Coated and Uncoated EBBC Pellets

Sample	Release Exponent (n)	Release Constant (K)	R^2(%)
D	0.4215	0.031	98.76
E	0.4162	0.028	96.43
F	0.4582	0.026	97.72
B	0.4521	0.028	99.10
Uncoated pellet	0.622	0.030	93.26

4.12.1 Leachate Characteristics Under Simulated Rainfall Events

The analysis of leachate characteristics and nutrient loss dynamics during simulated rainfall events clearly demonstrates the superior environmental performance of modified organic fertilizers, particularly encapsulated biochar-blended compost, in minimizing nutrient leaching relative to conventional synthetic fertilizers. Synthetic fertilizer treatments consistently produced extremely high electrical conductivity and total dissolved solids in their leachates, with values 20–30 times higher than those of the organic formulations, indicating rapid, massive flushing of soluble salts and nutrients immediately after application (**Table 4.12**). Such accelerated nutrient losses from synthetic fertilizers are well documented as major contributors to groundwater contamination and eutrophication, especially in high-rainfall environments (Hina, 2024; Rupp et al., 2024). In comparison, all biochar-blended compost treatments exhibited markedly lower EC and TDS, reflecting enhanced nutrient retention and slower solubilization within the soil matrix (Gao et al., 2025; Khan et al., 2023). A similar trend was observed for salinity: synthetic fertilizer leachates contained extremely high salinity levels (18–19 ppt), which are known to induce osmotic stress, root burn, and soil structural decline, whereas all organic treatments maintained salinity values below 1.1 ppt, indicating minimal salinity hazard (Liu et al., 2023; Peng et al., 2023; Tarolli et al., 2024). Notably, while unmodified BBC showed moderate nitrate release and Nano-BBC exhibited low but detectable nitrate concentrations, only EBBC achieved complete nitrogen retention, with no measurable nitrate detected in the leachates during both rainfall events. This exceptional performance can be attributed to the tight nutrient encapsulation and controlled-release behaviour of the EBBC matrix, which effectively prevents rapid nutrient flushing (Benlamlih et al., 2021; Faez et al., 2024; Helal et al., 2023).

In addition to its superior nutrient retention, EBBC also generated the lowest leachate volume (6.5 mL, compared with 18–20 mL from the other treatments), highlighting its enhanced water-holding capacity, an essential agronomic advantage in drought-prone cropping systems (Hao et al., 2024). The stable, mildly alkaline pH values recorded for EBBC and Nano-BBC leachates further suggest a beneficial buffering effect provided by the biochar–encapsulated matrix, reducing the risk of soil acidification (Hafez et al., 2020). Overall, these findings affirm that EBBC provides unmatched advantages in water retention, nitrogen conservation, and controlled nutrient release, resulting in near-zero leaching losses even under repeated rainfall

events. Accordingly, EBBC emerges as a highly effective, environmentally responsible fertilizer suitable for sustainable agriculture, particularly in sandy soils, highly permeable agroecosystems, and regions experiencing erratic or intense rainfall (Mikajlo et al., 2024).

Table 4.12: Leachate Physicochemical Properties of Fertilizer Treatments Under Successive Simulated Rainfall Event

	Fertilizer type	EC (µS/cm)	TDS (mg/l)	Ph	Salinity (ppt)	NO_3^- -N (mg/l)	NO_3^- (mg/l)	leachate (mL)
Rainfall event 1	Nano-BBC	821.90	327.10	8.00	0.35	3.10	13.80	18.5[a]
	EBBC	1,299.90	520.70	8.29	0.61	-	-	6.5[c]
	BBC	802.90	318.90	8.32	0.33	24.40	107.90	20[d]
	Synthetic	30,676.10	12,092.50	9.03	18.73	575.90	2,849.40	18[b]
	Control	502.60	298.80	8.40	0.31	15.20	3.40	20[b]
	CH	912.30	362.20	8.14	0.39	1.50	6.70	16[b]
Rainfall event 2	Nano-BBC	1,223.60	487.90	8.18	0.56	3.10	13.80	18[a]
	EBBC	2,189.90	821.00	7.87	1.01	-	-	6.50[c]
	BBC	1,570.10	616.90	8.02	0.74	0.10	0.20	20.00[d]
	Synthetic	30,280.60	12,005.11	8.99	19.22	475.90	2,949.40	18.00[b]
	Control	502.60	196.20	8.34	0.17	1.00	5.20	20.00[b]
	CH	1,107.10	438.80	8.33	0.50	1.00	5.20	16.00[b]

a – 24 h, b – 48 h, c – 50 h, d – 72 h

4.13 Germination Bioassay

This section reports the early agronomic performance of the engineered fertilizer formulations: biochar-blended compost and Nano-BBC as evaluated in a standardized 48-hour germination bioassay. The assay quantified germination response and initial seedling vigor to determine the extent to which mechanochemical modification improves the biological functionality of biochar-blended compost systems. The results indicate that mechanochemical milling produced notable improvements in fertilizer performance, reflected in higher germination indices, improved root development, and more vigorous shoot emergence compared with unmodified controls. These outcomes corroborate previous studies demonstrating that structural refinement of biochar–organic matrices can increase nutrient accessibility, mitigate the formation of phytotoxic intermediates, and stimulate early plant growth (Kumar et al., 2020; Shafiq et al., 2023; Yu et al., 2025)

4.13.1 Germination Index of Optimized BBC

The germination index (GI) is a sensitive bioassay parameter that integrates both seed germination rate and root elongation, providing an indicator of compost maturity and phytotoxicity (Ji et al., 2023; Kong et al., 2022). The optimized BBC formulation achieved a GI of 89.2%, exceeding the phytotoxicity threshold of 70% (**Table 4.13**). This performance indicates that the compost had reached biological maturity and was free from inhibitory compounds typically associated with immature poultry manure composts (Yang et al., 2021). The improvement in GI relative to the control compost (28.5%) is attributed to the synergistic amendment with *Tithonia diversifolia* biomass and biochar, both of which accelerated organic matter degradation and nitrogen stabilization. These effects are reflected in the reduced C/N ratio (9.8), consistent with mature compost characteristics (Mousavi et al., 2024). The incorporation of biochar likely enhanced microbial habitat stability and improved carbon mineralization efficiency, thereby lowering the C/N ratio through increased microbial turnover (Cui et al., 2017). **Table 4.13** summarizes the physicochemical attributes of the optimized compost at the determined optimum formulation (60 kg *Tithonia diversifolia*, 5.67 kg biochar, and 35 kg chicken manure). The nitrogen, phosphorus, and potassium concentrations all exceeded those in the control compost, confirming superior nutrient enrichment and stabilization. The optimized pH (7.02) further indicates a neutral and agronomically favorable compost, while the lower EC (205.5 µS/cm) relative to the control (3940.7 µS/cm) reflects reduced salinity stress, an important parameter for seed germination and seedling establishment (Hwang et al., 2020).

Table 4.13: Germination Index and Concentration of Biochar-Blended Compost (60kg *Tithonia Diversifolia*, 5.67kg Biochar and 35kg Chicken Manure)

Parameter	Optimized Compost	Control compost	Typical range ((Hwang et al., 2020; Ji et al., 2023; Kong et al., 2022; Mlangeni, 2013; Nurin et al., 2024; Ravindran et al., 2022)
Germination Index (%)	89.2	28.5	70 - 90
C/N ratio	9.8	24.2	0.8 - 23.5
pH	7.020	7.406	7.4 – 9.9
EC (µS/cm)	205.5	3940.7	1.2 - 8000
Nitrogen (g/kg)	26.52	12.8	18 - 25
Phosphorus (g/kg)	25.31	9.8	10.9
Potassium (g/kg)	27.93	15.1	25 - 27.6

4.13.2 Germination Index of Nano-BBC

Germination bioassays using white radish seeds confirmed the safety and effectiveness of all nano-BBC. Each treatment recorded GI values above the 80% phytotoxicity threshold (Kong et al., 2022; Yang et al., 2021). Among them, the ethanol-assisted Nano-BBC exhibited the highest GI exceeding 100% demonstrating a stimulatory effect on seedling emergence (**Figure 4.38**). This superior performance is attributed to the increased surface oxygenation and nanoscale refinement achieved during mechanochemical milling in ethanol, which enhanced nutrient solubilization and bioavailability (El-Moaty et al., 2024; Shafiq et al., 2023).

.

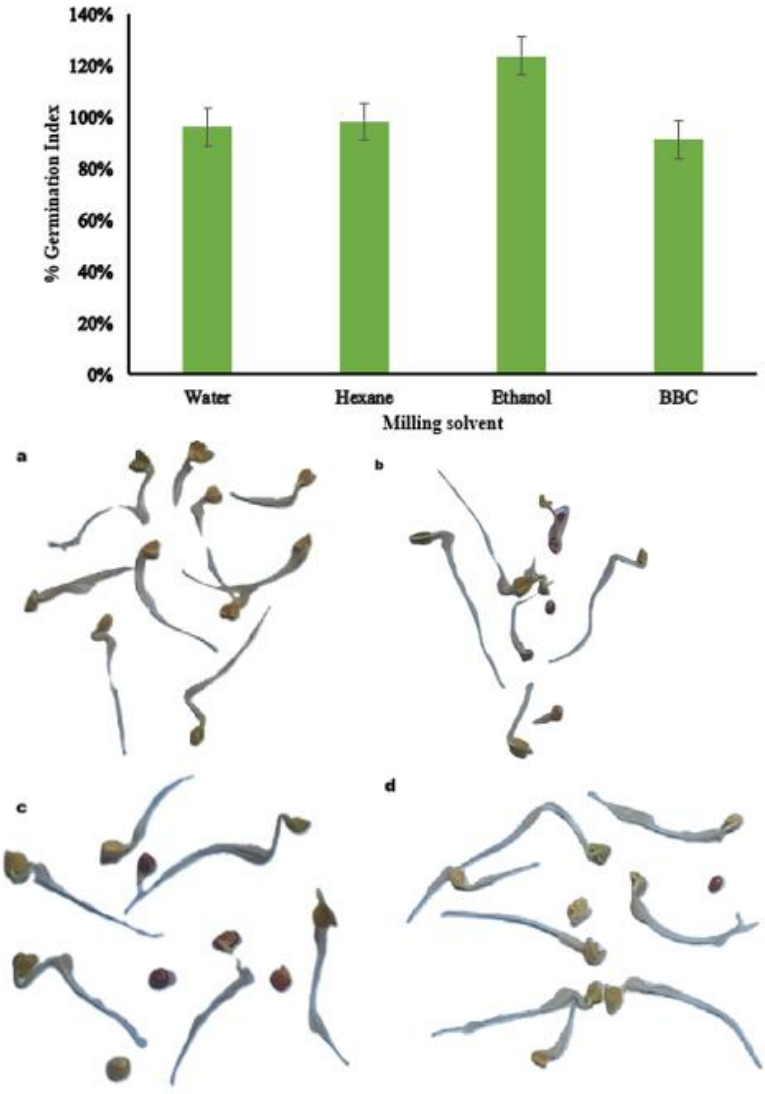

Figure 4.38: Phytotoxicity assessment and morphological differences of seeds treated with biochar-blended compost milled in different solvents. (a) Ethanol, (b) Hexane, (c) Water, and (d) control

In contrast, hexane- and water-assisted Nano-BBCs displayed slightly lower but still non-phytotoxic GI values, suggesting that solvent polarity strongly influences surface functionalization and biological response (Kumar et al., 2020). These observations corroborate previous reports indicating that nanosized fertilizers enhance root elongation, germination iindex, and nutrient uptake due to their increased surface area and improved nutrient diffusion kinetics (Kandil et al., 2020). The untreated BBC recorded the lowest GI, confirming that nanosizing and surface activation are key to transforming biochar–compost matrices from passive amendments into bioactive nutrient carriers.

4.14 Agronomic Performance in Semi-field Pot Experiments

The agronomic evaluation comprised two complementary phases: a 10-day seed emergence test in pots under semi-field conditions, followed by a 30-day vegetative growth study incorporating a controlled drought stress period. This approach integrated short-term physiological responses with longer-term plant performance outcomes. The assessment covered key indicators of early and sustained plant development, germination rate, seedling vigor, biomass accumulation, leaf development, and drought resilience, providing a comprehensive framework to elucidate how mechanochemical refinement and polymer encapsulation modulate amendment functionality and influence crop responses at the early stage of development.

4.14.1 Early Seedling Emergence (10-day open-environment germination)

The emergence data presented in **Table 4.14** show clear differences among fertilizer treatments. The biochar-blended compost consistently demonstrated the lowest germination rates and a suppressive effect on early seedling development, even after co-composting and optimization. This inhibition aligns with reports that even optimized biochar blends can exert phytotoxic effects or create suboptimal conditions for seed germination, depending on specific properties, application rates, or crop interactions (Buss et al., 2015; Kammann et al., 2015). While co-composting biochar generally aims to mitigate phytotoxicity and enhance beneficial properties (Mikajlo et al., 2024), complete elimination of inhibitory effects is not always guaranteed. Even after co-composting, residual mobile organic compounds from the biochar component can leach into the soil and disrupt seed imbibition, cellular metabolism, and radicle emergence, particularly in sensitive species such as maize (Backer et al., 2018; Thomas, 2021).

Furthermore, characteristics of the co-composted blend, such as elevated pH or high electrical conductivity, can lead to osmotic stress or nutrient imbalances, thereby hindering maize seed germination (Carril et al., 2023; Huang et al., 2019). Indeed, certain biochar-compost mixes have been shown to suppress seed germination in various crops, including corn, due to high pH and electrical conductivity (Huang et al., 2019). The variability in biochar and compost properties, even within optimized processes, means that specific blends may still present challenges for particular crops or soil conditions (Buss et al., 2015; Carril et al., 2023).

In contrast, the encapsulated biochar-blended compost markedly improved seed germination rate in soil, reaching 87% by day 10 as shown in **Figure 4.39**. This response is consistent with studies showing that encapsulation technologies create a favorable microenvironment by moderating nutrient release, buffering pH fluctuations, and reducing direct exposure to phytotoxic compounds (Paredes et al., 2023). The chitosan–starch coating likely acted as a controlled-release matrix, reducing nutrient shock and osmotic stress, both of which are critical for radicle emergence and early seedling vigor in soil media (Accinelli et al., 2023; Zhang et al., 2022). The superior performance of EBBC demonstrates the value of controlled nutrient delivery and physicochemical stabilization during early establishment. The comparatively lower germination observed in BBC further suggests that, although co-composting improves amendment quality, encapsulation provides an additional protective and regulatory function essential for optimizing germination, particularly in crops sensitive to soil amendments.

Table 4.14: Effect of Biochar–Compost Blends and Synthetic Fertilizer Treatments On 10-Day Seed Germination of Maize Grown in Pots Under Open Environmental Conditions

Treatment	**Germination on the days after sowing (%)**											**Total seeds germinated (N=15)**	**Germination (%)**
	0th	1st	2nd	3rd	4th	5th	6th	7th	8th	9th	10th		
Control	X	X	X	X	X	X	6	X	1	X	X	7	47%
Synthetic	X	X	X	X	X	X	3	3	2	1	1	10	67%
BBC	X	X	X	X	X	X	2	X	2	X	X	4	27%
EBBC	X	X	X	X	X	X	9	1	1	1	1	13	87%

X – Denotes no germination

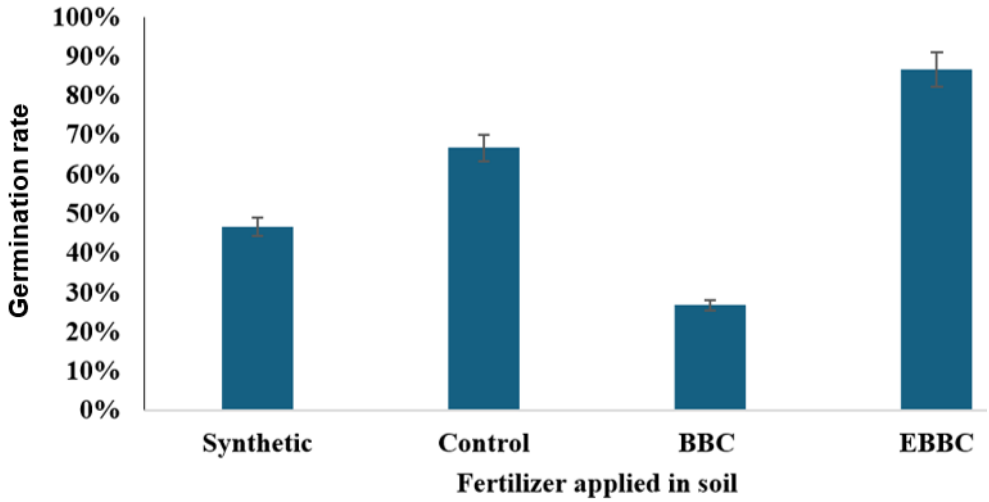

Figure 4.39: Germination rate Under Different Soil Amendments: Error Bars Represent Standard Error of the Mean.

4.14.2 Shoot Height Response to Fertilizer Treatments and Drought Stress (40-day growth period)

The 40-day growth study provides a longer-term perspective on how the germination-stage effects translated into overall plant vigor and resilience (**Figure 4.40**). Before drought induction (day 20), EBBC-treated plants exhibited the most excellent shoot height (47.0 cm), outperforming both synthetic fertilizer (42.92 cm) and the control (38.0 cm). BBC-treated plants showed the slowest early growth (31.17 cm), reflecting the poor emergence and early stress observed during germination. This weak initial establishment is consistent with reports that certain biochar–blended compost matrices may transiently immobilize nutrients or retain phytotoxic residues, delaying early vegetative growth.(Abban-Baidoo et al., 2024; Kammann et al., 2015; Mikajlo et al., 2024). Treatment differences became more pronounced after drought induction (days 20–25). EBBC maintained a strong growth advantage, reaching 65.35 cm by day 30 and 78.18 cm by day 40, significantly higher than synthetic fertilizer (64.73 cm), BBC (62.15 cm), and control (56.03 cm). The enhanced drought resilience of EBBC is consistent with the known benefits of biochar-based formulations in improving water retention, soil porosity (Anbuganesan et al., 2024; Danish et al., 2024; Hazman et al., 2023; Mannan & Shashi, 2019; Naeem et al., 2024; Rahman et al., 2025). Encapsulation further stabilizes moisture dynamics and nutrient release, strengthening plant tolerance under water-limited conditions (Acharya et al., 2024; Hagemann et al., 2017).

Synthetic fertilizer supported strong early growth but demonstrated reduced resilience during drought, ranking second at 64.73 cm by day 40. This pattern suggests that while Synthetic fertilizers provide rapid nutrient availability, their effectiveness diminishes more readily underwater stress compared with the sustained release and soil-enhancing properties of biochar-based formulations. Despite its slow start, the BBC showed substantial improvement by day 40 (62.15 cm), surpassing the control (56.03 cm). This later-stage recovery aligns with reports that biochar–compost amendments increasingly support nutrient availability and drought tolerance over time as soils equilibrate (Morales et al., 2023; Védère et al., 2022). Overall, EBBC demonstrated the strongest performance under both well-watered and drought conditions, reflecting the synergistic effects of encapsulation, enhanced soil porosity, and improved nutrient and moisture regulation (Hao et al., 2024; Ma et al., 2016; Naeem et al., 2024; Toková et al., 2023). These results reinforce the potential of advanced biochar-based fertilizers as effective, climate-resilient alternatives to synthetic inputs, particularly in drought-prone agroecosystems.

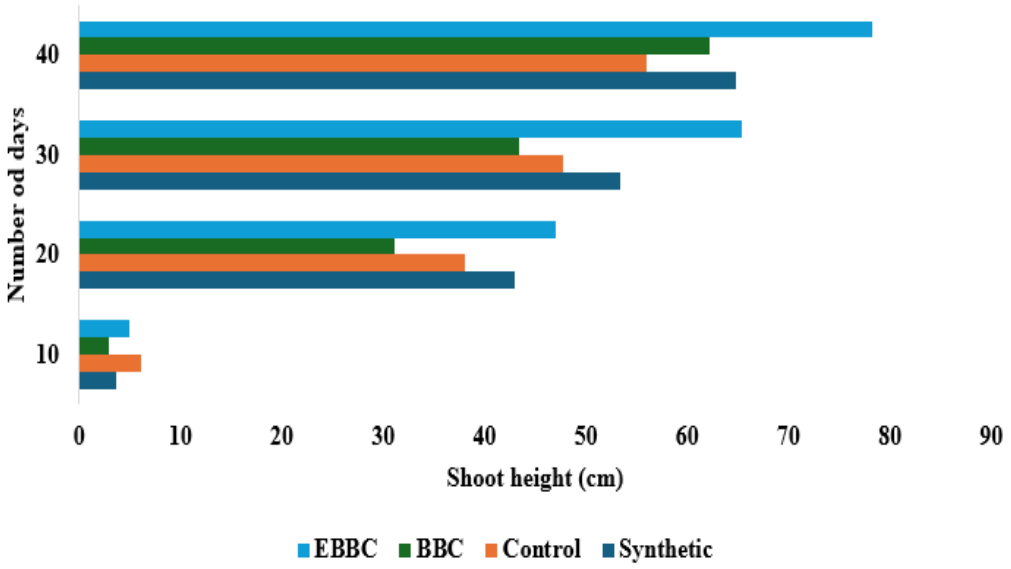

Figure 4.40: Comparative effect of different fertilizer treatments on shoot height over a 40-day growth period

4.14.3 Number of leaves in response to fertilizer treatments and drought stress

The number of leaves showed clear treatment-dependent patterns over the 40-day growth period, reflecting differences in vegetative vigor and drought resilience (**Figure 4.41**). On day 10, EBBC and the control recorded the highest early leaf numbers (4.0), suggesting a strong

initial canopy establishment. Synthetic fertilizer (3) and BBC (2.0) lagged slightly, indicating slower early development. By day 20, all treatments increased leaf numbers, but EBBC maintained its advantage (6 leaves), followed by synthetic fertilizer (6), the control (5), and BBC (5). After drought induction on day 20, divergence among treatments became more pronounced. By day 30, EBBC and BBC continued producing new leaves (7.0 and 5.0, respectively), demonstrating resilience under moisture limitation. Sustained leaf formation during drought is essential for maintaining photosynthetic capacity and biomass accumulation (Tayyab, 2018). These trends are consistent with research showing that biochar, particularly when co-composted or encapsulated, enhances soil water retention, nutrient availability, and physiological stability, ultimately improving drought tolerance (Fallah et al., 2023; Shabir et al., 2024; Wu et al., 2023). In contrast, the synthetic fertilizer and control treatments reduced leaf number, reflecting a diminished ability to buffer drought-induced stress. Synthetic fertilizers provide immediate nutrient boosts but lack the soil-conditioning properties needed to maintain water and nutrient balance under stress (Manea et al., 2023). The unamended control showed expected vulnerability, as soils without amendments typically experience rapid declines in water availability and nutrient status under drought (Hazman et al., 2023).

By day 40, EBBC remained the best amendment with 8 leaves, demonstrating strong canopy development despite episodic drought. This sustained vigor likely reflects improved porosity, water-holding capacity, and nutrient cycling (Tayyab, 2018; Védère et al., 2022; Wang et al., 2023). Numerous studies report that biochar enhances leaf production under drought by improving water-use efficiency and nutrient uptake (Danish et al., 2024; Naeem et al., 2024; Rahman et al., 2025; Wan et al., 2024). BBC also improved over time, reaching 7 leaves, surpassing the synthetic fertilizer treatment (6 leaves), which showed no further growth. The control declined to 4 leaves, signaling severe drought stress. BBC delayed but eventual improvement reflects the gradual nutrient release and soil-enhancing effects typical of biochar-blended compost, which stabilize over time as organic matter decomposes (Hazman et al., 2023; Rasul et al., 2025). Although BBC initially lagged due to slower nutrient availability or mild phytotoxicity, its long-term performance exceeded the unamended control. Overall, EBBC consistently supported the highest leaf proliferation and strongest drought resilience, showing the value of optimized biochar-based amendments for enhancing canopy development and sustaining growth under water-limited conditions. These findings highlight the importance

of advancing biochar formulations to support climate-resilient maize production in drought-prone regions (Abdou et al., 2024; Murtaza et al., 2024.

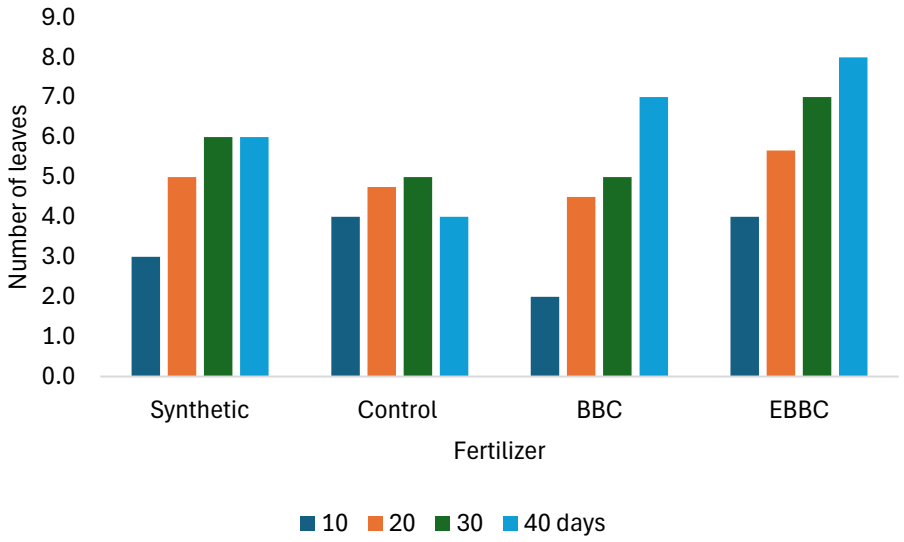

Figure 4.41: Comparative effect of different fertilizer treatments on the number of leaves over a 40-day growth period

4.14.4 Fresh Biomass Accumulation.

Fresh biomass accumulation varied substantially across treatments, with both shoot and root weights showing clear improvements under biochar-based amendments and synthetic fertilizer, particularly under drought stress (**Figure 4.42**). Shoot fresh weight ranged from 17.50 g in the unamended control to 26.13 g with EBBC. EBBC consistently produced the highest shoot biomass (26.13 g), followed by the co-composted biochar blend (BBC; 25.50 g) and synthetic fertilizer (24.67 g). The markedly lower shoot biomass in the control shows the essential role of nutrient inputs and soil amendments in sustaining physiological vigor (Rasul et al., 2025).

Root biomass showed an even more pronounced treatment response. EBBC generated the greatest root mass (13.50 g), substantially exceeding the synthetic fertilizer (10.83 g), BBC (8.50 g), and control (7.67 g). This enhancement reflects the well-documented capacity of biochar to improve soil structure, increase porosity, enhance water retention, and optimize nutrient dynamics within the rhizosphere (Kumar et al., 2023; Nawaz et al., 2022; Song et al., 2020). Biochar-based amendments also stimulate microbial activity, reduce soil toxicity, and promote nutrient uptake, collectively contributing to greater root development (Feng et al., 2021; Ibrahim et al., 2023; Wan et al., 2023; Zou et al., 2021). The encapsulation process in EBBC likely amplified these effects by creating a more stable microenvironment that supported

sustained root proliferation and nutrient accumulation in leaves (Wan et al., 2023). This sustained availability, combined with improved soil quality, supports higher biomass productivity (Mukhina et al., 2020).

Synthetic fertilizer enhanced shoot growth but was less effective in promoting root biomass compared to EBBC, reflecting the limitations of mineral fertilizers that supply nutrients rapidly but do not contribute to long-term soil health or water retention, which are key drivers of root expansion and drought resilience (Raza et al., 2021; Sun et al., 2023; Yan et al., 2023). Numerous studies demonstrate that integrating biochar with organic amendments yields higher biomass than inorganic fertilizers alone (Acharya et al., 2022; Ahmod et al., 2023; Lebrun et al., 2023; Mensah & Frimpong, 2018; Zahra et al., 2021).

BBC produced moderate gains relative to the control but did not match EBBC's performance, highlighting the additional value of encapsulation. Although biochar-blended compost has demonstrated its capacity to enhance biomass in many studies (Ahmod et al., 2023; Grafmüller et al., 2024; Melo & Sánchez-Monedero, 2024; Mikajlo et al., 2024; Mohamed et al., 2024) the superior biomass accumulation under EBBC indicates that advanced formulations unlock significantly greater agronomic potential. These finding position encapsulated amendments as a critical strategy for developing resilient, high-productivity cropping systems.

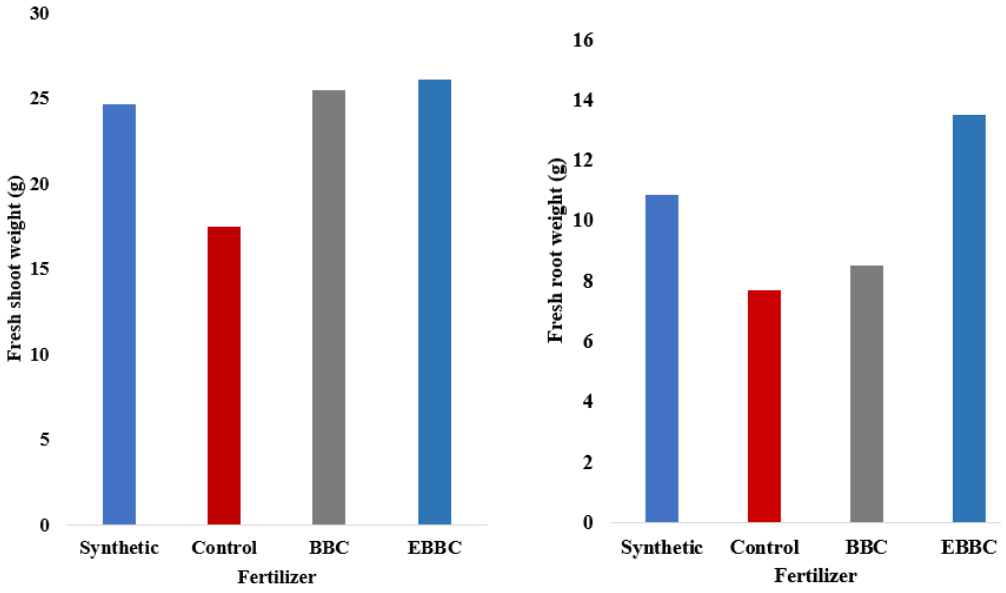

Figure 4.42: Fresh Shoot and Root Biomass Responses of Maize Under Drought Stress Across Different Fertilizer Treatments

4.14.5 N*utrient uptake responses across fertilizer treatments*

Nutrient uptake patterns varied significantly among treatments, demonstrating that fertilizer formulation profoundly influences elemental availability and subsequent plant assimilation (**Figure 4.43:** Concentrations of Major and Trace Elements in Zea mays Leaves after 40 Days). Nitrogen concentrations were predictably highest under synthetic fertilizer (149,127 mg/kg), reflecting the rapid ionic release and immediate uptake characteristic of inorganic sources. While BBC (99,127 mg/kg) and EBBC (81,980 mg/kg) recorded lower Nitrogen levels, these values indicate the moderated, sustained-release behavior typical of biochar-organic matrices. Such controlled-release systems are critical for synchronizing delivery with plant demand, thereby improving nitrogen-use efficiency by mitigating the high volatilization and leaching losses (often exceeding 50% in tropical soils) associated with synthetic urea (Abdala et al., 2024; Rafique et al., 2025). The dynamics of Phosphorus and Potassium highlight the clear superiority of the engineered organic formulations. EBBC exhibited the highest Phosphorus (2,454.51 mg/kg) and Potassium (45,421.81 mg/kg) concentrations, significantly outperforming synthetic fertilizer, which recorded the lowest uptake for both elements. This performance is attributed to biochar's ability to reduce P fixation in weathered soils and retain exchangeable P through its high cation exchange capacity and porous, silica-rich framework (Melo & Sánchez-Monedero, 2024). The fact that EBBC outperformed BBC suggests that the chitosan–starch biopolymer coating provided an additional stabilization layer, protecting these nutrients from early-season immobilization or runoff (Hamed et al., 2024). Micronutrient and secondary nutrient profiles reveal further mechanistic advantages of encapsulation. While Zinc uptake was highest under synthetic fertilizer (0.09 mg/kg), the moderated uptake in EBBC (0.03 mg/kg) is consistent with smart delivery systems that immobilize micronutrients initially to prevent early-stage toxicity, releasing them progressively as the polymer degrades (Arabzadeh Nosratabad et al., 2024). Similarly, EBBC achieved the highest Iron uptake (2.67 mg/kg), likely due to the chelating effect of the biopolymer matrix, which prevents oxidation and conversion into less available forms in aerobic soils. Conversely, the high Sodium spike in BBC (320.31 mg/kg) was effectively suppressed in the EBBC treatment (58.45 mg/kg), indicating that encapsulation can moderate the potentially saline elements found in raw manure-based composts (Mensah & Frimpong, 2018). Therefore, while synthetic fertilizers maximize short-term N accumulation, EBBC facilitates a more balanced and physiologically aligned nutrient

profile. By enhancing P, K, Fe, and Mg uptake while regulating Na and Zn, EBBC supports superior osmotic regulation and stress tolerance, essential traits for climate-resilient crop production in water-stressed tropical environments (Mahmoud et al., 2024).

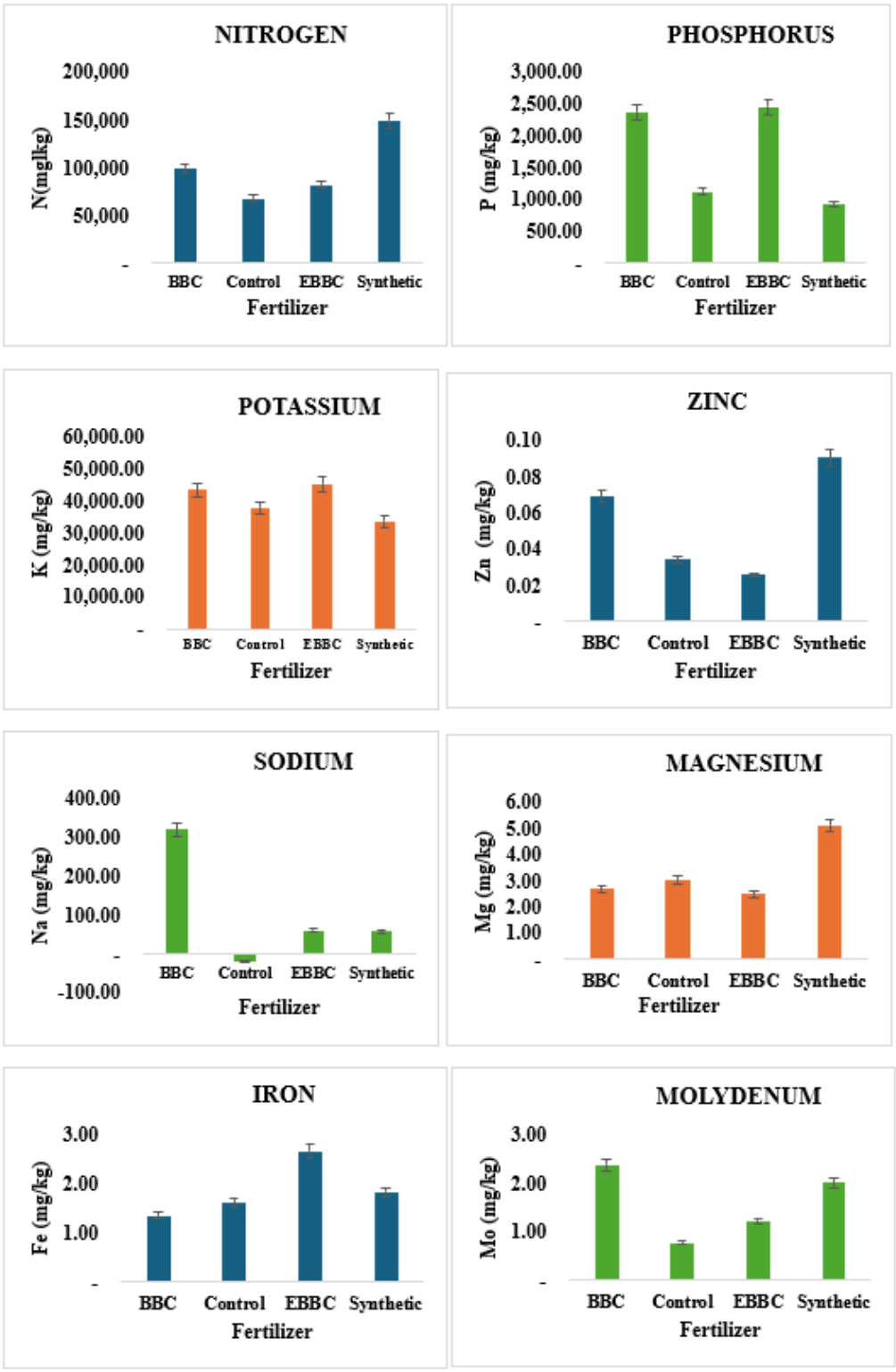

Figure 4.43: Concentrations of Major and Trace Elements in *Zea mays* Leaves after 40 Days

4.14.6 Environmental Safety: Heavy Metal Concentrations in Maize Leaves

Heavy metal concentrations in maize leaves sampled at 40 days were consistently low across all treatments, with mercury, chromium, copper, cobalt, nickel, cadmium, and lead remaining far below internationally accepted thresholds. These results indicate that the biochar-blended compost formulations support the production of environmentally safe maize, reinforcing their suitability for sustainable crop management and food-quality assurance. As illustrated in **Table 4.15**, Chromium, copper, and lead concentrations were substantially lower than FAO permissible limits and EU standards for leafy vegetables. Similarly, as shown in **Figure 4.44**, nickel levels remained comfortably below risk thresholds. Most importantly, cadmium was undetectable in maize leaves supplied with EBBC, which is a key finding because of its high phytotoxicity, strong mobility, and strict regulatory restrictions due to its persistence and potential health risks from food chain accumulation (Ahmad et al., 2021; Huo et al., 2023; Kaleem et al., 2022; Kolahi et al., 2023; Song et al., 2024; Zulfiqar et al., 2022). This is especially significant because maize is known to accumulate cadmium, with many studies reporting concentrations exceeding safety thresholds in contaminated soils (Akenga et al., 2017; Zha et al., 2023). Even under Cd-contaminated conditions, biochar has been shown to reduce Cd uptake in maize (Zha et al., 2023), consistent with the low levels observed in this study.

Table 4.15: FAO Maximum Permissible Limit in Edible Parts of Maize

Heavy Metal	FAO/ Maximum Permissible Limit in Edible Parts of Maize (mg/kg dry mass) (Crljenković et al., 2023)	EU Maximum Limit in Leafy Vegetables (mg/kg) (Ejaz et al., 2023) and (Kurtulus et al., 2021).	Maize Leaf Sample Range (mg/kg) (This study)
Cadmium	0.2	0.05 - 0.1 (depending on vegetable type)	Not Detected
Chromium	2.3	0.5 (leafy vegetables)	0.14–0.34
Copper	40	50 (all crops)	0.01–0.09
Lead	0.3	0.1 (all crops)	0.05–0.19
Nickel	4	50 (all crops)	0.051–0.093

Minor increases in Co (0.02–0.08 mg/kg) and Ni (0.051–0.093 mg/kg) were observed but remained far below regulatory concern. These low concentrations confirm that feedstock selection and the subsequent composting and biochar-blending processes effectively limited heavy-metal transfer to plant tissues. A frequent counterargument is that repeated long-term application of organic amendments may gradually increase trace metal concentrations in soils, potentially affecting future crop quality and human health (Liang et al., 2021; Roy et al., 2025). Indeed, some studies have documented the accumulation of Zn, Cu, and, occasionally, Cd in soils receiving continuous organic inputs (Baldi et al., 2020). However, the exceptionally low metal concentrations observed in this study, even after 40 days of plant growth, indicate that the EBBC and BBC system used here is intrinsically low risk. Overall, the consistently low heavy metal content in maize leaves demonstrates that these fertilizers are environmentally safe, comply with international food-safety standards, and pose minimal risk of heavy metal transfer, supporting their adoption in sustainable and climate-smart crop production systems as shown in **Figure 4.45**.

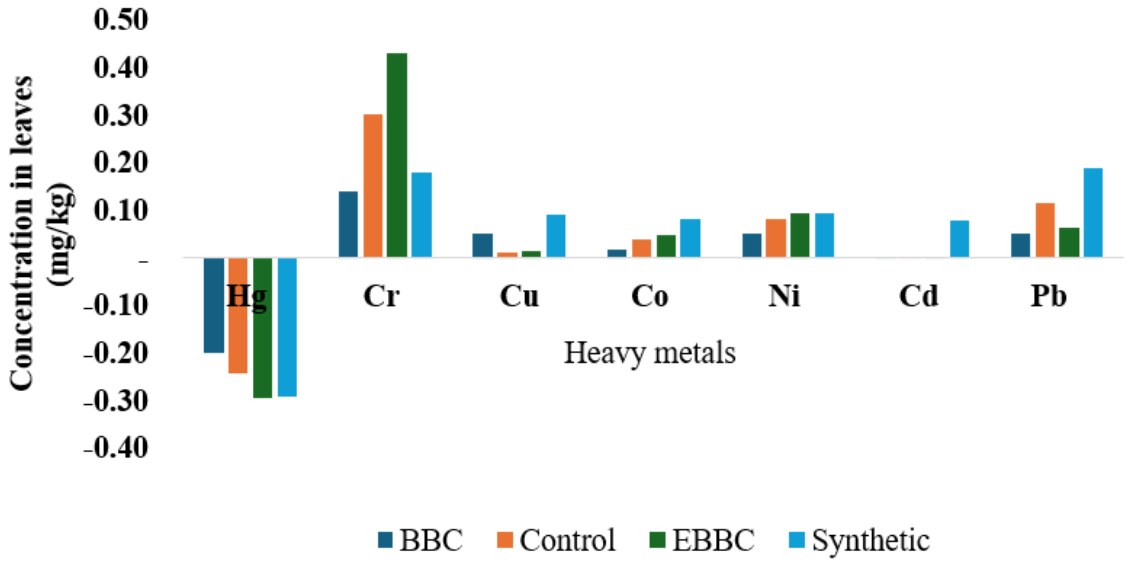

Figure 4.44: Variation in heavy metal and trace element concentrations in *Zea mays* after 40 days of application.

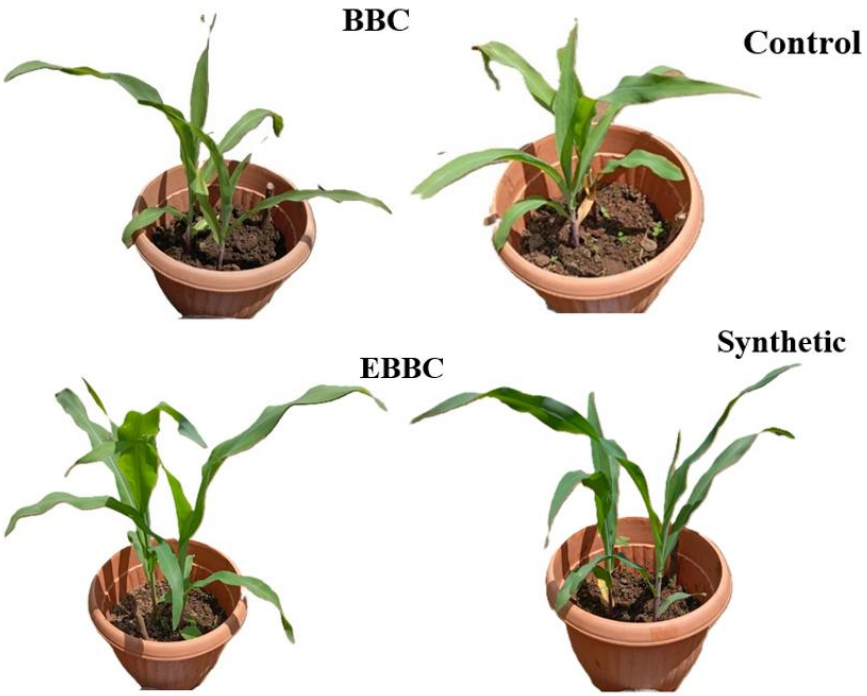

Figure 4.45: Shoot Biomass Accumulation and Vegetative Growth Under Drought Stress

4.15 Contribution to Knowledge

This research provides a reproducible method for producing nutrient-rich biochar-blended compost from locally available tropical feedstocks: chicken manure, *Tithonia diversifolia*, and rice husk biochar, addressing a key knowledge gap by systematically identifying optimal blending ratios that have previously lacked rigorous evaluation in smallholder contexts. Technologically, it introduced two innovations: Encapsulated Biochar-Blended Compost, using a biodegradable chitosan–starch coating for synchronized nutrient delivery; and Nano-Biochar-Blended Compost, synthesized via high-energy ball milling to enhance structural performance and nutrient bioavailability.

The study provided insights into the nutrient-release kinetics and water-retention behaviour of encapsulated organic fertilizers in tropical soils, particularly amid rapid mineralization. Agronomically, it bridged laboratory synthesis to semi-field application, demonstrating improved nutrient-use efficiency, early crop establishment, and drought resilience in *Zea mays*, supporting climate-smart agriculture. Aligning local needs with global sustainability, the study valorizes biomass and cuts reliance on imported synthetic fertilizers to advance an environmentally responsible agro-industry in Uganda.

CHAPTER 5: CONCLUSION AND RECOMMENDATIONS

5.1 Conclusion

This research successfully developed and validated biochar-blended compost (BBC) and its advanced derivatives, Encapsulated BBC (EBBC) and Nano-BBC, as high-performance organic fertilizers tailored for Uganda's smallholder farming systems. By integrating biopolymer encapsulation and nanoscale mechanochemical refinement, the study demonstrated that traditional organic amendments can be engineered to significantly improve nutrient use efficiency and soil-water interactions.

Using Response Surface Methodology, an optimal substrate composition was determined, consisting of 60% *Tithonia diversifolia* and 5.7% biochar, which achieved peak nutrient concentrations of 2.65% N, 2.53% P, and 2.79% K in chicken manure compost. This approach was extended in EBBC through a chitosan–starch matrix designed to control nutrient release; swelling kinetics assessments verified that these composite materials deliver the structural robustness required to inhibit early nitrate leaching. In parallel, Nano-BBC production via high-energy ball milling increased the functional group density and markedly improved cation exchange capacity.

.

In maize pot-scale experiments, these mechanisms proved particularly effective under simulated drought stress, where EBBC promoted superior macronutrient uptake, plant height, and root biomass. Agronomic evaluations confirmed that these advanced formulations are ecologically safe, with a Germination Index exceeding 100%. Ultimately, this study provides a scalable, evidence-based pathway for transforming local organic waste into sustainable, high-performance fertilizers, supporting food security and resilient soil management for resource-limited farmers in the tropics.

5.2 Recommendations

5.2.1 Agronomic Application

The robust efficacy of encapsulated biochar-blended compost (EBBC), as evidenced by enhanced seed germination rate, increased biomass production, and improved drought tolerance, shows its viability as an advanced organic fertilizer for maize cropping systems in Uganda. Its minimized leachate production and exceptional water-holding capacity render it

highly appropriate for the nutrient-poor, drought-susceptible Ferralsols prevalent throughout the region. EBBC is recommended for priority pilot implementation as a soil amendment in zones with unpredictable rainfall, harnessing its controlled-release attributes to sustain yields and maximize nutrient-use efficiency. To support scalability, multi-site field trials spanning Uganda's primary agroecological zones are essential for optimizing application rates and developing farmer-centric operational protocols.

.

5.2.2 Policy Recommendations

This present research aligns closely with the priorities outlined in Uganda's National Development Plan IV, particularly those emphasizing climate-smart agriculture and reducing dependence on costly synthetic fertilizers. Policymakers are advised to incorporate EBBC and its derivatives within national protocols for organic input certification, while promoting their adoption through extension initiatives such as farmer field schools. Inclusion of biochar-based fertilizers in national subsidy mechanisms or credit schemes would improve their economic accessibility. This strategic shift advances Sustainable Development Goals 2 (Zero Hunger), 12 (Responsible Consumption), and 13 (Climate Action) by valorizing local organic wastes as premium agricultural inputs.

5.2.3 Future Research Directions

While EBBC shows promise, further research is essential to characterize biopolymer degradation and its impact on the soil microbiome under varying tropical climates. Specifically, the influence of microbial enzymes on the longevity of chitosan- and starch-based coatings remains an underexplored frontier. Simultaneously, the agronomic potential of Nano-BBC warrants investigation, specifically regarding the mobility of submicron particles within the rhizosphere. Finally, interdisciplinary studies must address socio-economic barriers, such as the technical requirements for high-energy ball milling, to ensure these technologies are both accessible and scalable for resource-limited farmers.

REFERENCES

Abban-Baidoo, E., Manka'abusi, D., Apuri, L., Marschner, B., Frimpong, K. A., Manka'abusi, D., Apuri, L., Marschner, B., & Frimpong, K. A. (2024). Biochar addition influences C and N dynamics during biochar co-composting and the nutrient content of the biochar co-compost. *Scientific Reports*, *14*(1), 23781. https://doi.org/10.1038/s41598-024-67884-z

Abdala, D. B., da Silva, I. R., Vergütz, L., & Sparks, D. L. (2024). Synthesis of struvite-enriched slow-release fertilizer using magnesium-modified biochar: Desorption and leaching mechanisms. *Science of The Total Environment*, *926*, 172172. https://doi.org/10.1016/j.chemosphere.2014.07.029

Abdou, N. M., EL-Samnoudi, I. M., Ibrahim, A. E.-A. M., & El-Tawwab, A. R. A. (2024). Biochar Amendment Alleviates the Combined Effects of Salinity and Drought Stress on Water Productivity, Yield and Quality Traits of Sugar Beet (Beta vulgaris L.). *Journal of Soil Science and Plant Nutrition*, *24*(2), 2091–2110. https://doi.org/10.1007/s42729-024-01754-5

Abraham, A., Soloman, P. A., & Rejini, V. O. (2016). Preparation of Chitosan-Polyvinyl Alcohol Blends and Studies on Thermal and Mechanical Properties. *Procedia Technology*, *24*, 741–748. https://doi.org/10.1016/J.PROTCY.2016.05.206

Accinelli, C., Abbas, H. K., Morena, C., Bruno, V., Khambhati, V. H., Paulk, R. T., Little, N. S., Bellaloui, N., Walker, F., & Shier, W. T. (2023). Use of a biochar-based formulation for coating corn seeds. *Cogent Food \& Agriculture*, *9*(2). https://doi.org/10.1080/23311932.2023.2283956

Acharya, B. S., Dodla, S. K., Wang, J. J., Pavuluri, K., Darapuneni, M. K., Dattamudi, S., Maharjan, B., & Kharel, G. (2024). Biochar impacts on soil water dynamics: knowns, unknowns, and research directions. *Biochar*, *6*(1). https://doi.org/10.1007/s42773-024-00323-4

Acharya, N., Vista, S. P., Shrestha, S., Neupane, N., & Pandit, N. R. (2022). Potential of Biochar-Based Organic Fertilizers on Increasing Soil Fertility, Available Nutrients, and Okra Productivity in Slightly Acidic Sandy Loam Soil. *Nitrogen*, *4*(1), 1–15. https://doi.org/10.3390/nitrogen4010001

Agegnehu, G., Bass, A. M., Nelson, P. N., & Bird, M. I. (2016). Benefits of biochar, compost and biochar-compost for soil quality, maize yield and greenhouse gas

emissions in a tropical agricultural soil. *Science of the Total Environment*. https://doi.org/10.1016/j.scitotenv.2015.11.054

Aguilar-Pozo, V. B., Chimenos, J. M., Elduayen-Echave, B., Olaciregui-Arizmendi, K., López, A., Gómez, J., Guembe, M., García, I., Ayesa, E., & Astals, S. (2023). Struvite precipitation in wastewater treatment plants anaerobic digestion supernatants using a magnesium oxide by-product. *The Science of The Total Environment*, *890*, 164084. https://doi.org/10.1016/j.scitotenv.2023.164084

Agyarko-Mintah, E., Cowie, A., Van Zwieten, L., Singh, B. P., Smillie, R., Harden, S., & Fornasier, F. (2017). Biochar lowers ammonia emission and improves nitrogen retention in poultry litter composting. *Waste Management*, *61*, 129–137. https://doi.org/10.1016/j.wasman.2016.12.009

Ahmad, P., Raja, V., Ashraf, M., Wijaya, L., Bajguz, A., & Alyemeni, M. N. (2021). Jasmonic acid (JA) and gibberellic acid (GA3) mitigated Cd-toxicity in chickpea plants through restricted cd uptake and oxidative stress management. *Scientific Reports*, *11*(1). https://doi.org/10.1038/s41598-021-98753-8

Ahmod, Md. M., Rahman, Md. M. S., Moonmoon, S., Hossain, Md. S., Hasan, Md. K., & Rahman, Md. M. S. (2023). Kitchen Waste Biochar Reduces Inorganic Nourishments of Maize (Zea mays L.). *Journal of Agroforestry and Environment*, *16*(1), 17–25. https://doi.org/10.55706/jae1603

Akenga, T., Sudoi, V., Machuka, W., Kerich, E., & Ronoh, E. (2017). Heavy Metals Uptake in Maize Grains and Leaves in Different Agro Ecological Zones in Uasin Gishu County. *Journal of Environmental Protection*, *8*(12), 1435–1444. https://doi.org/10.4236/jep.2017.812087

Akinnawo, S. O. (2023). Eutrophication: Causes, consequences, physical, chemical and biological techniques for mitigation strategies. *Environmental Challenges*, *12*, 100733. https://doi.org/10.1016/J.ENVC.2023.100733

Alarefee, H. A., Ishak, C. F., Othman, R., & Karam, D. S. (2023). Effectiveness of mixing poultry litter compost with rice husk biochar in mitigating ammonia volatilization and carbon dioxide emission. *Journal of Environmental Management*, *329*, 117051. https://doi.org/10.1016/J.JENVMAN.2022.117051

Ali, A., Jabeen, N., Farruhbek, R., Chachar, Z., Laghari, A. A., Chachar, S., Ahmed, N., Ahmed, S., & Yang, Z. (2025). Enhancing nitrogen use efficiency in agriculture by

integrating agronomic practices and genetic advances. In *Frontiers in Plant Science* (Vol. 16). Frontiers Media. https://doi.org/10.3389/fpls.2025.1543714

Altamira-Algarra, B., Puigagut, J., Day, J. W., Mitsch, W. J., Vymazal, J., Hunter, R. G., & García, J. (2022). A review of technologies for closing the P loop in agriculture runoff: Contributing to the transition towards a circular economy. In *Ecological Engineering* (Vol. 177, p. 106571). Elsevier BV. https://doi.org/10.1016/j.ecoleng.2022.106571

Amusat, S. O., Kebede, T. G., Dube, S., & Nindi, M. M. (2021). Ball-milling synthesis of biochar and biochar–based nanocomposites and prospects for removal of emerging contaminants: A review. *Journal of Water Process Engineering*, *41*, 101993. https://doi.org/10.1016/J.JWPE.2021.101993

Amusat, S. O., Kebede, T. G., Nxumalo, E. N., Dube, S., & Nindi, M. M. (2023). Facile solvent-free modified biochar for removal of mixed steroid hormones and heavy metals: isotherm and kinetic studies. *BMC Chemistry*, *17*(1). https://doi.org/10.1186/s13065-023-01071-5

Anbuganesan, V., Vishnupradeep, R., Bruno, L. B., Sharmila, K., Freitas, H., & Rajkumar, M. (2024). Combined Application of Biochar and Plant Growth-Promoting Rhizobacteria Improves Heavy Metal and Drought Stress Tolerance in Zea mays. *Plants*, *13*(8), 1143. https://doi.org/10.3390/plants13081143

Antonangelo, J. A., Sun, X., & Zhang, H. (2021). The roles of co-composted biochar (COMBI) in improving soil quality, crop productivity, and toxic metal amelioration. *Journal of Environmental Management*, *277*, 111443. https://doi.org/10.1016/J.JENVMAN.2020.111443

Anyebe, O., Sadiq, F. K., Manono, B. O., & Matsika, T. A. (2025). Biochar Characteristics and Application: Effects on Soil Ecosystem Services and Nutrient Dynamics for Enhanced Crop Yields. *Nitrogen*, *6*(2), 31. https://doi.org/10.3390/nitrogen6020031

Arabzadeh Nosratabad, N., Yan, Q., Cai, Z., & Wan, C. (2024). Exploring nanomaterial-modified biochar for environmental remediation applications. *Heliyon*, *10*(18), e37123. https://doi.org/10.1016/j.heliyon.2024.e37123

Arefizadeh, M., Behvandi, D., Shahhosseini, S., & Ghaemi, A. (2024). Efficient CO2 adsorption by deoiled flaxseed hydrochar. *Scientific Reports*, *14*(1). https://doi.org/10.1038/s41598-024-78177-w

Asadu, C. O., Egbuna, S. O., Chime, T. O., Eze, C. N., Dibia, K. T., Mbah, G. O., & Ezema, C. A. (2019b). Survey on solid wastes management by composting: Optimization of key process parameters for biofertilizer synthesis from agro wastes using response surface methodology (RSM). *Artificial Intelligence in Agriculture*, *3*, 52–61. https://doi.org/10.1016/j.aiia.2019.12.002

Atakan, R., Martínez-González, I., Díaz-García, P., & Bonet-Aracil, M. (2023). Sustainable Dyeing and Functional Finishing of Cotton Fabric by Rosa canina Extracts. *Sustainability*, *16*(1), 227. https://doi.org/10.3390/su16010227

Ávila-Quezada, G. D., Ingle, A. P., Golińska, P., & Rai, M. (2022). Strategic applications of nano-fertilizers for sustainable agriculture: Benefits and bottlenecks. *Nanotechnology Reviews*, *11*(1), 2123–2140. https://doi.org/10.1515/ntrev-2022-0126

Awasthi, M. K., Duan, Y., Awasthi, S. K., Liu, T., Chen, H., Pandey, A., Zhang, Z., & Taherzadeh, M. J. (2020). Emerging applications of biochar: Improving pig manure composting and attenuation of heavy metal mobility in mature compost. *Journal of Hazardous Materials*, *389*, 122116. https://doi.org/10.1016/J.JHAZMAT.2020.122116

Azeem, B. (2025). Stimuli-Responsive Starch-Based Biopolymer Coatings for Smart and Sustainable Fertilizers. *Gels 2025, Vol. 11, Page 681*, *11*(9), 681. https://doi.org/10.3390/GELS11090681

Babaee, M., Garavand, F., Rehman, A., Jafarazadeh, S., Amini, E., & Cacciotti, I. (2022). Biodegradability, physical, mechanical and antimicrobial attributes of starch nanocomposites containing chitosan nanoparticles. *International Journal of Biological Macromolecules*, *195*, 49–58. https://doi.org/10.1016/J.IJBIOMAC.2021.11.162

Backer, R., Ghidotti, M., Schwinghamer, T., Saeed, W., Grenier, C., Dion-Laplante, C., Fabbri, D., Dutilleul, P., Séguin, P., & Smith, D. L. (2018). Getting to the root of the matter: Water-soluble and volatile components in thermally-treated biosolids and biochar differentially regulate maize (Zea mays) seedling growth. *PLoS ONE*, *13*(11). https://doi.org/10.1371/journal.pone.0206924

Badagliacca, G., Testa, G., Malfa, S. La, Cafaro, V., Presti, E. Lo, & Monti, M. (2024). Organic Fertilizers and Bio-Waste for Sustainable Soil Management to Support

Crops and Control Greenhouse Gas Emissions in Mediterranean Agroecosystems: A Review. In *Horticulturae* (Vol. 10, Number 5, p. 427). Multidisciplinary Digital Publishing Institute. https://doi.org/10.3390/horticulturae10050427

Baldi, E., Cavani, L., Mazzon, M., Marzadori, C., Quartieri, M., & Toselli, M. (2020). Fourteen years of compost application in a commercial nectarine orchard: effect on microelements and potential harmful elements in soil and plants. *The Science of The Total Environment*, *752*, 141894. https://doi.org/10.1016/j.scitotenv.2020.141894

Bass, A. M., Bird, M. I., Kay, G., & Muirhead, B. (2016). Soil properties, greenhouse gas emissions and crop yield under compost, biochar and co-composted biochar in two tropical agronomic systems. *Science of The Total Environment*. https://doi.org/10.1016/J.SCITOTENV.2016.01.143

Benlamlih, F. Z., Lamhamedi, M. S., Pépin, S., Benomar, L., & Messaddeq, Y. (2021). Evaluation of a New Generation of Coated Fertilizers to Reduce the Leaching of Mineral Nutrients and Greenhouse Gas (N2O) Emissions. *Agronomy*, *11*(6), 1129. https://doi.org/10.3390/agronomy11061129

Bhattacharya, S. (2021). Central Composite Design for Response Surface Methodology and Its Application in Pharmacy. In *IntechOpen eBooks*. IntechOpen. https://doi.org/10.5772/intechopen.95835

Bijay-Singh, & Craswell, E. (2021b). Fertilizers and nitrate pollution of surface and ground water: an increasingly pervasive global problem. *SN Applied Sciences 2021 3:4*. https://doi.org/10.1007/S42452-021-04521-8

Borges, B. M. M. N., Peixoto, F. R., Braga, M. de M., Brunozzi, B. de B., Silveira, M. L., & Coutinho, E. L. M. (2020). Response of bermudagrass to enhanced-efficiency fertilizers, application strategies and release under tropical conditions. *Australian Journal of Crop Science*, 108–115. https://doi.org/10.21475/ajcs.20.14.01.p1929

Bruand, A., Reatto, A., Brossard, M., Jouquet, P., & Martins, É. de S. (2023). Long-term activity of social insects responsible for the physical fertility of soils in the tropics. *Scientific Reports*, *13*(1), 12337. https://doi.org/10.1038/s41598-023-39654-w

Bruun, E., Ravenni, G., Müller-Stöver, D., & Petersen, C. T. (2023). Small biochar particles added to coarse sandy subsoil greatly increase water retention and affect hydraulic conductivity. *European Journal of Soil Science*, *74*(6). https://doi.org/10.1111/ejss.13442

Bryndum, S., Muschler, R., Nigussie, A., Magid, J., & de Neergaard, A. (2017). Reduced turning frequency and delayed poultry manure addition reduces N loss from sugarcane compost. *Waste Management*, *65*, 169–177. https://doi.org/10.1016/J.WASMAN.2017.04.001

Buss, W., Mašek, O., Graham, M., & Wüst, D. (2015). Inherent organic compounds in biochar–Their content, composition and potential toxic effects. *Journal of Environmental Management*, *156*, 150–157. https://doi.org/10.1016/j.jenvman.2015.03.035

Cao, G., Qiao, J., Ai, J., Ning, S., Sun, H., Chen, M., Zhao, L., Zhang, G., & Lian, F. (2022). Systematic Research on the Transport of Ball-Milled Biochar in Saturated Porous Media: Effect of Humic Acid, Ionic Strength, and Cation Types. *Nanomaterials*, *12*(6), 988. https://doi.org/10.3390/nano12060988

Carril, P., Ghorbani, M., Loppi, S., & Celletti, S. (2023). Effect of Biochar Type, Concentration and Washing Conditions on the Germination Parameters of Three Model Crops. *Plants*, *12*(12), 2235. https://doi.org/10.3390/plants12122235

Casini, D., Barsali, T., Rizzo, A. M., & Chiaramonti, D. (2021). Production and characterization of co-composted biochar and digestate from biomass anaerobic digestion. *Biomass Conversion and Biorefinery*, *11*(6), 2271–2279. https://doi.org/10.1007/S13399-019-00482-6/TABLES/4

Cecire, R., Diana, A., Giacomino, A., Abollino, O., Inaudi, P., Favilli, L., Bertinetti, S., Cavalera, S., Celi, L., & Malandrino, M. (2024). Rice Husk as a Sustainable Amendment for Heavy Metal Immobilization in Contaminated Soils: A Pathway to Environmental Remediation. *Toxics*, *12*(11), 790. https://doi.org/10.3390/TOXICS12110790/S1

Chaher, N. E. H., Chakchouk, M., Engler, N., Nassour, A., Nelles, M., & Hamdi, M. (2020). Optimization of Food Waste and Biochar In-Vessel Co-Composting. *Sustainability 2020, Vol. 12, Page 1356*, *12*(4), 1356. https://doi.org/10.3390/SU12041356

Chaubey, A. K., Pratap, T., Preetiva, B., Patel, M., Singsit, J. S., Pittman, C. U., & Mohan, D. (2024). Definitive Review of Nanobiochar. *ACS Omega*, *9*(11), 12331–12379. https://doi.org/10.1021/acsomega.3c07804

Chen, S., Yang, M., Ba, C., Yu, S., Jiang, Y., Zou, H., & Zhang, Y. (2018). Preparation and characterization of slow-release fertilizer encapsulated by biochar-based waterborne copolymers. *Science of The Total Environment*, *615*, 431–437. https://doi.org/10.1016/J.SCITOTENV.2017.09.209

Chen, Y., Xu, Y., Qu, F., Hou, F., Chen, H., & Li, X. (2020). Effects of different loading rates and types of biochar on passivations of Cu and Zn via swine manure composting. *Journal of Arid Land 2020 12:6*, *12*(6), 1056–1070. https://doi.org/10.1007/S40333-020-0026-5

Chi, W., Nan, Q., Liu, Y., Dong, D., Qin, Y., Li, S., & Wu, W. (2024). Stress resistance enhancing with biochar application and promotion on crop growth. *Biochar*, *6*(1). https://doi.org/10.1007/s42773-024-00336-z

Chiaregato, C. G., & Faez, R. (2021). Micronutrients encapsulation by starch as an enhanced efficiency fertilizer. *Carbohydrate Polymers*, *271*, 118419. https://doi.org/10.1016/j.carbpol.2021.118419

Corona, F., Hidalgo, D., Martín-Marroquín, J. M., Castro, J., Bedate, S. S., & Antolín, G. (2022). Study of the Crystallisation Reaction Behaviour to Obtain Struvite. *Waste and Biomass Valorization*, *13*(9), 3767–3786. https://doi.org/10.1007/s12649-022-01797-8

Crljenković, B., Mujkic, M., Čivić, H., Sijahovic, E., & Murtić, S. (2023). Heavy metals accumulation and distribution pattern in maize plants. *The Journal Agriculture and Forestry*, *69*(3). https://doi.org/10.17707/agricultforest.69.3.13

Danish, S., Hasnain, Z., Dawar, K., Fahad, S., Shah, A. N., Salmen, S. H., & Ansari, M. J. (2024). Enhancing maize resilience to drought stress: the synergistic impact of deashed biochar and carboxymethyl cellulose amendment. *BMC Plant Biology*, *24*(1). https://doi.org/10.1186/s12870-024-04843-w

De Paola, M. G., Paletta, R., Lopresto, C. G., Lio, G. E., De Luca, A., Chakraborty, S., & Calabrò, V. (2021). Stability of Film-Forming Dispersions: Affects the Morphology and Optical Properties of Polymeric Films. *Polymers 2021, Vol. 13, Page 1464*, *13*(9), 1464. https://doi.org/10.3390/POLYM13091464

Demirci, T., Gelen, T. T., & Bölgen, N. (2024). A Biopolymer Coating Strategy for the Slow Release of Urea from Urea Fertiliser. *Kemija u Industriji*. https://doi.org/10.15255/kui.2024.007

Dhiman, V. K., Dhiman, V. K., Rana, G., Kumar, R., Singh, D., Chauhan, A., Jabir, M. S., & Ghotekar, S. (2025). Recent advances in phosphorus nano-fertilizers: Impacts on crop productivity and soil sustainability. *Physiological and Molecular Plant Pathology*, *140*, 102885. https://doi.org/10.1016/j.pmpp.2025.102885

D'Hose, T., Debode, J., De Tender, C., Ruysschaert, G., & Vandecasteele, B. (2020). Has compost with biochar applied during the process added value over biochar or compost for increasing soil quality in an arable cropping system? *Applied Soil Ecology*, *156*. https://doi.org/10.1016/j.apsoil.2020.103706

Dobermann, A., Bruulsema, T., Çakmak, İ., Gérard, B., Majumdar, K., McLaughlin, M. J., Reidsma, P., Vanlauwe, B., Wollenberg, L., Zhang, F., & Zhang, X. (2021). *A New Paradigm for Plant Nutrition*. https://doi.org/10.48565/scfss2021-hg55

Dong, L., Li, L., Chen, H., Cao, Y., & Lei, H. (2025). Mechanochemistry: Fundamental Principles and Applications. *Advanced Science*, *12*(24), 2403949. https://doi.org/10.1002/ADVS.202403949

dos Santos Cotta, A. A. R., Ferreira, L. F., Borges, S. V., de Souza Nascimento, B., Cotta, A. A. C., & Dias, M. V. (2023). Biodegradation, Water Sorption Isotherms and Thermodynamic Properties of Extruded Packaging Composed of Cassava Starch with Tomato Peel. *Journal of Polymers and the Environment*, *32*(5), 2221–2238. https://doi.org/10.1007/s10924-023-03094-4

Duarte, S. de J., Hubach, A., & Glaser, B. (2022). Soil water balance and wettability methods in soil treated with biochar and/or compost. *Carbon Research*, *1*(1). https://doi.org/10.1007/s44246-022-00032-2

Dubadi, R., Huang, S. D., & Jaroniec, M. (2023). Mechanochemical Synthesis of Nanoparticles for Potential Antimicrobial Applications. In *Materials* (Vol. 16, Number 4, p. 1460). Multidisciplinary Digital Publishing Institute. https://doi.org/10.3390/ma16041460

Dudnik, O. V., Lakiza, S. M., Marek, I. O., Red'ko, V. P., Makudera, A. O., & Ruban, O. K. (2025). Advanced Approaches for Producing Nanocrystalline and Fine-Grained ZrO2-Based Powders(Review) I. Mechanical, Physical, and Chemical Methods (Excluding 'Wet' Chemistry). *Powder Metallurgy and Metal Ceramics 2025 63:5*, *63*(5), 318–342. https://doi.org/10.1007/S11106-025-00465-5

Eddarai, E. M., El Mouzahim, M., Ragaoui, B., Eladaoui, S., Bourd, Y., Bellaouchou, A., & Boussen, R. (2024). Review of current trends in chitosan based controlled and slow-release fertilizer: From green chemistry to circular economy. *International Journal of Biological Macromolecules*, *278*, 134982. https://doi.org/10.1016/J.IJBIOMAC.2024.134982

Ejaz, U., Khan, S. M., Khalid, N., Ahmad, Z., Jehangir, S., Rizvi, Z. F., Lho, L. H., Han, H., & Raposo, A. (2023). Detoxifying the heavy metals: a multipronged study of tolerance strategies against heavy metals toxicity in plants. In *Frontiers in Plant Science* (Vol. 14). Frontiers Media. https://doi.org/10.3389/fpls.2023.1154571

El-Damarawy, Y. A., Saleh, E., Ibrahim, O. M., Elrefaey, A., Saleh, M. E., & El-Gamal, E. H. (2025). Optimizing phosphorus released in calcareous soil amended with bone char and bone ash using response surface methodology and desirability function. *Scientific Reports*, *15*(1). https://doi.org/10.1038/s41598-025-13548-5

El-Moaty, H. I. A., El-Dissouky, A., Elhusseiny, A. F., Farag, K. M., Abu-Khudir, R., Alkuwayti, M. A., Abdulsalam, N. K. Al, & Rahman, S. M. A. (2024). Low-cost nano biochar: a sustainable approach for drought stress mitigation in faba bean (Vicia faba L.). *Frontiers in Plant Science*. https://doi.org/10.3389/FPLS.2024.1438893

Endriani, & Listyarini, D. (2023). Amelioration of dry land suboptimal using biochar and compost to improve soil physical properties and soybean yield. *BIO Web of Conferences*, *80*, 3001. https://doi.org/10.1051/bioconf/20238003001

Faez, R., Messa, L. L., & Souza, C. F. (2024). Distribution of nutrients from controlled-release polymers in sandy soil. *Ciência Agronômica/Revista Ciência Agronômica*, *55*. https://doi.org/10.5935/1806-6690.20240031

Fallah, N., Pang, Z., Lin, Z., Lin, W., Mbuya, S. N., Abubakar, A. Y., Fabrice, K. M. A., & Zhang, H. (2023). Plant growth and stress-regulating metabolite response to biochar utilization boost crop traits and soil health. *Frontiers in Plant Science*, *14*. https://doi.org/10.3389/fpls.2023.1271490

Fan, X., Wei, Y., Song, D., Zhou, T., Li, R., Su, X., Zhang, T., Cheng, S., & Xiao, R. (2025). Biochar enhanced co-composting for peat-free seedling substrate: A win-win solution for sustainable development of modern vegetable industry. *Process Safety and Environmental Protection*, *194*, 1504–1514. https://doi.org/10.1016/J.PSEP.2024.12.076

Fathy, R. F., Elagroudi, W., Taha, A. A., & Mosa, A. (2025). Modulating effects of biochar on phosphorus dynamics in soil–biota–plant system: a comprehensive review. In *Soil Ecology Letters* (Vol. 7, Number 3). Springer Science+Business Media. https://doi.org/10.1007/s42832-025-0325-z

Feng, L., Xu, W., Tang, G., Gu, M., & Geng, Z. (2021). Biochar induced improvement in root system architecture enhances nutrient assimilation by cotton plant seedlings. *BMC Plant Biology*, *21*(1), 269. https://doi.org/10.1186/s12870-021-03026-1

Ferrazza, A. C., Bieger, B. N., da Luz, G. L., Nesi, C. N., Lajús, C. R., & Fiori, M. A. (2018). Factorial Economic Planning Applied to Agricultural Experimentation. *International Journal of Advanced Engineering Research and Science*, *5*(6), 214–221. https://doi.org/10.22161/ijaers.5.6.35

Ferreira, L. F., de Abreu, G. F., Lago, A. M. T., Figueiredo, L. P., Borém, F. M., Martins, M. A., Borges, S. V., & Dias, M. V. (2018). Development and application of biopolymer coatings to specialty green coffee beans: Influence on water content, color and sensory quality. *LWT*, *96*, 274–280. https://doi.org/10.1016/j.lwt.2018.05.037

Fertahi, S., Ilsouk, M., Zeroual, Y., Oukarroum, A., & Barakat, A. (2020b). Recent trends in organic coating based on biopolymers and biomass for controlled and slow release fertilizers. In *Journal of Controlled Release* (Vol. 330, pp. 341–361). Elsevier BV. https://doi.org/10.1016/j.jconrel.2020.12.026

Fincheira, P., Hoffmann, N., Tortella, G., Ruíz, A., Cornejo, P., Díez, M. C., Seabra, A. B., Benavides-Mendoza, A., & Rubilar, O. (2023). Eco-Efficient Systems Based on Nanocarriers for the Controlled Release of Fertilizers and Pesticides: Toward Smart Agriculture. In *Nanomaterials* (Vol. 13, Number 13, p. 1978). Multidisciplinary Digital Publishing Institute. https://doi.org/10.3390/nano13131978

Firmanda, A., Fahma, F., Syamsu, K., Suryanegara, L., & Wood, K. (2022). Controlled/slow-release fertilizer based on cellulose composite and its impact on sustainable agriculture: review. *Biofuels, Bioproducts and Biorefining*, *16*(6), 1909–1930. https://doi.org/10.1002/BBB.2433

Fonseca-García, A., Jiménez-Regalado, E. J., & Aguirre-Loredo, R. Y. (2021). Preparation of a novel biodegradable packaging film based on corn starch-chitosan

and poloxamers. *Carbohydrate Polymers*, *251*, 117009. https://doi.org/10.1016/J.CARBPOL.2020.117009

Gale, N., Sackett, T. E., & Thomas, S. C. (2016). Thermal treatment and leaching of biochar alleviates plant growth inhibition from mobile organic compounds. *PeerJ*, *4*. https://doi.org/10.7717/peerj.2385

Ganetri, I., Essamlali, Y., Amadine, O., Dânoun, K., Aboulhrouz, S., & Zahouily, M. (2020). Controlling factors of slow or controlled-release fertilizers. In *Elsevier eBooks* (pp. 111–129). Elsevier BV. https://doi.org/10.1016/b978-0-12-819555-0.00007-8

Gao, L., Zhu, T., He, F., Ou, Z., Xu, J., & Ren, L. (2021). Preparation and Characterization of Functional Films Based on Chitosan and Corn Starch Incorporated Tea Polyphenols. *Coatings 2021, Vol. 11, Page 817*, *11*(7), 817. https://doi.org/10.3390/COATINGS11070817

Gao, S., Harrison, B. P., Thao, T., Gonzales, M., An, D., Ghezzehei, T. A., Díaz, G., & Ryals, R. (2023). Biochar co-compost improves nitrogen retention and reduces carbon emissions in a winter wheat cropping system. *GCB Bioenergy*, *15*(4), 462–477. https://doi.org/10.1111/gcbb.13028

Gao, S., Medina, M., Gonzalez-Ospina, L., Burce, K., Burce, K., & Melbourne, A. (2025). Boosting soil health and crop nutrients with locally sourced biochar and compost in Sacramento urban agriculture. *Frontiers in Sustainable Food Systems*, *9*. https://doi.org/10.3389/fsufs.2025.1546426

Gezahegn, S., Sain, M., & Thomas, S. C. (2020). Phytotoxic condensed organic compounds are common in fast but not slow pyrolysis biochars. *Bioresource Technology Reports*, *13*, 100613. https://doi.org/10.1016/j.biteb.2020.100613

Gigli, M., Fellet, G., Pilotto, L., Sgarzi, M., Marchiol, L., & Crestini, C. (2022). Lignin-based nano-enabled agriculture: A mini-review. In *Frontiers in Plant Science* (Vol. 13). Frontiers Media. https://doi.org/10.3389/fpls.2022.976410

Godlewska, P., Schmidt, H. P., Ok, Y. S., & Oleszczuk, P. (2017). Biochar for composting improvement and contaminants reduction. A review. *Bioresource Technology*, *246*, 193–202. https://doi.org/10.1016/J.BIORTECH.2017.07.095

Goiana, M. L., de Brito, E. S., Filho, E. G. A., de Castro Miguel, E., Fernandes, F. A. N., de Azeredo, H. M. C., & de Freitas Rosa, M. (2021). Corn starch based films treated

by dielectric barrier discharge plasma. *International Journal of Biological Macromolecules*, *183*, 2009–2016. https://doi.org/10.1016/j.ijbiomac.2021.05.210

Gondek, M., Weindorf, D. C., Thiel, C., & Kleinheinz, G. (2020). Soluble Salts in Compost and Their Effects on Soil and Plants: A Review. In *Compost Science \& Utilization* (Vol. 28, Number 2, pp. 59–75). Taylor \& Francis. https://doi.org/10.1080/1065657x.2020.1772906

Gong, M., He, J., Kong, M., Huo, Q., Jiang, Y., Song, J., Han, W., & Lv, G. (2023). A microencapsulation approach to design microbial seed coatings to boost wheat seed germination and seedling growth under salt stress. *Frontiers in Plant Science*, *14*. https://doi.org/10.3389/fpls.2023.1283590

Govil, S., Long, N. V. D., Escribà-Gelonch, M., & Hessel, V. (2024). Controlled-release fertiliser: Recent developments and perspectives. *Industrial Crops and Products*, *219*, 119160. https://doi.org/10.1016/j.indcrop.2024.119160

Govindasamy, P., Muthusamy, S., Bagavathiannan, M., Mowrer, J., Jagannadham, P. T. K., Maity, A., Halli, H. M., Sujayananad, G. K., Vadivel, R., K., D. T., Raj, R., Pooniya, V., Babu, S., Rathore, S. S., Muralikrishnan, L., & Tiwari, G. (2023). Nitrogen use efficiency—a key to enhance crop productivity under a changing climate. In *Frontiers in Plant Science* (Vol. 14). Frontiers Media. https://doi.org/10.3389/fpls.2023.1121073

Grafmüller, J., Möllmer, J., Muehe, E. M., Kammann, C., Kray, D., Schmidt, H., & Hagemann, N. (2024). Granulation compared to co-application of biochar plus mineral fertilizer and its impacts on crop growth and nutrient leaching. *Scientific Reports*, *14*(1). https://doi.org/10.1038/s41598-024-66992-0

Guarnieri, S. F., Nascimento, E. C. do, Costa, R. F., Faria, J. L. B., & Lobo, F. de A. (2021). Coconut fiber biochar alters physical and chemical properties in sandy soils. *Acta Scientiarum Agronomy*, *43*. https://doi.org/10.4025/actasciagron.v43i1.51801

Gumelar, M. D., Hamzah, M., Hidayat, A. S., Saputra, D. A., & Idvan. (2020). Utilization of Chitosan as Coating Material in Making NPK Slow Release Fertilizer. *Macromolecular Symposia*, *391*(1), 1900188. https://doi.org/10.1002/MASY.201900188

Hafeez, A., Pan, T., Tian, J., & Cai, K. (2022). Modified Biochars and Their Effects on Soil Quality: A Review. In *Environments* (Vol. 9, Number 5, p. 60).

Multidisciplinary Digital Publishing Institute. https://doi.org/10.3390/environments9050060

Hafez, M., Popov, A., & Rashad, M. (2020). Evaluation of the Effects of New Environmental Additives Compared to Mineral Fertilizers on the Leaching Characteristics of Some Anions and Cations under Greenhouse Plant Growth of Saline-Sodic Soils. *The Open Agriculture Journal*, *14*(1), 246–256. https://doi.org/10.2174/1874331502014010246

Hagemann, N., Joseph, S., Schmidt, H., Kammann, C., Harter, J., Borch, T., Young, R. B., Varga, K., Taherymoosavi, S., Elliott, K. W., McKenna, A. M., Albu, M., Mayrhofer, C., Obst, M., Conte, P., Dieguez-Alonso, A., Orsetti, S., Subdiaga, E., Behrens, S., & Kappler, A. (2017a). Organic coating on biochar explains its nutrient retention and stimulation of soil fertility. *Nature Communications*, *8*(1). https://doi.org/10.1038/s41467-017-01123-0

Hagemann, Nikolas., Kammann, C. I., Schmidt, H. P., Kappler, A., & Behrens, S. (2017b). Nitrate capture and slow release in biochar amended compost and soil. *PLOS ONE*, *12*(2), e0171214. https://doi.org/10.1371/JOURNAL.PONE.0171214

Haider, F. U., Cai, L., Coulter, J. A., Cheema, S. A., Wu, J., Zhang, R., Ma, W., & Farooq, M. (2021). Cadmium toxicity in plants: Impacts and remediation strategies. In *Ecotoxicology and Environmental Safety* (Vol. 211, p. 111887). Elsevier BV. https://doi.org/10.1016/j.ecoenv.2020.111887

Halbert-Howard, A., Häfner, F., Karlowsky, S., Schwarz, D., & Krause, A. (2021). Evaluating recycling fertilizers for tomato cultivation in hydroponics, and their impact on greenhouse gas emissions. *Environmental Science and Pollution Research*, *28*(42), 59284–59303. https://doi.org/10.1007/S11356-020-10461-4

Hamdi, M., Nasri, R., Azaza, Y. Ben, Li, S., & Nasri, M. (2020). Conception of novel blue crab chitosan films crosslinked with different saccharides via the Maillard reaction with improved functional and biological properties. *Carbohydrate Polymers*, *241*, 116303. https://doi.org/10.1016/j.carbpol.2020.116303

Hamed, R., Jodeh, S., & Alkowni, R. (2024b). Nano bio fertilizer capsules for sustainable agriculture. *Scientific Reports*, *14*(1). https://doi.org/10.1038/s41598-024-62973-5

Hao, J., Zhang, X., Zong, S., Zhuo, Y., Zhang, Y., Wang, S., Deng, Y., Zhang, X., & Li, J. (2024). Biochar as a highly efficient adsorption carrier for sewage sludge-derived

nutrients and biostimulants: component fixation and mechanism. *Biochar*, *6*(1). https://doi.org/10.1007/s42773-024-00335-0

Hassan, S. H., Chafik, Y., Sena-Vélez, M., Lebrun, M., Scippa, G. S., Bourgerie, S., Trupiano, D., Morabito, D. Importance of Application Rates of Compost and Biochar on Soil Metal(Loid) Immobilization and Plant Growth. *Plants*, *12*(11), 2077. https://doi.org/10.3390/plants12112077

Hazman, M., Fawzy, S., Hamdy, A., Khaled, A., Mahmoud, A., Khalid, E., Ibrahim, H. M., Gamal, M., Elyazeed, N. A., Saber, N., Ehab, M., & Kabil, F. (2023). Enhancing rice resilience to drought by applying biochar–compost mixture in low-fertile sandy soil. *Beni-Suef University Journal of Basic and Applied Sciences*, *12*(1). https://doi.org/10.1186/s43088-023-00411-7

Helal, M., El-Mogy, M. M., Khater, H., Fathy, M., Ibrahim, F. E., Y, L., Tong, Z., & Abdelgawad, K. F. (2023). A Controlled-Release Nanofertilizer Improves Tomato Growth and Minimizes Nitrogen Consumption. *Plants*, *12*(10), 1978. https://doi.org/10.3390/plants12101978

Herniou--Julien, C., Mendieta, J. R., & Gutiérrez, T. J. (2018). Characterization of biodegradable/non-compostable films made from cellulose acetate/corn starch blends processed under reactive extrusion conditions. *Food Hydrocolloids*, *89*, 67–79. https://doi.org/10.1016/j.foodhyd.2018.10.024

Hina, N. S. (2024). Global Meta-Analysis of Nitrate Leaching Vulnerability in Synthetic and Organic Fertilizers over the Past Four Decades. *Water*, *16*(3), 457. https://doi.org/10.3390/w16030457

Hossain, M. Z., Bahar, M. M., Sarkar, B., Bolan, N., & Donne, S. W. (2024). Fertilizer Value of Nutrient-Enriched Biochar and Response of Canola Crop. *Journal of Soil Science and Plant Nutrition*, *24*(2), 2123–2137. https://doi.org/10.1007/s42729-024-01784-z

Hossain, M. Z., Bahar, M. M., Sarkar, B., Donne, S. W., Ok, Y. S., Palansooriya, K. N., Kirkham, M. B., Chowdhury, S., & Bolan, N. (2020). Biochar and its importance on nutrient dynamics in soil and plant. *Biochar*, *2*(4), 379–420. https://doi.org/10.1007/s42773-020-00065-z

Hu, G., Lan, X., Peng, B., Liao, J., & Xiong, Y. (2024). Water resistant, biodegradable and flexible corn starch/carboxymethyl cellulose composite film for slow-release

fertilizer coating materials. *International Journal of Biological Macromolecules*, *260*, 129476. https://doi.org/10.1016/J.IJBIOMAC.2024.129476

Huang, H., Reddy, N. G., Huang, X., Chen, P., Pei-ying, W., Zhang, Y., Huang, Y., Lin, P., & Garg, A. (2021). Effects of pyrolysis temperature, feedstock type and compaction on water retention of biochar amended soil. *Scientific Reports*, *11*(1). https://doi.org/10.1038/s41598-021-86701-5

Huang, L., Yu, P., & Gu, M. (2019). Evaluation of Biochar and Compost Mixes as Substitutes to a Commercial Propagation Mix. *Applied Sciences*, *9*(20), 4394. https://doi.org/10.3390/app9204394

Huo, D., Hao, Y., Zou, J., Qin, L., Wang, C., & Du, D. (2023). Integrated transcriptome and metabonomic analysis of key metabolic pathways in response to cadmium stress in novel buckwheat and cultivated species. *Frontiers in Plant Science*, *14*. https://doi.org/10.3389/fpls.2023.1142814

Hwang, H. Y., Kim, S. H., Kim, M. S., Park, S. J., & Lee, C. H. (2020). Co-composting of chicken manure with organic wastes: characterization of gases emissions and compost quality. *Applied Biological Chemistry 2020 63:1*, *63*(1), 3-. https://doi.org/10.1186/S13765-019-0483-8

Ibrahim, E. A., El-Sherbini, M., & Selim, E.-M. M. (2023). Effects of biochar, zeolite and mycorrhiza inoculation on soil properties, heavy metal availability and cowpea growth in a multi-contaminated soil. *Scientific Reports*, *13*(1), 6621. https://doi.org/10.1038/s41598-023-33712-z

Iftikhar, A., & Tao, W. (2024). Recovery of struvite for organic production: Mineral-based magnesium supplementation and pH elevation. *Journal of Cleaner Production*, *452*, 142244. https://doi.org/10.1016/j.jclepro.2024.142244

Incrocci, L., Maggini, R., Cei, T., Carmassi, G., Botrini, L., Filippi, F., Clemens, R., Terrones, C., & Pardossi, A. (2020). Innovative Controlled-Release Polyurethane-Coated Urea Could Reduce N Leaching in Tomato Crop in Comparison to Conventional and Stabilized Fertilizers. *Agronomy*, *10*(11), 1827. https://doi.org/10.3390/agronomy10111827

Iqbal, H., Garcia-Perez, M., & Flury, M. (2015). Effect of biochar on leaching of organic carbon, nitrogen, and phosphorus from compost in bioretention systems. *Science of*

The Total Environment, *521–522*, 37–45. https://doi.org/10.1016/J.SCITOTENV.2015.03.060

Iqbal, M. K., Nadeem, A. M., Sherazi, F., & Khan, R. A. (2014). Optimization of process parameters for kitchen waste composting by response surface methodology. *International Journal of Environmental Science and Technology*, *12*(5), 1759–1768. https://doi.org/10.1007/s13762-014-0543-x

Irfan, S. A., Razali, R., KuShaari, K., & Mansor, N. (2017). Reaction-Multi Diffusion Model for Nutrient Release and Autocatalytic Degradation of PLA-Coated Controlled-Release Fertilizer. *Polymers*, *9*(3), 111. https://doi.org/10.3390/polym9030111

Islam, S. (2025). *Agriculture, food security, and sustainability: a review*. https://doi.org/10.37349/eff.2025.101082

Jama, B., Palm, C. A., Buresh, R. J., Niang, A., Gachengo, C., Nziguheba, G., & Amadalo, B. (2000). *Tithonia diversifolia as a green manure for soil fertility improvement in western Kenya: A review*. https://doi.org/https://doi.org/10.1023/A:1006339025728

Jankowski, K. J., Neill, C., Davidson, E. A., Macedo, M. N., Costa, C., Galford, G. L., Maracahipes-Santos, L., Lefebvre, P. A., Nunes, D., Cerri, C. E. P., McHorney, R., O'Connell, C. S., & Coe, M. T. (2018). Deep soils modify environmental consequences of increased nitrogen fertilizer use in intensifying Amazon agriculture. *Scientific Reports*, *8*(1). https://doi.org/10.1038/s41598-018-31175-1

Ji, Z., Zhang, L., Liu, Y., Li, X., & Li, Z. (2023). Evaluation of composting parameters, technologies and maturity indexes for aerobic manure composting: A meta-analysis. *Science of The Total Environment*, *886*, 163929. https://doi.org/10.1016/J.SCITOTENV.2023.163929

Jia, X., Wang, M., Yuan, W., Shah, S. B., Shi, W., Meng, X., Ju, X., & Yang, B. (2016). N2O Emission and Nitrogen Transformation in Chicken Manure and Biochar Co-Composting. *Transactions of the ASABE*, *59*(5), 1277–1283. https://doi.org/10.13031/trans.59.11685

Jiang, S., Duan, Q., Ma, L., Song, Y., Xie, H., Liu, H., Chen, L., & Yu, L. (2024). Preparation and characterization of slow-release fertilizer through coating acrylate epoxidized soybean oil. *Environmental Technology \& Innovation*. https://doi.org/10.1016/J.ETI.2024.103626

Jiang, T., Ma, X., Yang, J., Tang, Q., Yi, Z., Chen, M., & Li, G. (2016). Effect of different struvite crystallization methods on gaseous emission and the comprehensive comparison during the composting. *Bioresource Technology*, *217*, 219–226. https://doi.org/10.1016/J.BIORTECH.2016.02.046

Jiménez-Regalado, E. J., Caicedo, C., Fonseca-García, A., Rivera-Vallejo, C., & Aguirre–Loredo, R. Y. (2021). Preparation and Physicochemical Properties of Modified Corn Starch–Chitosan Biodegradable Films. *Polymers*, *13*(24), 4431. https://doi.org/10.3390/polym13244431

Jiménez-Rosado, M., Rubio-Valle, J. F., Perez-Puyana, V., Guerrero, A., & Romero, A. (2021). Eco-friendly protein-based materials for a sustainable fertilization in horticulture. *Journal of Cleaner Production*, *286*, 124948. https://doi.org/10.1016/J.JCLEPRO.2020.124948

Jindo, K., Sonoki, T., & Sánchez-Monedero, M. A. (2025). Stabilizing organic matter and reducing methane emissions during manure composting with biochar to strengthen the role of compost in soil health. *Soil & Environmental Health*, *3*(4), 100164. https://doi.org/10.1016/J.SEH.2025.100164

Jindo, K., Suto, K., Matsumoto, K., García, C., Sonoki, T., & Sanchez-Monedero, M. A. (2012). Chemical and biochemical characterisation of biochar-blended composts prepared from poultry manure. *Bioresource Technology*, *110*, 396–404. https://doi.org/10.1016/J.BIORTECH.2012.01.120

Joseph, S., Cowie, A. L., Van Zwieten, L., Bolan, N., Budai, A., Buss, W., Cayuela, M. L., Graber, E. R., Ippolito, J. A., Kuzyakov, Y., Luo, Y., Ok, Y. S., Palansooriya, K. N., Shepherd, J., Stephens, S., Weng, Z., & Lehmann, J. (2021). How biochar works, and when it doesn't: A review of mechanisms controlling soil and plant responses to biochar. *GCB Bioenergy*, *13*(11), 1731–1764 https://doi.org/10.1111/GCBB.12885

Joseph, S., Kammann, C. I., Shepherd, J. G., Conte, P., Schmidt, H. P., Hagemann, N., Rich, A. M., Marjo, C. E., Allen, J., Munroe, P., Mitchell, D. R. G., Donne, S., Spokas, K., & Graber, E. R. (2018). Microstructural and associated chemical changes during the composting of a high temperature biochar: Mechanisms for nitrate, phosphate and other nutrient retention and release. *Science of The Total Environment*. https://doi.org/10.1016/J.SCITOTENV.2017.09.200

Kakar, H., Memon, M., Rajpar, İ., & Chachar, Q. I. (2021). Slow Pyrolyzed Banana Leaf Waste Biochar Amended Calcareous Soil Properties and Maize Growth. *Indian Journal of Science and Technology*, *14*(21), 1791–1805. https://doi.org/10.17485/ijst/v14i21.2235

Kaleem, M., Shabir, F., Hussain, I., Hameed, M., Ahmad, M. S. A., Mehmood, A., Ashfaq, W., Riaz, S., Afzaal, Z., Maqsood, M. F., Iqbal, U., Shah, S. M. R., & Irshad, M. (2022). Alleviation of cadmium toxicity in Zea mays L. through up-regulation of growth, antioxidant defense system and organic osmolytes under calcium supplementation. *PLoS ONE*, *17*(6). https://doi.org/10.1371/journal.pone.0269162

Kalita, A., & Vaid, V. (2025). Nutrient release kinetics from bio-polymer coated slow-release fertilizers in agricultural soil: current advances and future prospects for environmental sustainability and agricultural productivity. *Polymer Bulletin*, *83*(1). https://doi.org/10.1007/s00289-025-06137-z

Kammann, C. I., Schmidt, H. P., Messerschmidt, N., Linsel, S., Steffens, D., Müller, C., Koyro, H. W., Conte, P., & Stephen, J. (2015b). Plant growth improvement mediated by nitrate capture in co-composted biochar. *Scientific Reports 2015 5:1*, *5*(1), 1–13. https://doi.org/10.1038/srep11080

Kavitha, B., Reddy, P. V. L., Kim, B., Lee, S. S., Pandey, S. K., & Kim, K. H. (2018). Benefits and limitations of biochar amendment in agricultural soils: A review. *Journal of Environmental Management*, *227*, 146–154. https://doi.org/10.1016/J.JENVMAN.2018.08.082

Kayarogannam, P., Njoku, C. N., Otisi, S. K., Lamidi, S., Olaleye, N., Bankole, Y., Obalola, A., Aribike, E., Adigun, I., Nguyen, N., Borkowski, J. J., Vuong, M. P., Ahmad, A., Alam, S., Sharma, M., & Sağbaş, A. (2022). Response Surface Methodology - Research Advances and Applications. In *IntechOpen eBooks*. IntechOpen. https://doi.org/10.5772/intechopen.102317

Kékedy-Nagy, L., Abolhassani, M., Bakovic, S. I. P., Anari, Z., Moore, J. P., Pollet, B. G., & Greenlee, L. F. (2020). Electroless Production of Fertilizer (Struvite) and Hydrogen from Synthetic Agricultural Wastewaters. *Journal of the American Chemical Society*, *142*(44), 18844–18858. https://doi.org/10.1021/jacs.0c07916

Ketheeswaran, K., Shetranjiwalla, S., Krishnapillai, M., & Galagedara, L. (2024). Incorporating biochar to make hydrogel composites with improved structural

properties, valorized from waste-paper mill sludge and forestry residues using energy efficient protocols. *RSC Sustainability*, *2*(11), 3478–3489. https://doi.org/10.1039/d4su00332b

Khaliq, M., Hanif, M. A., Bhatti, I. A., & Mushtaq, Z. (2023). A novel study for producing complexed and encapsulated nutrients at nanometric scale to enhance plant growth. *Scientific Reports*, *13*(1). https://doi.org/10.1038/s41598-023-37607-x

Khan, N., Bolan, N., Jospeh, S., Anh, M. T. L., Meier, S., Kookana, R., Borchard, N., Sánchez-Monedero, M. A., Jindo, K., Solaiman, Z. M., Alrajhi, A. A., Sarkar, B., Basak, B. B., Wang, H., Wong, J. W. C., Manu, M. K., Kader, M. A., Wang, Q., Li, R., … Qiu, R. (2023). Complementing compost with biochar for agriculture, soil remediation and climate mitigation. *Advances in Agronomy*, *179*, 1–90. https://doi.org/10.1016/bs.agron.2023.01.001

Khan, N., Clark, I., Sánchez-Monedero, M. A., Shea, S., Meier, S., Qi, F., Kookana, R. S., & Bolan, N. (2016). Physical and chemical properties of biochars co-composted with biowastes and incubated with a chicken litter compost. *Chemosphere*, *142*, 14–23. https://doi.org/10.1016/J.CHEMOSPHERE.2015.05.065

Khan, S., Irshad, S., Mehmood, K., Hasnain, Z., Nawaz, M., Rais, A., Gul, S., Wahid, M. A., Hashem, A., Abd_Allah, E. F., Ibrar, D., & Ibrar, (2024). Biochar Production and Characteristics, Its Impacts on Soil Health, Crop Production, and Yield Enhancement: A Review. *Plants 2024, Vol. 13, Page 166*, *13*(2), 166. https://doi.org/10.3390/PLANTS13020166

Khuntia, A., Prasanna, N. S., & Mitra, J. (2022b). Technologies for biopolymer-based films and coatings. *Biopolymer-Based Food Packaging: Innovations and Technology Applications*, 66–109. https://doi.org/10.1002/9781119702313.CH3

Khuri, A. I. (2017). Response Surface Methodology and Its Applications In Agricultural and Food Sciences. *Biometrics \& Biostatistics International Journal*, *5*(5). https://doi.org/10.15406/bbij.2017.05.00141

Kiani, A., Lamberti, E., Viscusi, G., Giudicianni, P., Grottola, C. M., Ragucci, R., Gorrasi, G., & Acocella, M. R. (2023). Eco-friendly one-shot approach for producing a functionalized nano-torrefied biomass: a new application of ball milling technology. *Materials Advances*, *5*(2), 695–704. https://doi.org/10.1039/d3ma00804e

Kolahi, M., Kazemi, E., Yazdi, M., Kazemian, M., & GOLDSON-BARNABY, A. (2023). Investigating the growth characteristics, oxidative stress, and metal absorption of chickpea (Cicer arietinum L.) under cadmium stress and in silico features of HMAs proteins. *Acta Agriculturae Slovenica*, *119*(3). https://doi.org/10.14720/aas.2023.119.3.12555

Kong, Y., Wang, G., Chen, W., Yang, Y., Ma, R., Li, D., Shen, Y., Li, G., Yuan, J., & Yuan. (2022). Phytotoxicity of farm livestock manures in facultative heap composting using the seed germination index as indicator. *Ecotoxicology and Environmental Safety*, *247*, 114251. https://doi.org/10.1016/J.ECOENV.2022.114251

Kong, Y., Zhang, J., Yang, Y., Liu, Y., Zhang, L., Wang, G., Liu, G., Dang, R., Li, G., & Yuan, J. (2023). Determining the extraction conditions and phytotoxicity threshold for compost maturity evaluation using the seed germination index method. *Waste Management*, *171*, 502–511. https://doi.org/10.1016/J.WASMAN.2023.09.040

Kotake, N., Kuboki, M., Kiya, S., & Kanda, Y. (2011). Influence of dry and wet grinding conditions on fineness and shape of particle size distribution of product in a ball mill. *Advanced Powder Technology*, *22*(1), 86–92. https://doi.org/10.1016/J.APT.2010.03.015

Kottegoda, N., Nimanka, S., Fernando, N., Silva, M. de, & Munaweera, I. (2023). Climate Smart Agriculture: The Role of Fertilizer Innovations and Efficient Plant Nutrient Management. *Vidyodaya Journal of Science*, *1*. https://doi.org/10.31357/vjs.v1is1.6709

Krishnamoorthy, N., Dey, B., Unpaprom, Y., Ramaraj, R., Maniam, G. P., Govindan, N., Jayaraman, S., Arunachalam, T., & Paramasivan, B. (2021). Engineering principles and process designs for phosphorus recovery as struvite: A comprehensive review. *Journal of Environmental Chemical Engineering*. https://doi.org/10.1016/J.JECE.2021.105579

Krystyjan, M., Khachatryan, G., Grabacka, M., Krzan, M., Witczak, M., Grzyb, J., & Woszczak, L. (2021). Physicochemical, Bacteriostatic, and Biological Properties of Starch/Chitosan Polymer Composites Modified by Graphene Oxide, Designed as New Bionanomaterials. *Polymers 2021, Vol. 13, Page 2327*, *13*(14), 2327. https://doi.org/10.3390/POLYM13142327

Ksheem, A. M., Bennett, J. M. L., Antille, D. L., & Raine, S. R. (2015). Towards a method for optimized extraction of soluble nutrients from fresh and composted chicken manures. *Waste Management*, *45*, 76–90. https://doi.org/10.1016/J.WASMAN.2015.02.011

Kucio, K., Sydorchuk, V., Khalameida, S., & Charmas, B. (2020). Mechanochemical and microwave treatment of precipitated zirconium dioxide and study of its physical–chemical, thermal and photocatalytic properties. *Journal of Thermal Analysis and Calorimetry 2020 147:1*, *147*(1), 253–262. https://doi.org/10.1007/S10973-020-10285-X

Kumar, A., Bhattacharya, T., Shaikh, W. A., Roy, A., Chakraborty, S., Vithanage, M., & Biswas, J. K. (2023). Multifaceted applications of biochar in environmental management: a bibliometric profile. *Biochar*, *5*(1). https://doi.org/10.1007/s42773-023-00207-z

Kumar, M., Xiong, X., Wan, Z., Sun, Y., Tsang, D. C. W. W., Gupta, J., Gao, B., Cao, X., Tang, J., & Ok, Y. S. (2020b). Ball milling as a mechanochemical technology for fabrication of novel biochar nanomaterials. *Bioresource Technology*, *312*, 123613. https://doi.org/10.1016/J.BIORTECH.2020.123613

Kumar, P., Singh, K., Singh, A. K., Singh, N., Singh, S., Agrawal, S., Das, R., Rajput, V. D., Minkina, T., Mishra, S. K., & Tiwari, K. N. (2024). Nano- and Nano-Biochar: Overview, Production, and Characteristics. *Nanomaterials and Nano-Biochar in Reducing Soil Stress: An Integrated Approach to Sustainable Agriculture*, 1–16. https://doi.org/10.1201/9781003503453-1

Kurtulus, Y. B., Bakircioglu, D., Kuscu, M., Topraksever, N., & Destanoğlu, O. (2021). Investigation of aflatoxin and metal concentrations in animal feeds and feed ingredients from Turkey. *Journal of Chemical Metrology*, (1), 52–64. https://doi.org/10.25135/jcm.56.21.01.1937

Kusumastuti, Y., Istiani, A., Rochmadi, & Purnomo, C. W. (2019). Chitosan-Based Polyion Multilayer Coating on NPK Fertilizer as Controlled Released Fertilizer. *Advances in Materials Science and Engineering*, *2019*(1), 2958021. https://doi.org/10.1155/2019/2958021

Lawrencia, D., Wong, S. K., Low, D. Y. S., Goh, B. H., Goh, J. K., Ruktanonchai, U., Soottitantawat, A., Lee, L., & Tang, S. Y. (2021). Controlled Release Fertilizers: A

Review on Coating Materials and Mechanism of Release. In *Plants* (Vol. 10, Number 2, p. 238). Multidisciplinary Digital Publishing Institute. https://doi.org/10.3390/plants10020238

Lebrun, M., Védère, C., Honvault, N., Rumpel, C., & Houben, D. (2023). Mixing ratio and Nitrogen fertilization drive synergistic effects between biochar and compost. *Nutrient Cycling in Agroecosystems*, *128*(3), 429–446. https://doi.org/10.1007/s10705-023-10320-x

Lee, P., Lin, X., Khan, F., Bennett, A. E., & Winter, J. O. (2022). Translating controlled release systems from biomedicine to agriculture. *Frontiers in Biomaterials Science*, *1*. https://doi.org/10.3389/fbiom.2022.1011877

Lewicka, K., Szymanek, I., Rogacz, D., Wrzalik, M., Łagiewka, J., Nowik-Zając, A., Zawierucha, I., Coseri, S., Puiu, I., Falfushynska, H., & Rychter, P. (2024). Current Trends of Polymer Materials' Application in Agriculture. *Sustainability 2024, Vol. 16, Page 8439*, *16*(19), 8439. https://doi.org/10.3390/SU16198439

Liang, B., Gao, D., Tajammal Munir, M., Yu, W., Wu, X., Huang, Y., Li, H., Young, B., Zhou, S., & Li, B. (2024). Struvite biomineralization as a promising solution to break the pollutant-resource paradox of phosphorus. *Chemical Engineering Journal*, *493*, 152437. https://doi.org/10.1016/J.CEJ.2024.152437

Liang, J., Shen, Y., Shou, Z., Yuan, H., Dai, X., & Zhu, N. (2018). Nitrogen loss reduction by adding KH2PO4-K2HPO4 buffer solution during composting of sewage sludge. *Bioresource Technology*, *264*, 116–122. https://doi.org/10.1016/j.biortech.2018.05.065

Liang, L., Xi, F., Tan, W., Meng, X., Hu, B., & Wang, X. (2021). Review of organic and inorganic pollutants removal by biochar and biochar-based composites. *Biochar*, *3*(3), 255–281. https://doi.org/10.1007/s42773-021-00101-6

Libutti, A., Francavilla, M., & Monteleone, M. (2021). Hydrological Properties of a Clay Loam Soil as Affected by Biochar Application in a Pot Experiment. *Agronomy*, *11*(3), 489. https://doi.org/10.3390/agronomy11030489

Liu, J., Xie, W., Yang, J., Yao, R., Wang, X., & Li, W. (2023). Effect of Different Fertilization Measures on Soil Salinity and Nutrients in Salt-Affected Soils. *Water*, *15*(18), 3274. https://doi.org/10.3390/w15183274

Liu, X., Li, Y., Zeng, L., Li, X., Chen, N., Bai, S., He, H., Wang, Q., & Zhang, C. (2022). A Review on Mechanochemistry: Approaching Advanced Energy Materials with Greener Force. *Advanced Materials*, *34*(46), 2108327. https://doi.org/10.1002/ADMA.202108327

Liu, X., Liao, J., Song, H., Yang, Y., Guan, C., & Zhang, Z. (2019). A Biochar-Based Route for Environmentally Friendly Controlled Release of Nitrogen: Urea-Loaded Biochar and Bentonite Composite. *Scientific Reports*, *9*(1). https://doi.org/10.1038/s41598-019-46065-3

López-Cano, I., Roig, A., Cayuela, M. L., Alburquerque, J. A., & Sánchez-Monedero, M. A. (2016). Biochar improves N cycling during composting of olive mill wastes and sheep manure. *Waste Management*, *49*(2), 553–559. https://doi.org/10.1016/j.wasman.2015.12.031

Lopez-Tenllado, F. J., Motta, I. L., & Hill, J. M. (2021). Modification of biochar with high-energy ball milling: Development of porosity and surface acid functional groups. *Bioresource Technology Reports*, *15*, 100704. https://doi.org/10.1016/J.BITEB.2021.100704

Luo, D., Wang, L., Nan, H., Cao, Y., Wang, H., Kumar, T. V., & Wang, C. (2022). Phosphorus adsorption by functionalized biochar: a review. *Environmental Chemistry Letters 2022 21:1*, *21*(1), 497–524. https://doi.org/10.1007/S10311-022-01519-5

Lyu, H., Gao, B., He, F., Zimmerman, A. R., Ding, C., Huang, H., & Tang, J. (2017). Effects of ball milling on the physicochemical and sorptive properties of biochar: Experimental observations and governing mechanisms. *Environmental Pollution*, *233*, 54–63. https://doi.org/10.1016/j.envpol.2017.10.037

Ma, F., Chen, Q., Quan, H., Zhao, C., Wang, Y., & Zhu, T. (2024). Combined Treatment for Chicken Manure and Kitchen Waste Enhances Composting Effect by Improving pH and C/N. *Waste and Biomass Valorization 2024 16:2*, *16*(2), 613–625. https://doi.org/10.1007/S12649-024-02676-0

Ma, N., Zhang, L., Zhang, Y., Yang, L., Yu, C., Yin, G., Doane, T. A., Zhi, W., Zhu, P., & Ma, X. (2016). Biochar Improves Soil Aggregate Stability and Water Availability in a Mollisol after Three Years of Field Application. *PLoS ONE*, *11*(5). https://doi.org/10.1371/journal.pone.0154091

Maaz, T. M., Dobermann, A., Lyons, S. E., & Thomson, A. M. (2025). Review of research and innovation on novel fertilizers for crop nutrition. *Npj Sustainable Agriculture*, *3*(1). https://doi.org/10.1038/s44264-025-00066-0

Madzokere, T. C., Murombo, L. T., & Chirariwa, H. (2021). Nano-based slow releasing fertilizers for enhanced agricultural productivity. *Materials Today Proceedings*, *45*, 3709–3715. https://doi.org/10.1016/j.matpr.2020.12.674

Magaletti, R., Pizzetti, F., Masi, M., & Rossi, F. (2023). Biobased Materials as Promising Tools for the Slow-Release of Urea. *ACS Agricultural Science \& Technology*, *3*(11), 957–969. https://doi.org/10.1021/acsagscitech.3c00450

Mahmoud, E., El-shahawy, A., Ibrahim, M., El-Halim, A. E.-H. A., Abo-Ogiala, A., Shokr, M. S., Mohamed, E. S., Rebouh, N. Y., & Ismail, S. M. (2024). Enhancing Maize Yield and Soil Health through the Residual Impact of Nanomaterials in Contaminated Soils to Sustain Food. *Nanomaterials*, *14*(4), 369. https://doi.org/10.3390/nano14040369

Mahmoud, N., Abdou, M. A. H., Salaheldin, S., Soliman, W. S., & Abbas, A. M. (2023). The Impact of Irrigation Intervals and NPK/Yeast on the Vegetative Growth Characteristics and Essential Oil Content of Lemongrass. *Horticulturae 2023, Vol. 9, Page 365*, *9*(3), 365. https://doi.org/10.3390/HORTICULTURAE9030365

Malomo, G. A., Bolu, S. A., Shuaibu Madugu, A., Usman, Z. S., Malomo, G. A., Bolu, S. A., Shuaibu Madugu, A., & Usman, Z. S. (2018). Nitrogen Emissions and Mitigation Strategies in Chicken Production. *Animal Husbandry and Nutrition*. https://doi.org/10.5772/intechopen.74966

Mancho, C., Diez-Pascual, S., Alonso, J., Gil-Díaz, M., & Lobo, M. C. (2023). Assessment of Recovered Struvite as a Safe and Sustainable Phosphorous Fertilizer. *Environments - MDPI*, *10*(2), 22. https://doi.org/10.3390/ENVIRONMENTS10020022/S1

Manea, A., Tabassum, S., Lambert, M., Cinantya, A., Ossola, A., & Leishman, M. R. (2023). Biochar, but not soil microbial additives, increase the resilience of urban plant species to low water availability. *Urban Ecosystems*, *26*(5), 1251–1261. https://doi.org/10.1007/s11252-023-01382-4

Matheri, F., Musafiri, C. M., Bautze, D., Durot, C., & Kiboi, M. (2025). Synergistic effect of biochar and post-thermophilic stage application of supplemental Tithonia

diversifolia on compost nutrient dynamics. *Discover Soil.*, *2*(1). https://doi.org/10.1007/s44378-025-00051-6

Md Saleh, Z., Mohamed, R. M. S. R., Al-Gheethi, A., Zainun, N. Y., & Nor Amani, N. A. F. (2020). Optimizing decomposition of food wastes using response surface methodology. *Materials Today: Proceedings*, *31*, 96–99. https://doi.org/10.1016/J.MATPR.2020.01.251

Melo, L. C. A., & Sánchez-Monedero, M. Á. (2024). How biochar-based fertilizers and biochar compost affect nutrient cycling and crop productivity. *Nutrient Cycling in Agroecosystems*, *128*(3), 411–414. https://doi.org/10.1007/s10705-024-10358-5

Melo, M. R. P., Martins, N., Melo, E. I. de, & Okura, M. H. (2020). Biochar as an additive in the composting process. *International Journal of Advanced Engineering Research and Science*, *7*(7), 267–276. https://doi.org/10.22161/ijaers.77.30

Mendes, J. F., Paschoalin, R. T., Carmona, V. B., Sena Neto, A. R., Marques, A. C. P., Marconcini, J. M., Mattoso, L. H. C., Medeiros, E. S., & Oliveira, J. E. (2016). Biodegradable polymer blends based on corn starch and thermoplastic chitosan processed by extrusion. *Carbohydrate Polymers*, *137*, 452–458. https://doi.org/10.1016/J.CARBPOL.2015.10.093

Mendes, P. M., Ribeiro, J. A., Martins, G. A., Lucia, T., Araújo, T. R., Fuentes-Guevara, M. D., Corrêa, L. B., & Corrêa, É. K. (2021). Phytotoxicity test in check: Proposition of methodology for comparison of different method adaptations usually used worldwide. *Journal of Environmental Management*, *291*, 112698. https://doi.org/10.1016/j.jenvman.2021.112698

Mensah, A. K., & Frimpong, K. A. (2018). Biochar and/or Compost Applications Improve Soil Properties, Growth, and Yield of Maize Grown in Acidic Rainforest and Coastal Savannah Soils in Ghana. *International Journal of Agronomy*, *2018*, 1–8. https://doi.org/10.1155/2018/6837404

Menya, E., Olupot, P. W., Storz, & H., Lubwama, & M., Kiros, Y., & John, M. J. (2020). Optimization of pyrolysis conditions for char production from rice husks and its characterization as a precursor for production of activated carbon. *Biomass Conversion and Biorefinery*. https://doi.org/10.1007/s13399-019-00399-0

Midamba, D. C., Agbolosoo, J. A., Ouya, F. O., & Kwesiga, M. (2025). The contribution of Socio-Economic factors to adoption of inorganic fertilizers among maize farmers

in Western Uganda. *Discover Sustainability*, *6*(1). https://doi.org/10.1007/s43621-025-01610-1

Miguel, N., López, A., Jojoa-Sierra, S. D., Gómez, J., & Ormad, M. P. (2025). Sustainable Management of the Organic Fraction of Municipal Solid Waste: Microbiological Quality Control During Composting and Its Application in Agriculture on a Pilot Scale. *Sustainability 2025, Vol. 17, Page 4169*, *17*(9), 4169. https://doi.org/10.3390/SU17094169

Miguel-Rojas, C., & Pérez-de-Luque, A. (2023). Nanobiosensors and nanoformulations in agriculture: new advances and challenges for sustainable agriculture. *Emerging Topics in Life Sciences*, *7*(2), 229–238. https://doi.org/10.1042/etls20230070

Mikajlo, I., Lerch, T. Z., Louvel, B., Hynšt, J., Záhora, J., Pourrut, B., & Pourrut, (2024). Composted biochar versus compost with biochar: effects on soil properties and plant growth. *Biochar*, *6*(1), 1–17. https://doi.org/10.1007/s42773-024-00379-2

Milon, A. R., Chang, S. W., & Ravindran, B. (2021). Biochar amended compost maturity evaluation using commercial vegetable crops seedlings through phytotoxicity germination bioassay. *Journal of King Saud University - Science*, *34*(2), 101770. https://doi.org/10.1016/j.jksus.2021.101770

Mim, J. J., Rahman, S., Khan, F., Paul, D., Sikder, S. S., DAS, H. P., Khan, S., Orny, N. T., Shuvo, M. I. M., & Hossain, N. (2025). Towards Smart Agriculture through Nano-Fertilizer-A Review. *Materials Today Sustainability*, 101100. https://doi.org/10.1016/j.mtsust.2025.101100

Minai, J., Libohova, Z., Kaizzi, K. C., Schulze, D. G., & Nkonya, E. (2023). Spatial Variability of Selected Soil Properties in Uganda Using Machine Learning Approaches. *SSRN Electronic Journal*. https://doi.org/10.2139/ssrn.4563998

Mishra, A. K., Yadav, P., Sharma, S., & Maurya, P. K. (2025). Comparison of microbial diversity and community structure in soils managed with organic and chemical fertilization strategies using amplicon sequencing of 16 s and ITS regions. *Frontiers in Microbiology*, *15*. https://doi.org/10.3389/fmicb.2024.1444903

Mlangeni, A. N. J. T. (2013). Effect of Tithonia diversifolia on Compost Pile Heat Built-Up and Physico-Chemical Quality Parameters of Chimato Compost. *Environment and Natural Resources Research*, *3*(3), 63–70. https://doi.org/10.5539/enrr.v3n3p63

Mlangeni, A. T., Sajidu, S., & Chiotha, S. (2013). Total Kjeldahl-N, Nitrate-N, C/N Ratio and pH Improvements in Chimato Composts Using Tithonia Diversifolia. *Journal of Agricultural Science*, *5*(10). https://doi.org/10.5539/jas.v5n10p1

Mohamed, I., Farid, I. M., Siam, H. S., Abbas, M. H. H., Tolba, M., Mahmoud, S. A., Abbas, H. H., Abdelhafez, A. A., Elkelish, A., Scopa, A., Drosos, M., Abdelrahman, M. A. E., & Bassouny, M. A. (2024). A brief investigation on the prospective of co-composted biochar as a fertilizer for Zucchini plants cultivated in arid sandy soil. *Open Agriculture*, *9*(1). https://doi.org/10.1515/OPAG-2022-0322

Morales, L., Boy, E. F., Madejón, E., & Domínguez, M. T. (2023). Soil legacy and organic amendment role in promoting the resistance of contaminated soils to drought. *Applied Soil Ecology*, *195*, 105226. https://doi.org/10.1016/j.apsoil.2023.105226

Mousavi, M., Goyette, B., Zhao, X., Couture, C., Talbot, G., & Rajagopal, R. (2024). Struvite-Driven Integration for Enhanced Nutrient Recovery from Chicken Manure Digestate. *Bioengineering*, *11*(2), 145. https://doi.org/10.3390/bioengineering11020145

Mujtaba, G., Hayat, R., Hussain, Q., & Ahmed, M. (2021). Physio-Chemical Characterization of Biochar, Compost and Co-Composted Biochar Derived from Green Waste. *Sustainability 2021, Vol. 13, Page 4628*, *13*(9), 4628. https://doi.org/10.3390/SU13094628

Mukhina, I., Rizhiya, E., & Банкина, T. A. (2020). Biochar Effect on Nutrients Availability to Barley. *Environmental Research Engineering and Management*, *76*(2), 43–53. https://doi.org/10.5755/j01.erem.76.2.21854

Murtaza, G., Usman, M., Iqbal, J., Tahir, M. N., Elshikh, M. S., Alkahtani, J., Toleikienė, M., Iqbal, R., Akram, M. I., & Gruda, N. S. (2024). The impact of biochar addition on morpho-physiological characteristics, yield and water use efficiency of tomato plants under drought and salinity stress. *BMC Plant Biology*, *24*(1), 356. https://doi.org/10.1186/s12870-024-05058-9

Naeem, M. B., Jahan, S., Rashid, A., Shah, A. A., Raja, V., & El-Sheikh, M. A. (2024). Improving maize yield and drought tolerance in field conditions through activated biochar application. *Scientific Reports*, *14*(1), 25000. https://doi.org/10.1038/s41598-024-76082-w

Naghdi, M., Taheran, M., Brar, S. K., Rouissi, T., Verma, M., Surampalli, R. Y., & Valero, J. R. (2017b). A green method for production of nanobiochar by ball milling-optimization and characterization. *Journal of Cleaner Production*, *164*, 1394–1405. https://doi.org/10.1016/J.JCLEPRO.2017.07.084

Nataliya, A., & Andrew, W. L. (2018). Cropping systems and soil quality and fertility in south-central Uganda. *African Journal of Agricultural Research*, *13*(15), 792–802. https://doi.org/10.5897/ajar2018.13056

Nawaz, F., Rafeeq, R., Majeed, S., Ismail, M. S., Ahsan, M., Ahmad, K. S., Akram, A., & Haider, G. (2022). Biochar Amendment in Combination with Endophytic Bacteria Stimulates Photosynthetic Activity and Antioxidant Enzymes to Improve Soybean Yield Under Drought Stress. *Journal of Soil Science and Plant Nutrition*, *23*(1), 746–760. https://doi.org/10.1007/s42729-022-01079-1

Nayak, P., Nandipamu, T. M. K., Chaturvedi, S., Dhyani, V. C., & Chandra, S. (2024). Synthesis, Properties, and Mechanistic Release-Kinetics Modeling of Biochar-Based Slow-Release Nitrogen Fertilizers and Their Field Efficacy. *Journal of Soil Science and Plant Nutrition*, *24*(4), 7460–7479. https://doi.org/10.1007/S42729-024-02052

Negi, P., Thakur, R., Manral, K., Tomar, K., Rawat, B. S., Ramola, B., & Ahmad, W. (2022). Coated Controlled-Release Fertilizers: Potential Solution for Sustainable Agriculture. *Nature Environment and Pollution Technology*, *21*(4), 1739–1745. https://doi.org/10.46488/nept.2022.v21i04.028

Nepal, J., Ahmad, W., Munsif, F., Khan, A., & Zou, Z. (2023). Advances and prospects of biochar in improving soil fertility, biochemical quality, and environmental applications. In *Frontiers in Environmental Science* (Vol. 11). Frontiers Media S.A. https://doi.org/10.3389/fenvs.2023.1114752

Ng, L. Y. F., Ariffin, H., Yasim-Anuar, T. A. T., Farid, M. A. A., & Hassan, M. A. (2022). High-Energy Ball Milling for High Productivity of Nanobiochar from Oil Palm Biomass. *Nanomaterials*, *12*(18), 3251. https://doi.org/10.3390/nano12183251

Njoroge, S., Mugi-Ngenga, E., Chivenge, P., Boulal, H., Zingore, S., & Majumdar, K. (2023). The Impact of the Global Fertilizer Crisis in Africa. *Growing Africa*, *2*(1), 3–8. https://doi.org/10.55693/ga21.xzvk8042

Nkonya, E., Pender, J., Kaizzi, K. C., Kato, E., Mugarura, S., Ssali, H., & Muwonge, J. (2008). Linkages between land management, land degradation, and poverty in Sub-

Saharan Africa: The case of Uganda. In *AgEcon Search (University of Minnesota, USA)*. University of Minnesota Rochester. https://doi.org/10.22004/ag.econ.47224

Nongbet, A., Mishra, A. K., Mohanta, Y. K., Mahanta, S., Ray, M. K., Khan, M., Baek, K.-H., & Chakrabartty, I. (2022b). Nanofertilizers: A Smart and Sustainable Attribute to Modern Agriculture. In *Plants* (Vol. 11, Number 19, p. 2587). Multidisciplinary Digital Publishing Institute. https://doi.org/10.3390/plants11192587

Novak, A., Li, L., Wason, J. W., Wang, J., & Zhang, Y. (2023). Characterization and modification of biochar from a combined heat and power (CHP) plant for amending sandy soils collected from wild blueberry fields. *BioResources*, *19*(1), 228–244. https://doi.org/10.15376/biores.19.1.228-244

Nurin, A. Y., Tee, T. P., Chin, N. L., Zainudin, M. H. M., & Nayan, N. (2024). Optimization of watermelon waste as a bulking agent for sustainable co-composting of livestock manures using response surface methodology. *Frontiers in Sustainable Food Systems*, *8*. https://doi.org/10.3389/fsufs.2024.1368970

Omolola, T. O. (2019). Phytochemical, Proximate and Elemental Composition of Tithonia diversifolia (Hemsley) A. Gray leaves. *International Annals of Science*, *8*(1), 54–61. https://doi.org/10.21467/ias.8.1.54-61

Opala, P. A. (2020). Recent Advances in the Use of Tithonia diversifolia Green Manure for Soil Fertility Management in Africa: A Review. *Agricultural Reviews*, *41*(03). https://doi.org/10.18805/ag.r-141

Othman, S. H., Ronzi, N. D. A., Shapi'i, R. A., Dun, M., Ariffin, S. H., & Mohammed, M. A. P. (2023). Biodegradability of Starch Nanocomposite Films Containing Different Concentrations of Chitosan Nanoparticles in Compost and Planting Soils. *Coatings 2023, Vol. 13, Page 777*, *13*(4), 777. https://doi.org/10.3390/COATINGS13040777

País-Chanfrau, J. M., Núñez-Pérez, J., del Carmen Espín-Valladares, R., Lara-Fiallos, M., & Trujillo, L. E. (2021). Uses of the Response Surface Methodology for the Optimization of Agro-Industrial Processes. In *IntechOpen eBooks*. IntechOpen. https://doi.org/10.5772/intechopen.98283

Palansooriya, K. N., Dissanayake, P. D., El-Naggar, A., Gayesha, E., Wijesekara, H., Krishnamoorthy, N., Cai, Y., & Chang, S. X. (2025). Biochar-based controlled-

release fertilizers for enhancing plant growth and environmental sustainability: a review. *Biology and Fertility of Soils 2025 61:4*, *61*(4), 701–715. https://doi.org/10.1007/S00374-025-01888-3

Panday, D., Bhusal, N., Das, S., & Ghalehgolabbehbahani, A. (2024). Rooted in Nature: The Rise, Challenges, and Potential of Organic Farming and Fertilizers in Agroecosystems. *Sustainability 2024, Vol. 16, Page 1530*, *16*(4), 1530. https://doi.org/10.3390/SU16041530

Pantoja, F. L., Sukmana, H., Beszédes, S., & László, Z. (2023). Removal of ammonium and phosphates from aqueous solutions by biochar produced from agricultural waste. *Journal of Material Cycles and Waste Management*, *25*(4), 1921–1934. https://doi.org/10.1007/s10163-023-01687-8

Paredes, A. O., Contreras, A. R., Delgado, A. M. S., Hernández, E. G., Delgado, R. S., Lara, T. L., & Zaragoza, J. B. H. (2023). Obtention and characterization of chitosan/starch/roselle films for the preservation of perishable fruits. *Emirates Journal of Food and Agriculture*. https://doi.org/10.9755/ejfa.2023.3157

Parra-Orobio, B. A., Rotavisky-Sinisterra, M. P., Pérez–Vidal, A., Marmolejo-Rebellón, L. F., & Torres–Lozada, P. (2021). Physicochemical, microbiological characterization and phytotoxicity of digestates produced on single-stage and two-stage anaerobic digestion of food waste. *Sustainable Environment Research*, *31*(1). https://doi.org/10.1186/s42834-021-00085-9

Peng, Y., Chen, Q., Lian, J., Zhang, W., Li, G., & Zhang, J. (2023). Combined Application of Organic Fertilizer with Microbial Inoculum Improved Aggregate Formation and Salt Leaching in a Secondary Salinized Soil. *Plants*, *12*(16), 2945. https://doi.org/10.3390/plants12162945

Peñuelas, J., Coello, F., & Sardans, J. (2023). A better use of fertilizers is needed for global food security and environmental sustainability. *Agriculture \& Food Security*, *12*(1). https://doi.org/10.1186/s40066-023-00409-5

Peterson, S. C., Jackson, M. A., Kim, S., & Palmquist, D. E. (2012). Increasing biochar surface area: Optimization of ball milling parameters. *Powder Technology*, *228*, 115–120. https://doi.org/10.1016/j.powtec.2012.05.005

Pezzolla, D., Cucina, M., Proietti, P., Calisti, R., Regni, L., & Gigliotti, G. (2021). The Use of New Parameters to Optimize the Composting Process of Different Organic

Wastes. *Agronomy 2021, Vol. 11, Page 2090*, *11*(10), 2090. https://doi.org/10.3390/AGRONOMY11102090

Piash, M. I., Itoh, T., Abe, K., & Iwabuchi, K. (2024). Superior nutrient recovery and release by chicken manure-derived biochar over hydrochar and compost for soil fertilization. *Geoderma Regional*, *40*. https://doi.org/10.1016/j.geodrs.2024.e00906

Piash, M. I., Iwabuchi, K., Itoh, T., & Uemura, K. (2021). Release of essential plant nutrients from manure- and wood-based biochars. *Geoderma*, *397*, 115100. https://doi.org/10.1016/j.geoderma.2021.115100

Pohshna, C., & Mailapalli, D. R. (2023). Modeling the particle size of nanomaterials synthesized in a planetary ball mill. *OpenNano*, *14*, 100191. https://doi.org/10.1016/J.ONANO.2023.100191

Pohshna, C., Mailapalli, D. R., & Laha, T. (2020). *Synthesis of Nanofertilizers by Planetary Ball Milling*. 75–112. https://doi.org/10.1007/978-3-030-33281-5_3

Pohshna, C., Mailapalli, D. R., & Mailapalli, C. P. (2023). Modeling the particle size of nanomaterials synthesized in a planetary ball mill. *OpenNano*, *14*, 100191. https://doi.org/10.1016/J.ONANO.2023.100191

Pokharel, P., & Chang, S. X. (2023). Biochar decreases and nitrification inhibitor increases phosphorus limitation for microbial growth in a wheat-canola rotation. *Science of The Total Environment*, *858*, 159773. https://doi.org/10.1016/J.SCITOTENV.2022.159773

Prost, K., Borchard, N., Siemens, J., Kautz, T., Séquaris, J.-M., Möller, A., & Amelung, W. (2013). Biochar Affected by Composting with Farmyard Manure. *Journal of Environmental Quality*, *42*(1), 164–172. https://doi.org/10.2134/JEQ2012.0064

Purakayastha, T. J., Bera, T., Bhaduri, D., Sarkar, B., Mandal, S., Wade, P., Kumari, S., Biswas, S., Menon, M., Pathak, H., & Tsang, D. C. W. (2019). A review on biochar modulated soil condition improvements and nutrient dynamics concerning crop yields: Pathways to climate change mitigation and global food security. In *Chemosphere* (Vol. 227, pp. 345–365). Elsevier BV. https://doi.org/10.1016/j.chemosphere.2019.03.170

Qian, J., Zhou, X., Cai, Q., Zhao, J., & Huang, X. (2023). The Study of Optimal Adsorption Conditions of Phosphate on Fe-Modified Biochar by Response Surface

Methodology. *Molecules 2023, Vol. 28, Page 2323*, *28*(5), 2323. https://doi.org/10.3390/molecules28052323

Qiao, Y., Zhang, L., & Sun, S. (2025). Biomass-based coated controlled-release fertilizers: a sustainable solution for tropical agriculture. *Tropical Plants*, *4*(1), 0. https://doi.org/10.48130/tp-0025-0001

Rabinovich, A., Heckman, J. R., Lew, B., & Rouff, A. A. (2021). Magnesium supplementation for improved struvite recovery from dairy lagoon wastewater. *Journal of Environmental Chemical Engineering*, *9*(4), 105628. https://doi.org/10.1016/j.jece.2021.105628

Raczkiewicz, M., Bogusz, A., Pan, B., Xing, B., & Oleszczuk, P. (2024). Contrasting environmental impacts of nano-biochar and conventional biochar on various organisms. *The Science of The Total Environment*, *957*, 177629. https://doi.org/10.1016/j.scitotenv.2024.177629

Radziemska, M., Gusiatin, Z. M., Cydzik-Kwiatkowska, A., Blazejczyk, A., Kumar, V., Kintl, A., & Brtnický, M. (2022). Effect of Biochar on Metal Distribution and Microbiome Dynamic of a Phytostabilized Metalloid-Contaminated Soil Following Freeze–Thaw Cycles. *Materials*, *15*(11), 3801. https://doi.org/10.3390/ma15113801

Rafique, M. I., Al-Wabel, M. I., Al-Farraj, A. S., Ahmad, M., Aouak, T., Al-Swadi, H. A., & Mousa, M. A. (2025). Incorporation of biochar and semi-interpenetrating biopolymer to synthesize new slow release fertilizers and their impact on soil moisture and nutrients availability. *Scientific Reports*, *15*(1), 9563. https://doi.org/10.1038/s41598-025-90367-8

Rafique, M. I., Al-Wabel, M. I., Al-Farraj, A. S., Ahmad, M., Aouak, T., Al-Swadi, H. A., & Mousa, M. awad. (2024). Semi-Interpenetrating Polymer Embedded Biochar Based Slow-Release Fertilizers: Fabrication, Characterization, and Nutrients Release Dynamics. *SSRN Electronic Journal*. https://doi.org/10.2139/ssrn.4960526

Rahman, A., Islam, K. R., Ahsan, S., Діденко, H. O., & Sundermeier, A. (2024). Predicting Accumulation and Potential Edge-of-Field Loss of Phosphorus to Surface Water from Diverse Ecosystems. *Water Air \& Soil Pollution*, *235*(12). https://doi.org/10.1007/s11270-024-07565-9

Rahman, S. U., Han, J., Yasin, G., Imtiaz, M. T., Zhao, X., Alharbi, S. A., Alfarraj, S., & Alarfaj, A. A. (2025). Synergetic effects of potassium and biochar on morphological,

physiological, and biochemical attributes of maize crop grown under different levels of drought stress. *BMC Plant Biology*, *25*(1). https://doi.org/10.1186/s12870-025-06391-3

Rajaonarivony, R. K., Rouau, X., Fabre, C., & Mayer-Laigle, C. (2022). Properties of biomass powders resulting from the fine comminution of lignocellulosic feedstocks by three types of ball-mill set-up. *Open Research Europe*, *1*, 125. https://doi.org/10.12688/openreseurope.14017.2

Ramos, S. J., Pinto, D. A., Guedes, R. S., Dias, Y. N., Caldeira, C. F., Gastauer, M., e Souza Filho, P. W. M., & Fernandes, A. R. (2021). Açaí Biochar and Compost Affect the Phosphorus Sorption, Nutrient Availability, and Growth of Dioclea apurensis in Iron Mining Soil. *Minerals*, *11*(7), 674. https://doi.org/10.3390/min11070674

Rani, M., Abideen, Z., Munir, N., Hasnain, M., Mehdizadeh, M., Qasim, M., & Radicetti, E. (2026). Enhancing soil fertility, nutrient recovery and carbon sequestration: the role of biochar, composted biochar, and biochar-compost mixtures in sustainable agriculture. *Journal of Trace Elements and Minerals*, *15*(3), 100276. https://doi.org/10.1016/j.jtemin.2025.100276

Ransom, C. J., Jolley, V. D., Blair, T. A., Sutton, L. E., & Hopkins, B. G. (2020). Nitrogen release rates from slow- and controlled-release fertilizers influenced by placement and temperature. *PLoS ONE*, *15*(6). https://doi.org/10.1371/journal.pone.0234544

Rashidzadeh, A., Olad, A., & Reyhanitabar, A. (2015). Hydrogel/clinoptilolite nanocomposite-coated fertilizer: swelling, water-retention and slow-release fertilizer properties. *Polymer Bulletin 2015 72:10*, *72*(10), 2667–2684. https://doi.org/10.1007/S00289-015-1428-Y

Rasul, F., Shahzad, S., Li, D., Naz, N., MUJAHID, N., Zafar, A., AL-KHAYRI, J. M., Al-Dossary, O., Ismail, M., Ghazzawy, H. S., Al-Mssallem, M. Q., & Almaghasla, M. I. (2025). Impact of biochar and compost on growth and physiological characteristics of maize (Zea mays l.). *Applied Ecology and Environmental Research*, *23*(5), 8741–8753. https://doi.org/10.15666/aeer/2305_87418753

Ravindran, B., Karmegam, N., Awasthi, M. K., Chang, S. W., Selvi, P. K., Balachandar, R., Chinnappan, S., Azelee, N. I. W., & Munuswamy-Ramanujam, G. (2022). Valorization of food waste and poultry manure through co-composting amending

saw dust, biochar and mineral salts for value-added compost production. *Bioresource Technology*, *346*, 126442. https://doi.org/10.1016/J.BIORTECH.2021.126442

Ravindran, B., Mupambwa, H. A., Silwana, S., & Mnkeni, P. N. S. (2017). Assessment of nutrient quality, heavy metals and phytotoxic properties of chicken manure on selected commercial vegetable crops. *Heliyon*, *3*(12), e00493. https://doi.org/10.1016/J.HELIYON.2017.E00493

Raza, M. A. S., Ibrahim, M. A., Ditta, A., Iqbal, R., Aslam, M. U., Muhammad, F., Ali, S., Çığ, F., Ali, B., Ikram, R. M., Muzamil, M. N., ur Rahman, M. H., Alwahibi, M. S., & Elshikh, M. S. (2023). Exploring the recuperative potential of brassinosteroids and nano-biochar on growth, physiology, and yield of wheat under drought stress. *Scientific Reports*, *13*(1). https://doi.org/10.1038/s41598-023-42007-2

Raza, S. T., Wu, J., Ali, Z., Anjum, R., Bazai, N. A., Feyissa, A., & Chen, Z. (2021). Differential Effects of Organic Amendments on Maize Biomass and Nutrient Availability in Upland Calcareous Soil. *Atmosphere*, *12*(8), 1034. https://doi.org/10.3390/atmos12081034

Ren, L., Yan, X., Zhou, J., Tong, J., & Su, X. (2017). Influence of chitosan concentration on mechanical and barrier properties of corn starch/chitosan films. *International Journal of Biological Macromolecules*, *105*, 1636–1643. https://doi.org/10.1016/J.IJBIOMAC.2017.02.008

Rosa, D., Petruccelli, V., Iacobbi, M. C., Brasili, E., Badiali, C., Pasqua, G., & Palma, L. Di. (2024). Functionalized biochar from waste as a slow-release nutrient source: Application on tomato plants. *Heliyon*, *10*(8). https://doi.org/10.1016/j.heliyon.2024.e29455

Rouzi, K., Abulikemu, A., Zhao, J., & Wu, B. (2017). A study on the synthesis and anion recognition of a chitosan-urea receptor. *RSC Advances*, *7*(80), 50920–50927. https://doi.org/10.1039/c7ra09431k

Roy, R., Hossain, A., Sharif, Md. O., Das, M., & Sarker, T. (2024). Optimizing biochar, vermicompost, and duckweed amendments to mitigate arsenic uptake and accumulation in rice (Oryza sativa L.) cultivated on arsenic-contaminated soil. *BMC Plant Biology*, *24*(1). https://doi.org/10.1186/s12870-024-05219-w

Roy, S., Khekare, G., Chhajed, S., & Victor, A. (2025). Integrating classification, regression, and time series models to assess biochar safety, optimize pollutant

removal, and predict environmental impacts. *Frontiers in Soil Science*, *5*. https://doi.org/10.3389/fsoil.2025.1661097

Rubel, R. I., Lin, W., Alanazi, S., Aldekhail, A., Cidreira, A. C. M., Yang, X., Wasti, S., Bhagia, S., & Zhao, X. (2024). Biochar-compost-based controlled-release nitrogen fertilizer intended for an active microbial community. *Frontiers of Agricultural Science and Engineering*, 0. https://doi.org/10.15302/j-fase-2024571

Rupp, H., Tauchnitz, N., & Meissner, R. (2024). The influence of increasing mineral fertilizer application on nitrogen leaching of arable land and grassland—results of a long-term lysimeter study. *Frontiers in Soil Science*, *4*. https://doi.org/10.3389/fsoil.2024.1345073

Rychel, K., Meurer, K., Getahun, G. T., Bergström, L., Kirchmann, H., & Kätterer, T. (2023). Lysimeter deep N fertilizer placement reduced leaching and improved N use efficiency. *Nutrient Cycling in Agroecosystems*, *126*, 213–228. https://doi.org/10.1007/s10705-023-10286-w

Saeed, A. A. H., Harun, N. Y., Sufian, S., Bilad, M. R., Nufida, B. A., Ismail, N. M., Zakaria, Z. Y., Jagaba, A. H., Ghaleb, A. A. S., & Al-dhawi, B. N. S. (2021). Modeling and Optimization of Biochar Based Adsorbent Derived from Kenaf Using Response Surface Methodology on Adsorption of Cd2+. *Water*, *13*(7), 999. https://doi.org/10.3390/w13070999

Sánchez-Monedero, M. A., Sánchez-García, M., Alburquerque, J. A., & Cayuela, M. L. (2019). Biochar reduces volatile organic compounds generated during chicken manure composting. *Bioresource Technology*, *288*, 121584. https://doi.org/10.1016/J.BIORTECH.2019.121584

Sarlaki, E., Kermani, A. M., Kianmehr, M. H., Asefpour Vakilian, K., Hosseinzadeh-Bandbafha, H., Ma, N. L., Aghbashlo, M., Tabatabaei, M., & Lam, S. S. (2021). Improving sustainability and mitigating environmental impacts of agro-biowaste compost fertilizer by pelletizing-drying. *Environmental Pollution*, *285*(2), 117412. https://doi.org/10.1016/j.envpol.2021.117412

Sary, D. H., & Abd El-Aziz, M. E. (2025). Synthesis and characterization of nano-micronutrient fertilizer and its effect on nutrient availability and maize (Zea Mays L.) productivity in calcareous soils. *Scientific Reports*, *15*(1), 1–11. https://doi.org/10.1038/S41598-025-11273-7

Sayara, T., Basheer-Salimia, R., Hawamde, F., & Sánchez, A. (2020). Recycling of Organic Wastes through Composting: Process Performance and Compost Application in Agriculture. *Agronomy 2020, Vol. 10, Page 1838*, *10*(11), 1838. https://doi.org/10.3390/AGRONOMY10111838

Schofield, H. K., Pettitt, T. R., Tappin, A. D., Rollinson, G., & Fitzsimons, M. F. (2019). Biochar incorporation increased nitrogen and carbon retention in a waste-derived soil. *The Science of The Total Environment*, *690*, 1228–1236. https://doi.org/10.1016/j.scitotenv.2019.07.116

Seligra, P. G., Medina Jaramillo, C., Famá, L., & Goyanes, S. (2016). Biodegradable and non-retrogradable eco-films based on starch–glycerol with citric acid as crosslinking agent. *Carbohydrate Polymers*, *138*, 66–74. https://doi.org/10.1016/J.CARBPOL.2015.11.041

Shabir, R., Li, Y., Megharaj, M., & Chen, C. (2024). Pyrolysis temperature affects biochar suitability as an alternative rhizobial carrier. *Biology and Fertility of Soils*, *60*(5), 681–697. https://doi.org/10.1007/s00374-024-01805-0

Shafiq, F., Anwar, S., Firdaus-e-Bareen, Zhang, L., & Ashraf, M. (2023). Nano-biochar: Properties and prospects for sustainable agriculture. *Land Degradation \& Development*, *34*(9), 2445–2463. https://doi.org/10.1002/LDR.4620

Shah, G. A., Mustafa, M., Asfour, H. Z., Shoukat, K., Yasin, A., Ali, N., Khan, M. B., Ondrašek, G., & Rashid, M. I. (2024). Nanobiochar-Coating Regulates N and P Release from DAP Fertilizer in Soil and Improves Maize Crop Productivity. *Journal of Soil Science and Plant Nutrition*. https://doi.org/10.1007/s42729-024-02004-4

Shahzadi, J., Zaib-un-Nisa, Ali, N., Iftikhar, M., Shah, A. A., Ashraf, M. Y., Chao, C., Shaffique, S., Gatasheh, M. K., 1∗, Z.-U.-N., Ali, N., Iftikhar, M., Shah, A. A., Ashraf, M. Y., Chao, C., Shaffique, S., & Gatasheh, M. K. (2025). Foliar application of nano biochar solution elevates tomato productivity by counteracting the effect of salt stress insights into morphological physiological and biochemical indices. *Scientific Reports 2025 15:1*, *15*(1), 3205-. https://doi.org/10.1038/s41598-025-87399-5

Sharma, P. P., Sharma, P. P., & Thakur, N. (2024). Sustainable farming practices and soil health: a pathway to achieving SDGs and future prospects. *Discover Sustainability*, *5*(1), 250-. https://doi.org/10.1007/s43621-024-00447-4

Sheokand, M., Jain, K., Rana, V., Dhaka, S., Rana, A., Singh, K. P., & Dhaka, R. K. (2023). *Nanobiochar-Based Formulations for Sustained Release of Agrochemicals in Precision Agriculture Practices* (pp. 2413–2438). https://doi.org/10.1007/978-3-031-16101-8_109

Shin, J. Du, & Park, S. W. (2018). Optimization of Blended Biochar Pellet by the Use of Nutrient Releasing Model. *Applied Sciences 2018, Vol. 8, Page 2274*, *8*(11), 2274. https://doi.org/10.3390/APP8112274

Shrestha, S., & Mahat, J. (2022). Sustainable food security: how to feed an increasing population? A review. In *inwascon Technology Magazine* (Vol. 4, pp. 15–18). Zibeline International Publishing. https://doi.org/10.26480/itechmag.04.2022.15.18

Sidorczuk, D., Kozanecki, M., Civalleri, B., Pernal, K., & Prywer, J. (2020). Structural and Optical Properties of Struvite. Elucidating Structure of Infrared Spectrum in High Frequency Range. *Journal of Physical Chemistry A*, *124*(42), 8668–8678. https://doi.org/10.1021/ACS.JPCA.0C04707

Siles-Castellano, A. B., López, M. J., López-González, J. A., Suárez-Estrella, F., Jurado, M. M., Estrella-González, M. J., & Moreno, J. (2020a). Comparative analysis of phytotoxicity and compost quality in industrial composting facilities processing different organic wastes. *Journal of Cleaner Production*, *252*. https://doi.org/10.1016/j.jclepro.2019.119820

Sim, D. H. H., Tan, I. A. W., Lim, L. L. P., & Hameed, B. H. (2021a). Encapsulated biochar-based sustained release fertilizer for precision agriculture: A review. *Journal of Cleaner Production*, *303*, 127018. https://doi.org/10.1016/J.JCLEPRO.2021.127018

Singh, K., Singh, R., Nwosu, N. J., Omara, P., Sharma, L., Dunn, B. L., & Singh, H. (2025). Optimizing Nutrient Delivery in Agronomic Crops: A Review of Enhanced Efficiency Fertilizers. *Journal of Plant Nutrition and Soil Science*, *188*(4), 570–584. https://doi.org/10.1002/JPLN.12010

Sofyane, A., Atlas, S., Lahcini, M., Vidović, E., Améduri, B., & Raihane, M. (2024). Insights into hydrophobic (meth)acrylate polymers as coating for slow-release fertilizers to reduce nutrient leaching. *Polymer Chemistry*, *15*(33), 3327–3340. https://doi.org/10.1039/d4py00573b

Song, J., Sun, Z., Saud, S., Fahad, S., & Nawaz, T. (2024). Exploring the deleterious effects of heavy metal cadmium on antioxidant defense and photosynthetic pathways in higher plants. *Plant Stress*, *15*, 100716. https://doi.org/10.1016/j.stress.2024.100716

Song, X., Razavi, B. S., Ludwig, B., Zamanian, K., Zang, H., Kuzyakov, Y., Dippold, M. A., & Gunina, A. (2020). Combined biochar and nitrogen application stimulates enzyme activity and root plasticity. *The Science of The Total Environment*, *735*, 139393. https://doi.org/10.1016/j.scitotenv.2020.139393

Stacey, N. E., Tea, T., Seefeldt, S. S., Bary, A., & Collins, D. P. (2024). Biochar-Poultry Manure Compost Alters Temperature and Nitrogen Dynamics during Composting and Improves Potato Growth Following Field Application. *Compost Science and Utilization*, *31*(3–4), 86–102. https://doi.org/10.1080/1065657X.2024.2366795

Su, B., Yan, Z., Li, Y., Tang, S., Pan, X., Zhang, X., Li, W., & Li, Y. (2022). Co-Compost Application of Magnesium Salts and Orthophosphate Adjusted Biochar and Cyanobacteria for Fixing Nitrogen, Improving Maize Quality, and Reducing Field Nutrient Loss. *Agronomy*, *12*(10), 2406. https://doi.org/10.3390/agronomy12102406

Sun, J., Lu, X., Wang, S., Tian, C., Chen, G., Luo, N., Zhang, Q., & Li, X. (2023). Biochar Blended with Nitrogen Fertilizer Promotes Maize Yield by Altering Soil Enzyme Activities and Organic Carbon Content in Black Soil. *International Journal of Environmental Research and Public Health*, *20*(6), 4939. https://doi.org/10.3390/ijerph20064939

Tagliaro, I., Seccia, S., Pellegrini, B., Bertini, S., & Antonini, C. (2022). Chitosan-based coatings with tunable transparency and superhydrophobicity: A solvent-free and fluorine-free approach by stearoyl derivatization. *Carbohydrate Polymers*, *302*, 120424. https://doi.org/10.1016/j.carbpol.2022.120424

Talboys, P. J., Heppell, J., Roose, T., Healey, J. R., Jones, D. L., & Withers, P. J. A. (2015). Struvite: a slow-release fertiliser for sustainable phosphorus management? *Plant and Soil 2015 401:1*, *401*(1), 109–123. https://doi.org/10.1007/S11104-015-2747-3

Tan, S. X., Ong, H. C., Andriyana, A., Lim, S., Pang, Y. L., Kusumo, F., & Ngoh, G. C. (2022). Characterization and Parametric Study on Mechanical Properties

Enhancement in Biodegradable Chitosan-Reinforced Starch-Based Bioplastic Film. *Polymers*, *14*(2), 278. https://doi.org/10.3390/polym14020278

Tarolli, P., Luo, J., Park, E., Barcaccia, G., & Masin, R. (2024). Soil salinization in agriculture: Mitigation and adaptation strategies combining nature-based solutions and bioengineering. *IScience*, *27*(2), 108830. https://doi.org/10.1016/j.isci.2024.108830

Tayyab, M. (2018). Biochar: an efficient way to manage low water availability in plants. *Applied Ecology and Environmental Research*, *16*(3), 2565–2583. https://doi.org/10.15666/aeer/1603_25652583

Tazebew, E., Addisu, S., Bekele, E., Alemu, A., Belay, B., & Sato, S. (2024). Sustainable soil health and agricultural productivity with biochar-based indigenous organic fertilizers in acidic soils: insights from Northwestern Highlands of Ethiopia. *Discover Sustainability*, *5*(1). https://doi.org/10.1007/S43621-024-00380-6

Thomas, S. C. (2021). Post-processing of biochars to enhance plant growth responses: a review and meta-analysis. In *Biochar* (Vol. 3, Number 4, pp. 437–455). Springer Nature. https://doi.org/10.1007/s42773-021-00115-0

Thu, T. T. P., & Loan, N. T. (2024). Multi-Component Composting of Agricultural By-Products Improves Compost Quality and Effects on the Growth and Yield of Cucumber. *Journal of Ecological Engineering*, *25*(6), 109–119. https://doi.org/10.12911/22998993/187036

Toková, L., Igaz, D., Hořák, J., & Aydın, E. (2023). Can application of biochar improve the soil water characteristics of silty loam soil? *Journal of Soils and Sediments*, *23*(7), 2832–2847. https://doi.org/10.1007/s11368-023-03505-y

Tomadoni, B., Casalongué, C., & Alvarez, V. A. (2019). Biopolymer-Based Hydrogels for Agriculture Applications: Swelling Behavior and Slow Release of Agrochemicals. *Polymers for Agri-Food Applications*, 99–125. https://doi.org/10.1007/978-3-030-19416-1_7

Tran, H. T., Bolan, N. S., Lin, C., Binh, Q. A., Nguyen, M. K., Luu, T. A., Le, V. G., Pham, C. Q., Hoang, H. G., & Vo, D. V. N. (2023). Succession of biochar addition for soil amendment and contaminants remediation during co-composting: A state of art review. *Journal of Environmental Management*, *342*, 118191. https://doi.org/10.1016/J.JENVMAN.2023.118191

Tsai, C. C., & Chang, Y. F. (2020). Effects of Biochar to Excessive Compost-Fertilized Soils on the Nutrient Status. *Agronomy 2020, Vol. 10, Page 683*, *10*(5), 683. https://doi.org/10.3390/AGRONOMY10050683

Urra, J., Alkorta, I., Lanzén, A., Mijangos, I., & Garbisu, C. (2019). The application of fresh and composted horse and chicken manure affects soil quality, microbial composition and antibiotic resistance. *Applied Soil Ecology*, *135*, 73–84. https://doi.org/10.1016/J.APSOIL.2018.11.005

Vadhel, A., Kumar, A., Bashir, S., Malik, T., & Mohan, A. (2023). Synergistic and non-synergistic impact of HAP-based nano fertilizer and PGPR for improved nutrient utilization and metabolite variation in hemp crops. *Environmental Science Nano*, *10*(11), 3101–3110. https://doi.org/10.1039/d3en00380a

Vandecasteele, B., Sinicco, T., D'Hose, T., Vanden Nest, T., & Mondini, C. (2016). Biochar amendment before or after composting affects compost quality and N losses, but not P plant uptake. *Journal of Environmental Management*, *168*, 200–209. https://doi.org/10.1016/J.JENVMAN.2015.11.045

Védère, C., Lebrun, M., Biron, P., Planchais, S., Bordenave-Jacquemin, M., Honvault, N., Firmin, S., Savouré, A., Houben, D., & Rumpel, C. (2022). The older, the better: Ageing improves the efficiency of biochar-compost mixture to alleviate drought stress in plant and soil. *The Science of The Total Environment*, *856*, 158920. https://doi.org/10.1016/j.scitotenv.2022.158920

Veljanoska, S. (2016). *Agricultural risk, remittances and climate change in rural Africa* (Doctoral dissertation, Université Panthéon-Sorbonne-Paris I). Accessed on 12/24/2025.

Verburg, K., Thorburn, P. J., Vilas, M. P., Biggs, J. S., Zhao, Z., & Bonnett, G. D. (2022). Why are the benefits of enhanced-efficiency fertilizers inconsistent in the field? Prerequisite conditions identified from simulation analyses. *Agronomy for*

Verma, R., Dutta, S., Kumar, A., Dabodiya, T. S., Kumar, N., Karuppasamy, K. S. K., Sangmesh, B., Jaiswal, A., & Jaiswal, K. K. (2023). Biochar-Based Nanocomposite Materials: Types, Characteristics, Physical Activation, and Diverse Application Scenarios. *Advances in Science, Technology and Innovation*, *Part F741*, 3–18. https://doi.org/10.1007/978-3-031-28873-9_1

Wan, H., Hou, J., Wei, Z., & Liu, F. (2024). Contrasting maize responses to soil phosphorus and potassium availability driven by biochar under reduced irrigation. *Plant and Soil*, *508*, 677–700. https://doi.org/10.1007/s11104-024-06824-2

Wan, H., Liu, X., Shi, Q., Chen, Y., Jiang, M., Zhang, J., Cui, B., Hou, J., Wei, Z., Hossain, M. A., & Liu, F. (2023). Biochar amendment alters root morphology of maize plant: Its implications in enhancing nutrient uptake and shoot growth under reduced irrigation regimes. *Frontiers in Plant Science*, *14*, 1122742. https://doi.org/10.3389/fpls.2023.1122742

Wan Yusof, W. R., Sabar, S., & Zailani, M. A. (2024). Starch-chitosan blends: A comprehensive review on the preparation, physicochemical properties and applications. *Biopolymers*, *115*(5), e23602. https://doi.org/10.1002/BIP.23602

Wang, G., Yang, Y., Kong, Y., Ma, R., Yuan, J., & Li, G. (2022). Key factors affecting seed germination in phytotoxicity tests during sheep manure composting with carbon additives. *Journal of Hazardous Materials*, *421*, 126809. https://doi.org/10.1016/J.JHAZMAT.2021.126809

Wang, L., Guan, J., Wei, J., Mahmood, A., Rasheed, A., Hassan, M. U., Al-Khayri, J. M., Al-Daej, M. I., Sattar, M. N., Rezk, A. A., Almaghasla, M. I., & Shehata, W. F. (2023). Biochar a promising amendment to mitigate the drought stress in plants: review and future prospective. *Notulae Botanicae Horti Agrobotanici Cluj-Napoca*, *51*(4), 13447. https://doi.org/10.15835/nbha51413447

Wang, S., Sun, K., Xiang, H., Zhao, Z., Shi, Y., Su, L., Tan, C., & Zhang, L. (2022). Biochar-seeded struvite precipitation for simultaneous nutrient recovery and chemical oxygen demand removal in leachate: From laboratory to pilot scale. *Frontiers in Chemistry*, *10*. https://doi.org/10.3389/fchem.2022.990321

Wang, X., Lou, T., Zhao, W., & Song, G. (2016b). Preparation of pure chitosan film using ternary solvents and its super absorbency. *Carbohydrate Polymers*, *153*(13), 253–257. https://doi.org/10.1016/j.carbpol.2016.07.081

Wang, X., Selvam, A., & Wong, J. W. C. (2016a). Influence of lime on struvite formation and nitrogen conservation during food waste composting. *Bioresource Technology*, *217*, 227–232. https://doi.org/10.1016/J.BIORTECH.2016.02.117

Wang, Y., Li, J., & Yang, X. (2021). The diffusion model of nutrient release from membrane pore of controlled release fertilizer. *Environmental Technology \& Innovation*, *25*, 102256. https://doi.org/10.1016/j.eti.2021.102256

Wei, Y., Wang, J., Chang, R., Zhan, Y., Wei, D., Zhang, L., & Chen, Q. (2021). Composting with biochar or woody peat addition reduces phosphorus bioavailability. *Science of The Total Environment*, *764*, 142841. https://doi.org/10.1016/J.SCITOTENV.2020.142841

Wenger, L. E., & Hanusa, T. P. (2023). Synthesis without solvent: consequences for mechanochemical reactivity. In *Chemical Communications* (Vol. 59, Number 96, pp. 14210–14222). Royal Society of Chemistry. https://doi.org/10.1039/d3cc04929a

Wesołowska, M., Rymarczyk, J., Góra, R., Baranowski, P., Sławiński, C., Klimczyk, M., Supryn, G., & Schimmelpfennig, L. (2021). New slow-release fertilizers – economic, legal and practical aspects: a Review. *International Agrophysics*, *35*(1), 11–24. https://doi.org/10.31545/intagr/131184

Wu, Y., Wang, X., Zhang, L., Zheng, Y., Liu, X., & Zhang, Y. (2023). The critical role of biochar to mitigate the adverse impacts of drought and salinity stress in plants. In *Frontiers in Plant Science* (Vol. 14, p. 1163451). Frontiers Media. https://doi.org/10.3389/fpls.2023.1163451

Xu, X., Xu, Z., Huang, J., Gao, B., Zhao, L., Qiu, H., & Cao, X. (2021). Sorption of reactive red by biochars ball milled in different atmospheres: Co-effect of surface morphology and functional groups. *Chemical Engineering Journal*, *413*, 127468. https://doi.org/10.1016/J.CEJ.2020.127468

Yameen, M. Z., Naqvi, S. R., Juchelková, D., & Khan, M. N. A. (2024). Harnessing the power of functionalized biochar: progress, challenges, and future perspectives in energy, water treatment, and environmental sustainability. *Biochar*, *6*(1). https://doi.org/10.1007/s42773-024-00316-3

Yan, B., Zhang, Y., Wang, Y., Rong, X., Peng, J., Fei, J., & Luo, G. (2023). Biochar amendments combined with organic fertilizer improve maize productivity and mitigate nutrient loss by regulating the C–N–P stoichiometry of soil, microbiome, and enzymes. *Chemosphere*, *324*, 138293. https://doi.org/10.1016/j.chemosphere.2023.138293

Yan, Y., Zhang, N., & Hu, X. (2019). Effects of wet and dry ball milling on the physicochemical properties of sawdust derived-biochar. *Instrumentation Science & Technology*, *48*(3), 287–300. https://doi.org/10.1080/10739149.2019.1708751

Yang, H., Zhang, H., Qiu, H., Anning, D. K., Li, M., Wang, Y., & Zhang, C. (2021). Effects of C/N Ratio on Lignocellulose Degradation and Enzyme Activities in Aerobic Composting. *Horticulturae 2021, Vol. 7, Page 482*, *7*(11), 482. https://doi.org/10.3390/HORTICULTURAE7110482

Yang, Y., Wang, G., Li, G., Ma, R., Kong, Y., & Yuan, J. (2021). Selection of sensitive seeds for evaluation of compost maturity with the seed germination index. *Waste Management*, *136*, 238–243. http://dx.doi.org/10.1016/j.wasman.2021.09.037

Yu, X., Wu, S., Zhang, Z., & Wang, C. (2025). Application of ball milling technology in removal of PFAS and ball milling modified materials: A review. *Journal of Hazardous Materials Advances*, *18*, 100709. https://doi.org/10.1016/J.HAZADV.2025.100709

Yusof, N. M., Jai, J., & Hamzah, F. (2019). Effect of Coating Materials on the Properties of Chitosan-Starch-Based Edible Coatings. *IOP Conference Series Materials Science and Engineering*, *507*, 12011. https://doi.org/10.1088/1757-899x/507/1/012011

Zain, A. H. M., Ab Wahab, M. K., & Ismail, H. (2017). Biodegradation Behaviour of Thermoplastic Starch: The Roles of Carboxylic Acids on Cassava Starch. *Journal of Polymers and the Environment*, *26*(2), 691–700. https://doi.org/10.1007/s10924-017-0978-5

Zha, Y., Zhao, L., Wei, J., Niu, T., Yue, E., Wang, X., Chen, Y., Shi, J., & Zhou, T. (2023). Effect of the application of peanut shell, bamboo, and maize straw biochars on the bioavailability of Cd and growth of maize in Cd-contaminated soil. *Frontiers in Environmental Science*, *11*. https://doi.org/10.3389/fenvs.2023.1240633

Zhang, D., Jiang, L., Zong, J., Chen, S., Ma, C., & Hong-jun, L. I. (2017). Incorporated α-amylase and starch in an edible chitosan–procyanidin complex film increased the release amount of procyanidins. *RSC Advances*, *7*(89), 56771–56778. https://doi.org/10.1039/c7ra11142h

Zhang, K., Khan, Z., Yu, Q., Qu, Z., Liu, J., Luo, T., Zhu, K., Bi, J., Hu, L., & Luo, L. (2022). Biochar Coating Is a Sustainable and Economical Approach to Promote Seed

Coating Technology, Seed Germination, Plant Performance, and Soil Health. In *Plants* (Vol. 11, Number 21, p. 2864). Multidisciplinary Digital Publishing Institute. https://doi.org/10.3390/plants11212864

Zhang, X., Teng, Z., Huang, R., & Catchmark, J. M. (2020). Biodegradable Starch/Chitosan Foam via Microwave Assisted Preparation: Morphology and Performance Properties. *Polymers 2020, Vol. 12, Page 2612*, *12*(11), 2612. https://doi.org/10.3390/POLYM12112612

Zhao, Y., Hu, Z., Lu, Y., Shan, S., Zhuang, H., Gong, C., Cui, X., Zhang, F., & Li, P. (2024). Facilitating mitigation of agricultural non-point source pollution and improving soil nutrient conditions: The role of low temperature co-pyrolysis biochar in nitrogen and phosphorus distribution. *Bioresource Technology*, *394*, 130179. https://doi.org/10.1016/J.BIORTECH.2023.130179

Zhou, R., Zhang, M., Zhou, J., & Wang, J. (2019). Optimization of biochar preparation from the stem of Eichhornia crassipes using response surface methodology on adsorption of Cd2+. *Scientific Reports*, *9*(1). https://doi.org/10.1038/s41598-019-54105-1

Zou, Z., Fan, L., Li, X., Dong, C., Zhang, L., Zhang, L., Fu, J., Han, W., & Yan, P. (2021). Response of Plant Root Growth to Biochar Amendment: A Meta-Analysis. *Agronomy*, *11*(12), 2442. https://doi.org/10.3390/agronomy11122442

Zouari, M., Marrot, L., & DeVallance, D. (2023). Effect of demineralization and ball milling treatments on the properties of Arundo donax and olive stone-derived biochar. *International Journal of Environmental Science and Technology*, *21*(1), 101–114. https://doi.org/10.1007/s13762-023-04968-9

APPENDICES

Encapsulated Biochar blended compost

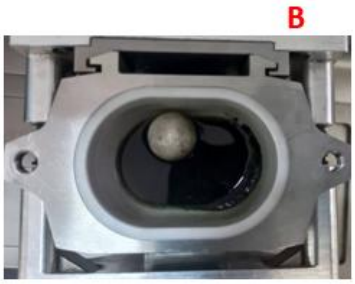

Nano Biochar blended compost

Finished product

Pot-scale semi-field experiments

Pots under drought stress